Interpreting environmental change using bivalve shell geochemistry

Sarah Tynan

January 2017

A thesis submitted for the degree of Doctor of Philosophy of

The Australian National University

Declaration

I confirm that this thesis is the product of my own original research. Where co-authors have contributed to chapters that are in the form of published (or to be published) manuscripts, individual contributions are indicated for each manuscript.

Signed:

Word count (excluding References and Appendices): 38 092

Acknowledgements

This has taken a long time, and I suspect some of these people don't even remember who I am, their involvement in this project long forgotten. But without their many and varied contributions, some huge, some small but significant, I could never have reached this point, and the journey to get here would have been all the more arduous.

Enormous and deep-felt thanks to Brad Opdyke, whose patience, optimism and good humour has seen this project through. Andrea Dutton provided valuable, direct and honest advice and support. David Ellis provided advice during the project's initial stages and Sara Beavis and Steve Eggins gave useful feedback, discussions and encouragement along the way. Maureen (Mo) Walczak's generosity with her time to provide guidance and mentoring has been crucial (read: saved my life). Patrick De Deckker thoughtfully established that connection in the first place.

Essential logistical assistance in setting up and maintaining the culturing experiments that formed the basis of this thesis are gratefully acknowledged:

Jane Clout and David Clout in Moreton Bay, and Hayden Dyke, Sue Dyke and Col Dyke in Little Swanport. These oyster farmers generously donated time, equipment, oysters, all-encompassing hospitality and true diligence and enthusiasm for the year-long responsibility of sample collection for the project.

At Pambula Lake, Pauline Millard and Karlene Belshaw ably assisted with sample collection. Special thanks to my parents Chris and Ray Tynan for, well, everything, but especially their diligence and commitment to assisting with the project and for (eventually) tactfully refraining from asking for updates.

Graham Moore from the Merimbula Office of the NSW Department of Environment provided a cultural context for the archaeological samples from the Severs Beach midden site. Bobby Maher and the Eden Aboriginal Land Council kindly supported this project. Sean Ulm and Jay Hall generously provided samples from archaeological sites in Queensland.

Tony Phimpsinane and John Vickers provided valuable guidance and assistance with the task of preparing shells into thick and thin sections

for sampling. Linda McMorrow assisted with analysis of water samples and Les Kinsley patiently (and repeatedly) helped with laser ablation analysis.

Simon Troelestra, Hubert Vonhoff, Suzanne Verdegaal and especially Emma Versteegh not only welcomed me into their lab at the Vrijie Universiteit Amsterdam, but generously helped with shell sampling and analysis. Patrick De Deckker (again!) kindly established that connection. Lora Windgate and KC Lohmann at the University of Michigan, along with Andy and Judy Meyers provided support and hospitality during my time in Ann Arbor.

Thank you to the friends who simply knew not to ask, or gave me other things to think about on the cricket pitch, the footy field, the stairwell, or in the boat on Lake Burley Griffin and at the coffee shop, lunch breaks, and of course the pub. Some deserve special mention: Julie Brown, Fern Beavis, Jill Sutton, Julia Jasonsmith, Luke Wallace and Al Usher, though the status of friend of all these people was called into doubt as one by one, they finished their PhDs in a sensible amount of time and left me to my fate. Thanks guys. And you're now forgiven. Sophie Lewis, Ulli Troitchsz, Megan Head and Sandra Gardam provided wise and unswerving counsel.

And finally, thank you Ben, for unmitigated support and reassurance, for helping me keep things in perspective, and for helping maintain an appreciation for the things that are truly important.

A PhD scholarship and financial support from the Cooperative Research Centre for Landscape Environments and Mineral Exploration is gratefully acknowledged. Visits to overseas laboratories to sample analysis and attendance at international conferences were enabled by an ANU Vice-Chancellor's HDR Travel Grant, a Betty Mayne Scientific Research Fund for Earth Sciences from the Linnaen Society of New South Wales and a Research School of Earth Sciences HDR Student Travel Grant. A Chrysalis Scholarship from the Association of Women Geoscientists is also facilitated continued work in the later stages of project.

ABSTRACT

To further our understanding of Earth's climate beyond historical records, a number of paleoclimate proxies are used to infer how climate has changed throughout Earth's history. Examined herein are two such geochemical proxies—the $\delta^{18}O$ of the shell of the Australian mud or flat oyster, *Ostrea angasi*, and the Mg/Ca ratio of the shells of the Sydney Rock oyster, *Saccostrea glomerata*, and the common mussel, *Mytilus galloprovincialis*.

The proxies were calibrated using *in situ* culturing experiments with modern specimens. Oysters and mussels were cultured for approximately one year in three locations representative of the broad distribution of the species along the east coast of Australia: Little Swanport, Tasmania (*O. angasi*, *M. galloprovincialis*); Pambula Lake, New South Wales (*O. angasi*, *S. glomerata*, *M. galloprovincialis*) and Moreton Bay, Queensland (*S. glomerata*). Temperature loggers were deployed with the specimens and water samples taken fortnightly.

The *O. angasi* shells were sampled using a Merchantek microsampling system at the Vrije Universiteit Amsterdam and the University of Michigan, and $\delta^{18}O$ was analysed via ICP-MS. The trace element ratios of *S. glomerata* shells were analysed via Laser Ablation ICP-MS at the Australian National University.

The data from the Pambula Lake and Little Swanport *O. angasi* were combined to produce a regression relationship between temperature and $\delta^{18}O_{shell}$ and $\delta^{18}O_{water}$. For *S. glomerata*, the Mg/Ca data from Pambula Lake and Moreton Bay were compiled to produce a mean Mg/Ca signal for the shells from each location. Linear regressions with temperature showed a significant difference in the *S. glomerata* Mg/Ca-temperature relationships

for the two locations. This difference was not evident when the D_{Mg}-temperature relationship was calculated, indicating that the underlying salinity or water chemistry can impact upon the *S. glomerata* shell Mg/Ca.

The Mg/Ca-temperature relationship within *M. galloprovincialis* shells from Pambula Lake and Little Swanport was also examined. The Little Swanport shells did not show a consistent relationship between Mg/Ca and temperature, while the Pambula Lake *M. galloprovincialis* Mg/Ca-temperature relationship compared well with published Mg/Ca-temperature relationships for other *Mytilus* species.

The derived proxy-temperature relationships for the oyster species were then applied to archaeological specimens of *O. angasi* from the Severs Beach midden site, Pambula Lake, and *S. glomerata* from the Sandstone Point midden site, Moreton Bay, to test the potential of these species for use as paleoclimate archives. Results show that while interpretation of paleoclimate information from these proxies within these species is not straightforward, both $\delta^{18}O$ in *O. angasi* and Mg/Ca in *S. glomerata* show good potential for use as paleoclimate proxies. Future work should focus on sampling a larger number of shells from a broader geographical area.

This is the first study to investigate these Australian species, and given the abundance of oyster and mussel shells within Aboriginal midden sites along the eastern coastline of Australia there is clearly potential for this approach to make a valuable contribution to understandings of paleoclimate in the Australian region, particularly for the mid to late Holocene, for which current records are scarce.

Table of Contents

List of Figures

List of Tables

Chapter 1

Introduction: Paleoclimate investigations

A persistent goal of Earth Sciences research is to understand how the planet we live on functions, and how it has changed over time. A major aspect of this is paleoenvironmental studies that seek to reconstruct past climatic conditions, tracking their fluctuations through glacial periods to epochs of warmer temperatures and higher sea levels. These studies inform our understanding of how Earth's climate has evolved to reach the point where it is today: on the cusp of dramatic change induced by anthropogenic activities. Only armed with a solid and comprehensive understanding of how climate has changed throughout Earth's evolution can scientists properly understand current conditions, and create the models needed to predict the impacts of ongoing climate change into the future.

The resources used for such paleoclimate reconstructions are many and varied, in type, resolution and chronology. There are ice cores from Antarctica that span eight glacial cycles (Jouzel et al. 2007; Kawamura et al. 2007; Augustin et al. 2014) and deep-sea sediment cores from various marine locations (e.g. Koutavas et al. 2002; Lisiecki and Raymo 2005). Records are also derived from lacustrine sediment cores (e.g. Lotter et al. 1992; Wick et al. 2003; Bookhagen et al. 2005). Coral records (e.g. Cobb et al. 2013; Tierney et al. 2015) and tree-ring (e.g. Cook et al. 2000) records are used to augment and extend the observational climate record back into the Holocene.

The proxies themselves are also numerous and diverse: physical parameters such as sedimentation rate (e.g. Romans et al. 2013), the presence of particular taxa of microfossils or pollen (e.g. Sabin and Pisias 1996), and geochemical analyses such as stable isotope and trace element

data (e.g. Campana 1999; Fairchild and Treble 2009; Martinez-Ruiz et al. 2015) all yield information about past climatic conditions.

One of the tools in the paleoclimatologist's arsenal is the sclerochronological record contained within the skeletons and shells of biogenic carbonates. Aquatic animals that produce a skeleton or shell of calcium carbonate extract the elements they require to build their skeleton (or shell) from the ambient water. In doing so, they capture a geochemical signature of that water, creating an archive of the environmental conditions it experienced as it grew. This provides a proxy record of that environment that will persist in the hard skeleton as it is preserved in the geological record.

The pioneering work that established the bedrock upon which biogenic carbonate paleoclimate proxies have been built occurred in the mid and latter half of the 20th century, initiated by Harold Urey's 1947 paper describing "The thermodynamic properties of isotopic substances" (Urey 1947). Samuel Epstein first described the concept of using the oxygen isotopes found within marine mollusc shells to derive a temperature record (Epstein et al. 1951; Epstein et al. 1953). Cesare Emiliani then used the isotopic analysis of foraminifera from marine sediment cores to assess and describe temperature and glacial fluctuations through the Pleistocene (Emiliani 1955). Nicholas Shackleton and Neil Opdyke further refined the development and application of these proxies (Shackleton and Opdyke 1973) and since then, paleoclimate investigations have been extended to a huge range of biogenic carbonates. Henderson (2002) provides an excellent review of the various proxies that have been developed since those first pioneering studies.

Many different biogenic carbonates have been investigated as recorders of environmental conditions, including corals (e.g. Cobb et al. 2013), coralline algae (e.g. Halfar et al. 2008), coralline sponges (e.g. Bohm et al. 2000), ostracods (e.g. Börner et al. 2013; De Deckker et al. 1999) gastropods (e.g. Szymanek 2016; Prendergast et al. 2016; Cespuglio 1999) fish otoliths (e.g. Bath et al. 2000; Hufthammer 2010) and even earthworm secretions (e.g. Versteegh et al. 2013) and emu eggshell (e.g. Miller et al. 2016).

1.1. Bivalves as a paleoclimate archive

The shells of bivalve molluscs, laid down in incremental growth layers throughout the duration of the animal's lifetime, also offer potential environmental archives. Although individual species are restricted to constrained geographical limits, collectively the class Bivalvia offers a virtually global distribution. Studies of bivalves have ranged from analysis of *Cucullaea* found in Antarctic waters (e.g. Dutton et al. 2002) to giant clams found in the tropics (e.g. Ayling et al. 2015; Warter et al. 2015; Elliot et al. 2009). Various northern hemisphere locations have been examined using the extremely long-lived *Arctica islandica* (e.g. Walliser et al. 2016; Wanamaker et al. 2011; Schöne et al. 2005) and the Pacific coast of South America has been investigated using the shells of *Mesodesma donacium* (e.g. Carré et al. 2014). Others have used *Mytilus edulis* to study measurements of glacial meltwater in Greenland (Versteegh et al. 2012) and other studies explore the extreme environments of deep-sea hydrothermal vents (e.g. Kádár and Costa 2006). Other work has examined freshwater mussels from the Himalayan and Ganja plain river system (Gajurel et al. 2006).

The longevity of the various bivalve species, and thus the length of the environmental record preserved in their shells, is also variable, with documented ages ranging between <10 and up to >500 years for some extremely long-lived bivalves, namely *Arctica islandica* (Butler et al. 2013) and *Neopycnodonte zibrowii* (Wisshak et al. 2009). Drawing on the work of dendrochronologists, many sclerochronology researchers have worked on ways to combine individual shell records to develop longer-term composite records (e.g. Marchitto et al. 2000).

A great advantage of bivalve shell sclerochronology is the high resolution of the record they can offer, as discussed in Schöne and Surge (2014 and references therein). The incremental growth structures in various different bivalves species have been found to range from the order of minutes–hours (Rodland et al. 2006) to diurnally (tidal), daily, or fortnightly-resolved records to those of seasonal and annual resolution. It is important to remember the role that seasonality and other environmental factors can play in controlling shell growth, and influencing the records shells contain.

1.2. Calibrating the environmental signals

Extensive research has been conducted into several different freshwater and marine bivalve species. The thermodynamic reactions that govern biogenic carbonate precipitation differ from inorganic carbonate precipitation thermodynamics, and different types of biogenic carbonates are mediated by biological controls in different ways. This shouldn't be surprising; corals, foraminifera and molluscs are very different creatures. As it is now well appreciated that calibrations developed for one type of biogenic carbonate do not necessarily translate to an accurate interpretation of the signal found

in a another, extensive research has focused on calibrating the environmental signals recorded in both the physical and chemical characteristics in specimens of living shells, along with assessing the potential uncertainties and inconsistencies that various species may exhibit in their shell geochemistry (e.g. *Mytilus edulis*: Wanamaker et al. 2006, Wanamaker et al. 2008; *Pecten maximus*: Owen et al. 2002; Freitas et al. 2012, *Mytilus trossulus*: Klein et al. 1996; Marchais et al. 2015; *Crassostrea virginica*: Surge et al. 2001, Surge and Lohmann 2008; *Arctica islandica*: Beirne et al. 2012; *Mesodesma donacium*: Carré et al. 2006; *Chione subrugosa*: Carré et al. 2006; *Tridacna gigas*: Elliot et al. 2009; *Panopea abrupta*: Hallmann et al. 2008; *Pinna nobilis*: Kennedy et al. 2001; *Ruditapes philippinarum*: Poulain et al. 2015; *Comptopallium radula*: Thébault et al. 2007).

These calibration studies have brought to light several issues that can complicate interpretations of environmental signals within bivalve shells. One such issue is heterogeneity of trace element incorporation, both within individual shells and between contemporaneous specimens (e.g. Freitas et al. 2005; Freitas et al. 2009; Schöne et al. 2010; Lazareth et al. 2013; Schöne et al. 2013). Ontogenetic effects have also been observed in a number of bivalve shell records, with isotopic fractionation and trace element incorporation regimes changing with increasing age of the animal (e.g. Strasser et al. 2008; Schöne et al. 2011). Similarly, growth rates can also affect shell isotopic and trace element signals (e.g. Owen et al. 2002; Carré et al. 2006). A number of studies have simply found no environmental signal within the shell geochemistry of some species (e.g. *Neopycnodonte zibrowii*, Wisshak et al. 2009).

1.3. Climate reconstructions

The logical next step is to apply the calibrated sclerochronological signals within a paleoenvironmental context. Despite the limitations discussed above, several studies have successfully used bivalve species to reconstruct records of climate variability for various epochs throughout the geological record and numerous locations around the globe. Reviews of such investigations are provided by Schöne and Gillikin (2013), Schöne and Surge (2014) and Twaddle et al. (2016). Table 1.1 is by no means an exhaustive list of all bivalve paleoclimate studies, but it provides an indication of the breadth of coverage that can be provided by bivalve sclerochronology.

Table 1.1. Selected paleoclimate studies using bivalve shells.

Time period	***Species***	**Citation**
Recent	*Arctica islandica*	Schöne et al. 2005
	Arctica islandica	Wanamaker et al. 2011
	Arctica islandica	Butler et al. 2013
Holocene	*Tridacna gigas*	Driscoll et al. 2014
	Donax variabilis	Jones et al. 2005
	Saxidomus giganteus	Hallmann et al. 2013
	Meretrix lamarckii	Chinzei et al. 1987
	Mesodesma donacium	Carré et al. 2014
	Phacosoma japonicum	Schöne et al. 2004
Pleistocene	*Crassostrea virginica*	Kirby et al. 1998
	Glycymeris, Aequipecten and Arctica	Crippa et al. 2016
Pliocene	*Mercenaria* spp.	Winkelstern et al. 2013
	Aequipecten opercularis, Atrina fragilis	Valentine et al. 2011
Miocene	*Diplodon* aff. *longulus, Diplodon longulus, Anodontites capax, Pachydon tenuis, Pachydon erectus*	Kaandorp et al. 2006
	Parreysia sp., *Lamelledens* sp.	Dettman et al. 2001
Oligocene	*Crassostrea gigantissima*	Kirby 2000
	Glycymeris planicostalis	Walliser et al. 2015
Eocene	*Cucullaea*	Dutton and Lohmann 2002
	Sphaerium	Buskirk et al. 2016
	Sokolowia bushii	Bougeois et al. 2014
Paleocene	*Camptochlamys alaskensis*	Bice et al. 1996
Cretaceous	*Vaccinites cornuvaccinium, Gorjanovicia, Vaccinites ultimus, Vaccinities vesiculousus, Yvaniella alpani, Vassinites grossouvrei, Durania, Torreites sanchezi milovanovici, Vaccinites macgillavryi*	Steuber 1999
Jurassic	oysters	Brigaud et al. 2008
	Praexogyra hebridica	Hendry and Kalin 1997
	belemnites, oysters, ammonites, nautiloids, trigoniid shells	Wierzbowski and Jaochimski 2007
Triassic	*Cornucardia hornigi,*	Nuetzel et al. 2010
Permian	brachiopod	Mazzullo et al. 2007
Carboniferous	*Neospirifer dunbari*	Roark et al 2016

1.4. Archaeological interpretations

One of the primary sources of paleo-samples of bivalves are archaeological sites that represent pre-historic human occupation. Accordingly, the records these shells can provide is not limited to environmental interpretations; they also provide insights into human-environment interactions, and the subsistence economies and lifestyles of these populations. This interplay between environmental interpretations and archaeology is complex: the environmental records obtained from archaeological shells must also be considered within the context of their provenance. Changes in seasonality that can be inferred from sclerochronological analysis would have impacted on resource availability for the people living in the landscape; the accumulation of shells within midden sites is a direct reflection of this human-environment interaction (Andrus 2011; Twaddle et al. 2016).

As such, a range of investigations have taken the climate information interpreted from shells and applied it to develop understandings of past human-climate interactions, and how people lived within the paleo-landscape.

In 1973, Shackleton published an interpretation of the occupation patterns of an archaeological site in South Africa, based on the $\delta^{18}O_{shell}$ values of the shells a gastropod (*Patella tabularis*) present in the site. By assessing the seasonal signal contained within the shells, then interpreting the most recent growth as being the season of collection, a regime of winter occupation was established for the site.

There are a number of limitations and cautions that must be exercised when interpreting these records, including an acknowledgement of

the uncertainties that may be inherent within a particular species' paleoclimate record (e.g. Bailey et al. 1983) or the potential impacts of diagenesis and human treatments of shells (e.g. Gaffey et al. 1991; Collins 2012; Loftus 2015). However, since the early work of Shackleton (1973), several studies have used sclerochronological methods to examine bivalves from various midden locations to inform archaeological and anthropological records of human occupation of the landscape, including the seasonality of site usage (e.g. Andrus and Crowe 2000; Killingley 1981) the intensity of shellfish collection and resource dependence and/or diversity (e.g. Deith 1986; Kennett and Voorhies 1996; Walker and Surge 2006; Brockwell et al. 2013; Eerkens et al. 2013) foraging distances and modes of travel to conduct shellfish collection (Andrus and Thompson 2012) and even the response of early European settlers in Virginia, USA, to conditions of drought (Harding et al. 2010).

1.5. Records of other environmental events

Sclerochronological approaches have been used to document other environmental events beyond climatic regimes. A significant area of focus is using the shells to assess levels of environmental pollution, as signals of environmental heavy metal contamination can be preserved in the shell as the animal grows (e.g. Jeffree et al. 1995; Al-Aasm et al. 1998; Brown et al. 2005; Daka 2005; Schöne et al. 2016). Other forms of pollution, such as eutrophication, can also be assessed (e.g. Kirby and Miller 2005).

Signals of marine upwelling events have been interpreted from the shells of *Donax gouldii* (Hatch et al. 2013) and *Mytilus californianus* (Killingley and Berger 1979). Events pertaining to aquatic and marine productivity such as phytoplankton blooms have been inferred from trace

element ratios with bivalve shells, such as Li/Ca in *Pecten maximus* (Thébault and Chauvaud 2013) Ba/Ca in *Saxidomus giganteus* (Gillikin et al. 2008) and Ba/Ca and $\delta^{13}C$ in *Crassostrea gigas* (Goodwin et al 2013).

Sclerochronological studies also extend to the investigation of the incursion of the invasive species *Crassostrea gigas* into the Bay of San Francisco (Goodwin et al. 2010). Assessments of hydrological regimes have also been conducted, for example, Schöne et al (2003) examined the impact of dam construction upon stream dynamics by analysing shells of *Chione cortezi* and *Chione fluctifraga* and Walther and Rowley (2013) used the shell records of *Crassostrea virginica* to investigate the flood and drought dynamics of an estuary in New Mexico.

1.6. The Australian context

However, amidst this extensive array of research pertaining to both modern day calibrations of environmentally-influenced geochemical signals in various different bivalves is a stark lack of studies pertaining to Australian species.

There have been a number of unpublished student theses on various freshwater mussel species, including the work on freshwater mussels *Alathyria pertexta* and *Velesunio wilsonii* (Durand 2002) *Alathyria spp.* (Prendergast 2004) and analysis of the estuarine cockle *Anadara trapezia* by Singh (2012) the bivalve *Polymesoda coaxans* by Hinton (2012) and a study of Holocene climate variability using bivalves from the Coorong region in South Australia (Chamberlayne 2016). Twaddle (2016) examined shells from Aboriginal middens in northern Australia, using sclerochronological techniques to infer Aboriginal site occupation patterns.

Published work includes a study of the incorporation of lead in the shell of the Ayokya pearl oyster, *Pinctada imbricata* (MacFarlane et al 2006) and a single study that examines the isotopic signals within shells at midden sites in tropical northern Australia (Brockwell et al. 2013).

This thesis begins to fill this gap, focusing primarily on two species of oyster endemic to Australia: *Ostrea angasi* (flat oyster or mud oyster) and *Saccostrea glomerata* (Sydney rock oyster). Through year-long *in-situ* field culturing experiments, in which water temperature and other chemical parameters were measured, the stable oxygen isotope records of shells of *O. angasi* and the Mg/Ca of *S. glomerata* were assessed as potential temperature proxies. The field culturing experiments were conducted at three locations along the east coast of Australia: Little Swanport estuary, Tasmania, Pambula Lake estuary, south coast of New South Wales, and Moreton Bay, southern Queensland.

Ostrea angasi was selected as it occurs over a wide range of temperatures along the east coast of Australia, from Tasmania to New South Wales. Selection of field culturing sites close to the southern (Little Swanport) and northern (Pambula Lake) extents of the species enabled the coverage of a broad temperature range. The $\delta^{18}O_{shell}$-temperature relationship was calibrated for *O. angasi*, (Chapter 2) and then this calibration was applied to shells sourced from an Aboriginal midden site on the Pambula River, to test the viability of using the calibration to make paleoclimate interpretations (Chapter 3).

Similarly, the Mg/Ca-temperature relationship was calibrated for specimens of *S. glomerata* (Chapter 4). This oyster was grown at both the Pambula Lake and Moreton Bay locations, which represent locations close

to the southern (Pambula Lake) and northern (Moreton Bay) extent of this species, again enabling the experiments to cover as broad a temperature range as possible. This relationship was then applied to a number of shells from a midden site located on the shore of Moreton Bay (Chapter 5).

The Mg/Ca-temperature relationship within the shell of the common blue mussel *Mytilus galloprovincialis* was also examined through *in situ* culturing experiments, at Little Swanport and Pambula Lake. This study contributes to the existing body of literature regarding sclerochronological analysis of various *Mytilus* species which span an essentially global distribution and is the first study of *Mytilus* within an Australian context (Chapter 6).

These bivalve species offer a unique means to probe past marine and near-shore environmental conditions. The high-resolution seasonal nature of the records they yield, along with the range of temperatures and latitudes they inhabit make them an ideal option for sclerochronological studies.

Furthermore, Australia has a wealth of Aboriginal midden sites, which are testament to the rich and enduring culture that has experienced and adapted to changes in climate long before Europeans settled the Australian continent. Midden sites are found along the entire coastline of eastern Australia, replete with shells of both *O. angasi* and *S. glomerata* (e.g. Bailey 1975; Sullivan 1982; Nell 2001). The application of these calibrations to a greater number of shells sourced from midden sites along the eastern Australian coast has the potential to provide valuable records and insights into climatic variation in eastern Australia during the late Holocene period. This is all the more valuable considering the current scarcity of high-resolution Holocene records for the Australian region. The

contribution analysis midden shell sclerochronological analysis can make to improving understandings of past human-environment interactions is also significant. It provides a clear avenue for multi-disciplinary work that will bolster our knowledge of the social and environmental history of the Australian continent, and particularly its coastal margins, during the Holocene.

1.7. References

Al-Aasm, I. S., Clarke, J. D., & Fryer, B. J. (1998). Stable isotopes and heavy metal distribution in *Dreissena polymorpha* (Zebra mussels) from western basin of Lake Erie, Canada. *Environmental Geology*, 33(2-3), 122-129.

Andrus, C. F. T., & Crowe, D. E. (2000). Geochemical analysis of *Crassostrea virginica* as a method to determine season of capture. *Journal of Archaeological Science*, 27(1), 33-42.

Andrus, C. F. T. (2011). Shell midden sclerochronology. *Quaternary Science Reviews*, 30(21-22), 2892-2905. doi:10.1016/j.quascirev.2011.07.016

Andrus, C. F. T., & Thompson, V. D. (2012). Determining the habitats of mollusk collection at the Sapelo Island shell ring complex, Georgia, USA using oxygen isotope sclerochronology. *Journal of Archaeological Science*, 39(2), 215-228. doi:10.1016/j.jas.2011.08.002

Augustin, L., Barbante, C., Barnes, P. R. F., Barnola, J. M., Bigler, M., Castellano, E., Epica Community Members (2004). Eight glacial cycles from an Antarctic ice core. *Nature*, 429(6992), 623-628. doi:10.1038/nature02599

Ayling, B. F., Chappell, J., Gagan, M. K., & McCulloch, M. T. (2015). ENSO variability during MIS 11(424-374 ka) from *Tridacna gigas* at Huon Peninsula, Papua New Guinea. *Earth and Planetary Science Letters*, 431, 236-246. doi:10.1016/j.epsl.2015.09.037

Bailey, G. N., Deith, M. R., & Shackleton, N. J. (1983). Oxygen-isotope analysis and seasonality determinations - limits and potential of a new technique. *American Antiquity*, 48(2), 390-398.

Bath, G. E., Thorrold, S. R., Jones, C. M., Campana, S. E., McLaren, J. W., & Lam, J. W. H. (2000). Strontium and barium uptake in aragonitic otoliths of marine fish. *Geochimica Et Cosmochimica Acta*, 64(10), 1705-1714. doi:10.1016/s0016-7037(99)00419-6

Beirne, E. C., Wanamaker, A. D., & Feindel, S. C. (2012). Experimental validation of environmental controls on the delta C-13 of *Arctica islandica* (ocean quahog) shell carbonate. *Geochimica Et Cosmochimica Acta*, 84, 395-409. doi:10.1016/j.gca.2012.01.021

Bice, K. L., Arthur, M. A., & Marincovich, L. (1996). Late Paleocene Arctic Ocean shallow-marine temperatures from mollusc stable isotopes. *Paleoceanography*, 11(3), 241-249.

Bohm, F., Joachimski, M. M., Dullo, W. C., Eisenhauer, A., Lehnert, H., Reitner, J., & Worheide, G. (2000). Oxygen isotope fractionation in marine aragonite of coralline sponges. *Geochimica Et Cosmochimica Acta*, 64(10), 1695-1703.

Bookhagen, B., Thiede, R. C., & Strecker, M. R. (2005). Late Quaternary intensified monsoon phases control landscape evolution in the northwest Himalaya. *Geology*, 33(2), 149-152. doi:10.1130/g20982.1

Borner, N., De Baere, B., Yang, Q. C., Jochum, K. P., Frenzel, P., Andreae, M. O., & Schwalb, A. (2013). Ostracod shell chemistry as proxy for paleoenvironmental change. *Quaternary International*, 313, 17-37. doi:10.1016/j.quaint.2013.09.041

Bougeois, L., de Rafelis, M., Reichart, G. J., de Nooijer, L. J., Nicollin, F., & Dupont-Nivet, G. (2014). A high resolution study of trace elements and stable isotopes in oyster shells to estimate Central Asian Middle Eocene seasonality. *Chemical Geology*, 363, 200-212. doi:10.1016/j.chemgeo. 2013.10.037

Brigaud, B., Puceat, E., Pellenard, P., Vincent, B., & Joachimski, M. M. (2008). Climatic fluctuations and seasonality during the Late Jurassic (Oxfordian-Early Kimmeridgian) inferred from delta O-18 of Paris Basin oyster shells. *Earth and Planetary Science Letters*, 273(1-2), 58-67. doi:10.1016/j.epsl.2008.06.015

Brockwell, S., Marwick, B., Bourke, P., Faulkner, P., & Willan, R. (2013). Late Holocene Climate Change and Human Behavioural Variability in the Coastal Wet-Dry Tropics of Northern Australia: Evidence from a pilot study of oxygen isotopes in marine bivalve shells from archaeological sites. *Australian Archaeology* 76, 21-33.

Brown, M. E., Kowalewski, M., Neves, R. J., Cherry, D. S., & Schreiber, M. E. (2005). Freshwater mussel shells as environmental chronicles: Geochemical and taphonomic signatures of mercury-related extirpations in the North Fork Holston River, Virginia. *Environmental Science & Technology*, 39(6), 1455-1462. doi:10.1021/es048573p

Buskirk, B. L., Bourgeois, J., Meyer, H. W., & Nesbitt, E. A. (2016).

Freshwater molluscan fauna from the Florissant Formation, Colorado: paleohydrologic reconstruction of a latest Eocene lake. *Canadian Journal of Earth Sciences*, 53(6), 630-643. doi:10.1139/cjes-2015-0168

Butler, P. G., Wanamaker, A. D., Scourse, J. D., Richardson, C. A., & Reynolds, D. J. (2013). Variability of marine climate on the North Icelandic Shelf in a 1357-year proxy archive based on growth increments in the bivalve *Arctica islandica*. *Palaeogeography Palaeoclimatology Palaeoecology,* 373, 141-151. doi:10.1016/j.palaeo.2012.01.016

Campana, S. E. (1999). Chemistry and composition of fish otoliths: pathways, mechanisms and applications. *Marine Ecology Progress Series*, 188, 263-297. doi:10.3354/meps188263

Carré, M., Bentaleb, I., Bruguier, O., Ordinola, E., Barrett, N. T., & Fontugne, M. (2006). Calcification rate influence on trace element concentrations in aragonitic bivalve shells: Evidences and mechanisms. *Geochimica Et Cosmochimica Acta,* 70(19), 4906-4920.

Carré, M., Sachs, J. P., Purca, S., Schauer, A. J., Braconnot, P., Falcon, R. A., Julien, M. & Lavallee, D. (2014). Holocene history of ENSO variance and asymmetry in the eastern tropical Pacific. *Science,* 345(6200), 1045-1048. doi:10.1126/science.1252220

Cespuglio, G., Piccinetti, C., & Longinelli, A. (1999). Oxygen and carbon isotope profiles from *Nassa mutabilis* shells (Gastropoda): accretion rates and biological behaviour. *Marine Biology*, 135(4), 627-634.

Chamberlayne, B. (2016). *Late Holocene seasonal and multicentennial hydroclimate variability in the Coorong Lagoon, South Australia: evidence from stable isotopes and trace element profiles of bivalve molluscs.* (Bachelor of Science (Hons)), University of Adelaide, Adelaide.

Chinzei, K., Koike, H., Oba, T., Matsushima, Y., & Kitazato, H. (1987). Secular changes in the oxygen isotope ratios of mollusk shells during the Holocene of Central Japan. *Palaeogeography Palaeoclimatology Palaeoecology,* 61(1-2), 155-166.

Cobb, K. M., Westphal, N., Sayani, H. R., Watson, J. T., Di Lorenzo, E., Cheng, H., Edwards, R. L., & Charles, C. D. (2013). Highly Variable El Nino-Southern Oscillation Throughout the Holocene. Science, 339(6115), 67-70. doi:10.1126/science.1228246

Collins, J. D. (2012). Assessing mussel shell diagenesis in the modern vadose zone at Lyon's Bluff (22OK520), Northeast Mississippi. *Journal of Archaeological Science, 39*(12), 3694-3705. doi:10.1016/j.jas.2012.06.012

Cook, E. R., Buckley, B. M., D'Arrigo, R. D., & Peterson, M. J. (2000). Warm-season temperatures since 1600 BC reconstructed from Tasmanian tree rings and their relationship to large-scale sea surface temperature anomalies. *Climate Dynamics,* 16(2-3), 79-91. doi:10.1007/s003820050006

Crippa, G., Angiolini, L., Bottini, C., Erba, E., Felletti, F., Frigerio, C., Hennisen, J. A. I., Leng, M. J., Petrizzo, M. R., Raffi, I., Raineri, G., & Stephenson, M. H. (2016). Seasonality fluctuations recorded in fossil bivalves during the early Pleistocene: Implications for climate change. *Palaeogeography Palaeoclimatology Palaeoecology*, 446, 234-251. doi:10.1016/j.palaeo.2016.01.029

Daka, E. R. (2005). Heavy metal concentrations in *Littorina saxatilis* and *Enteromorpha intestinalis* from Manx Estuaries. *Marine Pollution Bulletin,* 50(11), 1451-1456.

De Deckker, P., Chivas, A. R., & Shelley, J. M. G. (1999). Uptake of Mg and Sr in the euryhaline ostracod *Cyprideis* determined from in vitro experiments. *Palaeogeography Palaeoclimatology Palaeoecology*, 148(1-3), 105-116. doi:10.1016/s0031-0182(98)00178-3

Deith, M. R. (1986). Subsistence strategies at a Mesolithic camp site - evidence from stable isotope analyses of shells. *Journal of Archaeological Science,* 13(1), 61-78.

Dettman, D. L., Kohn, M. J., Quade, J., Ryerson, F. J., Ojha, T. P., & Hamidullah, S. (2001). Seasonal stable isotope evidence for a strong Asian monsoon throughout the past 10.7 m.y. *Geology,* 29(1), 31-34. doi:10.1130/0091-7613(2001)029<0031:ssiefa>2.0.co;2

Driscoll, R., Elliot, M., Russon, T., Welsh, K., Yokoyama, Y., & Tudhope, A. (2014). ENSO reconstructions over the past 60 ka using giant clams (*Tridacna* sp.) from Papua New Guinea. *Geophysical Research Letters,* 41(19), 6819-6825. doi:10.1002/2014gl061446

Dutton, A. L., Lohmann, K. C., & Zinsmeister, W. J. (2002). Stable isotope and minor element proxies for Eocene climate of Seymour Island,

Antarctica. *Paleoceanography,* 17(2). doi:10.1029/2000pa000593

Eerkens, J. W., Byrd, B. F., Spero, H. J., & Fritschi, A. K. (2013). Stable isotope reconstructions of shellfish harvesting seasonality in an estuarine environment: implications for Late Holocene San Francisco Bay settlement patterns. *Journal of Archaeological Science,* 40(4), 2014-2024. doi:10.1016/j.jas.2012.12.018

Elliot, M., Welsh, K., Chilcott, C., McCulloch, M., Chappell, J., & Ayling, B. (2009). Profiles of trace elements and stable isotopes derived from giant long-lived *Tridacna gigas* bivalves: Potential applications in paleoclimate studies. *Palaeogeography Palaeoclimatology Palaeoecology,* 280(1-2), 132-142. doi:10.1016/j.palaeo.2009.06.007

Emiliani, C. (1955). Pleistocene temperatures. *Journal of Geology,* 63(6), 538-578.

Epstein, S., Buchsbaum, R., Lowenstam, H., & Urey, H. C. (1951). Carbonate-water isotopic temperature scale. *Geological Society of America Bulletin,* 62(4), 417-426. doi:10.1130/0016-7606(1951)62[417:cits]2.0.co;2

Epstein, S., Buchsbaum, R., Lowenstam, H. A., & Urey, H. C. (1953). Revised carbonate-water isotopic temperature scale. *Bulletin of the Geological Society of America,* 64, 1315-1326.

Fairchild, I. J., & Treble, P. C. (2009). Trace elements in speleothems as recorders of environmental change. *Quaternary Science Reviews,* 28(5-6), 449-468. doi:10.1016/j.quascirev.2008.11.007

Freitas, P., Clarke, L. J., Kennedy, H., Richardson, C., & Abrantes, F. (2005). Mg/Ca, Sr/Ca, and stable-isotope (delta O-18 and delta C-13) ratio profiles from the fan mussel *Pinna nobilis*: Seasonal records and temperature relationships. *Geochemistry Geophysics Geosystems,* 6. doi:10.1029/2004gc000872

Freitas, P. S., Clarke, L. J., Kennedy, H., & Richardson, C. A. (2009). Ion microprobe assessment of the heterogeneity of Mg/Ca, Sr/Ca and Mn/Ca ratios in *Pecten maximus* and *Mytilus edulis* (bivalvia) shell calcite precipitated at constant temperature. *Biogeosciences,* 6(7), 1209-1227.

Freitas, P. S., Clarke, L. J., Kennedy, H., & Richardson, C. A. (2012). The potential of combined Mg/Ca and delta O-18 measurements within the shell of the bivalve *Pecten maximus* to estimate seawater delta O-18

composition. *Chemical Geology,* 291, 286-293. doi:10.1016/j.chemgeo.2011.10.023

Gaffey, S. J., Kolak, J. J., & Bronnimann, C. E. (1991). Effects of drying, heating, annealing, and roasting on carbonate skeletal material, with geochemical and diagenetic implications. *Geochimica Et Cosmochimica Acta,* 55(6), 1627-1640.

Gajurel, A. P., France-Lanord, C., Huyghe, P., Guilmette, C., & Gurung, D. (2006). C and O isotope compositions of modem fresh-water mollusc shells and river waters from the Himalaya and Ganga plain. *Chemical Geology,* 233(1-2), 156-183.

Gillikin, D. P., Lorrain, A., Paulet, Y. M., Andre, L., & Dehairs, F. (2008). Synchronous barium peaks in high-resolution profiles of calcite and aragonite marine bivalve shells. *Geo-Marine Letters,* 28(5-6), 351-358. doi:10.1007/s00367-008-0111-9

Goodwin, D. H., Cohen, A. N., & Roopnarine, P. D. (2010). Forensics on the half shell: a sclerochronological investigation of a modern biological invasion in San Francisco Bay, United States. *Palaios,* 25(11-12), 742-753. doi:10.2110/palo.2010.p10-015r

Goodwin, D. H., Gillikin, D. P., & Roopnarine, P. D. (2013). Preliminary evaluation of potential stable isotope and trace element productivity proxies in the oyster *Crassostrea gigas*. *Palaeogeography Palaeoclimatology Palaeoecology,* 373, 88-97. doi:10.1016/j.palaeo.2012.03.034

Halfar, J., Steneck, R. S., Joachimski, M., Kronz, A., & Wanamaker, A. D. (2008). Coralline red algae as high-resolution climate recorders. *Geology,* 36(6), 463-466. doi:10.1130/g24635a.1

Hallmann, N., Burchell, M., Brewster, N., Martindale, A., & Schöne, B. R. (2013). Holocene climate and seasonality of shell collection at the Dundas Islands Group, northern British Columbia, Canada—A bivalve sclerochronological approach. *Palaeogeography, Palaeoclimatology, Palaeoecology,* 373(0), 163-172. doi:http://dx.doi.org/10.1016/j.palaeo.2011.12.019

Hallmann, N., Schone, B. R., Strom, A., & Fiebig, J. (2008). An intractable climate archive - Sclerochronological and shell oxygen isotope analyses of the Pacific geoduck, *Panopea abrupta* (bivalve mollusk) from

Protection island (Washington State, USA). *Palaeogeography Palaeoclimatology Palaeoecology*, 269(1-2), 115-126. doi:10.1016/j.palaeo.2008.08.010

Harding, J. M., Spero, H. J., Mann, R., Herbert, G. S., & Sliko, J. L. (2010). Reconstructing early 17th century estuarine drought conditions from Jamestown oysters. *Proceedings of the National Academy of Sciences of the United States of America*, 107(23), 10549-10554. doi:10.1073/pnas.1001052107

Hatch, M. B. A., Schellenberg, S. A., & Carter, M. L. (2013). Ba/Ca variations in the modern intertidal bean clam *Donax gouldii*: An upwelling proxy? *Palaeogeography Palaeoclimatology Palaeoecology*, 373, 98-107. doi:10.1016/j.palaeo.2012.03.006

Henderson, G. M. (2002). New oceanic proxies for paleoclimate. *Earth and Planetary Science Letters*, 203(1), 1-13. doi:10.1016/s0012-821x(02)00809-9

Hendry, J. P., & Kalin, R. M. (1997). Are oxygen and carbon isotopes of mollusc shells reliable palaeosalinity indicators in marginal marine environments? A case study from the Middle Jurassic of England. *Journal of the Geological Society*, 154, 321-333.

Hinton, J. (2012). *Life in a Shell: Using Archaeological Shell Assemblages for Paleoenvironmental Reconstruction: Preliminary Isotope Analysis of Polymesoda (Gelonia) coaxans (Gmelin, 1791) from Bentinck Island, Gulf of Carpentaria.* (Bachelor of Arts (Hons)), The University of Queensland, Brisbane.

Hufthammer, A. K., Hoie, H., Folkvord, A., Geffen, A. J., Andersson, C., & Ninnemann, U. S. (2010). Seasonality of human site occupation based on stable oxygen isotope ratios of cod otoliths. *Journal of Archaeological Science*, 37(1), 78-83. doi:10.1016/j.jas.2009.09.001

Jeffree, R. A., Markich, S. J., Lefebvre, F., Thellier, M., & Ripoll, C. (1995). Shell microlaminations of the fresh-water bivalve *Hyridella depressa* as an archival monitor of manganese water concentration - experimental investigation by depth profiling using secondary-ion mass-spectrometry (SIMS). *Experientia*, 51(8), 838-848. doi:10.1007/bf01922440

Jones, D. S., Quitmyer, I. R., & Andrus, C. F. T. (2005). Oxygen isotopic

evidence for greater seasonality in Holocene shells of *Donax variabilis* from Florida. *Palaeogeography Palaeoclimatology Palaeoecology*, 228(1-2), 96-108. doi:10.1016/j.palaeo.2005.03.046

Jouzel, J., Masson-Delmotte, V., Cattani, O., Dreyfus, G., Falourd, S., Hoffmann, G., Minster, B., Nouet, J., Barnola, J. M., Chappellaz, J., Fischer, H., Gallet, J. C., Johnsen, S., Leuenberger, M., Loulergue, L., Luethi, D., Oerter, H., Parrenin, F., Raisbeck, G., Raynaud, D., Schilt, A., Schwander, J., Selmo, E., Souchez, R., Spahni, R., Stauffer, B., Steffensen, J. P., Stenni, B., Stocker, T. F., Tison, J. L., Werner, M., & Wolff, E. W. (2007). Orbital and millennial Antarctic climate variability over the past 800,000 years. Science, 317(5839), 793-796. doi:10.1126/science.1141038

Kaandorp, R. J. G., Wesselingh, F. P., & Vonhof, H. B. (2006). Ecological implications from geochemical records of Miocene Western Amazonian bivalves. *Journal of South American Earth Sciences,* 21(1-2), 54-74.

Kadar, E., & Costa, V. (2006). First report on the micro-essential metal concentrations in bivalve shells from deep-sea hydrothermal vents. *Journal of Sea Research, 56*(1), 37-44. doi:10.1016/j.seares.2006.01.001

Kawamura, K., Parrenin, F., Lisiecki, L., Uemura, R., Vimeux, F., Severinghaus, J. P., Hutterli, M. A., Nakazawa, T., Aoki, S., Jouzel, J., Raymo, M. E., Matsumoto, K., Nakata, H., Motoyama, H., Fujita, S., Goto-Azuma, K., Fujii, Y., & Watanabe, O. (2007). Northern Hemisphere forcing of climatic cycles in Antarctica over the past 360,000 years. Nature, 448(7156), 912-U914. doi:10.1038/nature06015

Kennedy, H., Richardson, C. A., Duarte, C. M., & Kennedy, D. P. (2001). Oxygen and carbon stable isotopic profiles of the fan mussel, *Pinna nobilis*, and reconstruction of sea surface temperatures in the Mediterranean. *Marine Biology*, 139(6), 1115-1124.

Kennett, D. J., & Voorhies, B. (1996). Oxygen isotopic analysis of archaeological shells to detect seasonal use of wetlands on the southern Pacific coast of Mexico. *Journal of Archaeological Science,* 23(5), 689-704.

Killingley, J. S. (1981). Seasonality of mollusk collecting determined from O-18 profiles of midden shells. *American Antiquity*, 46(1), 152-158.

Killingley, J. S., & Berger, W. H. (1979). Stable isotopes in a mollusk shell

- detection of upwelling events. *Science, 205*(4402), 186-188.

Kirby, M. X. (2000). Paleoecological differences between tertiary and Quaternary *Crassostrea* oysters, as revealed by stable isotope sclerochronology. *Palaios,* 15(2), 132-141.

Kirby, M. X., & Miller, H. M. (2005). Response of a benthic suspension feeder (*Crassostrea virginica* Gmelin) to three centuries of anthropogenic eutrophication in Chesapeake Bay. *Estuarine Coastal and Shelf Science,* 62(4), 679-689.

Kirby, M. X., Soniat, T. M., & Spero, H. J. (1998). Stable isotope sclerochronology of pleistocene and recent oyster shells (*Crassostrea virginica*). *Palaios,* 13(6), 560-569.

Klein, R. T., Lohmann, K. C., & Thayer, C. W. (1996). Bivalve skeletons record sea-surface temperature and delta O-18 via Mg/Ca and O-18/O-16 ratios. *Geology,* 24(5), 415-418.

Koutavas, A., Lynch-Stieglitz, J., Marchitto, T. M., & Sachs, J. P. (2002). El Nino-like pattern in ice age tropical Pacific sea surface temperature. *Science,* 297(5579), 226-230. doi:10.1126/science.1072376

Lazareth, C. E., Le Cornec, F., Candaudap, F., & Freydier, R. (2013). Trace element heterogeneity along isochronous growth layers in bivalve shell: Consequences for environmental reconstruction. *Palaeogeography Palaeoclimatology Palaeoecology,* 373, 39-49. doi:10.1016/j.palaeo. 2011.04.024

Lisiecki, L. E., & Raymo, M. E. (2005). A Pliocene-Pleistocene stack of 57 globally distributed benthic delta O-18 records. *Paleoceanography,* 20(1). doi:10.1029/2004pa001071

Loftus, E., Rogers, K., & Lee-Thorp, J. (2015). A simple method to establish calcite: aragonite ratios in archaeological mollusc shells. *Journal of Quaternary Science,* 30(8), 731-735. doi:10.1002/jqs.2819

Lotter, A. F., Eicher, U., Siegenthaler, U., & Birks, H. J. B. (1992). Late-glacial climatic oscillations as recorded in Swiss lake-sediments. *Journal of Quaternary Science, 7*(3), 187-204.

MacFarlane, G. R., Markich, S. J., Linz, K., Gifford, S., Dunstan, R. H., O'Connor, W., & Russell, R. A. (2006). The Akoya pearl oyster shell as an archival monitor of lead exposure. *Environmental Pollution,* 143(1), 166-173. doi:10.1016/j.envpol.2005.10.042

Marchais, V., Richard, J., Jolivet, A., Flye-Sainte-Marie, J., Thebault, J., Jean, F., Richard, P., Paulet, Y. M., Clavier, J., & Chauvaud, L. (2015). Coupling experimental and field-based approaches to decipher carbon sources in the shell of the great scallop, *Pecten maximus* (L.). *Geochimica Et Cosmochimica Acta*, 168, 58-69. doi:10.1016/j.gca.2015.07.010

Marchitto, T. M., Jones, G. A., Goodfriend, G. A., & Weidman, C. R. (2000). Precise temporal correlation of Holocene mollusk shells using sclerochronology. *Quaternary Research*, 53(2), 236-246.

Martinez-Ruiz, E., Kastner, M., Gallego-Torres, D., Rodrigo-Gamiz, M., Nieto-Moreno, V., & Ortega-Huertas, M. (2015). Paleoclimate and paleoceanography over the past 20,000 yr in the Mediterranean Sea Basins as indicated by sediment elemental proxies. *Quaternary Science Reviews*, 107, 25-46. doi:10.1016/j.quascirev.2014.09.018

Mazzullo, S. J., Boardman, D. R., Grossman, E. L., & Dimmick-Wells, K. (2007). Oxygen-carbon isotope stratigraphy of upper Carboniferous to lower Permian marine deposits in midcontinent USA (Kansas and NE Oklahoma): Implications for sea water chemistry and depositional cyclicity. *Carbonates and Evaporites*, 22(1), 55-72.

Miller, G. H., & Fogel, M. L. (2016). Calibrating delta O-18 in *Dromaius novaehollandiae* (emu) eggshell calcite as a paleo-aridity proxy for the Quaternary of Australia. *Geochimica Et Cosmochimica Acta*, 193, 1-13. doi:10.1016/j.gca.2016.08.004

Nutzel, A., Joachimski, M., & Lopez Correa, M. (2010). Seasonal climatic fluctuations in the Late Triassic tropics - High-resolution oxygen isotope records from aragonitic bivalve shells (Cassian Formation, Northern Italy). *Palaeogeography Palaeoclimatology Palaeoecology*, 285(3-4), 194-204. doi:10.1016/j.palaeo.2009.11.011

Owen, R., Kennedy, H., & Richardson, C. (2002). Experimental investigation into partitioning of stable isotopes between scallop (*Pecten maximus*) shell calcite and sea water. *Palaeogeography Palaeoclimatology Palaeoecology*, 185(1-2), 163-174.

Poulain, C., Gillikin, D. P., Thebault, J., Munaron, J. M., Bohn, M., Robert, R., Paulet, Y. M., & Lorrain, A. (2015). An evaluation of Mg/Ca, Sr/Ca, and Ba/Ca ratios as environmental proxies in aragonite bivalve shells. *Chemical Geology*, 396, 42-50. doi:10.1016/j.chemgeo.2014.12.019

Prendergast, A. L. (2004). *Late Quaternary environments of the Murray River valley in northwestern Victoria.* (Bachelor of Science, (Hons)), The University of Melbourne, Melbourne.

Prendergast, A. L., Stevens, R. E., O'Connell, T. C., Hill, E. A., Hunt, C. O., & Barker, G. W. (2016). A late Pleistocene refugium in Mediterranean North Africa? Palaeoenvironmental reconstruction from stable isotope analyses of land snail shells (Haua Fteah, Libya). *Quaternary Science Reviews,* 139, 94-109. doi:10.1016/j.quascirev.2016.02.014

Roark, A., Grossman, E. L., & Lebold, J. (2016). Low seasonality in central equatorial Pangea during a late Carboniferous highstand based on high-resolution isotopic records of brachiopod shells. *Geological Society of America Bulletin,* 128(3-4), 597-608. doi:10.1130/b31330.1

Romans, B. W., & Graham, S. A. (2013). A Deep-Time Perspective of Land-Ocean Linkages in the Sedimentary Record. *Annual Review of Marine Science,* 5(5), 69-94. doi:10.1146/annurev-marine-121211-172426

Sabin, A. L., & Pisias, N. G. (1996). Sea surface temperature changes in the northeastern Pacific Ocean during the past 20,000 years and their relationship to climate change in northwestern North America. *Quaternary Research*, 46(1), 48-61. doi:10.1006/qres.1996.0043

Schöne, B. R., Fiebig, J., Pfeiffer, M., Gless, R., Hickson, J., Johnson, A. L. A., Dreyer, W., & Oschmann, W. (2005). Climate records from a bivalved Methuselah (*Arctica islandica*, Mollusca; Iceland). Palaeogeography Palaeoclimatology Palaeoecology, 228(1-2), 130-148.

Schöne, B. R., Flessa, K. W., Dettman, D. L., & Goodwin, D. H. (2003). Upstream dams and downstream clams: growth rates of bivalve mollusks unveil impact of river management on estuarine ecosystems (Colorado River Delta, Mexico). *Estuarine Coastal and Shelf Science,* 58(4), 715-726. doi:10.1016/s0272-7714(03)00175-6

Schöne, B. R., & Gillikin, D. P. (2013). Unraveling environmental histories from skeletal diaries - Advances in sclerochronology. *Palaeogeography Palaeoclimatology Palaeoecology,* 373, 1-5. doi:10.1016/j.palaeo.2012.11.026

Schöne, B. R., & Krause, R. A. (2016). Retrospective environmental biomonitoring - Mussel Watch expanded. *Global and Planetary Change*, 144, 228-251. doi:10.1016/j.gloplacha.2016.08.002

Schöne, B. R., Oschmann, W., Tanabe, K., Dettman, D., Fiebig, J., Houk, S. D., & Kanie, Y. (2004). Holocene seasonal environmental trends at Tokyo Bay, Japan, reconstructed from bivalve mollusk shells - implications for changes in the East Asian monsoon and latitudinal shifts of the Polar Front. *Quaternary Science Reviews*, 23(9-10), 1137-1150.

Schöne, B. R., Zhang, Z., Jacob, D., Gillikin, D. P., Tutken, T., Garbe-Schonberg, D., McConnaughey, T, & Soldati, A. (2010). Effect of organic matrices on the determination of the trace element chemistry (Mg, Sr, Mg/Ca, Sr/Ca) of aragonitic bivalve shells (*Arctica islandica*)-Comparison of ICP-OES and LA-ICP-MS data. *Geochemical Journal*, 44(1), 23-37.

Schöne, B. R., Zhang, Z. J., Radermacher, P., Thebault, J., Jacob, D. E., Nunn, E. V., & Maurer, A. F. (2011). Sr/Ca and Mg/Ca ratios of ontogenetically old, long-lived bivalve shells (Arctica islandica) and their function as paleotemperature proxies. *Palaeogeography Palaeoclimatology Palaeoecology*, 302(1-2), 52-64. doi:10.1016/j.palaeo.2010.03.016

Schöne, B., & Surge, D. (2014). Bivalve shells: ultra-high resolution paleoclimate archives. *PAGES magazine*, 22(1), 20-21.

Schöne, B. R., Radermacher, P., Zhang, Z., & Jacob, D. E. (2013). Crystal fabrics and element impurities (Sr/Ca, Mg/Ca, and Ba/Ca) in shells of *Arctica islandica*—Implications for paleoclimate reconstructions. *Palaeogeography, Palaeoclimatology, Palaeoecology*, 373(0), 50-59. doi:http://dx.doi.org/10.1016/j.palaeo.2011.05.013

Shackleton, N. J. (1973). Oxygen isotope analysis as a means of determining season of occupation of prehistoric midden sites. *Archaeometry*, 15(1), 133-141.

Shackleton, N. J., & Opdyke, N. D. (1973). Stable oxygen isotope analysis on sediment core V28-238. In Supplement to: Shackleton, NJ; Opdyke, ND (1973): Oxygen isotope and paleomagnetic stratigraphy of equatorial Pacific Core V28-238: oxygen isotope temperatures and ice volume on a 105 year and 106 year scale. *Quaternary Research*, 3, 39-55,

doi:10.1016/0033-5894(73)90052-5: PANGAEA.

Singh, D. (2012). *Palaeoenvironmental reconstruction of south-eastern Australia during MIS 5e and the early Holocene and comparison between present conditions using the shell geochemistry of Anadara trapezia and Katelysia spp.* (Bachelor of Science (Hons)), The Australian National University, Canberra.

Steuber, T. (1999). Isotopic and chemical intra-shell variations in low-Mg calcite of rudist bivalves (Mollusca-Hippuritacea): disequilibrium fractionations and late Cretaceous seasonality. *International Journal of Earth Sciences,* 88(3), 551-570.

Strasser, C. A., Mullineaux, L. S., & Walther, B. D. (2008). Growth rate and age effects on *Mya arenaria* shell chemistry: Implications for biogeochemical studies. *Journal of Experimental Marine Biology and Ecology,* 355(2), 153-163. doi:10.1016/j.jembe.2007.12.022

Surge, D., & Lohmann, K. C. (2008). Evaluating Mg/Ca ratios as a temperature proxy in the estuarine oyster, *Crassostrea virginica*. *Journal of Geophysical Research-Biogeosciences,* 113(G2). doi:G0200110.1029/ 2007jg000623

Surge, D., Lohmann, K. C., & Dettman, D. L. (2001). Controls on isotopic chemistry of the American oyster, *Crassostrea virginica*: implications for growth patterns. *Palaeogeography Palaeoclimatology Palaeoecology,* 172(3-4), 283-296.

Szymanek, M. (2016). Stable isotope composition of the Holsteinian (MIS 11) freshwater snail *Valvata piscinalis* (O. F. Muller, 1774) from eastern Poland and its palaeoenvironmental implications. *Journal of Quaternary Science,* 31(6), 622-630. doi:10.1002/jqs.2885

Thebault, J., & Chauvaud, L. (2013). Li/Ca enrichments in great scallop shells (*Pecten maximus*) and their relationship with phytoplankton blooms. *Palaeogeography Palaeoclimatology Palaeoecology,* 373, 108-122. doi:10.1016/j.palaeo.2011.12.014

Thebault, J., Chauvaud, L., Clavier, J., Guarini, J., Dunbar, R. B., Fichez, R., Mucciarone, D. A., & Morize, E. (2007). Reconstruction of seasonal temperature variability in the tropical Pacific Ocean from the shell of the scallop, *Comptopallium radula*. *Geochimica Et Cosmochimica Acta,* 71(4), 918-928.

Tierney, J. E., Abram, N. J., Anchukaitis, K. J., Evans, M. N., Giry, C., Kilbourne, K. H., Saenger, C. P., Wu, H. C., & Zinke, J. (2015). Tropical sea surface temperatures for the past four centuries reconstructed from coral archives. *Paleoceanography,* 30(3), 226-252. doi:10.1002/2014pa002717

Twaddle, R. (2016). *A novel application of sclerochronology: forging new understandings of Aboriginal occupation in the South Wellesley archipelago, Gulf of Carpentaria.* (PhD), James Cook University, Townsville.

Twaddle, R. W., Ulm, S., Hinton, J., Wurster, C. M., & Bird, M. I. (2016). Sclerochronological analysis of archaeological mollusc assemblages: methods, applications and future prospects. *Archaeological and Anthropological Sciences,* 8(2), 359-379. doi:10.1007/s12520-015-0228-5

Urey, H. C. (1947). The thermodynamic properties of isotopic substances. *Journal of the Chemical Society* (May), 562-581. doi:10.1039/jr9470000562

Valentine, A., Johnson, A. L. A., Leng, M. J., Sloane, H. J., & Balson, P. S. (2011). Isotopic evidence of cool winter conditions in the mid-Piacenzian (Pliocene) of the southern North Sea Basin. *Palaeogeography Palaeoclimatology Palaeoecology*, 309(1-2), 9-16. doi:10.1016/j.palaeo.2011.05.015

Versteegh, E. A. A., Black, S., Canti, M. G., & Hodson, M. E. (2013). Earthworm-produced calcite granules: A new terrestrial palaeothermometer? *Geochimica Et Cosmochimica Acta,* 123, 351-357. doi:10.1016/j.gca.2013.06.020

Versteegh, E. A. A., Blicher, M. E., Mortensen, J., Rysgaard, S., Als, T. D., & Wanamaker, A. D. (2012). Oxygen isotope ratios in the shell of *Mytilus edulis*: archives of glacier meltwater in Greenland? *Biogeosciences,* 9(12), 5231-5241. doi:10.5194/bg-9-5231-2012

Walker, K. J., & Surge, D. (2006). Developing oxygen isotope proxies from archaeological sources for the study of Late Holocene human-climate interactions in coastal southwest Florida. *Quaternary International,* 150, 3-11.

Walliser, E. O., Lohmann, G., Niezgodzki, I., Tutken, T., & Schone, B. R. (2016). Response of Central European SST to atmospheric pCO(2)

forcing during the Oligocene - A combined proxy data and numerical climate model approach. *Palaeogeography Palaeoclimatology Palaeoecology*, 459, 552-569. doi:10.1016/j.palaeo.2016.07.033

Walliser, E. O., Schone, B. R., Tutken, T., Zirkel, J., Grimm, K. I., & Pross, J. (2015). The bivalve *Glycymeris planicostalis* as a high-resolution paleoclimate archive for the Rupelian (Early Oligocene) of central Europe. *Climate of the Past*, 11(4), 653-668. doi:10.5194/cp-11-653-2015

Walther, B. D., & Rowley, J. L. (2013). Drought and flood signals in subtropical estuaries recorded by stable isotope ratios in bivalve shells. *Estuarine Coastal and Shelf Science*, 133, 235-243. doi:10.1016/j.ecss.2013.08.032

Wanamaker, A. D., Kreutz, K. J., Borns, H. W., Introne, D. S., Feindel, S., & Barber, B. J. (2006). An aquaculture-based method for calibrated bivalve isotope paleothermometry. *Geochemistry Geophysics Geosystems*, 7, 13. doi:Q09011Artn q09011

Wanamaker, A. D., Kreutz, K. J., Schone, B. R., & Introne, D. S. (2011). Gulf of Maine shells reveal changes in seawater temperature seasonality during the Medieval Climate Anomaly and the Little Ice Age. *Palaeogeography Palaeoclimatology Palaeoecology*, 302(1-2), 43-51. doi:10.1016/j.palaeo.2010.06.005

Wanamaker, A. D., Kreutz, K. J., Wilson, T., Borns, H. W., Introne, D. S., & Feindel, S. (2008). Experimentally determined Mg/Ca and Sr/Ca ratios in juvenile bivalve calcite for *Mytilus edulis*: implications for paleotemperature reconstructions. *Geo-Marine Letters*, 28(5-6), 359-368. doi:10.1007/s00367-008-0112-8

Warter, V., Muller, W., Wesselingh, F. P., Todd, J. A., & Renema, W. (2015). Late Miocene seasonal to subdecadal climate variability in the indo-west pacific (East Kalimantan, Indonesia) preserved in giant clams. *Palaios*, 30(1), 66-82. doi:10.2110/palo.2013.061

Wick, L., Lemcke, G., & Sturm, M. (2003). Evidence of Late glacial and Holocene climatic change and human impact in eastern Anatolia: high-resolution pollen, charcoal, isotopic and geochemical records from the laminated sediments of Lake Van, Turkey. *Holocene*, 13(5), 665-675. doi:10.1191/0959683603hl653rp

Wierzbowski, H., & Joachimski, M. (2007). Reconstruction of late Bajocian-Bathonian marine palaeoenvironments using carbon and oxygen isotope ratios of calcareous fossils from the Polish Jura Chain (central Poland). *Palaeogeography Palaeoclimatology Palaeoecology*, 254(3-4), 523-540.

Winkelstern, I., Surge, D., & Hudley, J. W. (2013). Multiproxy sclerochronological evidence for Plio-Pleistocene regional warmth: United States Mid-Atlantic coastal plain. *Palaios,* 28(9-10), 649-660. doi:10.2110/palo.2013.p13-010r

Wisshak, M., Lopez Correa, M., Gofas, S., Salas, C., Taviani, M., Jakobsen, J., & Freiwald, A. (2009). Shell architecture, element composition, and stable isotope signature of the giant deep-sea oyster *Neopycnodonte zibrowii* sp n. from the NE Atlantic. *Deep-Sea Research Part I-Oceanographic Research Papers,* 56(3), 374-407. doi:10.1016/ j.dsr.2008.10.002

Chapter 2

Oxygen isotope records of the Australian flat oyster (*Ostrea angasi*) as a potential temperature archive

This paper was published in *Marine Geology*, 2014, 357 pp195–209

Authors and contributions:

Sarah Tynan: 85% conceived study, conducted field work, sampling and data analysis

Bradley Opdyke 5% overarching guidance and support, feedback on written drafts

Andrea Dutton 5% overarching guidance and support, feedback on written drafts

Steven Eggins 5% overarching guidance and support, feedback on written drafts

ABSTRACT

The response of the oxygen isotope ratio ($\delta^{18}O$) in shells of the Australian native flat oyster *Ostrea angasi* to changes in water temperature has been assessed using growth experiments conducted for one year at two locations on the east coast of Australia. The analysed $\delta^{18}O$ of the oyster shells ($\delta^{18}O_{shell}$) closely follows the predicted oyster shell $\delta^{18}O$ constructed from measured $\delta^{18}O$ in the water ($\delta^{18}O_{water}$) and water temperature.

Influxes of freshwater that occur in the estuarine habitats of *O. angasi* can modify the $\delta^{18}O_{water}$, and consequently $\delta^{18}O_{shell}$. Salinity fluctuations can also cause interruptions to shell growth in this species. This can cause overestimated temperatures in *O. angasi* $\delta^{18}O_{shell}$ temperature reconstructions.

A $\delta^{18}O_{shell}$-temperature calibration was established for *O. angasi*, yielding the relationship: $T^{o}C = 13.97 - 3.57(\delta^{18}O_{shell} - \delta^{18}O_{water}) + 0.17(\delta^{18}O_{shell} - \delta^{18}O_{water})^2$, n = 79, $R^2 = 0.79$, which, within the experimental uncertainties of the data, is similar to other published biogenic carbonate paleotemperature equations.

Keywords:

Bivalve; oyster; *Ostrea angasi*; oxygen isotopes; paleotemperature

2.1. Introduction

Since the pioneering work of Epstein et al. (1951; 1953), analysis of the $\delta^{18}O$ of biogenic carbonates has become an established method for paleoenvironmental reconstruction. Provided biogenic carbonate is precipitated in isotopic equilibrium with the ambient water, its $\delta^{18}O$ will vary with fluctuations in water temperature and the $\delta^{18}O$ of the water ($\delta^{18}O_{water}$).

A wide variety of bivalve mollusc species have been investigated with respect to their potential to record climatic variation, in marine, estuarine and freshwater environments (e.g. marine: Romanek et al., 1987; Kennedy et al., 2001; Schöne et al. 2003; Chauvaud et al., 2005; Freitas et al., 2005; Schöne et al., 2005; Thébault et al., 2007; estuarine: Goodwin et al., 2001; Dettman et al., 2004; Schöne et al., 2004a; Gillikin et al., 2005; freshwater: Dettman, et al., 1999; Schöne et al., 2004b; Versteegh et al., 2011). The wide geographic distribution of bivalve species adds to their value as climate archives, as many can provide records from regions where other biogenic carbonates that can provide paleoenviromental proxies, such as corals, are not available.

Oysters, although not as widely studied in the literature as some other bivalves, have been used to both reconstruct climate regimes (Wang et al., 1995; Kirby et al., 1998; Surge et al., 2003; Brigaud et al., 2008) and contribute to archaeological investigations (Custer and Doms, 1990; Andrus and Crowe, 2000; Milner 2002; Harding et al., 2010; Andrus and Thompson, 2012).

Many previous studies have focussed upon determining whether oysters precipitate their shell in equilibrium with the ambient water, and how the $\delta^{18}O_{shell}$ correlates with temperature. Ullman et al. (2010) examined the $\delta^{18}O$ of a *Crassostrea gigas* shell from the North Sea, and concluded that this species is indeed a reliable proxy for seawater temperature, although care must be taken to ensure that temperatures of growth cessation (during summer or winter extremes) are understood to avoid misinterpretation of fossil shell temperature records. Similarly, the American oyster, *Crassostrea virginica* has been shown to precipitate its shell in isotopic equilibrium with ambient seawater (Kirby et al., 1998; Surge et al., 2001; Lécuyer et al., 2004), although it also is subject to 'heat shock', whereby these oysters cease shell precipitation during the height of summer (Kirby et al., 1998). Titschack et al., (2010) studied the giant oyster *Hyotissa hyotis*, which is found in coral reef environments, and concluded that although its $\delta^{18}O_{shell}$ reflects sea surface temperature, it specifically reflects the oyster's immediate environment, which can differ from that of the open ocean.

Other studies have used $\delta^{18}O_{shell}$ analysis of fossil or sub-fossil oyster shells, along with modern analogues, to investigate changes in climatic and environmental conditions over time. For example, Brigaud et al. (2008) interpreted information about Jurassic climate conditions from oysters from the Paris Basin. Wang et al. (1995) used the $\delta^{18}O_{shell}$ of contemporary and mid-Holocene specimens of *C. gigas* to infer environmental changes in the Bohai Bay system in the Bohai Sea, China. Similarly, specimens of *C. virginica* have been used to reconstruct Pleistocene $\delta^{18}O_{water}$ and temperature in Chesapeake Bay, USA (Kirby et al.,

1998), investigate estuary dynamics over the past 1000 years in the northwestern Ten Thousand Islands, Florida, USA (Surge et al., 2003), and the response of 17th century European settlers to conditions of drought in the Chesapeake Bay area (Harding et al., 2010).

Structural analysis, sometimes in conjunction with geochemical analysis, of oysters has been used to determine the season of death of the animal and the seasonality of use of midden (shell refuse) sites in Europe (*Ostrea edulis*: Milner, 2002), and the USA (*C. virginica*: Custer and Doms, 1990; Andrus and Crowe, 2000). Sclerochronological analysis of *C. virginica* also enabled Andrus and Thompson (2012) to analyse Archaic peoples' habitation patterns and infer the use of boats for shellfish collection on the coast of Georgia, USA. Sclerochronological analysis has also be used to investigate more recent events, such as the timing and dynamics of the invasion of the exotic *C. gigas* in San Francisco Bay, California, USA (Goodwin et al., 2010).

These diverse studies illustrate the potential of oyster shells to contribute to knowledge of past environments, from paleoclimate, archaeological and ecological perspectives. However, different species can have different optimum temperatures for growth and variable seasonal growth patterns, such as periods of growth cessation, where temperatures will not be recorded in the $\delta^{18}O_{shell}$ (Chauvaud et al., 2005; Freitas et al., 2005; Gillikin et al., 2005; Schöne et al., 2005; Wanamaker et al., 2006; Wanamaker et al., 2007). Thus, it is necessary to carefully examine each individual species. Australian oyster species have not been the subject of previous study except for the use of the shell of *Pinctada imbricata* (the

Akoya pearl oyster) as an archival monitor of environmental lead (MacFarlane et al., 2006).

Herein we examine changes in the $\delta^{18}O_{shell}$ of the oyster *Ostrea angasi*, with the aim of determining the $\delta^{18}O_{shell}$ response as a function of water temperature and assessing its potential as a paleoclimate archive. This species is prevalent in midden sites along the south east coast of Australia (Taylor 1892; Lourandos 1968; Sullivan 1982). Records of Holocene climate from near-shore Australian waters are relatively scarce, and so this oyster has the potential to provide valuable environmental information for this region.

2.2. Background and Study Sites

2.2.1. *O. angasi* and its habitat

O. angasi is morphologically very similar to the European oyster, *O. edulis*, which has been shown to faithfully record environmental changes in its $\delta^{18}O_{shell}$ (Milner, 2002), supporting the viability of using *O. angasi* in similar investigations. *O. angasi* is native to the southern and southeastern coastlines of Australia (Nell 2001). Juvenile *O. angasi* usually begin life cemented to a hard substrate, from which they subsequently separate and spend most of their life living on soft sediment, although no time scales for these life cycle changes have been reported. Unlike many other oyster species that occupy the intertidal zone, *O. angasi* is exclusively subtidal, living in shallow waters down to 20 m depth (Nell, 2001). A field survey of

O. angasi conducted on the New South Wales coast found the majority of oysters lived 1–4 m below the low water mark (Heasman et al., 2004). That *O. angasi* inhabits subtidal environments, and will therefore experience more consistent temperature and salinity regimes (and thus $\delta^{18}O_{water}$) than those of surface and intertidal regions, increases this oyster's potential to be a useful environmental archive.

The range of temperatures which *O. angasi* can tolerate remains undefined, beyond unpublished data indicating an upper temperature limit of 28ºC (S. O'Connor, personal communication, 2008). A single study reports that growth of *O. angasi* in Tasmanian waters slowed significantly over the colder austral autumn and winter months (May–September) (Mitchell et al., 2000). The preferred salinity range of *O. angasi* is 26–36 (Nell & Livanos, unpublished data, in Nell & Gibbs 1986; reported as 25–35 g l^{-1}), though the oyster can tolerate salinities of 21–46 (Nell & Gibbs 1986; reported as 20–45 g l^{-1}).

Two east coast locations, representative of different environmental regimes within the range of *O. angasi*'s geographic distribution were selected to conduct *in situ* field culture experiments: Pambula Lake, on the far south coast of New South Wales and Little Swanport, located on the mid-east coast of Tasmania (Figure 2.1). The general characteristics of each location are given in Table 2.1.

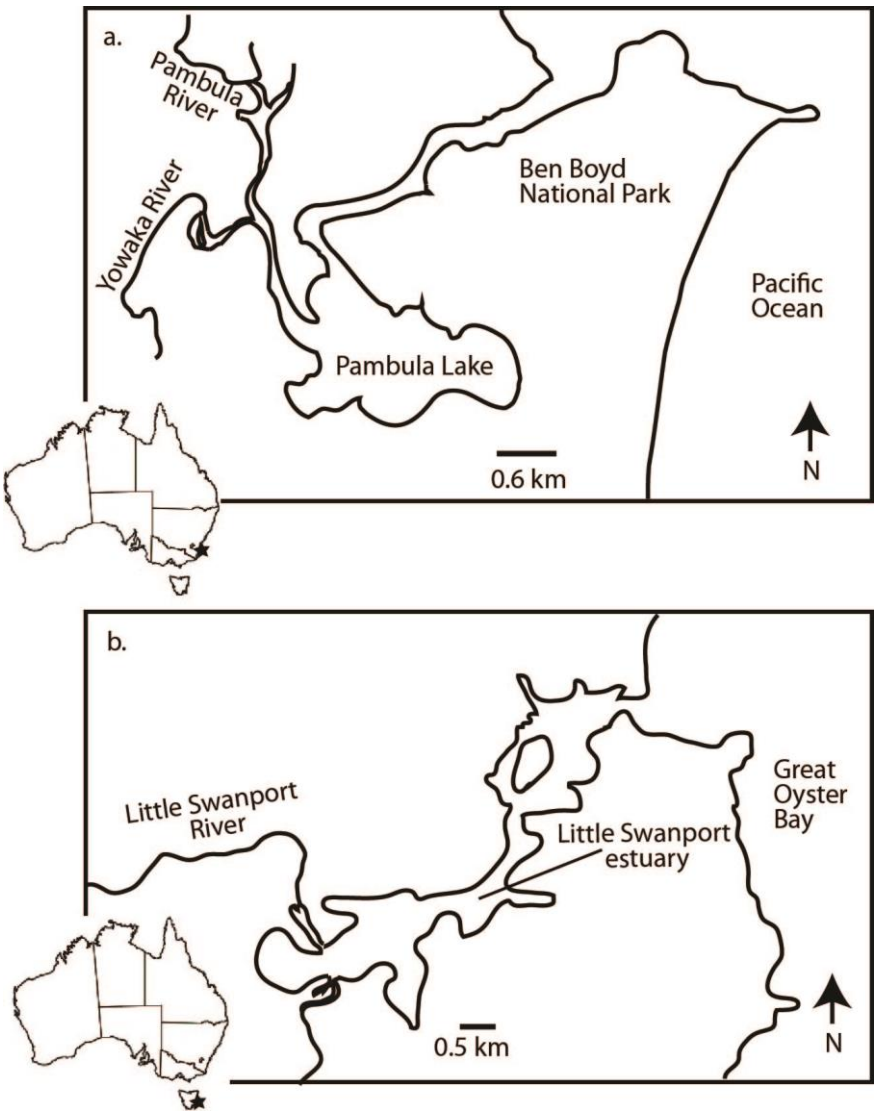

Figure 2.1. Location map of a. Pambula Lake, New South Wales, and

b. Little Swanport, Tasmania

Table 2.1. Environmental characteristics of the Pambula Lake and Little Swanport field sites.

	Estuary type	Annual temperature range (ºC)	Mean monthly temperature (ºC)	Annual rainfall range (mm)	Mean annual rainfall (mm)	Catchment area (km^2)	Residence time (days)
Pambula Lake	Tidal lake	16.4 (July) – 24.6 (Jan/ Feb)[a]	20.6[a]	101 (Feb) – 31 (Aug)[a]	651[a]	296.5[b]	~1.5[b, c]
Little Swanport	Marine-dominated estuary	13.1 (July) – 22 (January)[d]	17.6[d]	18 (May) – 69 (Feb)[e]	701[e]	600[f]	~1–1.5[f]

[a] Australian Bureau of Meteorology, Merimbula field station, data from 1998–2010; http://www.bom.gov.au/climate/da
[b] NSW Government Office of Environment and Heritage; http://www.environment.nsw.gov.au/estuaries/stats/PambulaRiver.htm
[c] Calculated by the volume of the estuary (9773.7 ML) divided by the mean tidal flux (2.96×10^6 m^3), data from [b]
[d] Australian Bureau of Meteorology, Orford field station, data from 1951–2010; http://www.bom.gov.au/climate/data
[e] Australian Government Bureau of Meteorology, Little Swanport (Wineglass Cottage) field station, data from 1995–2011; http://www.bom.gov.au/climate/data
[f] Crawford and Mitchell (1999)

2.3. Methods

2.3.1. *In situ* field culture experiments

In situ field culture experiments were conducted at each location. Commercial oyster farms at each location provided infrastructure for the experiments.

2.3.1.1. Pambula Lake

O. angasi specimens used in the monitoring experiment at Pambula Lake were hatchery grown before being transferred to the lake when they were a few months old. The aquaculture methods employed to farm these oysters prevent the overgrowth of other oysters, and each of the oysters was consequently regular in shape.

Each specimen was measured along the maximum growth axis (Figure 2.2), using digital calipers (accuracy ±0.1 mm) and labelled with a plastic fish tag (Hallprint® labels) glued to a clean and dry section of the shell with either Araldite® or Selleys Supa Glue®. The oysters were put into a covered plastic mesh tray, measuring 1.5 × 3 m, and placed in the lake alongside an oyster farm rack. The tray was submerged at all times, so as to simulate the oysters' natural habitat. The water depth was typically ~2 m at high tide and ~0.5 m at low tide.

The oysters' shell length along the maximum growth axis was measured every 4–6 weeks to obtain a record of growth rates, with care taken to minimise the amount of time the oysters were exposed to air. The new growth of *O. angasi* is very fine and brittle, and handling during measurement and shifting of oysters with tidal movements caused some breakage of new growth. Assuming that calcification of the hinge region (the region of the oyster where sampling is

conducted) occurs in proportion to shell extension these growth measurements provide a useful, but not necessarily definitive, measure of the oysters' growth.

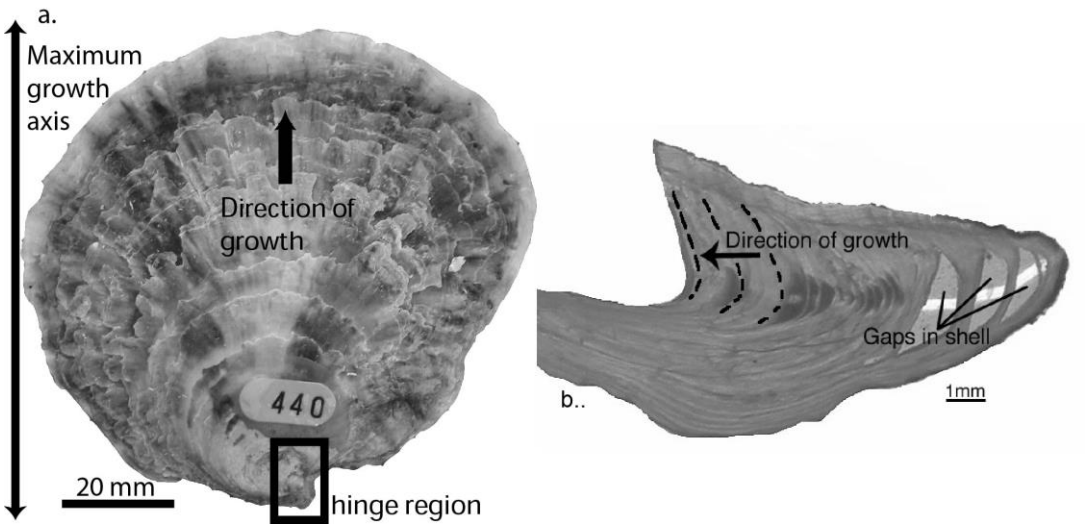

Figure 2.2. *Ostrea angasi*. a. Top view of entire shell. b. A cross section through the hinge region of the shell, showing growth layers perpendicular to the growth axis. Dotted lines indicate examples of isotope sample paths.

HOBO® U22 Water Temp Pro v2 temperature loggers (accuracy ±0.2ºC) were deployed along with the oysters and recorded temperature every 30 minutes. Water samples and salinity readings, using a TPS AQUA-CP Handheld pH Conductivity meter, calibrated to TPS pH Buffer 4.01 and TPS pH Buffer 9.18, were taken fortnightly. Water samples were collected from the lake at the location of the field culturing experiment, brought back to shore and filtered through a Millipore Millex-GN Nylon 0.2 µm filter. All water samples were kept refrigerated. The duration of the field culture experiment at Pambula Lake was 13 months, from June 2006–July 2007.

2.3.1.2. Little Swanport

O. angasi occurs naturally at Little Swanport, but they are particularly susceptible to infection by the protozoan parasite *Bonamia* sp. present in this location, which can kill the animal in times of environmental stress. As such, *O. angasi* are not farmed commercially in this area, and all the animals collected were wild specimens. As a consequence, both shell growth and morphology were rather irregular compared to the Pambula Lake. *O. angasi*.

The Little Swanport oysters were collected, measured and labelled, then placed in closed baskets and suspended below an oyster rack on a rope strung between two posts, ensuring the oysters were constantly submerged. Following advice from the local oyster farmers, the oysters were placed in a location where salinity fluctuations resulting from freshwater input from the Little Swanport River would be minimal.

Water temperatures were logged and samples collected fortnightly, following the same methods as described for Pambula Lake. The duration of the experiment at Little Swanport was 10 months, from September 2006–July 2007.

2.3.2. Sampling and analysis

2.3.2.1. XRD analysis

X-ray diffraction analysis was conducted on a sample from the hinge region of an *O. angasi* shell. The sample was milled by hand in an agate mortar in acetone and suspended on a quartz low background holder. The analysis was carried out with a SIEMENS D501 Bragg-Brentano diffractometer equipped with a graphite monochromator and scintillation detector, using CuK radiation. The scan range was 20 to 55° 2-theta, at a step width of 0.02°, and a scan speed of 1° per minute.

The results were interpreted using the SIEMENS software package Diffracplus Eva 10 (2003) for identification, and Siroquant V3 for quantification.

2.3.2.1. Isotope analysis

Like that of many other oysters, *O. angasi* shell growth is somewhat irregular. The hinge region exhibits the most consistent growth relative to the rest of the shell that is most suitable to be sampled for isotopic analysis (Figure 2.2).

Hinge sections of the left valves of the oysters were set in epoxy resin and sliced parallel to the growth axis of the hinge, through the resilifer (the central groove that runs down the centre of the oyster hinge surface), to expose a cross-section of the growth layers. Thick sections (~100 µm) were prepared from the cut blocks, which facilitated both high definition viewing and milling of incremental growth layers for stable isotope analysis. Sampling was undertaken using a Merchantek MicroMill®, at a resolution of 120 to 500 µm. Full sampling details are provided in Table 2.2.

Samples were a minimum weight of 10 µg for the University of Michigan analysis and 20 µg for the Vrije Universiteit analysis. Analysis of small samples sizes such as these is standard practice for each of these laboratories, however a number of samples collected in this study were too small for analysis (see Table 2.2).

It was not feasible to employ a consistent temporal sampling resolution throughout all specimens, with shells PLOa421 and PLOa472 yielding 29 and 32 samples per year respectively, (i.e., greater than fortnightly resolution) as compared to PLOa410 and PLOa440, which provided 10 and 11 samples per year, respectively (i.e., quasi-monthly resolution) for the same time interval. Shells LSOa754, LSOa756 and LSOa793 yielded 107, 44 and 52 samples respectively.

Table 2.2. Sampling details for $\delta^{18}O$ analysis. VU: Vrije Universiteit, Amsterdam, UM: University of Michigan.

	Sampling location	$\delta^{18}O$ analysis location	Depth (µm)	Drill speed (%)	Scan speed (%)	No. of passes	No. of samples	Sampling resolution (µm)	Samples run	Unsuitable sample size
PLOa410	VU	VU	240	80	70	1	50	lines 2-23: 135 gap in shell lines 24-34: 128 lines 34-43: 243 gap in shell lines 44-46: 477 gap in shell lines 47-48: 127 gap in shell lines 49-50: 215	every second	1, 12, 13
PLOa421	UM	UM	45	5	100	3	37	lines 1-8: 269 lines 9-15: 257 lines 16-22: 287 lines 23-31: 281 lines 32-35: 328 gap in shell line 36 gap in shell line 37 (drill depth shallower)	all	nil

	Sampling location	$\delta^{18}O$ analysis location	Depth (µm)	Drill speed (%)	Scan speed (%)	No. of passes	No. of samples	Sampling resolution (µm)	Samples run	Unsuitable sample size
PLOa440	UM	UM	20	5	100	6	31	lines 1-4: 241 lines 5-8: 276 lines 9-15: 245 lines 16-19: 324 lines 20-21: 326 lines 22-27: 319 gap in shell lines28-29: 269 gap in shell line 30 gap in shell line 31	every second	nil
PLOa472	VU	VU	240	80	70	1	49	lines 1- 23: 192 lines 24-41: 211 gap in shell lines 42-48: 393 gap in shell	all	7, 23, 33, 48, 49
LSOa754	VU	VU	240	80	70	1	107	lines 1-2: 220 lines 3-14: 150 lines 14-23: 204 lines 23-33: 154 lines 33-49: 163 lines 49-64: 167 lines 64-83: 228 lines 83-100: 249 lines 100-105: 214	all	7-10, 14, 16, 24, 29, 32, 34-38, 41, 45, 47, 60-65, 71, 72, 76, 77, 85, 86

	Sampling location	$\delta^{18}O$ analysis location	Depth (µm)	Drill speed (%)	Scan speed (%)	No. of passes	No. of samples	Sampling resolution (µm)	Samples run	Unsuitable sample size
LSOA756	UM	UM	15	5	100	lines 1-41: 8 lines 42-44: 11	44	lines 1-4: 302 lines 5-13: 356 lines 14-18: 326 lines 19-24: 343 lines 25-30: 329 lines 31-35: 301 lines 36-38: 382 lines 39-41: 342	all	nil
LSOa793	VU	VU	240	80	70	1	52	lines 1-16: 203 lines 16-34: 215 lines 35-38: 591 gap in shell lines 39-47: 237 lines 47-49: 187 gap in shell lines 50-52: 557	all	nil

Stable isotope analysis was conducted at the Vrije Universiteit in Amsterdam and the University of Michigan, Ann Arbor. Analyses conducted at the Vrije Universiteit, Amsterdam, (PLOa 410, PLOa472, LSOa754, LSOa793) were carried out on a Finnigan Delta^{+} mass spectrometer with GasBench-II preparation device, using internal standards regularly calibrated to NBS 18, 19 and 20. The long-term standard deviation of these standards is <0.1 ‰. Samples obtained at the University of Michigan (PLOa421, PLOa440, LSoa756) were analysed on a Finnigan MAT Kiel IV preparation device coupled directly to the inlet of a Finnigan MAT 253 triple collector isotope ratio mass spectrometer. O^{17} corrected data were corrected for acid fractionation and source mixing by calibration to a best-fit regression line defined by NBS standards 18 and 19. Precision and accuracy of data are monitored through daily analysis of a variety of powdered carbonate standards. At least four standards are reacted and analysed daily. Results are reported in standard δ-notation, relative to V-PDB, with measured precision of better than 0.1 ‰.

2.3.2.2. $\delta^{18}O_{water}$ analysis

δ^{18}O analysis of water samples was conducted at The Australian National University, Canberra, using a Picarro cavity ring-down laser absorption device, model number L1102-i. Each sample was injected 5 times and each injection was about 1 µL. The needle was washed with 1-methyl-2-pyrrolidinone between injections. The data are calibrated against internal standards, which are regularly calibrated to IEAA standards SLAP, GISP and VSMOW. Results are reported in standard δ-notation, relative to V-SMOW, with a precision of 0.25 ‰.

2.3.3. Predicted $\delta^{18}O_{shell}$

To confirm that *O. angasi* shell is precipitated in equilibrium with the ambient water, a predicted $\delta^{18}O_{shell}$ profile was calculated for each location, based on measured water temperatures and $\delta^{18}O_{water}$ (Kirby et al., 1998; Surge et al., 2001; Ullman et al., 2010). Two $\delta^{18}O$-temperature calibration equations were evaluated: the equation derived from empirical study of biogenic carbonate by Epstein et al. (1953):

$$T\ (^{o}C) = 16.5 - 4.3(\delta^{18}O_{shell} - \delta^{18}O_{water}) + 0.14(\delta^{18}O_{shell} - \delta^{18}O_{water})^2 \quad \text{(Eq. 2.1)}$$

where both $\delta^{18}O_{shell}$ and $\delta^{18}O_{water}$ are relative to the V-PBD standard (0.27 was subtracted from $\delta^{18}O_{water}$ values to convert from V-SMOW to V-PBD, as per Hut (1987), in Gonfiantini et al. (1995)), and also a calibration derived by Kim and O'Neil (1997) from inorganic carbonate precipitation experiments:

$$1000 ln\alpha_{cc\text{-}w} = 18.03(10^3 T^{-1}) - 32.42 \quad \text{(Eq. 2.2)}$$

where T is temperature in Kelvin and α_{cc-w} is the isotope fractionation factor between calcite and water (with $\delta^{18}O_{shell}$ and $\delta^{18}O_{water}$ both relative to the V-SMOW standard).

However, in the $\delta^{18}O$ analysis used to derive their equation, Kim and O'Neil (1997) used an acid fractionation factor of 1.01050, (as opposed to 1.01025, see Wanamaker et al., 2006; Coplen, 2007), which resulted in an offset in their calcite $\delta^{18}O$ data of 0.25 ‰. As such, their equation must be modified slightly. Wanamaker et al. (2006) adjusted the Kim and O'Neil (1997) dataset, and

obtained the modified equation:

$$T\ (^{o}C) = 15.07 - 4.6(\delta^{18}O_{calcite} - \delta^{18}O_{water}) + 0.09(\delta^{18}O_{calcite} - \delta^{18}O_{water})^2 \quad \text{(Eq. 2.3)}$$

where $\delta^{18}O_{calcite}$ is relative to V-PDB, and $\delta^{18}O_{water}$ relative to V-SMOW.

Of the previous studies of oyster $\delta^{18}O_{shell}$, the majority use the Epstein et al. (1953) equation (Wang et al., 1995; Kirby et al., 1998; Harding et al., 2010), or a variation upon this equation developed by Anderson and Arthur (1983) (Brigaud et al., 2008; Lartaud et al., 2010; Titschack et al., 2010). Other authors use equations derived from equilibrium experiments of synthetic carbonates conducted by Tarutani et al. (1969) (Surge et al., 2001; Ullmann et al., 2010) or Friedman and O'Neil (1977) (Goodwin et al., 2010), which are very similar to the Kim and O'Neil (1997) equation.

2.4. Results

2.4.1. *O. angasi* shell structure

The X-Ray diffraction analysis confirmed that *O. angasi* shell is comprised of calcite. Thin section analysis of the *O. angasi* shell structures did not reveal any features that can be readily linked to an annual or seasonal periodicity; however, incremental growth layers are visible (Figure 2.2b). Small, crescent-shaped gaps are visible in the Pambula Lake shell cross sections. These gaps do not appear to correlate temporally between the shells, nor be linked to particular environmental events or influences. These gaps also occur, but are not as prevalent, in the Little Swanport shells.

2.4.2. *O. angasi* growth rates

All of the Pambula Lake *O. angasi* samples show significant growth over the 13-month experiment period, with average monthly shell extension rates between 1.0–5.0 mm/month (Figure 2.3).

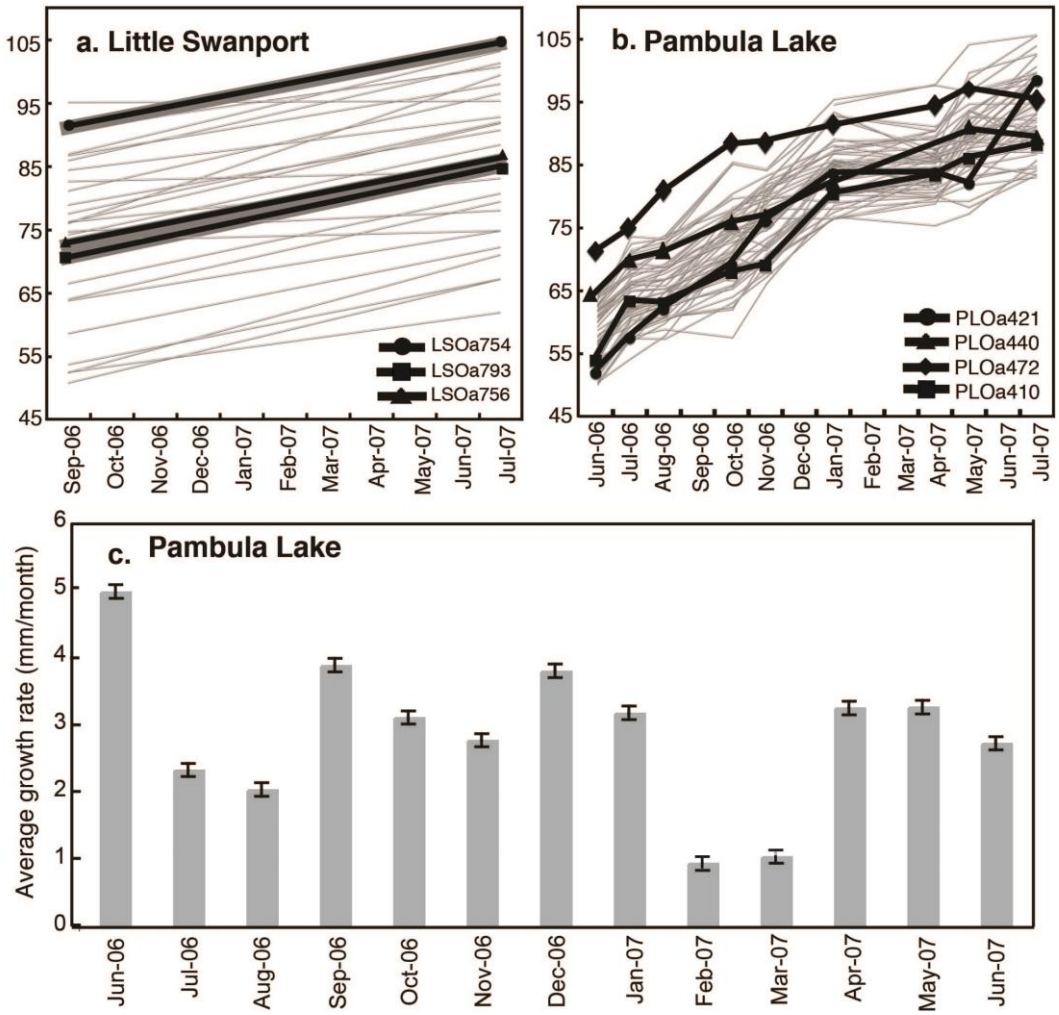

Figure 2.3. *Ostrea angasi* growth rate data. a: Little Swanport *O. angasi*; b, c: Pambula Lake *O. angasi*. The black lines in a. and b. indicate the *O. angasi* for which $\delta^{18}O_{shell}$ was analysed, grey lines indicate other *O. angasi* included in the experiment, but not sampled for $\delta^{18}O_{shell}$. The Pambula Lake *O. angasi* shells show decreased growth during February–March 2007, co-incident with an intense rainfall event.

It is evident from the growth rate records that the Pambula Lake shells do not grow at a consistent rate throughout the year. The average monthly growth rates show a marked slowing, and possible cessation (of unknown duration) in

growth during the late summer and early autumn months of February to April 2007 (Figure 2.3c). Growth rates for the months of February and March 2007 are only 1.0 and 1.1 mm/month respectively, less than one third of the average monthly growth rate of 3.2 mm/month (1σ = 0.8 mm/month) for the other months (excluding February and March 2007) of the experiment period. While the growth rates for the months of July and August 2006 (2.31 and 2.01 mm/month respectively) are also lower than average, there is no evidence for a winter-temperature induced growth cessation.

Due to logistical constraints, the Little Swanport *O. angasi* shells were measured only at the beginning and end of the experiment period. Calculated growth rates for the experiment period average 1.3 mm/month (1σ = 0.1 mm/month) for the shells sampled, 1.1 mm/month (1σ = 0.5 mm/month) for all shells at Little Swanport) and provide no indication as to whether the oysters may have stopped growing or varied their growth rate at certain times during the experiment. Previous studies of *O. angasi* in Tasmanian waters have found growth rates to be higher during the summer months, with little to no growth during winter (Dix, 1980; Mitchell et al., 2000). The Little Swanport oysters exhibit slower growth rates than those from Pambula Lake. Given that the Little Swanport oysters were larger, and presumably older, than the Pambula Lake oysters at the time of collection, this may be an ontogenetic effect whereby growth slows with increasing age (e.g. Gosling 2003; *Arctica islandica*: Schöne et al. 2005; *C. gigas*: Mouchi et al. 2012).

2.4.3. Pambula Lake and Little Swanport water chemistry

The various water chemistry parameters that were measured over the experiment periods in both locations are shown in Figure 2.4. The water temperature at Pambula Lake ranged from 11.6–24.7 ºC, and salinity ranged from 1.8–34.

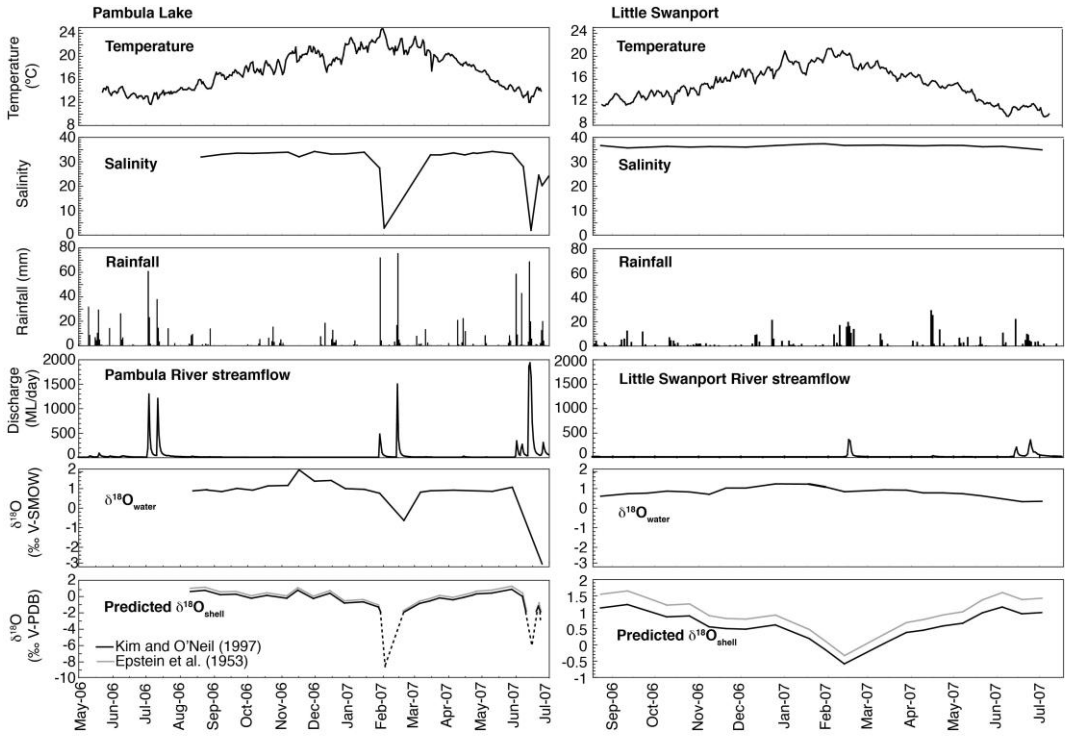

Figure 2.4. Environmental conditions of temperature, salinity, rainfall, streamflow and $\delta^{18}O_{water}$ recorded at Pambula Lake and Little Swanport over the duration of the *in situ* field culture experiments, along with predicted $\delta^{18}O_{shell}$ profiles for each location. The Pambula Lake data show increased rainfall during the winter or 2006 and an intense rainfall event in February 2007. The dotted line in the predicted $\delta^{18}O_{shell}$ for Pambula Lake indicates the $\delta^{18}O_{shell}$ values that fall below the established threshold for Pambula Lake $\delta^{18}O_{shell}$.

The minimum $\delta^{18}O_{water}$ recorded was −2.88 ‰ V-SMOW (July 2007), with a maximum of 1.93 ‰ V-SMOW (December 2006) with an average of 0.77 ‰ V-SMOW (1σ = 0.98 ‰) over the duration of the experiment (salinity and $\delta^{18}O_{water}$ data are given in Table 2.3). The salinity-$\delta^{18}O_{water}$ relationship, derived from

comparison of in situ salinity measurements with contemporaneous water samples analysed for $\delta^{18}O_{water}$ is described by:

$$\delta^{18}O_{water}\ (‰) = 0.25_{\pm 0.07} * \text{salinity} - 7.20_{\pm 2.29} \qquad \text{(Eq. 2.4)}$$

$R^2 = 0.76$, n = 22

The errors provided above are for the 95 % confidence interval. Root Mean Square Error (RMSE) = ±0.95 ‰.

The water temperature in the Little Swanport estuary during the experiment period ranged from 9.4 to 21.2 ºC. The salinity range was 34.6–37.1, with an average of 36.1, slightly higher than average marine salinity, most likely due to evaporation from the estuary. The minimum $\delta^{18}O_{water}$ recorded was 0.30 ‰ V-SMOW (July 2007), with a maximum of 1.21 ‰ V-SMOW (December 2006) with an average of 0.77 ‰ (1σ = 0.25 ‰) V-SMOW over the duration of the experiment. The relationship between salinity and $\delta^{18}O_{water}$ is described by:

$$\delta^{18}O_{water}\ (‰) = 0.29_{\pm 0.08} * \text{salinity} - 9.52_{\pm 2.72} \qquad \text{(Eq. 2.5)}$$

$R^2 = 0.43$, n = 21

The errors provided above are for the 95 % confidence interval, RMSE = ±0.36 ‰.

Table 2.3. Pambula Lake and Little Swanport salinity and $\delta^{18}O_{water}$ data.

Pambula Lake				**Little Swanport**		
Date	Salinity	$\delta^{18}O$		Date	Salinity	$\delta^{18}O$
08/07/06		1.40		7/09/06	36.4	0.58
08/09/06	31.7	0.90		26/09/06	35.4	0.71
22/09/06	32.8	0.82		10/10/06	35.7	0.74
06/10/06	33.3	0.98		24/10/06	36.0	0.84
20/10/06	33.2	0.89		9/11/06	35.8	0.8
03/11/06	33.4	1.11		23/11/06	36.0	0.68
21/11/06	33.7	1.13		5/12/06	35.9	1
01/12/06	31.8	1.93		19/12/06	35.8	1
15/12/06	34	1.35		9/01/07	36.4	1.21
30/12/06	32.9	1.39		2/02/07	37.1	1.2
12/01/07	33	0.97		13/02/07	37.1	1.06
29/01/07	33.7	0.93		27/02/07	36.4	0.81
12/02/07	27.2	0.73		27/03/07	36.6	0.9
16/02/07	2.67			12/04/07	36.4	0.89
06/03/07		-0.66		24/04/07	36.3	0.75
21/03/07		0.79		8/05/07	36.5	0.75
30/03/07	32.60	0.86		22/05/07	36.4	0.71
08/04/07	32.60			5/06/07	35.9	0.59
20/04/07	33.40	0.89		19/06/07	36.0	0.45
30/04/07	32.60			3/07/07	35.4	0.3
08/05/07	33.40			17/07/07	34.6	0.32
11/05/07	33.20					
25/05/07	34.00	0.83				
12/06/07	33.10	1.04				
22/06/07	27.80					
29/06/07	1.76					
06/07/07	24.30					
09/07/07	20.00	-2.88				
16/07/07	24.50					

2.4.4. $\delta^{18}O_{shell}$ and $\delta^{13}C_{shell}$

The complete *O. angasi* $\delta^{18}O_{shell}$ profiles include growth that occurred prior to and during the experiment periods at both sites. Despite differences in their sampling resolution, all four Pambula Lake shells show consistent $\delta^{18}O_{shell}$ profiles that reflect seasonal changes from high $\delta^{18}O_{shell}$ during the cooler winter months and low $\delta^{18}O_{shell}$ during warmer summer months. In the Little Swanport *O. angasi*, seven complete seasonal cycles are evident in shell LSOa754, five in LSOa756, and two in LSOa793 (Figure 2.5).

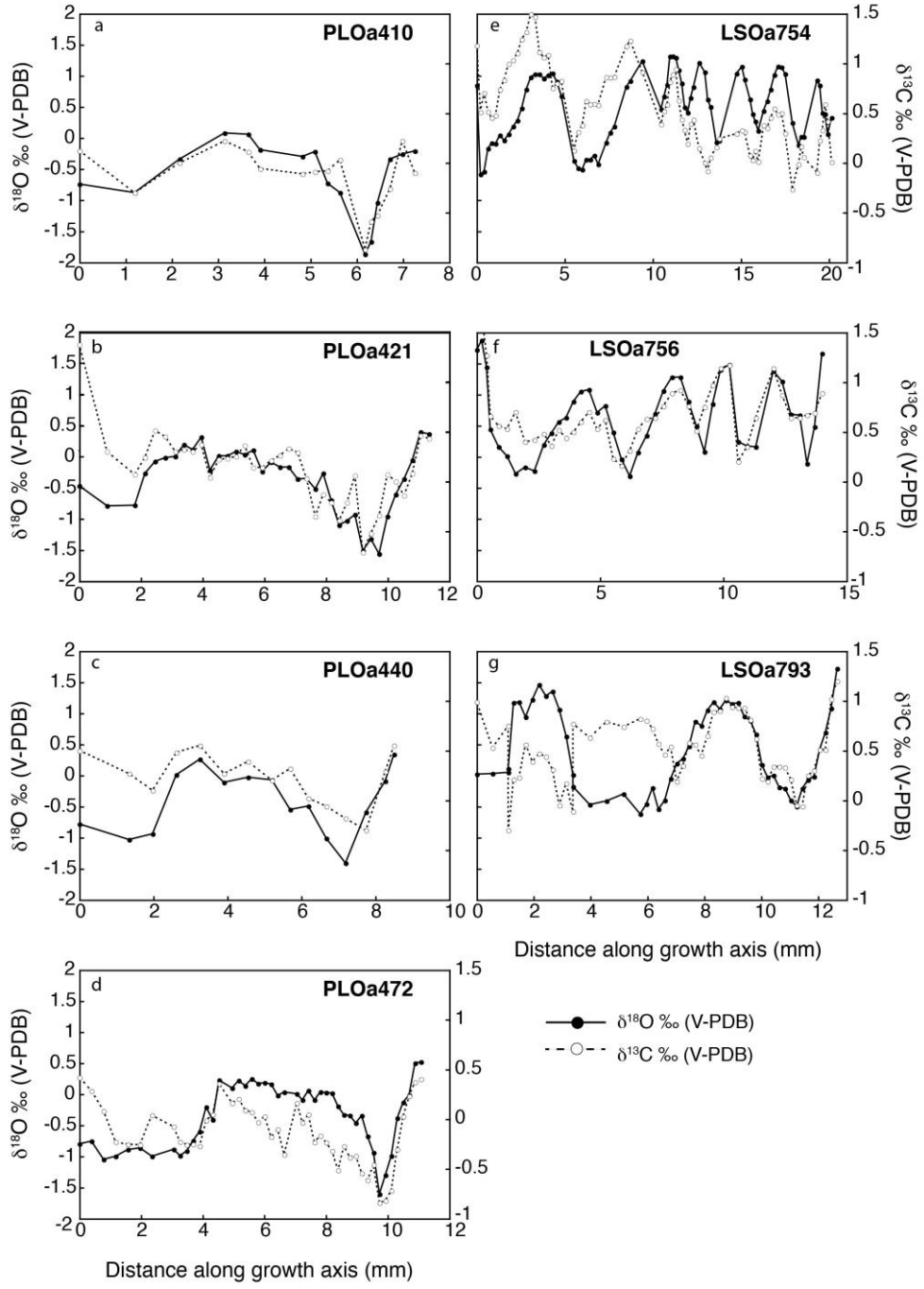

Figure 2.5. Pambula Lake (a–d) and Little Swanport (e–g) *O. angasi* entire shell $\delta^{18}O_{shell}$ and $\delta^{13}C_{shell}$ profiles. All shells show clear seasonal cycles. The Pambula Lake *O. angasi* show ~1.5 years of growth, while the Little Swanport shells are clearly older, with seven seasonal cycles visible in shell LSOa754, five in LSOa756 and 2.5 in LSOa793.

Except for a notable offset during the early stages of the Pambula Lake *O. angasi* growth, the $\delta^{13}C_{shell}$ closely follows $\delta^{18}O_{shell}$ in each of the *O. angasi*. In the older Little Swanport *O. angasi*, $\delta^{13}C_{shell}$ follows a similar pattern in shells LSOa754 and LSOa756. Shell LSOa793 shows a different pattern of $\delta^{13}C_{shell}$, where in the first year of the oyster's growth, the $\delta^{18}O_{shell}$ and $\delta^{13}C_{shell}$ are distinctly out of phase, then become aligned in the second year of growth.

2.5. Discussion

2.5.1. *O. angasi* shell structure

Similar gaps to those seen in the hinge region of the Pambula Lake *O. angasi* shells have been noted in *O. edulis* shells, and attributed to rapid growth rates, common in the early stages of bivalve growth (Milner, 2002). Given that the Pambula Lake shells are juveniles, and were growing quickly during this period, this explanation is plausible, and also explains why the gaps are less prominent in the Little Swanport shells, where the less favourable environmental conditions result in slower overall growth rates.

Although some studies report that darker bands in oyster shell cross sections are time dependent (Kirby et al., 1998), Surge et al., (2001) found that the visible structures found in *C. virginica* could not be used to provide a temporal context for calcification and Wang et al. (1995), found that using the shell ligamental structures in *C. gigas* as an indication of age could result in an overestimation of shell ages. No structures that could be related to a temporal context were found in the *O. angasi* shells of this study.

2.5.2. *O. angasi* growth

The growth rates reported in section 2.4.2 for the Pambula Lake *O. angasi* are typical of the rapid growth rate of juvenile bivalves (Gosling, 2003).

Growth cessation or slower growth in the Pambula Lake *O. angasi* most likely relates to changes in salinity. Each period of low growth in the Pambula Lake oysters corresponds to a time of high rainfall, and low salinity in the estuary (Figure 2.4). While salinity data corresponding to the high rainfall of the 2006 winter months was not obtained, it is clear that the high rainfall of both February and June 2007 resulted in a significant freshening of the estuary, with salinity dropping to 2.7 and 1.8 respectively. Despite the short residence time of the Pambula Lake estuary, which would see a return to normal salinity in ~2 days, the rainfall at these times was not confined to a single event, resulting in persistently low salinity within the estuary. As such, it is reasonable to assume that these salinities, well below the known tolerance range for *O. angasi*, were the cause of the lower growth rates, and possible growth cessation. Other factors, such as increased pollutant load or turbidity, which might also affect the oysters' growth, are not significant in this estuary.

2.5.3. *O. angasi* $\delta^{18}O_{shell}$

The $\delta^{18}O$ profiles of the Pambula Lake *O. angasi* are consistent with the oysters having grown for approximately 1.5 years—commencing growth during summer or autumn, then experiencing a full winter and summer before being collected for analysis.

The $\delta^{18}O_{shell}$ profiles of LSOa754, LSOa756 and LSOa793 indicate they are 8, 5 and 2.5 years old, respectively (Figure 2.5). After the first two years of growth, the older shells LSOa754 and LSOa756 show a significant decrease in

hinge extension rate between the first two years of growth and subsequent years, with compressed annual $\delta^{18}O_{shell}$ cycles, and attenuation of the $\delta^{18}O_{shell}$ amplitudes. This slowing of growth with ontogeny, and accompanying attenuation in $\delta^{18}O_{shell}$ amplitudes has been documented in a number of bivalve studies (e.g. Krantz et al., 1987; Harrington, 1989; Kennedy et al., 2001; Freitas et al., 2005; Schöne, 2008).

This attenuation is most marked in the summer temperatures following the first two years of growth. The reduced growth rate results in reduced calcification and a lower sampling resolution. This can dampen the degree of variation in the isotopic profile, whereby short-term extreme conditions become averaged with surrounding less extreme conditions (Wang et al., 1995; Kennedy et al., 2001; Goodwin et al., 2003) The $\delta^{18}O_{shell}$ of the first two years of growth in shells LSOa754 and LSOa756 are similar to the amplitude observed in the younger shell, LSOa793.

2.5.4. Predicted *vs.* observed $\delta^{18}O_{shell}$

Salinity in the Pambula Lake estuary is variable and influenced by non-systematic patterns induced by rainfall events and evaporation. The high rainfall events of February and June 2007, and the consequent influx of fresh water with a more negative $\delta^{18}O$ value results in the prediction of low $\delta^{18}O_{shell}$ values of –8.5 and –6 ‰ V-PDB. It is presumed that the low salinity coincident with these extreme rain events was such that the oysters ceased to precipitate calcium carbonate at these times. Accordingly, these negative $\delta^{18}O_{shell}$ values are not recorded in the *O. angasi* isotopic profiles, and are indicated by the dashed lines in the Pambula Lake predicted $\delta^{18}O_{shell}$ profile in Figure 2.4. This is supported by the shell extension rates (Figure 3), which show reduced growth rates for February (the

actual low salinity event) and March (the recovery period) of approximately two thirds the average growth rate for the entire experiment period. It follows that the oysters may have ceased calcite precipitation during this event, and so the shells do not record the predicted extreme $\delta^{18}O_{shell}$ values.

In the absence of observable growth structures that provide a temporal context for shell precipitation and that can be matched to the predicted $\delta^{18}O_{shell}$ profile, the predicted and observed *O. angasi* $\delta^{18}O_{shell}$ profiles were compared using AnalySeries software (Version 2.4.0.2). This program facilitated the comparison of the predicted and observed curves via manual determination of multiple discrete tie-points, and scaling of the x-axis (distance along the shell growth axis, i.e. growth rate). This accounts for the variable growth rate common to oysters and evident in the *O. angasi* growth records. As it is assumed that *O. angasi* will cease to precipitate any calcite during low salinity (and correspondingly negative $\delta^{18}O_{water}$) events, a threshold of -1.87 ‰ V-PDB, the minimum value observed in the Pambula Lake *O. angasi*, was assigned for the Pambula Lake predicted $\delta^{18}O_{shell}$ (Figure 4).

Comparisons of the predicted $\delta^{18}O_{shell}$ and the analysed $\delta^{18}O_{shell}$ for the *O. angasi* from each location are shown in Figure 2.6. Overall, the $\delta^{18}O_{shell}$ of the Pambula Lake *O. angasi* shows good agreement with the predicted $\delta^{18}O_{shell}$ profile. However, two sharp peaks of relatively high $\delta^{18}O$ that are not seen in the measured *O. angasi* $\delta^{18}O_{shell}$ profiles occur in the predicted $\delta^{18}O_{shell}$ profile in mid-November 2006 and mid-December 2006. These correlate to sharp drops in temperature of ~1 week in duration. It appears that the sampled *O. angasi* $\delta^{18}O_{shell}$ record is of insufficient resolution to record these brief temperature excursions, with the isotopic record being averaged over the time period that the sample covers, thus smoothing out the temperature extremes. A higher sampling

resolution would result in greater fidelity between the predicted and observed $\delta^{18}O_{shell}$ records.

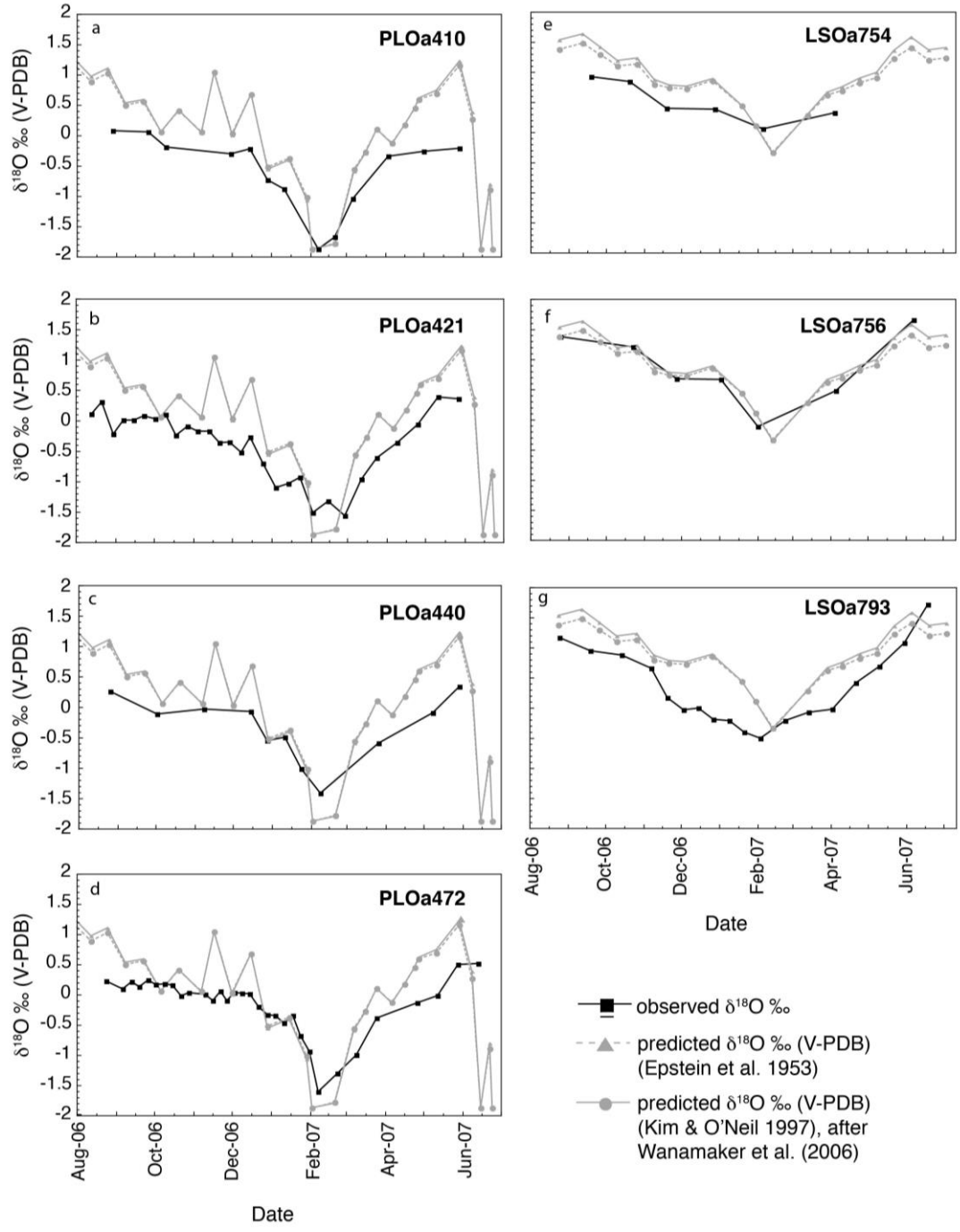

Figure 2.6. Comparisons of predicted and observed $\delta^{18}O_{shell}$ for Pambula Lake and Little Swanport *O. angasi*. These records correspond to the portion of shell growth that occurred during the experiment period, i.e. the most recent year of growth only. Pambula Lake predicted $\delta^{18}O_{shell}$ was assigned a threshold value of −1.87 ‰ V-PDB. While overall the *O. angasi* $\delta^{18}O_{shell}$ records from both locations show good agreement with the predicted $\delta^{18}O_{shell}$ profiles, there are some notable discrepancies in the Pambula Lake *O. angasi* during the winter months of 2006.

It is also apparent that the Pambula Lake *O. angasi* possibly do not record values greater than ~0.4 ‰ V-PDB in their $\delta^{18}O_{shell}$. This could be explained if shell growth ceases or is greatly reduced at lower winter temperatures. However, this does not seem likely, as although the shell extension rates (Figure 2.3) for the 2006 winter period are lower than the average growth rate, there is no evidence for a complete cessation of growth. Moreover, the longer-lived *O. angasi* from the Little Swanport site consistently record $\delta^{18}O_{shell}$ values more positive than 0.4 ‰ V-PDB, (up to 1.87 ‰ V-PDB) and thus continue to grow at considerably lower temperatures.

Given the spatial extent between the two sites, it is possible that there exists some genetic variability between the two populations of *O. angasi*, which may exert some influence upon the $\delta^{18}O_{shell}$, as discussed in Wanamaker et al. (2007). Evidence for genetic introgression with the New Zealand flat oyster, *Ostrea chilensis* (=*Tiostrea chilensis = Tiostrea lutaria = Ostrea lutaria*) has been found among Tasmanian *O. angasi* (W. O'Connor, personal communication 2012). Significant similarities with *O. edulis* have been reported for *O. angasi* populations in Albany, Western Australia (Morton et al., 2003). It has also been found that individual cohorts of *O. angasi* juveniles do not necessarily represent the genetic variability of the entire population (W. O'Connor, personal communication 2012). However, further rigorous genetic and geochemical studies would be required to 1) confirm the potential effects of genetic variability on variations between *O. angasi* populations, and 2) reasonably attribute differences in the $\delta^{18}O_{shell}$ of the *O. angasi* from different geographical locations to any such genetic variability.

2.5.5. $\delta^{18}O_{shell}$-temperature reconstructions

2.5.5.1. Pambula Lake

To assess the accuracy of a temperature record obtained from *O. angasi* $\delta^{18}O_{shell}$, paleotemperature Equations 2.1 and 2.3 were used to reconstruct temperature records from the $\delta^{18}O_{shell}$. As it was not possible to ascribe a temporal context to the oyster $\delta^{18}O_{shell}$ from structural analysis, we were unable to constrain variations in $\delta^{18}O_{water}$, so average values for $\delta^{18}O_{water}$ of 0.77‰ (V-SMOW) were used for both Pambula Lake and Little Swanport. This unavoidably introduces an error into the temperature records, as the $\delta^{18}O_{water}$ is clearly affected by sporadic influxes of fresh water in both estuaries. However, any application of the $\delta^{18}O_{shell}$ temperature proxy in a paleoclimate context requires this assumption, as exact values for paleo-$\delta^{18}O_{water}$ will not be known (Brigaud et al., 2008; Freitas et al., 2012).

Figure 2.7 shows comparisons of the temperature record constructed from the Pambula Lake *O. angasi* shells using the two paleotemperature equations described earlier with the instrumental water temperature recorded during the experiment period.

The precision of the $\delta^{18}O$ measurements in this study, (i.e. better than 0.1 ‰ V-PDB) equates to a maximum temperature uncertainty at $\delta^{18}O_{shell}$ of −1.87 ‰ of 0.5 ºC for both Equation 2.1 and 2.3. This uncertainty decreases slightly at the highest reported $\delta^{18}O_{shell}$ of 1.87 ‰ to 0.4ºC for each equation.

The Pambula Lake *O. angasi* show a sharp peak in summer temperature, rather than the comparatively sustained period of ~23ºC in the instrumental temperature record. This is attributable to the growth cessation that resulted from the high rainfall event of February 2007.

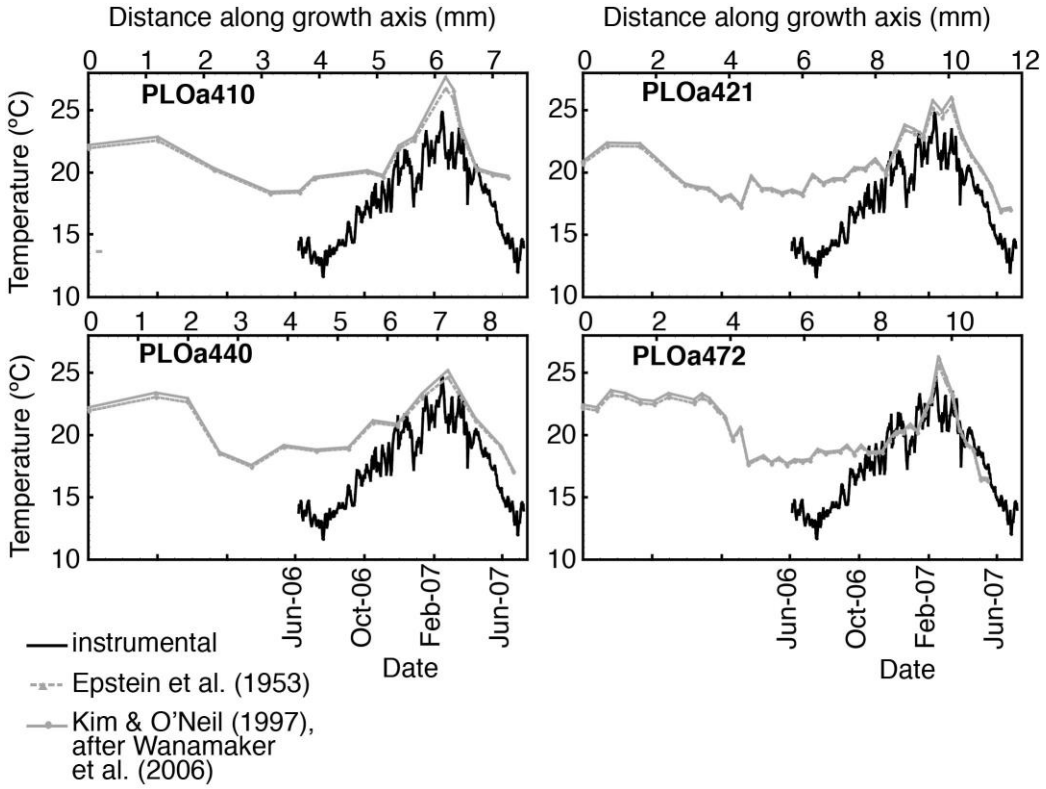

Figure 2.7. Comparison of observed temperatures recorded during the *in situ* field culture experiments at Pambula Lake with *O. angasi* $\delta^{18}O_{shell}$-reconstructed temperatures using the equations of Epstein et al. (1953) and Kim & O'Neil (1997), after Wanamaker et al. (2006). The *O. angasi* $\delta^{18}O_{shell}$-reconstructed temperatures tend to overestimate winter temperatures and show a distinct peak in summer temperature rather than the comparatively sustained temperatures in the observed temperature record.

It is also notable that the $\delta^{18}O_{shell}$-temperature profiles constructed from both calibration equations over-estimate calcification temperatures during each winter of the experiment period (Table 2.4 Figure 2.7). As previously discussed, it is unlikely that this is caused by a growth cessation at low temperature during the winter, as shell measurements indicate continued growth during winter, and lower temperatures than those experienced at Pambula Lake are recorded in the shells from Little Swanport. A possible explanation for the discrepancy is the use of a single average value for $\delta^{18}O_{water}$ (0.77 ‰ V-SMOW) for the entire temperature reconstruction period. Sustained high rainfall ($\delta^{18}O_{rainwater}$ = −13.48 ‰ V-SMOW)

during the first winter of the experiment period would have driven the Pambula Lake $\delta^{18}O_{water}$ to more negative values than the average $\delta^{18}O_{water}$ value of 0.77 ‰ V-SMOW. More negative $\delta^{18}O_{water}$ values during this winter period would cause reconstructed temperatures to appear warmer than true calcification temperatures.

The range of $\delta^{18}O_{water}$ values required to match shell calcification temperatures with instrumental temperatures of 12–14ºC during the 2006 winter period is −0.75−0.45 ‰ V-SMOW, which is equivalent to a salinity of ~25.5–27 (from Equation 2.4). These salinity values are plausible given the amount of rainfall received during this period, and fall within the tolerance range for *O. angasi* and so are unlikely to have caused a low-salinity growth cessation. Furthermore, despite the relatively short residence time of water in Pambula Lake of ~1.5 days, the prolonged nature of this rainfall event, where four out of the six days between 25 February and 2 March 2007 received appreciable rainfall, would have resulted in a persistently lower salinity within the lake.

The winter of 2007 experienced even higher rainfall, low salinity and $\delta^{18}O_{water}$ below the threshold value of 1.87 ‰ V-SMOW. Hence, the failure of the Pambula Lake *O. angasi* to record the low winter temperatures of this time could result from a low-salinity-induced growth cessation potentially compounded by the error introduced by using an average $\delta^{18}O_{water}$ value in the temperature calculation.

Table 2.4. Temperatures reconstructed from Pambula Lake *O. angasi* $\delta^{18}O_{shell}$, using the equations of Epstein et al. (1953) and Kim & O'Neil (1997), after Wanamaker et al. (2006), compared to the instrumental temperature recorded over the experiment periods (July 2006–June 2007). The offset between the reconstructed and instrumental temperature is shown in square brackets.

Growth period	**Pambula Lake temperature**	**PLOa410 Epstein et al. (1953)**	**PLOa410 Kim & O'Neil (1997), after Wanamaker et al. (2006)**	**PLOa421 Epstein et al. (1953)**	**PLOa421 Kim & O'Neil (1997), after Wanamaker et al. (2006)**	**PLOa440 Epstein et al. (1953)**	**PLOa440 Kim & O'Neil (1997), after Wanamaker et al. (2006)**	**PLOa472 Epstein et al. (1953)**	**PLOa472 Kim & O'Neil (1997), after Wanamaker et al. (2006)**
2006 winter	11.6	18.3 [6.7]	18.2 [6.6]	17.3 [5.7]	17.1 [5.5]	17.6 [6.0]	17.4 [5.8]	17.7 [6.1]	17.6 [6.0]
2006-07 summer	24.7	27.5 [2.8]	26.6 [1.9]	25.7 [1.0]	25.1 [0.4]	25.2 [0.5]	24.7 [0]	26.2 [1.5]	25.5 [0.8]
2007 winter	11.9	19.6 [7.7]	19.5 [7.6]	17.0 [5.1]	16.8 [4.9]	17.2 [5.3]	17.0 [5.1]	16.4 [4.5]	16.2 [4.3]
2006-07 annual mean	17.5	21.4 [3.9]	21.1 [3.6]	20.5 [3]	20.3 [2.8]	20.3 [2.8]	20.3 [2.8]	20.1 [2.6]	19.8 [2.3]

Table 2.5. Temperatures reconstructed from Little Swanport *O. angasi* $\delta^{18}O_{shell}$, using the equations of Epstein et al. (1953) and Kim & O'Neil (1997), after Wanamaker et al. (2006), compared to the instrumental temperature recorded over the experiment periods (September 2006–July 2007). Historical temperatures were calculated from the relationship between the Little Swanport water temperature and air temperature at the Orford Bureau of Meteorology field station. Also shown is the instrumental temperature record from the Maria Island Integrated Marine Observing System-Australian National Moorings Network National Reference Station, ~30km from the Little Swanport estuary. The offset between the reconstructed and instrumental temperature is shown in square brackets.

Growth period	Maria Island temperature	Little Swanport (Orford) temperature	LSOa754 Epstein et al. (1953)	LSOa754 Kim & O'Neil (1997), after Wanamaker et al. (2006)	LSOa756 Epstein et al. (1953)	LSOa756 Kim & O'Neil (1997), after Wanamaker et al. (2006)	LSOa793 Epstein et al. (1953)	LSOa793 Kim & O'Neil (1997), after Wanamaker et al. (2006)
1999 winter	12.8	11.3	15.0 [3.7]	14.7 [3.4]				
1999-00 summer	17.8	19.4	21.3 [1.9]	21.1 [1.8]				
2000 winter	12.9	11.0	14.3 [3.3]	13.9 [2.9]				
2000-01 summer	18.9	20.1	21.0 [0.8]	20.8 [0.7]				
2001 winter	13.3	11.7	13.4 [1.7]	12.9 [1.2]				
2001-02 summer	17.5	17.5	16.7 [-0.8]	16.5 [-1.0]				
2002 winter	13.0	11.6	13.1 [1.5]	12.5 [1.0]	10.9 [-0.7]	9.9 [-1.7]		
2002-03 summer	18.6	19.6	16.9 [-2.7]	16.7 [-2.9]	19.9 [0.3]	19.8 [0.1]		
2003 winter	13.0	10.9	13.5 [2.6]	13.0 [2.1]	14.1 [3.1]	13.6 [2.7]		
2003-04 summer	17.4	18.1	19.0 [0.9]	18.9 [0.8]	20.1 [2.0]	19.9 [1.9]		

2004 winter	12.0	9.9	13.8 [3.8]	13.3 [3.4]	13.2 [3.3]	12.7 [2.8]		
2004-05 summer	16.7	18.1	18.2 [0.1]	18.0 [0]	18.3 [0.3]	18.2 [0.2]	18.6 [0.5]	18.5 [0.4]
2005 winter	12.2	11.4	13.8 [2.4]	13.3 [1.9]	12.4 [1.1]	11.8 [0.4]	12.5 [1.2]	11.9 [0.5]
2005-06 summer	16.1	18.5	19.2 [0.7]	19.1 [0.5]	18.0 [-0.5]	17.8 [-0.7]	21.1 [2.6]	20.9 [2.4]
2006 winter	12.4	10.5	14.7 [4.1]	14.3 [3.8]	12.8 [2.3]	12.2 [1.7]	13.5 [3.0]	13.0 [2.5]
2006-07 summer	17.8	19.2	18.4 [-0.7]	18.3 [-0.9]	19.2 [0]	19.0 [-0.1]	20.9 [1.8]	20.8 [1.6]
2007 winter	13.7	9.9	17.3 [7.3]	17.1 [7.1]	11.7 [1.7]	10.9 [0.9]	11.5 [1.5]	10.6 [0.7]
1999-00 annual mean	15.0	15.0	17.4 [2.4]	17.2 [2.2]				
2000-01 annual mean	15.9	15.1	18.0 [2.8]	17.7 [2.6]				
2001-02 annual mean	15.6	14.7	14.8 [0]	14.4 [-0.3]				
2002-03 annual mean	15.4	15.0	14.9 [-0.1]	14.6 [-0.4]	16.6 [1.5]	16.3 [1.2]		
2003-04 annual mean	14.7	14.4	16.0 [1.7]	15.8 [1.4]	16.3 [1.9]	16.0 [1.7]		
2004-05 annual mean	13.5	14.4	16.0 [1.6]	15.7 [1.3]	15.1 [0.7]	14.8 [0.4]		
2005-06 annual mean	13.8	14.6	16.5 [1.9]	16.3 [1.6]	16.5 [1.9]	16.2 [1.6]	17.3 [2.7]	17.1 [2.4]
2006-07 annual mean	15.0	14.8	16.5 [1.8]	16.3 [1.5]	15.0 [0.2]	14.7 [-0.1]	17.1 [2.3]	16.8 [2.0]

2.5.5.2. Little Swanport

Comparisons of the Little Swanport *O. angasi* $\delta^{18}O_{shell}$ temperature reconstructions with recorded temperatures are shown in Figure 2.8. The greater sampling resolution achieved in the fast-growing earlier years compared to later years of the Little Swanport *O. angasi* shells growth is clearly evident. After the first two years of shell growth, the seasonal records appear to be truncated during the summer in the older shells. The early years of growth in shells LSOa754 and LSOa756 show seasonal amplitudes equivalent to that observed in the younger shell LSOa793.

Water temperature data for the Little Swanport estuary encompassing the entirety of the older Little Swanport *O. angasi* growth were not available. An estimate of water temperatures was calculated via comparison of air temperature records from the Orford Bureau of Meteorology field station (located close to the Little Swanport site) and the water temperature in the Little Swanport estuary over the monitoring period. Assuming a constant relationship between these datasets (i.e. an offset of ~2ºC) water temperature records were constructed for the Little Swanport estuary over the last eight years for the purpose of comparison with the earlier years of growth in shells LSOa754 and LSOa756 (Table 2.5, Figure 2.8). Also shown are water temperatures obtained from the Integrated Marine Observing System-Australian National Moorings Network National Reference Station at Maria Island (IMOS platform code: NRSMAI; http://www.imos.org.au/html), which is located ~30 km from the Little Swanport estuary. Temperature at this marine location undergoes a smaller degree of temperature fluctuation than in an estuarine setting. Furthermore, the available temperature record from Maria Island is of low resolution, with the number of data points for individual years ranging between three and eight. The uncertainties

and limitations associated with these two comparative datasets preclude an in-depth interpretation, but still enable a basic comparison of the environmental temperature with the *O. angasi* $\delta^{18}O_{shell}$ records.

The Little Swanport *O. angasi* $\delta^{18}O_{shell}$-reconstructed temperatures agree well with the instrumental temperatures over the experiment period, although summer maxima are underestimated in shells LSOa754 and LSOa756 (Table 2.5, Figure 2.8). This is most likely due to the lower sampling resolution resulting from the reduced growth rate of the older shells. The consequent time-averaging of the record results in dampened peak summer temperatures. Despite this underestimation of summer temperature in the experiment period, the majority of the other summer maxima in shells LSOa754 and LSOa756 overestimate the summer maxima of the instrumental temperature record.

As mentioned previously, this truncation appears to occur consistently in the summer time of shells LSOa754 and LSOa756 after the first two years of growth, while winter $\delta^{18}O_{shell}$ values remain consistent throughout the shell (albeit with an overestimation of winter minima by ~3ºC). A number of studies discuss the effect of ontogeny upon bivalve $\delta^{18}O_{shell}$ (Krantz et al., 1987; Harrington, 1989; Krantz et al., 1989; Kennedy et al., 2001; Freitas et al., 2005; Schöne, 2008), describing the attenuation of $\delta^{18}O_{shell}$ amplitude as the animal ages. Freitas et al., (2005), in their study of the fan mussel, *Pinna nobilis*, describe this phenomenon as mainly affecting the most positive (winter) $\delta^{18}O_{shell}$ values. Goodwin et al. (2003) discuss $\delta^{18}O_{shell}$ isotopic amplitude attenuation in *Chione cortezi* as being the product of reduced growth in terms of both shorter growth periods and also a decreased volume of carbonate precipitation, whereby *C. cortezi* exhibits an ongoing reduction in the amplitude of winter $\delta^{18}O_{shell}$ peaks,

whereas summer peaks remain comparatively constant. A similar, if reversed, pattern is seen in the Little Swanport *O. angasi*.

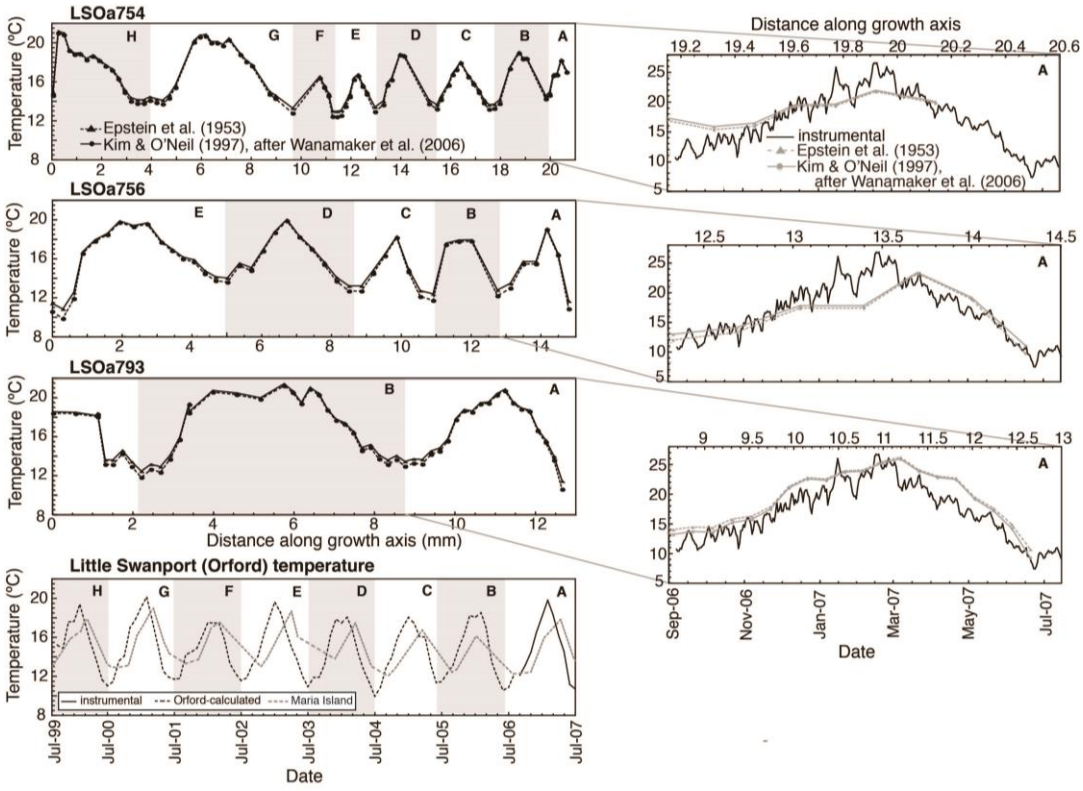

Figure 2.8. Comparison of Little Swanport *O. angasi* $\delta^{18}O_{shell}$-reconstructed temperatures with water temperatures. Water temperatures beyond the most recent year of growth were calculated via a comparison of Little Swanport temperatures over the field culture experiment period with air temperature records from Orford and water temperature records from Maria Island. The enlarged panels show comparison of $\delta^{18}O_{shell}$-reconstructed temperatures for the latest year of growth with the observed temperature during the Little Swanport *in situ* field culture experiments. All three shells show good agreement between the recorded and $\delta^{18}O_{shell}$-reconstructed temperatures, in particular, the younger shell LSOa793.

It has been suggested that bivalve $\delta^{18}O_{shell}$ may be disrupted due to biologically-induced reductions in shell growth rates or growth cessations, related to the onset of sexual maturity and gametogenesis (Romanek et al., 1987; Surge et al., 2001). However, unlike other bivalves, the sexual maturity, fecundity and reproductive cycle of *O. angasi* are variable and not restricted to certain times of the year. Furthermore, sexual maturity can be reached as early as eight months of age (S. O'Connor, personal communication, 2012). Hence, this is not a likely explanation for the underestimation of summer temperatures after the first two years of growth in the Little Swanport shells.

Other authors have attributed disequilibrium precipitation in biogenic carbonates resulting from kinetic fractionation effects (McConnaughey, 1989a; 1989b), where higher growth rates result in a greater incorporation of ^{16}O, pushing the $\delta^{18}O_{shell}$ to more negative values and the temperature record to warmer temperatures. Owen et al. (2002a) reported a significant kinetic fractionation effect upon the $\delta^{18}O_{shell}$ of *Pecten maximus*, whereby higher growth rates in the early years of growth (combined with a growth cessation at low temperatures) resulted in a more negative median $\delta^{18}O_{shell}$ value that overestimated actual median temperature by ~1.5ºC. A similar offset is seen in the Little Swanport *O. angasi*, where annual mean temperatures for the first two years of growth are overestimated in shells LSOa754 and LSOa793 by >2ºC and by nearly 2ºC in LSOa793 (Table 2.5). Further long-term calibration experiments would be required to confirm the existence of a kinetic fractionation effect in *O. angasi*.

Shells LSOa754 and LSOa756 both underestimate summer maxima in the summers of 2001–02 and 2002–03. This corresponds to a time of extreme drought in south-eastern Australia, and annual rainfall for 2002 in the Little Swanport

region was considerably below average (Australian Government Bureau of Meteorology, Little Swanport (Wineglass Cottage) field station, data from 1995–2011; http://www.bom.gov.au/climate/data). High rates of evaporation in the Little Swanport estuary may have resulted in more positive $\delta^{18}O_{water}$, which is then reflected in the underestimated $\delta^{18}O_{shell}$-derived temperatures.

The *O. angasi* from each location give consistently overestimated mean annual temperatures, by up to nearly 4ºC for the Pambula Lake (Table 2.5) and by up to ~3ºC for the Little Swanport. This could be in part due to the variable growth rates throughout the year biasing the average temperature towards warmer temperatures. These temperature offsets are similar to those reported for other oyster studies: *C. virginica* can overestimate temperature by up to 4 ºC (Surge et al., 2001); *C. gigas* by ~5 ºC (Lartaud et al., 2010; Ullman et al., 2010).

2.5.6. *O. angasi* $\delta^{18}O_{shell}$-temperature calibration

The application of different paleotemperature equations in the various studies of oyster and other bivalve $\delta^{18}O_{shell}$ studies suggests that different species can exhibit subtle differences in their $\delta^{18}O$-temperature relationships. Owen et al. (2002b) derived a $\delta^{18}O_{shell}$-temperature calibration under constrained conditions for the scallop *P. maximus*, and Wanamaker et al. (2006) calibrated the $\delta^{18}O_{shell}$-temperature relationship for *Mytilus edulis* and found slight differences between the equation they developed and other existing $\delta^{18}O$-temperature equations. Similarly, this study has found consistent offsets between the instrumental temperature record and the temperatures obtained from the *O. angasi* $\delta^{18}O_{shell}$ temperatures reconstructed from the Epstein et al. (1953) and Kim & O'Neil (1997) equations. While these temperature offsets are in a large part due to the

assumption of a constant (average) $\delta^{18}O_{water}$ value in the estuarine setting where $\delta^{18}O_{water}$ can and does vary, it is also possible that subtle differences also exist between the *O. angasi* $\delta^{18}O_{shell}$-temperature relationship and the existing $\delta^{18}O$-temperature calibrations.

Accordingly, an *O. angasi*-specific $\delta^{18}O_{shell}$-temperature calibration was calculated from a combined dataset of the Pambula Lake and Little Swanport *O. angasi* $\delta^{18}O_{shell}$. The scaling of the $\delta^{18}O_{shell}$ datasets using the AnalySeries program assigned dates to the $\delta^{18}O_{shell}$ record, and average temperatures were calculated for the time periods represented by $\delta^{18}O_{shell}$ samples. These were then matched with corresponding $\delta^{18}O_{water}$ data. Some smoothing of the Pambula Lake $\delta^{18}O_{shell}$ datasets was necessary to obtain a consistent temporal resolution with that of the $\delta^{18}O_{water}$ data. For the Little Swanport *O. angasi*, the $\delta^{18}O_{water}$ dataset was of higher resolution and so required smoothing to obtain a consistent temporal resolution with the *O. angasi* $\delta^{18}O_{shell}$ data. The calibration curve obtained for *O. angasi* is shown in Figure 9. Data corresponding to February 2007 and June 2007 for the Pambula Lake *O. angasi* were not included in the calibration calculation, as it is believed shell precipitation had ceased at these times (these data points shown as open circles in Figure 2.9a).

Despite the limitations upon this calibration resulting from the low resolution of the $\delta^{18}O_{water}$ data and the inherent uncertainties associated with the temporal designation of the $\delta^{18}O_{shell}$ data via the matching of the predicted and observed $\delta^{18}O_{shell}$ records, this calibration produces an equation similar to existing $\delta^{18}O$-temperature equations, and is represented by:

$$T\ (^{o}C) = 13.97_{(\pm 0.53)} - 3.57_{(\pm 0.85)}(\delta^{18}O_{shell} - \delta^{18}O_{water}) + 0.17_{(\pm 0.53)}(\delta^{18}O_{shell} - \delta^{18}O_{water})^2$$

$$n= 79,\ R^2 = 0.79 \qquad \text{(Eq. 2.6)}$$

where, following the method of Wanamaker et al. (2006), the $\delta^{18}O_{shell}$ is given in reference to the V-PDB scale, and the $\delta^{18}O_{water}$ on the V-SMOW scale, thus omitting the need for conversions and corrections between the different scales. The errors given for the slope and intercept are calculated at the 95 % CI and the RMSE calculated at the 95 % CI for the calibration is ±2.5 ºC. These errors are quite large, though not unexpected given the uncertainties associated with the development of this calibration. Within this error range, the calibration matches well with the existing $\delta^{18}O$-temperature equations.

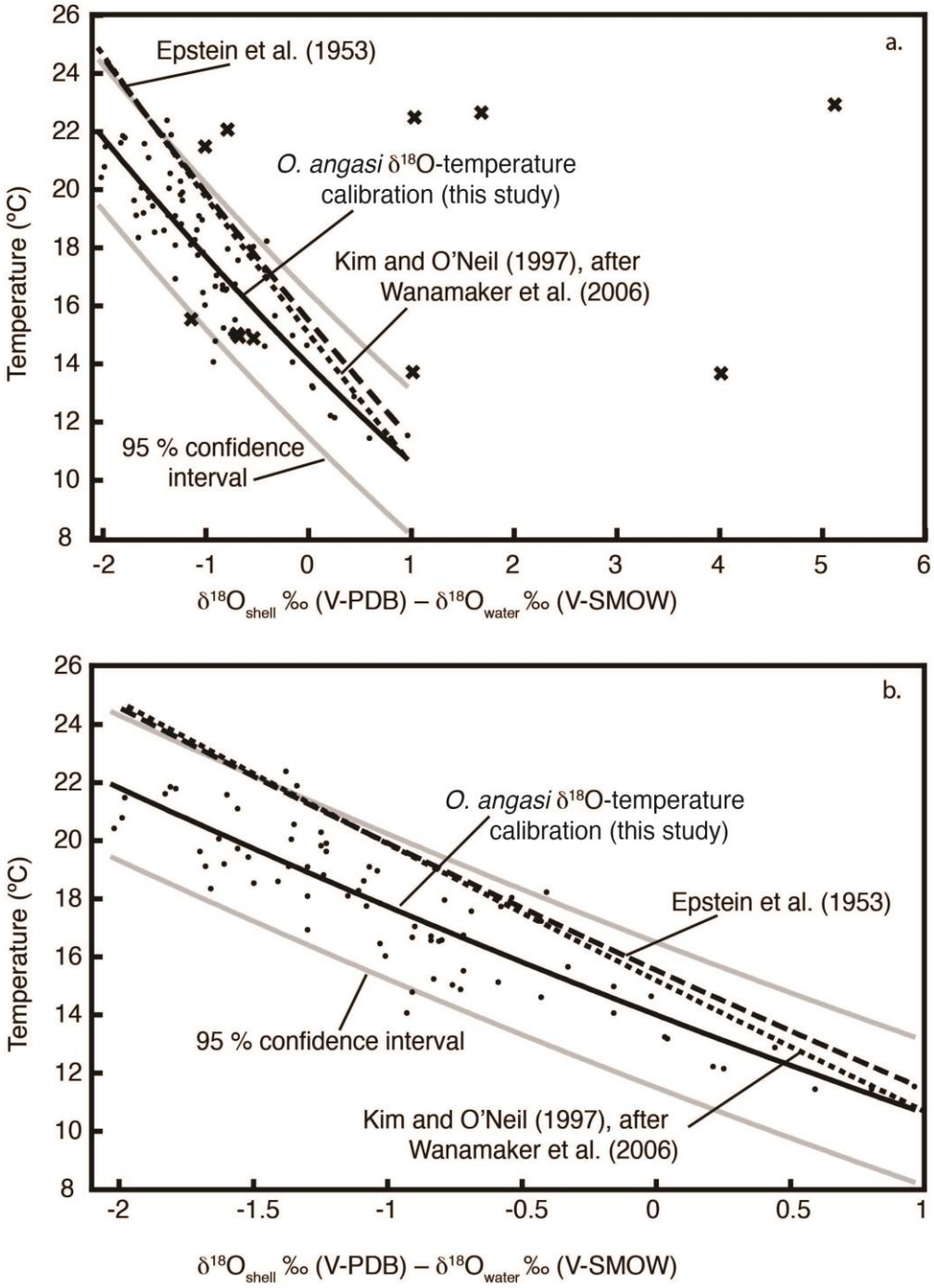

Figure 2.9. The $\delta^{18}O_{shell}$-temperature calibration curve constructed for *O. angasi*, compared with the calibrations of Epstein et al. (1953) (dashed line), Kim and O'Neil (1997, after Wanamaker et al. 2006) (dotted line) where a. includes the data points that correspond to dates for which it was assumed that no carbonate was precipitated and were omitted from the calibration, and b. shows a direct comparison of the three equations.

2.6. Conclusion—*O. angasi* shells as climate records

O. angasi $\delta^{18}O_{shell}$ is sensitive to ambient water temperature during shell calcification. However, changes in $\delta^{18}O_{water}$ associated with freshwater inputs to *O. angasi*'s estuarine habitat, along with consequent fluctuations in salinity complicate $\delta^{18}O_{shell}$ records and can bias apparent calcification temperatures by several degrees. Temperatures will also not be recorded during any low-salinity-induced growth cessations in *O. angasi*, which may occur in some locations. This makes the derivation of robust $\delta^{18}O_{shell}$-derived temperature records feasible only in environments that experience minimal salinity variation. However, in areas where rainfall is intense but sporadic, and the residence time of the estuary water is sufficiently low, a seasonal signal can be obtained from *O. angasi*. The rapid growth of the first two years of *O. angasi* growth provides a higher resolution $\delta^{18}O_{shell}$ record, with subsequent years showing truncated summer temperatures.

Given that the temperature record obtained from the *O. angasi* $\delta^{18}O_{shell}$ using the existing Epstein et al. (1953) and Kim and O'Neil (1997) equations showed consistent offsets with the instrumental temperatures, an *O. angasi*-specific $\delta^{18}O_{shell}$-temperature calibration was developed from the results of this study. This equation matches well with other published $\delta^{18}O$-temperature equations (Epstein et al., 1953; Kim and O'Neil, 1997; Wanamaker et al., 2006; 2007), albeit with errors which result in an uncertainty of ± ~2.5ºC for paleotemperature reconstruction. Further refinement of this calibration to reduce this uncertainty is desirable, however, given the prevalence of *O. angasi* throughout Holocene midden sites in Australia the calibration developed here provides a useful tool for elucidating past climates in the region, where other such records are scarce.

Acknowledgements

Funding for this study was provided by CRC LEME. Travel to the Vrije Universiteit and the University of Michigan to conduct the sampling and analysis was enabled by an ANU Vice-Chancellor Travel Grant and the Betty Mayne Scientific Research Fund for Earth Sciences from the Linnean Society of New South Wales. Thank you to Suzan Verdegaal, Hubert Vonhoff, Simon Troelstra and Emma Versteegh at the Vrije Universiteit, Amsterdam and K. C. Lohmann and Lora Wingate at the University of Michigan for invaluable assistance and discussion regarding shell sampling and isotope analysis, and Hilary Stuart-Williams at The Australian National University for water isotope analysis. Thanks also to David Ellis, Sara Beavis and Patrick De Deckker for valuable discussion throughout this project.

2.7. References

Anderson, T.F., Arthur, M.A., 1983. Stable Isotopes of Oxygen and Carbon and Their Application to Sedimentologic and Paleoenvironmental Problems, in: Arthur, M.A., Anderson, T.F., Kaplan, I.R., Veizer, J., Land, L. (Eds.), *Stable Isotopes in Sedimentary Geology*, SEPM Short Course No. 10. SEPM, Georgia, USA, pp. 1-151.

Andrus, C.F.T., Crowe, D.E., 2000. Geochemical analysis of *Crassostrea virginica* as a method to determine season of capture. *Journal of Archaeological Science* 27, 33-42.

Andrus, C.F.T., Thompson, V.D., 2012. Determining the habitats of mollusk collection at the Sapelo Island shell ring complex, Georgia, USA using oxygen isotope sclerochronology. *Journal of Archaeological Science* 39, 215-228.

Australian Government Bureau of Meteorology, 2012. Climate Data Online. http://www.bom.gov.au/climate/data/, accessed 23/5/2012.

Brigaud, B., Puceat, E., Pellenard, P., Vincent, B., Joachimski, M.M., 2008.

Climatic fluctuations and seasonality during the Late Jurassic (Oxfordian-Early Kimmeridgian) inferred from delta O-18 of Paris Basin oyster shells. *Earth and Planetary Science Letters* 273, 58-67.

Chauvaud, L., Lorrain, A., Dunbar, R.B., Paulet, Y.M., Thouzeau, G., Jean, F., Guarini, J.M., Mucciarone, D., 2005. Shell of the Great Scallop *Pecten maximus* as a high-frequency archive of paleoenvironmental changes. *Geochemistry Geophysics Geosystems* 6.

Coplen, T.B., 2007. Calibration of the calcite-water oxygen-isotope geothermometer at Devils Hole, Nevada, a natural laboratory. *Geochimica Et Cosmochimica Acta* 71, 3948-3957.

Crawford, C., Mitchell, I., 1999. Physical and chemical parameters of several oyster growing areas in Tasmania, in: Gardner, C. (Ed.), Technical Report Series. Tasmanian Aquaculture and Fisheries Institute, University of Tasmania, Tasmania.

Custer, J.F., Doms, K.R., 1990. Analysis of microgrowth patterns of the American oyster (*Crassostrea virginca*) in the middle Atlantic region of eastern North America–archaeological applications. *Journal of Archaeological Science* 17, 151-160.

Dettman, D.L., Flessa, K.W., Roopnarine, P.D., Schone, B.R., Goodwin, D.H., 2004. The use of oxygen isotope variation in shells of estuarine mollusks as a quantitative record of seasonal and annual Colorado River discharge. *Geochimica Et Cosmochimica Acta* 68, 1253-1263.

Dettman, D.L., Reische, A.K., Lohmann, K.C., 1999. Controls on the stable isotope composition of seasonal growth bands in aragonitic fresh-water bivalves (unionidae). *Geochimica Et Cosmochimica Acta* 63, 1049-1057.

Dix, T., 1980. Growth of the native oyster Ostrea angasi using raft culture in Tasmania, Australia. *Aquaculture* 19, 109-115.

Epstein, S., Buchsbaum, R., Lowenstam, H., Urey, H.C., 1951. Carbonate-water isotopic temperature scale. *Geological Society of America Bulletin* 62, 417-426.

Epstein, S., Buchsbaum, R., Lowenstam, H.A., Urey, H.C., 1953. Revised carbonate-water isotopic temperature scale. *Bulletin of the Geological Society of America* 64, 1315-1326.

Freitas, P., Clarke, L.J., Kennedy, H., Richardson, C., Abrantes, F., 2005. Mg/Ca, Sr/Ca, and stable-isotope (δ18O and δ13C) ratio profiles from the fan mussel *Pinna nobilis*: Seasonal records and temperature relationships. *Geochemistry*

Geophysics Geosystems 6.

Freitas, P.S., Clarke, L.J., Kennedy, H., Richardson, C.A., 2012. The potential of combined Mg/Ca and $\delta^{18}O$ measurements within the shell of the bivalve *Pecten maximus* to estimate seawater $\delta^{18}O$ composition. *Chemical Geology* 291, 286-293.

Friedman, I., O'Neil, J.R., 1977. Compilation of stable isotope fractionation factors of geochemical interest., in: Fleischer, M. (Ed.), *Data of Geochemistry*, 6th Edition: U.S. Geological Survey (USGS) Professional Paper 440-KK, 6th ed. United States Geological Survey, p. 12.

Gillikin, D.P., De Ridder, F., Ulens, H., Elskens, M., Keppens, E., Baeyens, W., Dehairs, F., 2005. Assessing the reproducibility and reliability of estuarine bivalve shells (*Saxidomus giganteus*) for sea surface temperature reconstruction: Implications for paleoclimate studies. *Palaeogeography Palaeoclimatology Palaeoecology* 228, 70-85.

Gonfiantini, R., Stichler, W., Rozanski, K., 1995. Standards and intercomparison materials distributed by the International Atomic Energy Agency for stable isotope measurements., Reference and intercomparison materials for stable isotopes of light elements : proceedings of a consultants meeting held in Vienna, 1-3 December 1993. International Atomic Energy Agency, pp. 13-29.

Goodwin, D.H., Flessa, K.W., Schone, B.R., Dettman, D.L., 2001. Cross-calibration of daily growth increments, stable isotope variation, and temperature in the Gulf of California bivalve mollusk *Chione cortezi*: Implications for paleoenvironmental analysis. *Palaios* 16, 387-398.

Goodwin, D.H., Schone, B.R., Dettman, D.L., 2003. Resolution and fidelity of oxygen isotopes as paleotemperature proxies in bivalve mollusk shells: Models and observations. *Palaios* 18, 110-125.

Goodwin, D.H., Cohen, A.N., Roopnarine, P.D., 2010. Forensics on the half shell: a sclerochronological investigation of a modern biological invasion in San Francisco Bay, United States. *Palaios* 25, 742-753.

Gosling, E., 2003. *Bivalve Molluscs: Biology, Ecology and Culture Fishing*. Fishing News Books, Oxford.

Grossman, E.L., Ku, T.L., 1986. Oxygen and carbon isotope fractionation in biogenic aragonite – temperature effects. *Chemical Geology* 59, 59-74.

Harding, J.M., Spero, H.J., Mann, R., Herbert, G.S., Sliko, J.L., 2010. Reconstructing early 17th century estuarine drought conditions from Jamestown

oysters. *Proceedings of the National Academy of Sciences of the United States of America* 107, 10549-10554.

Harrington, R.J., 1989. Aspects of the growth deceleration in bivalves – clues to understanding the seasonal δ18O and δ13C record – a comment. *Palaeogeography Palaeoclimatology Palaeoecology* 70, 399-403.

Heasman, M., Diggles, B.K., Hurwood, D., Mather, P., Pirozzi, I., Dworjanyn, S., 2004. Paving the way for continued rapid development of the flat (angasi) oyster (*Ostrea angasi*) farming industry in New South Wales, NSW Final Report Series, New South Wales.

Hong, W., Keppens, E., Nielsen, P., Vanriet, A., 1995. Oxygen and Carbon-Isotope Study of the Holocene Oyster Reefs and Paleoenvironmental Reconstruction on the Northwest Coast of Bohai Bay, China. *Marine Geology* 124, 289-302.

Hut, G., 1987. Report to the Director General, Consultants group meeting on stable isotope reference samples for geochemical and hydrological investigations. International Atomic Energy Agency, Vienna, p. 42.

Integrated Marine Observing System 2012, Australian Government National Collaborative Research Infrastructure Strategy Australian Government Super Science Initiative CSIRO Tasmanian Marine Analysis Network CSIRO Tasmanian ICT Centre. http://www.imos.org.au/html, date accessed 23/5/2012.

Kennedy, H., Richardson, C.A., Duarte, C.M., Kennedy, D.P., 2001. Oxygen and carbon stable isotopic profiles of the fan mussel, *Pinna nobilis*, and reconstruction of sea surface temperatures in the Mediterranean. Marine Biology 139, 1115-1124.

Kim, S.T., Oneil, J.R., 1997. Equilibrium and nonequilibrium oxygen isotope effects in synthetic carbonates. *Geochimica Et Cosmochimica Acta* 61, 3461-3475.

Kirby, M.X., Soniat, T.M., Spero, H.J., 1998. Stable isotope sclerochronology of pleistocene and recent oyster shells (*Crassostrea virginica*). *Palaios* 13, 560-569.

Krantz, D.E., Jones, D.S., Williams, D.F., 1989. Aspects of growth deceleration in bivalves – clues to understanding the seasonal δ18O and δ13C record – reply. *Palaeogeography Palaeoclimatology Palaeoecology* 70, 403-407.

Krantz, D.E., Williams, D.F., Jones, D.S., 1987. Ecological and paleoenvironmental information using stable isotope profiles from living and fossil mollusks. *Palaeogeography Palaeoclimatology Palaeoecology* 58, 249-

266.

Lartaud, F., Emmanuel, L., de Rafelis, M., Ropert, M., Labourdette, N., Richardson, C.A., Renard, M., 2010. A latitudinal gradient of seasonal temperature variation recorded in oyster shells from the coastal waters of France and The Netherlands. *Facies* 56, 13-25.

Lécuyer, C., Reynard, B., Martineaua, F., 2004. Stable isotope fractionation between mollusc shells and marine waters from Martinique Island. *Chemical Geology* 213, 293-305.

Lourandos, H., 1968. Dispersal of Activities - the East Tasmanian Aboriginal Sites. *Papers and Proceedings of the Royal Society of Tasmania* 102, 41–46.

MacFarlane, G.R., Markich, S.J., Linz, K., Gifford, S., Dunstan, R.H., O'Connor, W., Russell, R.A., 2006. The Akoya pearl oyster shell as an archival monitor of lead exposure. *Environmental Pollution* 143, 166-173.

McConnaughey, T., 1989a. C-13 and O-18 isotopic disequilibrium in biological carbonates 1. Patterns. *Geochimica Et Cosmochimica Acta* 53, 151–162.

McConnaughey, T., 1989b. C-13 and O-18 isotopic disequilibrium in biological carbonates 2. Invitro simulation of kinetic isotope effects. *Geochimica Et Cosmochimica Acta* 53, 163–171.

Milner, N., 2002. *Incremental Growth of the European Oyster Ostrea Edulis*. Archaeopress, Oxford.

Mitchell, I.M., Crawford, C.M., Rushton, M.J., 2000. Flat oyster (*Ostrea angasi*) growth and survival rates at Georges Bay, Tasmania (Australia). *Aquaculture* 191, 309-321.

Morton, B., Lam, K., Slack-Smith, S., 2003. First report of the European flat oyster *Ostrea edulis*, identified genetically, from Oyster Harbour, Albany, south-western Western Australia. *Molluscan Research* 23, 199-208.

Mouchi, V., de Rafélis, M., Lartaud, F., Fialin, M., Verrecchia, E., 2013. Chemical labelling of oyster shells used for time-calibrated high-resolution Mg/Ca ratios: A tool for estimation of past seasonal temperature variations. *Palaeogeography, Palaeoclimatology, Palaeoecology* 373, 66-74.

Nell, J.A., 2001. The history of oyster faming in Australia. *Marine Fisheries Review*.

Nell, J.A., Gibbs, P.J., 1986. Salinity tolerance and absorption of L-methionine by some Australian bivalve mollusks. *Australian Journal of Marine and Freshwater Research* 37, 721–727.

NSW Government Office of Environment and Heritage, 2012. Estuaries of NSW: Physical characteristics, tidal surveys and hydrographic surveys, Pambula River. http://www.environment.nsw.gov.au/estuaries/stats/PambulaRiver.htm, accessed 22/1/2013

Owen, R., Kennedy, H., Richardson, C., 2002a. Experimental investigation into partitioning of stable isotopes between scallop (*Pecten maximus*) shell calcite and sea water. *Palaeogeography Palaeoclimatology Palaeoecology* 185, 163-174.

Owen, R., Kennedy, H., Richardson, C., 2002b. Isotopic partitioning between scallop shell calcite and seawater: Effect of shell growth rate. *Geochimica Et Cosmochimica Acta* 66, 1727-1737.

Romanek, C.S., Jones, D.S., Williams, D.F., Krantz, D.E., Radtke, R., 1987. Stable isotopic investigation of physiological and environmental changes recorded in shell carbonate from the giant clam *Tridacna maxima*. Marine Biology 94, 385–393.

Schöne, B.R., 2003. A clam-ring master-chronology constructed from a short-lived bivalve mollusc from the northern Gulf of California, USA. *Holocene* 13, 39-49.

Schöne, B.R., Tanabe, K., Dettman, D.L., Sato, S., 2003. Environmental controls on shell growth rates and delta O-18 of the shallow-marine bivalve mollusk *Phacosoma japonicum* in Japan. *Marine Biology* 142, 473-485.

Schöne, B.R., Dunca, E., Mutvei, H., Norlund, U., 2004. A 217-year record of summer air temperature reconstructed from freshwater pearl mussels (*M. margarifitera*, Sweden) (vol 23, p 1803, 2004). *Quaternary Science Reviews* 23, 2057-2057.

Schöne, B.R., Oschmann, W., Tanabe, K., Dettman, D., Fiebig, J., Houk, S.D., Kanie, Y., 2004. Holocene seasonal environmental trends at Tokyo Bay, Japan, reconstructed from bivalve mollusk shells - implications for changes in the East Asian monsoon and latitudinal shifts of the Polar Front. *Quaternary Science Reviews* 23, 1137-1150.

Schöne, B.R., Fiebig, J., Pfeiffer, M., Gless, R., Hickson, J., Johnson, A.L.A., Dreyer, W., Oschmann, W., 2005. Climate records from a bivalved Methuselah (*Arctica islandica*, Mollusca; Iceland). *Palaeogeography Palaeoclimatology Palaeoecology* 228, 130-148.

Schöne, B.R., 2008. The curse of physiology - challenges and opportunities in the interpretation of geochemical data from mollusk shells. *Geo-Marine Letters* 28, 269-285.

Surge, D., Lohmann, K.C., Dettman, D.L., 2001. Controls on isotopic chemistry of the American oyster, *Crassostrea virginica*: implications for growth patterns. *Palaeogeography Palaeoclimatology Palaeoecology* 172, 283-296.

Surge, D.M., Lohmann, K.C., Goodfriend, G.A., 2003. Reconstructing estuarine conditions: oyster shells as recorders of environmental change, Southwest Florida. *Estuarine Coastal and Shelf Science* 57, 737-756.

Sullivan, M., 1982. *Aboriginal shell middens in the coastal landscape of New South Wales*. PhD Thesis, The Australian National University, Canberra, p. 284.

Tarutani, T., Clayton, R.N., Mayeda, T.K., 1969. Effect of polymorphism and magnesium substitution on oxygen isotope fractionation between calcium carbonate and water. *Geochimica Et Cosmochimica Acta* 33, 987–996.

Taylor, A.J., 1892. Notes on the Shell-Mounds at Seaford, Little Swanport. *Papers and Proceedings of the Royal Society of Tasmania*.

Thebault, J., Chauvaud, L., Clavier, J., Guarini, J., Dunbar, R.B., Fichez, R., Mucciarone, D.A., Morize, E., 2007. Reconstruction of seasonal temperature variability in the tropical Pacific Ocean from the shell of the scallop, *Comptopallium radula*. *Geochimica Et Cosmochimica Acta* 71, 918-928.

Titschack, J., Zuschin, M., Spotl, C., Baal, C., 2010. The giant oyster *Hyotissa hyotis* from the northern Red Sea as a decadal-scale archive for seasonal environmental fluctuations in coral reef habitats. *Coral Reefs* 29, 1061-1075.

Ullmann, C.V., Wiechert, U., Korte, C., 2010. Oxygen isotope fluctuations in a modern North Sea oyster (*Crassostrea gigas*) compared with annual variations in seawater temperature: Implications for palaeoclimate studies. *Chemical Geology* 277, 160-166.

Versteegh, E.A.A., Vonhof, H.B., Troelstra, S.R., Kroon, D., 2011. Can shells of freshwater mussels (Unionidae) be used to estimate low summer discharge of rivers and associated droughts? *International Journal of Earth Sciences* 100, 1423–1432.

Wanamaker, A.D., Kreutz, K.J., Borns, H.W., Introne, D.S., Feindel, S., Barber, B.J., 2006. An aquaculture-based method for calibrated bivalve isotope paleothermometry. *Geochemistry Geophysics Geosystems* 7, 13.

Wanamaker, A.D., Kreutz, K.J., Borns, H.W., Introne, D.S., Feindel, S., Funder, S., Rawson, P.D., Barber, B.J., 2007. Experimental determination of salinity, temperature, growth, and metabolic effects on shell isotope chemistry of *Mytilus edulis* collected from Maine and Greenland. Paleoceanography 22, 12.

Chapter 3

Late Holocene inter-annual temperature variability reconstructed from the $\delta^{18}O$ of archaeological *Ostrea angasi* shells.

This paper was published in *The Australian Journal of Earth Sciences* 2017, 64(6) pp 779-791

Slight differences exist between this chapter and the published paper; the published version is included as Appendix 4.

Authors and contributions:

Sarah Tynan: 85% conceived study, conducted field work, sampling and data analysis

Bradley Opdyke 5% overarching guidance and support, feedback on written drafts

Maureen Walczak 5% overarching guidance and support, feedback on written drafts

Andrea Dutton 5% overarching guidance and support, feedback on written drafts

ABSTRACT

Two multi-year oxygen isotope ($\delta^{18}O$) records were obtained from archaeological *Ostrea angasi* shells. High-resolution $\delta^{18}O_{shell}$ samples from the *O. angasi* clearly display seasonal variability, confirming the potential of this species to provide valuable environmental records for the late Holocene period in southeastern Australia and offer insight into past climate conditions in a region where such information is presently limited.

The oxygen isotope record in *O. angasi* reflects a combined temperature-salinity signal. Observations of $\delta^{18}O_{shell}$ data from modern specimens are used as a point of reference to assist in decoupling these two influences, with the two archaeological samples compared to the $\delta^{18}O_{shell}$ profile of four modern *O. angasi*. Assuming similar paleo-$\delta^{18}O_{water}$ values at the collection sites, data from these archaeological shells present a record of temperatures during the period of their growth that are consistently lower than modern day, with mean annual temperatures ~2 ºC cooler.

Key words: oyster, *Ostrea angasi*, $\delta^{18}O$, salinity, paleoclimate, late Holocene, midden

3.1. Introduction

3.1.1. Late Holocene climate in southeast Australia

Recent reviews have highlighted the paucity of Holocene climate records for the Australian region (Neukom and Gergis 2012; Reeves et al. 2013). Indeed, there is only a single high-resolution paleoclimate record spanning the Holocene: namely, a tree-ring record from Tasmania (Cook et al. 2000). There are several other dendrochronology studies from Tasmania but mainland Australia lacks the long-lived tree species suitable for obtaining these records (Barr et al. 2014).

Lower-resolution (centennial to millennial-scale) late Holocene records for southeast Australia are also scarce and geographically scattered. A sedimentation record from Barrington Tops in northern New South Wales suggests that the early Holocene was wetter and warmer, and at ~3500–3000 years before present (BP) conditions became cooler and drier than present (Dodson 1987). Evidence for a wetter early–mid Holocene period ~9000–6000 years BP, followed by a shift to drier conditions following ~6000 years BP was also found in a lacustrine core from Little Llangothlin Lagoon by Woodward et al. (2014).

Further south, a sedimentary record from Lake Keilambete in southwestern Victoria indicates a wetter climate at ~2000–1800 years BP, followed by cooler and drier conditions from ~1750–1425 years BP (Bowler 1981; Mooney 1997). More recent work from Lake Keilambete, as well as two additional inland lakes in southwestern Victoria (Lake Gnotuk and Lake Bullenmerri) show high lake water levels at ~7200 years BP, indicating higher precipitation in the early Holocene. This is supported by speleothem records from Lynds Cave in northern Tasmania, which also indicate that the early Holocene was a time of increased precipitation (Xia et al. 2001). The Victorian lake levels

then drop during the mid-Holocene, oscillate around modern levels from ~5000 years BP onwards, and reach a minimum during the late Holocene: ~1800 years BP in Lake Keilambete, and ~1300 years BP in Lake Gnotuk (De Deckker 1982; Wilkins et al. 2013). Wilkins et al. (2013) suggested that these lake records reflected the Holocene precipitation regime, with the low lake levels indicative of reduced precipitation. Comparison with other records led them to surmise that this precipitation regime was connected to cooler temperatures.

Further evidence for reduced southeast Australian precipitation in the late Holocene comes from a study of Port Phillip Bay, in southern Victoria, which suggests that the bay dried out sometime between ~2800 and ~1000 years BP (Holdgate et al. 2011). The trend of higher precipitation during the early Holocene, followed by a shift to a drier late Holocene is also corroborated by studies from Lake George, in the southeastern highlands of New South Wales, which indicate conditions were significantly wetter during the early and middle Holocene, with a shift at ~2500 years BP to drier and more variable conditions, similar to those of the present day (Coventry 1976; Fitzsimmons and Barrows 2010). In apparent contrast, records from Blue Lake, in southeastern South Australia, provide evidence of a variable evaporation/precipitation regime during the late Holocene (Gouramanis et al. 2010), with wetter conditions at ~2000 years BP.

The southeastern Australia region is beyond the range of tropical and sub-tropical corals, and the limited extent of the continental shelf precludes obtaining marine sediment cores, meaning that there are few studies that provide a marine perspective on Holocene climate for this region. An exception is a study of relic assemblages of marine species from the Port Hacking region of New South Wales, which found evidence for sea surface temperatures cooler than present day

at ~2400 years BP (Baker et al. 2001). Cooler temperatures on land were implicated for a shift to alpine vegetation in the Micalong Swamp region, in the southern tablelands of New South Wales at 2700–900 years BP (Kemp and Hope 2014).

It is noteworthy that the majority of available research to date on southeastern Australian climate history consists primarily of discrete qualitative observations. A new climate archive for southeastern Australia that affords the potential for independently-dated and quantitative estimates of environmental variability from a marine perspective would be a significant contribution to knowledge of Holocene climate variability. One potential and as-yet-unexplored source of Australian climate information is the sclerochronological records of mollusc shells, i.e. the archives of ambient environmental conditions that are recorded in the physical (growth increment size and periodicity) and geochemical ($\delta^{18}O$ and trace element) characteristics of the shell, neatly embedded in a temporal context as the animal's shell grows incrementally over the course of its lifetime (see Schöne and Gillikin 2013 and Schöne and Surge 2014 for reviews of molluscan sclerochronology).

A number of studies have illustrated how modern climatic conditions are reflected in the $\delta^{18}O_{shell}$ of various oyster species. Tynan et al .(2014) showed that the $\delta^{18}O$ of the shell of *Ostrea angasi*, the native mud or flat oyster, endemic to southeastern Australia, recorded seasonal variation in calcification temperatures. Milner (2001; 2002) investigated the growth structures of the European oyster *Ostrea edulis* and used these to determine the season of death, a useful application for studies of archaeological specimens. The growth structures and $\delta^{18}O$ signals within shells of the American oyster, *Crassostrea virginica,* have been extensively studied and compared to the modern shells to Pleistocene specimens

of the *C. virginica* (Kirby et al. 1998) and Oligocene specimens of *Crassostrea gigantissima* (Kirby 2000) to assess how growth patterns in the oyster have changed and evolved over time.

Surge et al. (2001) also studied the stable isotope signals within the shell of *C. virginica* and then used these signals to interpret environmental changes within an estuarine system in Florida (Surge et al 2003). Studies of *Crassostrea gigas* by Ullmann et al. (2010) and Ullmann et al. 2013 assess the integrity of the environmental control of $\delta^{18}O$, $\delta^{13}C$ and trace element incorporation in the shell and confirm the reliability of this species to record ambient environmental conditions. Hong et al. (1995) use the isotopic records within *C. gigas* specimens to infer environmental change during the mid-Holocene. Both of these species were also examined by Mouchi et al. (2013) who calibrated the $\delta^{18}O$ and Mg/Ca signals for oysters from different locations.

The $\delta^{18}O$ within the shell of the giant tropical oyster *Hyotissa hyotis* was assessed by Titschack et al. (2010) and was also found to provide a good record of sea surface temperature, albeit the authors caution that local environmental dynamics can cause departures from expected equilibrium $\delta^{18}O$ fractionation and this must be taken into account in paleoenvironmental studies.

With several such studies confirming that the $\delta^{18}O_{shell}$ of various oyster species do indeed record ambient environmental conditions, records from fossil or archaeological specimens can be used for paleoenvironmental reconstructions (e.g. Hong et al. 1995; Kirby et al. 1998; Milner 2002; Brigaud et al. 2008; Harding et al. 2010; Brockwell et al. 2013; Mouchi et al. 2013; Bougeois et al. 2014; Bougeois et al. 2016; Twaddle et al. 2016). This paper presents a temperature record derived from the $\delta^{18}O_{shell}$ of archaeological specimens of *O. angasi* as a promising potential source of Holocene climate information.

3.1.2. Middens as sources of environmental information

Archaeological shell middens, also known as kitchen middens or more descriptively as ‘shell heaps’, represent accumulations of shells and/or bones and other debris or artefacts resulting from human activity. Middens represent dedicated marine subsistence economies or flexible coastal subsistence (Rowland and Ulm, 2012, and references therein). As the shell species found in midden sites are generally of local origin, they can provide a range of information representative of that local area and the people that collected them (e.g. Burchell et al. 2013; Prendergast et al. 2016).

Some midden studies have examined how changes in the dominant species of shellfish within the stratigraphy of a midden can offer information about the prevailing environmental conditions, as different species of shellfish have different environmental tolerances and inhabit different habitats (e.g. Sandweiss et al. 1996). Analysis of the individual shellfish found within a midden can also yield significant cultural information. It has been suggested that the size of midden shells can offer insight into resource use and management; a distinct shift to smaller shell sizes throughout the midden stratigraphy could indicate a change in environmental factors that control the shell growth and maximum size and/or signify the collection of smaller animals as a result of increased exploitation by humans (e.g. Bailey et al. 1983; Walton 2012; Zangrando et al. 2017). There have also been a number of studies that focus upon the seasonality of shellfish collection and midden creation. The fact that shellfish resources are often available all year round does not necessarily mean that they would have been

continually harvested. For various reasons, many midden sites were occupied only at particular times of the year (Shackleton 1973; Killingley 1981; Sullivan 1982).

The microstructures within shells and the information provided by $\delta^{18}O_{shell}$ analysis have been used to estimate the season of death of the shellfish and thus the time of collection and site occupation (Shackleton 1973; Bailey 1975; Killingley 1981, 1983; Deith 1986; Talma et al. 1992; Andrus and Crowe 2000; Milner 2002; Mannino et al. 2003). Generally, the season of death is inferred from a high-resolution $\delta^{18}O_{shell}$ signal, which varies as a function of changes in temperature and/or salinity on a seasonal timescale. For example, a study of archaeological clam (*Polymesoda radiata*) shells from the south Pacific coast of Mexico, where the tropical water temperatures do not exhibit significant seasonal variation, the $\delta^{18}O_{shell}$ record was linked to changes in estuarine salinity, which changes during the rainy season (Kennett and Voorhies 1996).

A study of shells of the American oyster, *Crassostrea virginica*, found in abandoned well sites in the Chesapeake Bay area of the eastern United States, used the $\delta^{18}O_{shell}$ profiles of the oysters to reconstruct the environmental conditions from the early 1600s and identified the response of early European settlers' of the area to conditions of drought during that time (Harding et al. 2010). Another study has also used *C. virginica* from a Late Archaic shell ring site on the coast of Georgia, USA, to determine the provenance of the shellfish and infer foraging behaviours (Andrus and Thompson 2012). However, there have been very few studies as yet examining the sclerochronological record of mollusc shells within midden sites in Australia (e.g. Godfrey 1988; Brockwell et al. 2013).

3.1.3. Midden characteristics and distribution along the southeastern coast of Australia

Aboriginal midden sites are ubiquitous along the Australian coastline, with a chronological perspective that spans the Holocene (Bailey 1975; Sullivan 1982; Nell 2001), although it has been noted more recently that the majority of sites are younger than ~2000 yrs BP (Rowland and Ulm 2012). They represent areas of great cultural importance, providing evidence of occupation, sustained resource management and insights into the practices and rituals of the people that created them. Sullivan (1982) reports that the New South Wales coast alone has at least 801 midden sites and there are 6325 New South Wales midden sites recorded in the Aboriginal Heritage Information Management System maintained by the New South Wales Department of Environment (http://www.environment.nsw.gov.au /licences/AboriginalHeritageInformationManagementSystem.htm). However, not all sites are easily recognisable, and many have been significantly altered and damaged by natural weathering and erosion as well as changes in land use and development since European settlement. Some midden sites were also exploited as a source of shell for the creation of lime (Taylor 1891; Sullivan 1982; Nell 2001).

Midden accumulations are generally above ground level, with any burial being the result of more recent sedimentation processes. Many middens have a mounded morphology, which generally correlates with the content of the midden being dominantly or wholly shells of estuarine species. Midden locations are not arbitrary: they represent the deliberate repeated use of a place with favourable environmental conditions. Most middens are found in very close proximity to the exploited shell populations (Lourandos 1968). Thus, it can be assumed that the

provenance of bivalve shells found within a midden is local, and any climatic information procured from analysis of their shells will be representative of the area.

Tasmanian middens are primarily composed of *Ostrea angasi* (the Australian flat oyster, or mud oyster) shells, as are those in southern mainland Australia. Progressively further north, *O. angasi* diminishes in prevalence in the midden sites, and *Saccostrea glomerata* (the Sydney Rock oyster) becomes the dominant estuarine species (Nell 2001). This pattern broadly reflects the modern day distribution of the oysters. *Mytilus galloprovincialis* (the common blue mussel) is also found in many middens throughout New South Wales (Sullivan 1982). Some of the taxonomic differences in middens along the New South Wales coast are related to substrate, with the northern New South Wales coast middens dominated by estuarine and beach species, while in the southern New South Wales middens rock platform species are more important, reflecting the varied morphology of the New South Wales coastline.

3.2. Study site

3.2.1. Ostrea angasi

Ostrea angasi is found along the eastern and southern coastlines of Australia, and inhabits estuarine and near shore environments. The oyster can tolerate salinities of 20–45, with a preferred range of 26–36 (Nell & Livanos, unpublished data, in Nell & Gibbs 1986; reported in g l^{-1}). Unlike many other oysters, *O. angasi* usually lives on top of soft sediment, rather than cemented to a hard substrate. Previous work has determined that *O. angasi* $\delta^{18}O_{shell}$ can be used to determine

water temperature (Tynan et al. 2014). Well-preserved sub-fossil shells of *O. angasi*, or shells excavated from Aboriginal midden sites therefore have the potential to provide a valuable calibrated archive of past environmental conditions.

Two shells are analysed in this study: SBOa001 and SBOa004, from an Aboriginal midden site located at Severs Beach on the Pambula River, New South Wales (New South Wales Parks and Wildlife Cultural Heritage Database site number: 62-6-0012). These shells were excavated by Marjorie Sullivan in 1979 as part of a detailed examination of the midden (Sullivan 1982). Although two shells is a small sample size, both the labour intensive sampling method and constraints surrounding the excavation and subsequent destruction through sampling of items of a culturally significant nature precluded the use of a greater number of shells in this investigation into the viability of archaeological *O. angasi* as paleotemperature archives.

The shells used in this study were part of the collection from the Severs Beach Midden that is now in the possession of the Australian Museum. The shells were sampled with the permission of the Australian Museum, the New South Wales Office of Environment and Heritage, and in consultation with the Eden Local Aboriginal Land Council.

3.2.2. The Severs Beach Midden, Pambula River

The mouth of the Pambula estuary is located on the southern end of Pambula Beach, and the Pambula River travels ~5 km before opening into Pambula Lake, which is fed by both the Yowaka and Pambula rivers (Figure 3.1). Pambula Lake is a tidal lake with residence time of ~1.5 days (Tynan et al. 2014), and the Pambula River mouth is an unconstricted estuary. As such, predominantly marine conditions persist within Pambula River up to and including Pambula Lake.

The lake is vegetated predominantly with mangroves, and the banks of the river near the Severs Beach midden site are lined with sclerophyll forest, including tea tree scrub and gum trees (*Eucalyptus muellarana* and *E. gummifera*), along with introduced and native grasses (*Lomandra longifolia*). Some small-scale farming occurs within the Pambula River catchment area, but the flow regime of the Pambula and Yowaka rivers has not been significantly impacted by anthropogenic activities.

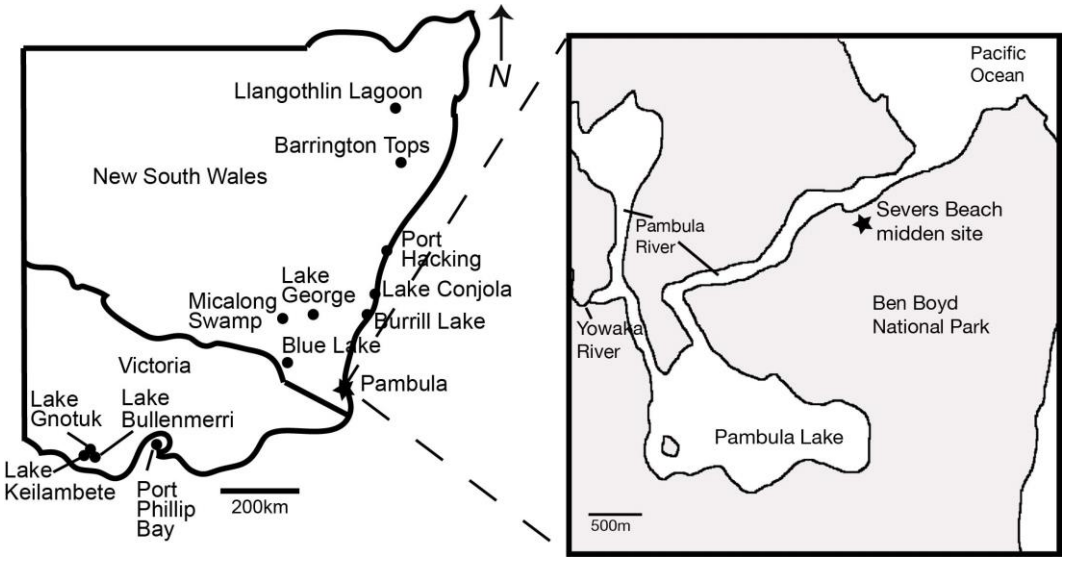

Figure 3.1. Location map, showing the sites of late Holocene climate data and the midden at Severs Beach, Pambula River.

Midden sites of various sizes are found along the banks of both the Pambula River and Lake. The sites were first described by William Anderson, a geological surveyor, who identified 17 sites in 1890, then revisited by Marjorie Sullivan in 1978, who identified another four sites. Sullivan excavated one of these middens, the Severs Beach complex, and carried out a comprehensive examination of one particular mound, called the PLA mound. Following is a brief summary of her findings and conclusions, as reported in her PhD Thesis (1982).

The entire Severs Beach complex covers an area of around 4000 m^2, with several mounds of various sizes, ranging from <1 m to >10 m in diameter. The estimated volume of the site is 20,000 m^3. The site is now largely covered by honeyrush and introduced grasses. There is evidence of rabbit activity in the area, and a section of the mound had been disturbed. Upon excavation of a trench 1 m x 0.5 m x 1.2 m deep, within the PLA mound, the midden was divided into three main sections (upper, middle, lower) based primarily on the dominant shellfish species present (Sullivan 1982).

Radiocarbon dating analysis was conducted by Sullivan (1982) at the Australian National University on shell and charcoal samples from various depths within the midden. Shell radiocarbon dates were corrected for the marine reservoir environmental effect by subtracting 450±80 years, after Gillespie and Temple (1977). Ages ranged from 2700±175 years at 90–100 cm depth to 90±80 years at 0–25 cm depth. The region of the midden where the two shells in this study were located contained a charcoal sample that was dated at 1850 years old ±80 years. We assume the incorporated charcoal is contemporaneous with the harvest and consumption of the shells of this study. As such, the shells within the midden present a record of climatic conditions in southeast Australia for a time period for which very little other data currently exists in the literature (PAGES 2k Consortium, 2013; Reeves et al. 2013).

The upper section (0–40 cm deep) contains mainly *Mytilus galloprovincialis* (Sullivan's classification: *Mytilus planulatus*) (blue mussel) shells, with a few *Trichomya hirsutus* (hairy mussel) shells, and was dated at ~1200 years old. The middle section (~40–95 cm deep) is predominantly comprised of *T. hirsutus*, with appreciable amounts of *O. angasi*, and spans the period of ~1200–2300 years old. This section also contains discrete lenses of each

T. hirsutus and *O. angasi* shells, probably indicative of specific shellfish gathering events. *O. angasi* dominates the lower section (~95–120 cm deep), which ranges from ~2300–3000 years old. The general distribution of bivalves throughout the entire midden is ~4.5% *O. angasi*, ~2.5% *Sassostrea glomerata* (Sullivan's classification: *Crassostrea commercialis*) ~18% *M. galloprovincialis*, ~67.4% *T. hirsutus*, and ~7.6% other species.

The stratigraphy demonstrates that for the first ~700 years of occupation of the site, *O. angasi* was the dominant shellfish species exploited. This was followed by ~1100 years of *T. hirsutus* combined with *O. angasi*, then in the last ~1200 years *M. galloprovincialis* was most important. The driver behind this change is not clear, though similar shifts are seen in other New South Wales midden sites, and they seem to correspond with the timing of the introduction of the use of fish hooks (Sullivan 1982).

Sullivan (1982) concluded that the Severs Beach midden represents an occupation site, as opposed to a dinner-time camp or shell refuse site. This is indicated by the relatively high number of stone artefacts also found within the midden, which would have been carried into the site from elsewhere. Additionally, the presence of a range of fish of different sizes and species, that show distinct seasonal patterns today, suggests that the site was used all year round (Sullivan 1982). A comprehensive analysis of a large number of shells from the midden site could provide further insight into this question, as it may be possible to infer a consistent season of death (and therefore capture and consumption) of the shellfish. Sullivan (1982) also provides a synopsis of the ethnographical information available for the Pambula Lake region and while there are several accounts of mens' fishing activities, there is no mention of shellfish collection.

3.3. Methods

3.3.1. Shell sampling and analysis

O. angasi exhibits visible growth increments, but does not contain any structures that have a clear temporal association with the timing of carbonate deposition within the shell. Despite this, high-resolution profiles of the $\delta^{18}O_{shell}$ of modern *O. angasi* from New South Wales and Tasmania contain a clear seasonal signal (Tynan et al. 2014). The two shells that are the focus of this study, SBOa001 and SBOa004, are shown in Figure 3.2, along with cross sections of their hinge regions, which is the most consolidated region of the shell and contains the full range of growth increments for high-resolution sampling (e.g. Surge et al. 2001).

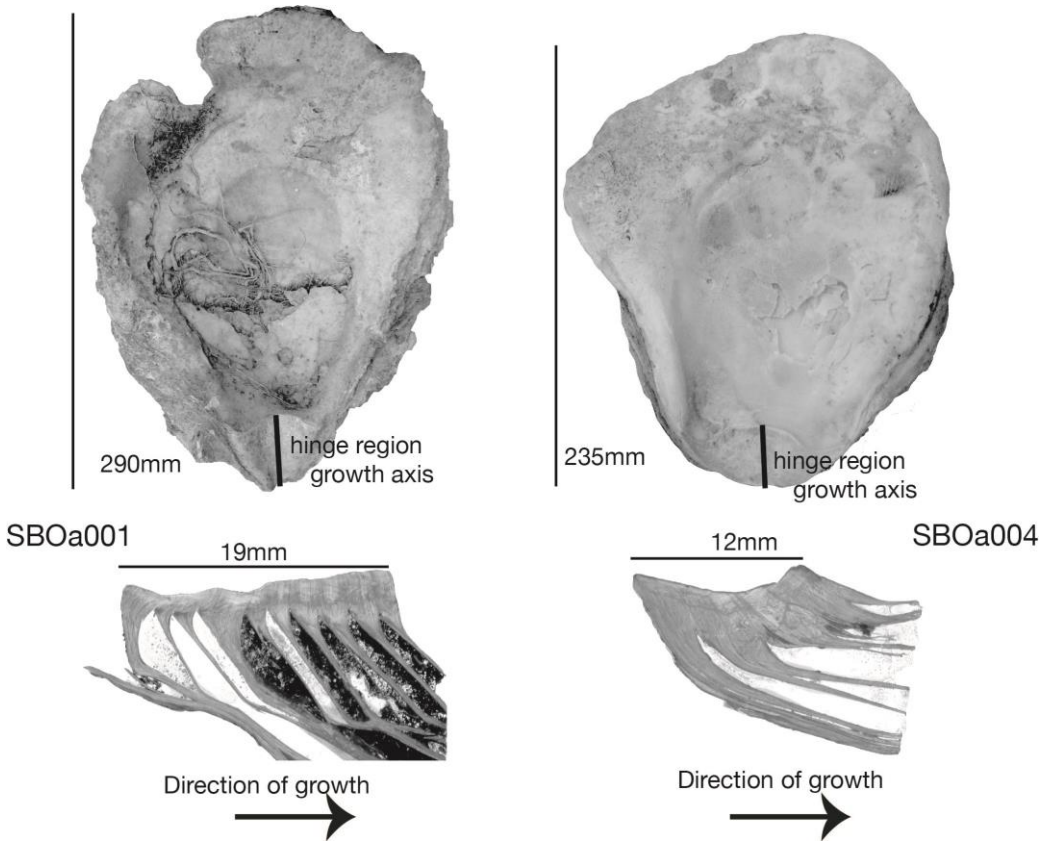

Figure 3.2. Images of the entire shells of SBOa001 and SBOa004 and cross sections of the hinge regions. Sampling was conducted by milling consecutive transects parallel to growth layers, perpendicular to the direction of growth in the hinge.

Sampling and analysis for stable oxygen and carbon isotopes were conducted at the University of Michigan, Ann Arbor. Samples were collected using a Merchantek Micromill by milling powder from incremental paths ~400 µm apart, parallel to the visible growth increments and perpendicular to the growth axis within the hinge region of the oyster. As such, a series of temporally sequential samples were obtained for analysis. Shell SBOa001 yielded 38 samples for analysis; 30 samples were obtained from SBOa004.

Samples of a minimum weight of 10 µg were roasted at 200°C *in vacuo* for one hour to remove volatile contaminants and water, then placed in individual borosilicate reaction vessels and reacted at 77±1°C with 4 drops of anhydrous phosphoric acid for 8 minutes in a Finnigan MAT Kiel IV preparation device coupled directly to the inlet of a Finnigan MAT 253 triple collector isotope ratio mass spectrometer. O^{17}-corrected data account for acid fractionation and source mixing by calibration to a best-fit regression line defined by two NBS standards, NBS 18 and NBS 19. Precision and accuracy of data were monitored through daily analysis of a variety of at least four powdered carbonate standards. Results are reported in standard δ-notation, relative to VPDB, with measured precision of better than 0.1‰.

3.3.2. Comparison with modern *O. angasi* $\delta^{18}O_{shell}$

The estuarine habitat of *O. angasi* can undergo a degree of localised environmental variability that does not necessarily reflect the open marine environment. Additionally, shell precipitation may cease if the oyster experiences unfavourable conditions, such as a pulse of freshwater. As such, comparison with a local modern analogue that can be presumed to have experienced similar environmental conditions offers the most robust method of interpreting the

$\delta^{18}O_{shell}$-temperature record from archaeological shells. Ideally, this would be done in conjunction with geomorphological studies that evaluate the environmental setting for the archaeological shells, although given the stable tectonic setting it is likely the current morphology of the Pambula River estuary has varied little during the late Holocene.

The $\delta^{18}O_{shell}$ data from four modern *O. angasi* grown in the Pambula River estuary, reported in Tynan et al. (2014), were used to calibrate the midden $\delta^{18}O_{shell}$ data. A chronology was assigned to each of the four modern $\delta^{18}O_{shell}$ profiles via correlation to the surface ocean temperatures recorded throughout the period of growth using the AnalySeries 2.0 software package. Tie-points between the modern $\delta^{18}O_{shell}$ records and the temperature record were assigned manually by matching maxima, minima and the overall shape of the records. The rescaled data from the four shells were interpolated to a consistent temporal resolution and stacked in order to construct a composite $\delta^{18}O_{shell}$ record. The differences between the midden and modern *O. angasi* $\delta^{18}O_{shell}$ values were converted into temperature differences using an *O. angasi*-specific $\delta^{18}O_{shell}$-temperature equation, derived by Tynan et al. (2014) from empirical study of *O. angasi* in southeast Australia:

$$T\ ^{o}C = 13.97_{(\pm 0.53)} - 3.57_{(\pm 0.85)}(\delta^{18}O_{shell} - \delta^{18}O_{water}) + 0.17_{(\pm 0.53)}(\delta^{18}O_{shell} - \delta^{18}O_{water})^2 \quad \text{(Eq 3.1)}$$

where $\delta^{18}O_{shell}$ is relative to VPDB, and $\delta^{18}O_{water}$ to VSMOW. The root mean square error (RMSE) within a 95% confidence interval (CI) on the Tynan et al. (2014) equation is ±2.5 ºC. Although this uncertainty is quite large relative to other published $\delta^{18}O_{shell}$-temperature calibrations, it was derived specifically for *O. angasi*, and its use is appropriate given that other studies have reported

variations between bivalve species in isotopic fractionation associated with calcification temperature (Owen et al. 2002; Wanamaker et al. 2007). The temperatures obtained from the two *O. angasi* shells using other $\delta^{18}O_{shell}$-temperature equations from Epstein et al. (1953) and Kim and O'Neil (1997) lie within the 95% CI uncertainty of the Tynan et al. (2014) equation.

A paleo-$\delta^{18}O_{water}$ value of 1.03‰ VSMOW was used for the temperature calculations. This value was calculated from the data for Pambula Lake reported in Tynan et al. (2014), omitting two values that corresponded to times of high rainfall. High rainfall events result in a significant freshening of the lake, and salinity levels can drop below the growth tolerance of *O. angasi*. Given the reasonable assumption that precipitation of new shell carbonate during these events is negligible, freshwater-dominated $\delta^{18}O_{water}$ values are not relevant to an *O. angasi* $\delta^{18}O_{shell}$ paleotemperature reconstruction.

3.4. Results

3.4.1. Modern *O. angasi* $\delta^{18}O_{shell}$ temperature records

The modern shells grew during the years 2006–07. This period coincided with the transition from a weak El Niño influence to that of a weak La Niña. El Niño conditions typically result in warmer temperatures and lower precipitation in southeast Australia, and La Niña typically results in higher precipitation (e.g. Dai and Wigley 2000; Ummenhofer et al. 2009). However, temperature and precipitation observed at the sample location in 2006–07 is not anomalous relative to the variability observed in the available temperature (record from Australian Bureau of Meteorology (BOM) Moruya Head Pilot station no. 069018) or precipitation (record from BOM Pambula Post Office station no. 069024) records

spanning the previous 40 years from this region. These records, along with the Southern Oscillation Index (SOI) record, (a measure of the difference in air pressure between Darwin and Tahiti, and is used as an indication of the intensity of El Niño and La Niña events) indicate the $\delta^{18}O_{shell}$ from the modern *O. angasi* can be taken as representative of an essentially neutral ENSO phase.

However, as documented in Tynan et al. (2014), the temperatures derived from the modern *O. angasi* $\delta^{18}O_{shell}$ for the winter period show a positive bias. This was attributed to prolonged precipitation events resulting in a more negative ambient $\delta^{18}O_{water}$ and thus apparently warmer temperature as recorded in the *O. angasi* shells.

A mean value for the modern $\delta^{18}O_{shell}$ was calculated by smoothing the $\delta^{18}O_{shell}$ record to a ~monthly resolution, to match that of the midden shells (maximum 12 data points per annual $\delta^{18}O_{shell}$ cycle). The mean for this smoothed curve was 0.32‰ VPDB.

3.4.2. Midden *O. angasi* $\delta^{18}O_{shell}$

The $\delta^{18}O_{shell}$ data from each midden shell is presented in Table 3.1. Both shells show a clear seasonal signal oscillating between summer and winter within their $\delta^{18}O_{shell}$ profiles (Figure 3.3).

Table 3.1. Oxygen isotope analysis data from shells SBOa001 and SBOa004. Temperatures calculated from the *Ostrea angasi* δ^{18}O-temperature equation of Tynan et al. (2014).

Sample	Distance along growth axis (mm)	δ^{18}O (VPDB)	Temperature ºC (Tynan et al. 2014)
SBOa001 - 1	0.00	-0.64	20.4
SBOa001 - 2	0.57	0.01	17.8
SBOa001 - 3	1.14	0.15	17.2
SBOa001 - 4	1.70	0.88	14.5
SBOa001 - 5	2.27	0.90	14.4
SBOa001 - 6	2.93	0.37	16.4
SBOa001 - 7	3.59	-0.17	18.5
SBOa001 - 8	4.24	0.03	17.7
SBOa001 - 9	4.89	-0.37	19.3
SBOa001 - 10	5.54	-0.56	20.1
SBOa001 - 11	6.10	-0.49	19.8
SBOa001 - 12	6.65	-0.86	21.3
SBOa001 - 13	7.21	-0.42	19.5
SBOa001 - 14	7.76	0.80	14.8
SBOa001 - 15	8.31	1.23	13.3
SBOa001 - 16	8.87	0.45	16.1
SBOa001 - 17	9.66	0.06	17.6
SBOa001 - 18	10.44	-0.51	19.9
SBOa001 - 19	11.00	0.36	16.4
SBOa001 - 20	11.56	1.26	13.2
SBOa001 - 21	12.12	0.08	17.5
SBOa001 - 22	12.60	-0.19	18.6
SBOa001 - 23	13.07	0.53	15.8
SBOa001 - 24	13.54	1.07	13.8
SBOa001 - 25	14.01	0.44	16.1
SBOa001 - 26	14.49	-0.17	18.5
SBOa001 - 27	14.97	0.61	15.5
SBOa001 - 28	15.45	1.03	14.0
SBOa001 - 29	15.93	-0.44	19.6
SBOa001 - 30	16.41	-0.36	19.3
SBOa001 - 31	16.91	-0.15	18.4
SBOa001 - 32	17.40	0.52	15.8
SBOa001 - 33	17.90	1.05	13.9
SBOa001 - 34	18.40	-0.19	18.6
SBOa001 - 35	18.86	-0.79	21.0
SBOa001 - 36	19.29	-0.44	19.6
SBOa001 - 37	19.72	0.32	16.6
SBOa001 - 38	19.86	1.03	14.0
SBOa004 - 1	0.00	-0.34	18.9
SBOa004 - 2	0.60	0.08	17.4
SBOa004 - 3	1.20	0.66	15.3
SBOa004 - 4	1.81	0.68	15.3
SBOa004 - 5	2.41	0.44	16.1
SBOa004 - 6	3.01	0.23	16.8
SBOa004 - 7	3.61	-0.43	19.2
SBOa004 - 8	4.20	-0.39	19.1
SBOa004 - 9	4.78	-0.49	19.5

SBOa004 - 10	5.37	-0.53	19.6
SBOa004 - 11	5.96	-0.35	18.9
Sample	**Distance along growth axis (mm)**	**δ18O (VPDB)**	**Temperature ºC (Tynan et al. 2014)**
SBOa004 - 12	6.49	0.56	15.7
SBOa004 - 13	6.96	1.28	13.3
SBOa004 - 14	7.44	0.91	14.5
SBOa004 - 15	7.92	0.20	16.9
SBOa004 - 16	8.39	-0.56	19.7
SBOa004 - 17	8.98	-0.68	20.2
SBOa004 - 18	9.68	-0.29	18.7
SBOa004 - 19	10.13	0.34	16.5
SBOa004 - 20	10.57	0.99	14.2
SBOa004 - 21	11.02	0.47	16.0
SBOa004 - 22	11.47	-0.02	17.7
SBOa004 - 23	11.91	-0.33	18.8
SBOa004 - 24	12.37	-0.48	19.4
SBOa004 - 25	12.84	-0.88	21.0
SBOa004 - 26	13.31	0.01	17.6
SBOa004 - 27	13.81	1.07	14.0
SBOa004 - 28	14.33	0.06	17.4
SBOa004 - 29	14.81	0.58	15.6
SBOa004 - 30	15.26	0.96	14.3

Shell SBOa001 shows six distinct cycles in $\delta^{18}O_{shell}$, indicating that its growth records a time period of six years. Shell SBOa004 contains three full annual cycles in its $\delta^{18}O_{shell}$ profile, and a final cycle indicating at least a partial fourth year of growth with an apparently truncated summer growth period. The full annual range of $\delta^{18}O$ values is ~2‰ VPDB in each of the midden shells, ranging from −0.86 to 1.26‰ VPDB in SBOa001 and −0.88 to 1.28‰ VPDB in SBOa004.

The values between the first and last maxima of the full annual cycles captured in the midden $\delta^{18}O_{shell}$ profiles were used to calculate a mean annual $\delta^{18}O_{shell}$ value for each midden shell. SBOa001 has a mean annual $\delta^{18}O_{shell}$ of 0.18‰ VPDB, and the mean annual $\delta^{18}O_{shell}$ of SBOa004 is 0.08‰ VPDB. The winter minima, summer maxima, and mean $\delta^{18}O_{shell}$ values for both the modern and midden *O. angasi* are given in Table 3.2.

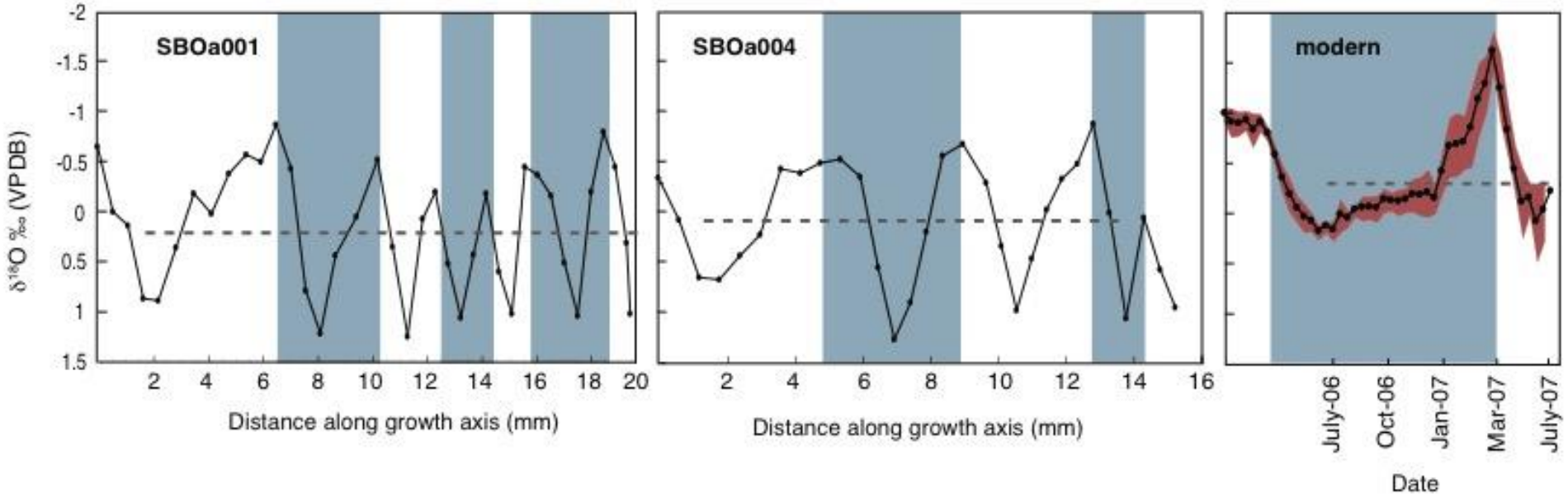

Figure 3.3. $\delta^{18}O$ profiles from the two midden *O. angasi* shells, alongside the mean $\delta^{18}O_{shell}$ profile constructed for four modern *O. angasi* from Pambula Lake. Dashed grey lines indicate the mean $\delta^{18}O_{shell}$ values. The shaded bars on the midden shell profiles represent time periods of one year. The shaded region on the modern $\delta^{18}O_{shell}$ profile represents one standard deviation of the mean derived from the four modern $\delta^{18}O_{shell}$ profiles. Note the inversion of the y-axis to align the more negative $\delta^{18}O_{shell}$ values with inferred warmer temperature.

Table 3.2. Mean, maximum and minimum seasonal $\delta^{18}O_{shell}$ values and reconstructed temperatures for the modern and midden *O. angasi*, *along with the recorded temperature from Pambula Lake for the 2006–2007 period.*

	Modern shells			**SBOa001**		**SBOa004**	
	$\delta^{18}O_{shell}$ ‰ VPDB	**ºC**	**ºC (recorded)**	**$\delta^{18}O_{shell}$ ‰ VPDB**	**ºC**	**$\delta^{18}O_{shell}$ ‰ VPDB**	**ºC**
Summer maximum	-1.60	24.53	24.7	-0.86 (0.74)	21.26 (-3.27)	-0.88 (0.72)	21.41 (-3.13)
Mean summer	-1.60	24.53	--	-0.49 (1.11)	19.6 (-4.93)	-0.7 (0.90)	20.52 (-4.01)
Winter minimum	0.18	17.13	11.6	1.26 (1.08)	13.16 (-3.97)	1.28 (1.10)	13.09 (-4.04)
Mean winter	0.14	17.28	11.75	1.09 (0.95)	12.83 (-4.45)	1.01 (0.87)	13.17 (-4.11)
Mean annual	-0.30	19.02	17.5	0.18 (0.48)	16.69 (-2.33)	0.08 (0.38)	17.12 (-1.90)
Seasonal amplitude	1.73	7.25	12.95	1.58 (-0.15)	6.77 (-0.48)	1.71(-0.02)	7.35 (0.10)

3.4.3. Comparison of modern and midden *O. angasi* $\delta^{18}O_{shell}$

The interpolated and averaged $\delta^{18}O_{shell}$ profiles of the four modern shells are shown in Figure 3.3. The four shells had consistent $\delta^{18}O_{shell}$ profiles, with mean $\delta^{18}O_{shell}$ values of −0.50, −0.39, −0.36 and −0.32 VPDB, and the standard deviation of the shell means is depicted as the shaded region in Figure 3.3. Their $\delta^{18}O_{shell}$ range is 1.79‰ VPDB, from −1.61‰ to 0.18‰ VPDB. There is a difference of ~0.4–0.5‰ VPDB between the mean annual $\delta^{18}O_{shell}$ values of the midden and modern *O. angasi* (Table 3.2, Figure 3.3). Mean summer maxima are offset by +1.11 ‰ VPDB (SBOa001) and +0.9 ‰ VPDB (SBOa004) in the midden *O. angasi* when compared to average summer maximum of the modern *O. angasi*.

Mean winter minimum $\delta^{18}O_{shell}$ values are also more positive in the midden shells than the modern *O. angasi*. Shell SBOa001 shows an offset of +0.95‰ VPDB, while SBOa004 an offset of +0.87‰ VPDB.

3.5. Discussion

3.5.1. Comparison of *O. angasi* $\delta^{18}O_{shell}$ annual mean, amplitude and seasonality

The two midden shells show good agreement in both the annual mean and seasonal structure of their $\delta^{18}O_{shell}$ records, supporting the assumption that they grew in similar climatologic regimes and likely at a similar time. If we assume that the paleo-hydrological conditions in this estuary have remained similar to those of the modern day over the past 2000 years, the difference in $\delta^{18}O_{shell}$ between the midden and modern *O. angasi* would be attributable to a change in

temperature. Using the equation relating calcification temperature to $\delta^{18}O_{shell}$ derived for *O. angasi* developed by Tynan et al (2014) we infer from the isotopic composition of the midden shells that mean annual water temperature in Pambula Lake was ~2 ºC cooler ~1850 years BP. Although this is within the error of the *O. angasi* $\delta^{18}O_{shell}$-temperature equation, the consistently positive offset in the $\delta^{18}O_{shell}$ of the midden *O. angasi* suggests this is a valid signal.

The temperature difference of surface waters in the Pambula River estuary 2000 years ago implied by this end-member scenario is dramatic, and there are no previously published quantitative records of Holocene sea surface temperature from the region with which to compare. There is some qualitative evidence for cooler conditions around this time period (e.g. Baker et al. 2001; Kemp and Hope 2014) which corroborates the direction of temperature offset indicated by the midden *O. angasi*.

An alternative explanation is that the difference in $\delta^{18}O_{shell}$ between the midden and modern *O. angasi* is attributable wholly or in part to a change in the $\delta^{18}O_{water}$ and predominant salinity of the estuary, rather than temperature. In this scenario, the paleo-$\delta^{18}O_{water}$ required to drive a change in $\delta^{18}O_{shell}$ of this magnitude would be 1.93–2.06‰ SMOW. According to the $\delta^{18}O_{water}$-salinity relationship determined by Tynan et al. (2014), this corresponds to a salinity of ~36.5–37. Modern open ocean salinities in this range are generally only found in the subtropical Atlantic (http://aquarius.umaine.edu/cgi/gal_salinity.htm#annual). Very high evaporation rates would be required within the Pambula Lake estuary to produce a consistent salinity of this value.

Such a different hydrological regime could only be the result of marked geomorphological changes within the Pambula Lake system since the late Holocene—a significantly lower sea level, resulting in Pambula Lake being more

isolated from the ocean. Although no geomorphological study has been conducted at Pambula Lake, Sloss et al. (2007) report that a study of Burrill Lake, ~180 km north of Pambula Lake, indicates sea level ~2000 years BP was in fact up to 1.5 m higher than present, not lower. A study of Lake Conjola, close to Burrill Lake, and ~195 km from Pambula Lake, produced evidence of a sea-level highstand at ~5000–3000 years BP (Sloss et al. 2010). From Bateman's Bay, a site closer to Pambula Lake (~140 km away) Switzer et al. (2010) also report a sea level at least 1 m higher for the period ~2500–5000 years BP. This regional evidence of a late Holocene sea-level highstand, albeit slightly earlier than the age of the *O. angasi* of this study, makes it unlikely that Pambula Lake was indeed more isolated from the ocean during the time the midden *O. angasi* were growing. Furthermore, owing to the northward direction of the littoral drift of sediments on the Australian east coast, it is generally only estuaries with outlets on the northern end of the embayments that tend to become closed to the ocean; the Pambula estuary outlet is located on the southern end of the Pambula Beach embayment adjacent to a rocky headland. As such, it seems unlikely that increased evaporation in the Pambula Lake could have driven paleo-$\delta^{18}O_{water}$ and thus $\delta^{18}O_{shell}$ of the midden *O. angasi* to more positive values sufficient to result in the cooler inferred temperatures.

Furthermore, it is impossible to pinpoint the exact location where the midden shells grew. They could have been collected from the river channel itself, where due to the open connection to the ocean salinity would be more consistent. It is also possible the midden *O. angasi* grew in a localised region of higher evaporation within the lake, subject to hypersaline conditions, but given that their natural growth habitat is purely subtidal (Nell, 2001), living at the sediment-water interface, it seems unlikely they would have been consistently subjected to

periods of higher salinity resulting from increased evaporation of surface waters. Indeed, Heasman et al., (2004) found that the majority of *O. angasi* observed on the New South Wales coast lived 1–4 m below the low water mark (Heasman et al., 2004).

However, it must be noted that modern *O. angasi* $\delta^{18}O_{shell}$ is biased towards warmer annual average temperatures if there is input of depleted $\delta^{18}O_{water}$ during episodes of anomalously high precipitation and/or fluvial input to the estuary. This bias could go part way to explaining the temperature difference between the modern and midden *O. angasi* $\delta^{18}O_{shell}$ records if there were fewer extreme freshwater input events on an annual basis 2000 years ago. However this is unlikely to account for the entire discrepancy, as the influence of extreme freshwater events observed in the modern shells was sporadic in nature while the offset of the midden $\delta^{18}O_{shell}$ values relative to the modern persists year-round and over several annual cycles (Figure 3.3).

With regard to the marked difference in the summer maxima recorded by the midden *O. angasi* compared to the modern shells, a possible explanation is that the midden oysters failed to record maximum summer temperatures. A number of studies have reported growth cessations in oysters during times of either high or low temperature extremes (Kirby et al. 1998; Surge et al. 2001). However, this explanation too is unlikely as overall the midden *O. angasi* are offset towards cooler temperatures/higher $\delta^{18}O_{shell}$ and modern day *O. angasi* from Pambula Lake precipitate $\delta^{18}O_{shell}$ as low as –1.87 ‰ (which corresponds to a temperature of ~24 ºC (Tynan et al. 2014).

Clearly, interpretation of the $\delta^{18}O_{shell}$-temperature relationships and their use to reconstruct paleo-temperatures in estuarine environments is not straightforward. Uncertainties surrounding the paleo-precipitation regime allow

for the potential influence of changing fluvial input on $\delta^{18}O_{water}$, especially as several records indicate drier conditions during the late Holocene period in which the midden shells were harvested (De Deckker et al. 1982; Fitzsimmons and Barrows 2010; Holdgate et al. 2011; Wilkins et al. 2013; Woodward et al. 2014). However, as it is unlikely the morphology of the Pambula River estuary has changed dramatically over the past two millennia, changes in freshwater input would have to be extreme to overwhelm the moderating effect of tidal mixing with the coastal ocean (Tynan et al., 2014). Due to the persistence of the positive offset observed in the $\delta^{18}O_{shell}$ of the midden *O. angasi* relative to modern specimens over several annual cycles, we conclude these observations are likely predominantly driven by cooler than modern temperatures for the period ~1850 years BP, though the magnitude of this shift needs to be treated with caution and investigated with further study.

It would be useful to develop independent temperature and salinity proxies to enable the decoupling of the salinity ($\delta^{18}O_{water}$)-temperature signal of the *O. angasi* $\delta^{18}O_{shell}$ and allow for a more conclusive assessment of the temperature record. A number of studies have examined the Mg/Ca of oyster carbonate as a temperature proxy that is independent of salinity, with varying degrees of success (Surge and Lohmann 2008; Mouchi et al. 2013; Ullmann et al. 2013; Bougeois et al. 2014). A preliminary assessment of modern *O. angasi* (unpublished data) indicates that Mg/Ca shows a large degree of variation between individual shells and thus is not, at this stage, a viable alternative or complement to $\delta^{18}O_{shell}$ as a paleotemperature proxy.

Analysis of clumped isotopes is another potential avenue for further study, as this method provides information on mineralisation temperature, independent

of the water isotopic composition (e.g. Zaruur et al. 2016; Winkelstern et al. 2017).

While is it not possible to present more than a 'snapshot' of paleotemperature from the two shells of this study, the clear, high-resolution seasonal records obtained from the midden *O. angasi* shells emphasise the potential of this species for future paleoclimate studies. The abundance of midden deposits, the time periods archived by their creation, and the marine context of the shells they contain offers a potentially vast resource that could significantly contribute to the understanding of late Holocene climate for the eastern Australian region, and in particular, the timing and dynamics of the shift to ENSO-dominated modern climate conditions documented by other studies (e.g. Wilkins et al. 2013; Fitzsimmons and Barrows 2010; Woodward et al. 2014).

More extensive sampling of shells to provide an increased sample size would increase the confidence of climate interpretations. Generating a composite record from multiple shells (e.g. Carré et al 2014), including samples from different strata of the midden deposit, as well as other middens along the eastern coastline of Australia would also enable a more robust and temporally complete reconstruction of Holocene paleoclimate.

3.5.2. Potential archaeological interpretations

The $\delta^{18}O_{shell}$ profiles of each of the midden *O. angasi* terminate at values that are close to the maximum $\delta^{18}O_{shell}$ values recorded by the shells, indicating the season of death for both shells was wintertime. Analysis of a greater number of shells to determine if this is a consistent pattern throughout the midden site would make a valuable contribution to the other archaeological evidence used by Sullivan (1982) to determine the nature and timing of PLA midden site occupation.

3.6. Conclusion—paleotemperature records from *O. angasi*

The two Severs Beach midden *O. angasi* $\delta^{18}O_{shell}$ records presented in this study offer a multi-year, seasonal reconstruction of Pambula River estuarine climate from the period ~1850 years BP.

The Severs Beach midden *O. angasi* $\delta^{18}O_{shell}$ values are consistently higher than those of four modern *O. angasi* from Pambula Lake, an effect likely partially or predominantly driven by cooler temperatures during the period ~1850 years BP. Mean annual temperatures calculated from the *O. angasi* $\delta^{18}O$-temperature calibration of Tynan et al. (2014) are ~2 ºC cooler than present temperatures, with the greatest offsets observed in summer. Further analysis of a greater number of shells, along with geomorphological investigations of the region would improve confidence in our interpretation of this calibrated result. However, the internally consistent signal obtained from these two midden *O. angasi* shells confirms that climate information can be inferred from archaeological (or fossil) specimens of this species.

Given the limited availability of other data for this time and region, this high-resolution snapshot of late Holocene climate in southeast Australia is a valuable record. Given the broad geographical distribution of mid to late Holocene middens along the Australian coastline, the $\delta^{18}O_{shell}$-derived temperature records from *O. angasi* shells have the potential to provide a valuable contribution to Holocene climate records currently available for the southeast Australia region.

Acknowledgements

This study was funded by CRC LEME. The authors would like to acknowledge the valuable work of Marjorie Sullivan, in carrying out the excavation of the Severs Beach midden that provided the samples for this project. We would like to thank Marjorie Sullivan, the Australian Museum, the Eden Local Aboriginal Land Council and the NSW Department of Parks and Wildlife for providing the permission to use the samples for this research. Thanks also to Lora Wingate and K.C Lohmann for valuable technical assistance with sampling and analysis, along with an anonymous reviewer whose constructive comments greatly improved and clarified the manuscript.

3.7. References

Andrus, C. F. T., & Crowe, D. E. (2000). Geochemical analysis of *Crassostrea virginica* as a method to determine season of capture. Journal of Archaeological Science, 27(1), 33-42.

Andrus, C. F. T., & Thompson, V. D. (2012). Determining the habitats of mollusk collection at the Sapelo Island shell ring complex, Georgia, USA using oxygen isotope sclerochronology. *Journal of Archaeological Science*, 39(2), 215-228. doi:10.1016/j.jas.2011.08.002

Bailey, G. N. (1975). The role of molluscs in coastal economies: The results of midden analysis in Australia. *Journal of Archaeological Science*, 2, 45-62.

Bailey, G. N., Deith, M. R., & Shackleton, N. J. (1983). Oxygen-isotope analysis and seasonality determinations—limits and potential of a new technique. *American Antiquity*, 48(2), 390-398.

Baker, R. G. V., Haworth, R. J., & Flood, P. G. (2001). Warmer or cooler late Holocene marine palaeoenvironments?: interpreting southeast Australian and Brazilian sea-level changes using fixed biological indicators and their delta O-18 composition. *Palaeogeography Palaeoclimatology Palaeoecology*, 168(3-4), 249-272.

Barr, C., Tibby, J., Gell, P., Tyler, J., Zawadzki, A., & Jacobsen, G. E. (2014).

Climate variability in south-eastern Australia over the last 1500 years inferred from the high-resolution diatom records of two crater lakes. *Quaternary Science Reviews*, 95, 115-131. doi:10.1016/j.quascirev.2014.05.001

Bougeois, L., de Rafelis, M., Reichart, G. J., de Nooijer, L. J., & Dupont-Nivet, G. (2016). Mg/Ca in fossil oyster shells as a palaeotemperature proxy, an example from the Palaeogene of Central Asia. *Palaeogeography Palaeoclimatology Palaeoecology*, 441, 611-626. doi:10.1016/j.palaeo.2015.09.052

Bougeois, L., de Rafelis, M., Reichart, G. J., de Nooijer, L. J., Nicollin, F., & Dupont-Nivet, G. (2014). A high resolution study of trace elements and stable isotopes in oyster shells to estimate Central Asian Middle Eocene seasonality. *Chemical Geology*, 363, 200-212. doi:10.1016/j.chemgeo.2013.10.037

Bowler, J. M. (1981). Australian salt lakes—a paleohydrologic approach. *Hydrobiologia*, 81(2), 431-444.

Brigaud, B., Puceat, E., Pellenard, P., Vincent, B., & Joachimski, M. M. (2008). Climatic fluctuations and seasonality during the Late Jurassic (Oxfordian-Early Kimmeridgian) inferred from delta O-18 of Paris Basin oyster shells. *Earth and Planetary Science Letters*, 273(1-2), 58-67. doi:10.1016/j.epsl.2008.06.015

Brockwell, S., Marwick, B., Bourke, P., Faulkner, P., & Willan, R. (2013). Late Holocene climate change and human behavioural variability in the coastal wet-dry tropics of northern Australia: Evidence from a pilot study of oxygen isotopes in marine bivalve shells from archaeological sites. *Australian Archaeology*, 76, 21-33.

Burchell, M., Cannon, A., Hallmann, N., Schwarcz, H. P., and Schone, B. R. (2013). Inter-site variability in the season of shellfish collection on the central coast of British Columbia: *Journal of Archaeological Science*, 40(1), 626-636.

Carré, M., Sachs, J. P., Purca, S., Schauer, A. J., Braconnot, P., Falcon, R. A., Julien, M. & Lavallee, D. (2014). Holocene history of ENSO variance and asymmetry in the eastern tropical Pacific. *Science*, 345(6200), 1045-1048. doi:10.1126/science.1252220

Cook, E. R., Buckley, B. M., D'Arrigo, R. D., & Peterson, M. J. (2000). Warm-season temperatures since 1600 BC reconstructed from Tasmanian tree rings and their relationship to large-scale sea surface temperature anomalies. *Climate Dynamics*, 16(2-3), 79-91. doi:10.1007/s003820050006

Coventry, R. J. (1976). Abandoned shorelines and the late Quaternary history of Lake George, New South Wales. *Journal of the Geological Society of Australia*,

23, 249-273.

Dai, A., & Wigley, T. M. L. (2000). Global patterns of ENSO-induced precipitation. *Geophysical Research Letters*, 27(9), 1283-1286. doi:10.1029/1999gl011140

De Deckker, P. (1982). Holocene history of four maar lakes in SE Australia, illustrated by the recovery of ostracods and other invertebrate and fish remains. *Proceedings of the Royal Society of Victoria* 94, 183-220.

Deith, M. R. (1986). Subsistence strategies at a Mesolithic camp site—evidence from stable isotope analyses of shells. *Journal of Archaeological Science*, 13(1), 61-78.

Dodson, J. R. (1987). Mire development and environmental change, Barrington Tops, New South Wales, Australia. *Quaternary Research*, 27(1), 73-81.

Epstein, S., Buchsbaum, R., Lowenstam, H. A., & Urey, H. C. (1953). Revised carbonate-water isotopic temperature scale. *Bulletin of the Geological Society of America*, 64, 1315-1326.

Fitzsimmons, K. E., & Barrows, T. T. (2010). Holocene hydrologic variability in temperate southeastern Australia: An example from Lake George, New South Wales. *The Holocene*, 20(4), 585-597. doi:10.1177/0959683609356589

Gillespie, R., & Temple, R. B. (1977). Radiocarbon dating of shell middens. *Archaeology and Physical Anthropology in Oceania*, 12, 26-37.

Godfrey, M. (1988). Oxygen isotope analysis: a means for determining the seasonal gathering of the pipi (*Donax deltoides*) by Aborigines in prehistoric Australia. *Archaeology in Oceania*, 23, 17-21. doi:10.1002/j.1834-4453.1988.tb00179.x

Gouramanis, C., Wilkins, D., & De Deckker, P. (2010). 6000 years of environmental changes recorded in Blue Lake, South Australia, based on ostracod ecology and valve chemistry. *Palaeogeography Palaeoclimatology Palaeoecology*, 297(1), 223-237. doi:10.1016/j.palaeo.2010.08.005

Harding, J. M., Spero, H. J., Mann, R., Herbert, G. S., & Sliko, J. L. (2010). Reconstructing early 17th century estuarine drought conditions from Jamestown oysters. *Proceedings of the National Academy of Sciences of the United States of America*, 107(23), 10549-10554. doi:10.1073/pnas.1001052107

Heasman, M., Diggles, B.K., Hurwood, D., Mather, P., Pirozzi, I., Dworjanyn, S., 2004. Paving the way for continued rapid development of the flat (angasi) oyster (*Ostrea angasi*) farming industry in New South Wales, NSW Final Report Series,

New South Wales.

Holdgate, G. R., Wagstaff, B., & Gallagher, S. J. (2011). Did Port Phillip Bay nearly dry up between 2800 and 1000 cal. yr BP? Bay floor channelling evidence, seismic and core dating. *Australian Journal of Earth Sciences*, 58(2), 157-175. doi:10.1080/08120099.2011.546429

Hong, W., Keppens, E., Nielsen, P., & Vanriet, A. (1995). Oxygen and carbon-isotope study of the Holocene oyster reefs and paleoenvironmental reconstruction on the northwest coast of Bohai Bay, China. *Marine Geology*, 124(1-4), 289-302. doi:10.1016/0025-3227(95)00046-2

Kemp, J., & Hope, G. (2014). Vegetation and environments since the Last Glacial Maximum in the Southern Tablelands, New South Wales. *Journal of Quaternary Science*, 29(8), 778-788. doi:10.1002/jqs.2749

Kennett, D. J., & Voorhies, B. (1996). Oxygen isotopic analysis of archaeological shells to detect seasonal use of wetlands on the southern Pacific coast of Mexico. *Journal of Archaeological Science*, 23(5), 689-704.

Killingley, J. S. (1981). Seasonality of mollusk collecting determined from O-18 profiles of midden shells. *American Antiquity*, 46(1), 152-158.

Killingley, J. S. (1983). Seasonality determination by oxygen-isotopic profile—a reply to Bailey et al. *American Antiquity*, 48(2), 399-403.

Kim, S. T., & O'Neil, J. R. (1997). Equilibrium and nonequilibrium oxygen isotope effects in synthetic carbonates. *Geochimica et Cosmochimica Acta*, 61(16), 3461-3475.

Kirby, M. X. (2000). Paleoecological differences between Tertiary and Quaternary *Crassostrea* oysters, as revealed by stable isotope sclerochronology. *Palaios*, 15(2), 132-141.

Kirby, M. X., Soniat, T. M., & Spero, H. J. (1998). Stable isotope sclerochronology of Pleistocene and recent oyster shells (*Crassostrea virginica*). *Palaios*, 13(6), 560-569.

Lourandos, H. (1968). Dispersal of activities - the east Tasmanian Aboriginal sites. *Papers and Proceedings of the Royal Society of Tasmania*, 102(2), 41-46.

Mannino, M. A., Spiro, B. F., & Thomas, K. D. (2003). Sampling shells for seasonality: oxygen isotope analysis on shell carbonates of the inter-tidal gastropod *Monodonta lineata* (da Costa) from populations across its modern range and from a Mesolithic site in southern Britain. *Journal of Archaeological Science*, 30(6), 667-679.

Milner, N. (2001). At the cutting edge: Using thin sectioning to determine season of death of the European oyster, *Ostrea edulis*. *Journal of Archaeological Science*, 28(8), 861-873. doi:10.1006/jasc.2000.0618

Milner, N. (2002). *Incremental Growth of the European Oyster Ostrea Edulis.* Oxford: Archaeopress.

Mooney, S. (1997). A fine-resolution paleoclimatic reconstruction of the last 2000 years, from Lake Keilambete, southeastern Australia. *The Holocene*, 7(2), 139-149.

Mouchi, V., de Rafélis, M., Lartaud, F., Fialin, M., & Verrecchia, E. (2013). Chemical labelling of oyster shells used for time-calibrated high-resolution Mg/Ca ratios: A tool for estimation of past seasonal temperature variations. *Palaeogeography, Palaeoclimatology, Palaeoecology*, 373, 66-74. doi:http://dx.doi.org/10.1016/j.palaeo.2012.05.023

Nell, J. A. (2001). The history of oyster farming in Australia. *Marine Fisheries Review*, 63(3), 14-25.

Nell, J. A., & Gibbs, P. J. (1986). Salinity tolerance and absorption of L-methionine by some Australian bivalve mollusks. *Australian Journal of Marine and Freshwater Research*, 37(6), 721-727.

Neukom, R., & Gergis, J. (2012). Southern Hemisphere high-resolution palaeoclimate records of the last 2000 years. *The Holocene*, 22(5), 501-524. doi:10.1177/0959683611427335

Owen, R., Kennedy, H., & Richardson, C. (2002). Experimental investigation into partitioning of stable isotopes between scallop (*Pecten maximus*) shell calcite and sea water. *Palaeogeography Palaeoclimatology Palaeoecology*, 185(1-2), 163-174.

PAGES 2k Consortium (2013). Continental-scale temperature variability during the past two millennia. *Nature Geoscience*, 6(5), 339-346. doi:10.1038/ngeo1797

Prendergast, A. L., Stevens, R. E., O'Connell, T. C., Fadlalak, A., Touati, M., al-Mzeine, A., Schone, B. R., Hunt, C. O., and Barker, G. (2016) Changing patterns of eastern Mediterranean shellfish exploitation in the Late Glacial and Early Holocene: Oxygen isotope evidence from gastropod in Epipaleolithic to Neolithic human occupation layers at the Haua Fteah cave, Libya. *Quaternary International*, 407, 80-93.

Reeves, J. M., Barrows, T. T., Cohen, T. J., Kiem, A. S., Bostock, H. C., Fitzsimmons, K. E., Jansen, J.D., Kemp, J., Krause, C., Petherick, L., Phipps, S. J., & Oz-Intimate Members (2013). Climate variability over the last 35,000 years recorded in marine and terrestrial archives in the Australian region: an OZ-INTIMATE compilation. *Quaternary Science Reviews*, 74, 21-34. doi:10.1016/j.quascirev.2013.01.001

Rowland, M. J., & Ulm, S. (2012). Key issues in the conservation of the Australian coastal archaeological record: natural and human impacts. *Journal of Coastal Conservation*, 16(2), 159-171. doi:10.1007/s11852-010-0112-5

Sandweiss, D. H. (1996). Environmental Change and Its Consequences for Human Society on the Central Andean Coast: A Malacological Perspective. In E. J. Reitz, L. A. Newsom, & S. J. Scudder (Eds.), *Case Studies in Environmental Archaeology* (pp. 127-146). New York: Plenum Press.

Schöne, B., & Gillikin, D. (2013) Unraveling environmental histories from skeletal diaries—Advances in sclerochronology. Palaeogeography, Palaeoclimatology, Palaeoecology, 373 1–5. doi: http://dx.doi.org/10.1016/ j.palaeo.2012.11.026

Schöne, B., & Surge, D. (2014). Bivalve shells: ultra high-resolution paleoclimate archives. *PAGES* Magazine, 22, 20-21.

Shackleton, N. J. (1973). Oxygen isotope analysis as a means of determining season of occupation of prehistoric midden sites. *Archaeometry*, 15(1), 133-141.

Sloss, C. R., Jones, B. G., Switzer, A. D., Nichol, S., Clement, A. J. H., & Nicholas, A. W. (2010). The Holocene infill of Lake Conjola, a narrow incised valley system on the southeast coast of Australia. *Quaternary International*, 221(1-2), 23-35. doi:10.1016/j.quaint.2009.06.027

Sloss, C. R., Murray-Wallace, C. V., & Jones, B. G. (2007). Holocene sea-level change on the southeast coast of Australia: a review. *The Holocene*, 17(7), 999-1014. doi:10.1177/0959683607082415

Sullivan, M. (1982). *Aboriginal shell middens in the coastal landscape of New South Wales*. (PhD thesis), The Australian National University, Canberra.

Surge, D., & Lohmann, K. C. (2008). Evaluating Mg/Ca ratios as a temperature proxy in the estuarine oyster, *Crassostrea virginica*. *Journal of Geophysical Research-Biogeosciences*, 113(G2). doi:G0200110.1029/2007jg000623

Surge, D., Lohmann, K. C., & Dettman, D. L. (2001). Controls on isotopic

chemistry of the American oyster, *Crassostrea virginica*: implications for growth patterns. *Palaeogeography Palaeoclimatology Palaeoecology*, 172(3-4), 283-296.

Surge, D. M., Lohmann, K. C., & Goodfriend, G. A. (2003). Reconstructing estuarine conditions: oyster shells as recorders of environmental change, southwest Florida. *Estuarine Coastal and Shelf Science*, 57(5-6), 737-756.

Switzer, A. D., Sloss, C. R., Jones, B. G., & Bristow, C. S. (2010). Geomorphic evidence for mid-late Holocene higher sea level from southeastern Australia. *Quaternary International*, 221(1-2), 13-22. doi:10.1016/j.quaint.2009.06.035

Talma, A. S., Donner, J. J., & Ellis, S. D. (1992). Stable isotopic composition of marine shells along the southern African coast. *South African Journal of Science*, 88(9-10), 499-504.

Taylor, A. J. (1891). Notes on the Shell-Mounds at Seaford, Little Swanport. *Papers and Proceedings of the Royal Society of Tasmania*, 89-94.

Titschack, J., Zuschin, M., Spotl, C., & Baal, C. (2010). The giant oyster *Hyotissa hyotis* from the northern Red Sea as a decadal-scale archive for seasonal environmental fluctuations in coral reef habitats. *Coral Reefs*, 29(4), 1061-1075. doi:10.1007/s00338-010-0665-7

Twaddle, R. W., Ulm, S., Hinton, J., Wurster, C. M., & Bird, M. I. (2016). Sclerochronological analysis of archaeological mollusc assemblages: methods, applications and future prospects. *Archaeological and Anthropological Sciences*, 8(2), 359-379. doi:10.1007/s12520-015-0228-5

Tynan, S., Dutton, A., Eggins, S., Opdyke, B., &. (2014). Oxygen isotope records of the Australian flat oyster (*Ostrea angasi*) as a potential temperature archive. *Marine Geology*, 357, 195-209. doi:10.1016/j.margeo.2014.07.009

Ullmann, C. V., Boehm, F., Rickaby, R. E. M., Wiechert, U., & Korte, C. (2013). The Giant Pacific Oyster (*Crassostrea gigas*) as a modern analog for fossil ostreoids: Isotopic (Ca, O, C) and elemental (Mg/Ca, Sr/Ca, Mn/Ca) proxies. *Geochemistry Geophysics Geosystems*, 14(10), 4109-4120. doi:10.1002/ggge.20257

Ullmann, C. V., Wiechert, U., & Korte, C. (2010). Oxygen isotope fluctuations in a modern North Sea oyster (*Crassostrea gigas*) compared with annual variations in seawater temperature: Implications for palaeoclimate studies. *Chemical Geology*, 277(1-2), 160-166. doi:10.1016/j.chemgeo.2010.07.019

Ummenhofer, C. C., England, M. H., McIntosh, P. C., Meyers, G. A., Pook, M.

J., Risbey, J. S., Gupta, A. S., & Taschetto, A. S. (2009). What causes southeast Australia's worst droughts? *Geophysical Research Letters*, 36. doi:10.1029/2008gl036801

Walton, R. C. (2012). *Sucking the Shell Beds Dry? The morphometric analysis of oyster (Saccostrea glomerata), cockle (Anadara trapezia) and whelk (Pyrazus ebeninus) to interpret the intensity of human exploitation of molluscs at the Sandstone Point shell midden complex, southeast Queensland.* (Bachelor of Social Science (Hons)), The University of Queensland, Queensland.

Wanamaker, A. D., Kreutz, K. J., Borns, H. W., Introne, D. S., Feindel, S., Funder, S., Rawson, P. D., & Barber, B. J. (2007). Experimental determination of salinity, temperature, growth, and metabolic effects on shell isotope chemistry of *Mytilus edulis* collected from Maine and Greenland. *Paleoceanography*, 22(2), 12. doi:Pa2217Artn pa2217

Wilkins, D., Gouramanis, C., De Deckker, P., Fifield, L. K., & Olley, J. (2013). Holocene lake-level fluctuations in Lakes Keilambete and Gnotuk, southwestern Victoria, Australia. *The Holocene*, 23(6), 784-795. doi:10.1177/0959683612471983

Winkelstern, I. Z., Rowe, M. P., Lohmann, K. C., Defliese, W. F., Petersen, S. V., & Brewer, A. W. (2017). Meltwater pulse recorded in Last Interglacial mollusk shells from Bermuda. *Paleoceanography*, 32(2), 132-145. doi:10.1002/2016pa003014

Woodward, C., Shulmeister, J., Bell, D., Haworth, R., Jacobsen, G., & Zawadzki, A. (2014). A Holocene record of climate and hydrological changes from Little Llangothlin Lagoon, south eastern Australia. *The Holocene*, 24(12), 1665-1674. doi:10.1177/0959683614551218

Xia, Q. K., Zhao, J. X., & Collerson, K. D. (2001). Early-Mid Holocene climatic variations in Tasmania, Australia: multi-proxy records in a stalagmite from Lynds Cave. *Earth and Planetary Science Letters*, 194(1-2), 177-187.

Zangrando, A. F., Vargas, G. P., and Tivoli, A. M. (2017) Decreased foraging return in shellfishing? Species composition and shell size of blue mussel (*Mytilus edulis*) from a Late Holocene site of the South Coast of Tierra del Fuego. *Quaternary International*, 427, 160-169.

Zaarur, S., Affek, H. P., & Stein, M. (2016). Last glacial-Holocene temperatures and hydrology of the Sea of Galilee and Hula Valley from clumped isotopes in Melanopsis shells. *Geochimica Et Cosmochimica Acta*, 179, 142-155.

Chapter 4

Assessment of Mg/Ca in *Saccostrea glomerata* (the Sydney Rock oyster) shell as a potential temperature record.

This paper was published on in *Paleogeography, Paleoclimatology, Paleoecology*, 2017, 484, pp79-88

Authors and contributions:

Sarah Tynan: 80% conceived study, conducted field work, sampling and data analysis

Bradley Opdyke: 5% overarching guidance and support, feedback on written drafts

Andrea Dutton: 5% overarching guidance and support, feedback on written drafts

Maureen Walczak: 10% guidance with data analysis, feedback on written drafts

ABSTRACT

Bivalve shell Mg/Ca records can be important potential tracers of paleo-temperature, but evidence has shown that the temperature dependence of trace metal incorporation ratios can vary significantly between different species and even within the same species. This study aims to assess one such bivalve species as a potential temperature proxy for the east coast of Australia. Specimens of the Sydney Rock oyster (*Saccostrea glomerata*) were cultured for approximately one year at two locations on the east coast of Australia: Moreton Bay, Queensland, a semi-enclosed bay with consistently marine conditions, and Pambula Lake, New South Wales, a tidal lake which can undergo significant variations in salinity as a result of rainfall and river discharge. Transects of the oysters' growth axis were analysed via LA-ICP-MS. Mg/Ca-temperature relationships for the oysters show a robust temperature dependence but there is also a clear discrepancy between the two sites. However, this discrepancy was not evident when the temperature dependence of Mg partition coefficients (D_{Mg}) was determined, indicating that the difference seen in the direct Mg/Ca_{shell}-temperature relationships can be accounted for by variation in salinity at the estuarine site of Pambula Lake. This has implications for the use of Mg/Ca as a paleo-temperature tracer within estuarine fauna as knowledge of the water chemistry is required to determine D_{Mg} values. However, *S. glomerata* Mg/Ca remains a promising paleo-temperature tracer as the direct Mg/Ca-temperature relationships can still be applied to samples from environments that experience little variation in salinity. Combined analysis of Mg/Ca coupled with $\delta^{18}O_{shell}$ records has the potential to enable the deconvolution of the combined salinity/temperature signal in the $\delta^{18}O_{shell}$ and Mg/Ca_{shell} records.

Keywords: bivalve, oyster, Mg/Ca, temperature, *Saccostrea glomerata*, D_{Mg}

4.1. Introduction

In the absence of instrumental climate records that extend back further than a few hundred years, paleoclimate studies rely on various proxy records such as the geochemical signals of biogenic carbonates. These include $\delta^{18}O_{carbonate}$ and trace element ratios found in corals (e.g. Corrége 2006), bivalves (e.g. Driscoll et al. 2014; Elliot et al. 2009; Dutton and Lohmann 2002), gastropods (e.g. Sisma-Ventura et al. 2009) and foraminifera (e.g. Rosenthal et al. 1997; Lea et al. 1999). However, the utility of $\delta^{18}O_{carbonate}$ as a temperature tracer can be somewhat limited as it is influenced not only by precipitation temperature, but also $\delta^{18}O_{water}$. The record obtained from $\delta^{18}O_{carbonate}$ in locations where $\delta^{18}O_{water}$ is markedly variable, usually concurrent with changes in salinity, is often a combined temperature-salinity signal from which it can be difficult to isolate a temperature record.

As it is generally accepted that Mg/Ca remains constant in seawater unless salinity falls below 10 (Dodd and Crisp 1982), Mg/Ca presents a potential temperature tracer that is comparatively independent of salinity. Trace element ratios of biogenic carbonates, most commonly Mg/Ca in biogenic calcite and Sr/Ca in aragonite, have been widely investigated as potential temperature proxies to serve as complements or alternatives to $\delta^{18}O_{carbonate}$. Mg/Ca-temperature calibration curves have been successfully developed for foraminifera (Lea et al.1999; Elderfield and Ganssen 2000), ostracods (e.g. Elmore et al. 2012; Ingram et al. 1998), and gastropods (e.g. Ingram et al. 1998).

Table 4.1. Published bivalve Mg/Ca-temperature relationships.

Species	Equation	R^2	Temperature range (ºC)	Environment	Comments	Citation
Crassostrea virginica	Mg/Ca = 0.72T – 0.23	0.3	19.1–31.4	Estuarine	Older (most recent) growth only	Surge and Lohmann 2008
Mytilus edulis	Mg/Ca = 0.70T – 0.63	0.91	5–20	Estuarine (intertidal bay)	Younger growth only	Vander Putten et al. 2000
Mytilus edulis	$Mg/Ca = 0.26_{(\pm 0.06)}T + 1.56_{(\pm 0.84)}$	0.37	10–20	Laboratory culture		Freitas et al. 2008
Mytilus edulis	$Mg/Ca = 0.82_{(\pm 0.24)}T + 3.6_{(\pm 3.24)}$	0.82	7–20	Laboratory culture	Juvenile (<2 years) growth, low salinity	Wanamaker et al. 2008
Mytilus edulis	$Mg/Ca = 0.75_{(\pm 0.22)}\ T + 5.44_{(\pm 0.31)}$	0.49	7–20	Laboratory culture	Juvenile (<2 years) growth	Wanamaker et al. 2008
Pecten maxiumus	$Mg/Ca = 0.52_{(\pm 0.19)}\ T + 9.89_{(\pm 0.84)}$	0.21	10–20	Laboratory culture	Outer shell section	Freitas et al. 2008
Pecten maxiumus	$Mg/Ca = 0.17_{(\pm 0.03)}\ T + 2.56_{(\pm 0.42)}$	0.77	10–20	Laboratory culture	Inner shell section	Freitas et al. 2012
Mytilus trossulus	$Mg/Ca = 0.30_{(\pm 0.04)}\ T + 2.25_{(\pm 0.63)}$	0.74		Estuarine (shallow tidal inlet)		Klein et al. 1996
Pinna nobilis	$Mg/Ca = \exp 0.022_{(\pm 0.04)}T + 17.16_{(\pm 1.95)}$	0.62	10–22.5	Marine (seagrass meadow)	Younger (<4.5 years) growth only	Freitas et al. 2005
Crassostrea gigas	Mg/Ca = 0.27T – 0.5		4.8–23	Marine	Juvenile (<2 years) growth	Mouchi et al. 2013
Saccostrea glomerata Moreton Bay	$Mg/Ca = 0.71_{(\pm 0.02)}T + 2.31_{(\pm 0.61)}$	0.46	11–30	Marine	Juvenile (1–2 years) growth	This study
Saccostrea glomerata Pambula Lake	$Mg/Ca\ \ 0.81_{(\pm 0.02)}T – 2.35_{(\pm 0.32)}$	0.52	10–26	Estuarine	Juvenile (1–2 years) growth	This study

Obtaining a robust temperature record from bivalve shell Mg/Ca ratios has proved somewhat problematic, as a number of factors other than temperature have been reported to influence bivalve shell Mg/Ca ratios, including ontogenetic and developmental factors (e.g. Freitas et al. 2005; Surge and Lohmann 2008; Takesue et al. 2008; Freitas et al. 2009; Schöne et al. 2011), growth rate and other biological factors (e.g. Carré et al. 2006; Strasser et al. 2008; Heinemann et al. 2011) and a tendency for some elements to be incorporated into organic components of the shell rather than the crystal lattice (Takesue et al. 2008; Schöne 2010). Variability of Mg/Ca ratios between contemporaneous individuals and also intra-shell variability can further limit the reliability of a temperature tracer offered by shell Mg/Ca ratios in some bivalve species (e.g. mussel *Mytilus edulis*, scallop *Pecten maximus*: Freitas et al. 2008; clam *Tridacna gigas*: Elliot et al. 2009).

Despite these complications, a number of studies have yielded (qualified) Mg/Ca-temperature equations for various bivalves (Table 4.1). For a number of these equations, the Mg/Ca-temperature relationship is valid only for certain periods of the bivalve's life: Surge and Lohmann (2008) found that Mg/Ca in the oyster *Crassostrea virginica* exhibited a temperature dependence only in the later period of their growth, while other studies have reported a significant relationship between Mg/Ca ratios and temperature only in the juvenile portions of shell growth in the oyster *Crassostrea gigas* (Mouchi et al. 2013) and the mussel *M. edulis* (Vander Putten et al. 2000). Some calibration relationships are limited to certain regions of the bivalve shell (Freitas et al. 2008; Elliot et al. 2009; Freitas et al. 2012; Ullmann et al. 2013), while other modern bivalve studies have identified weak correlations between Mg/Ca ratios and temperature but were unable to derive a quantitative calibration, such as that reported by Ullmann et al. (2013) for

C. gigas, Elliot et al. (2009) for *T. gigas*, Freitas et al. (2006) for *P. maximus*. Indeed, the latter study found that the Mg/Ca-temperature relationship showed a positive correlation within some portions of the shell, and an inverse correlation in others. In addition to the compelling evidence for species-specific Mg/Ca-temperature relationships, marked differences can also be seen for calibrations derived for the same species by different studies: Wanamaker et al (2008) derived a significantly different Mg/Ca-temperature relationship to that of Freitas et al. (2008) for the mussel *M. edulis*, which is different again to that observed by Vander Putten et al. (2000).

This paper examines the Mg/Ca-temperature relationship in the shell of two geographically distinct populations of the Sydney rock oyster, *Saccostrea glomerata*, to assess this species' potential as a paleotemperature tracer and to derive a robust Mg/Ca-temperature relationship that can be applied to archaeological or fossil samples. This oyster is endemic to Australia and is prevalent within Holocene-age archaeological midden sites along the Australian east coast. If a robust Mg/Ca-temperature relationship can be established for this species, it has the potential to be a valuable source of Holocene climate information, particularly as this is a region for which few such records exist (see Reeves et al. 2013; Petherick et al. 2013).

4.2. Methods and materials

4.2.1. *Saccostrea glomerata* (Sydney rock oyster)

Saccostrea glomerata is found along the east, north and west coasts of Australia, from northern Victoria through New South Wales and Queensland and through the tropics to Shark Bay in Western Australia (Malcolm 1971; Kailola et al. 1993; Nell 2001). *Saccostrea glomerata* is almost always cemented to a hard substrate

and while it prefers an estuarine intertidal habitat, can be found in up to 3 m water depth, surviving completely submerged conditions (Malcolm 1971; Kailola et al. 1993).

The reported preferred temperature tolerance for *S. glomerata* is 12–25 ºC. *S. glomerata* in New Zealand exhibit the greatest growth between temperatures of 17–20°C (Dinamani 1991), while Nell and Dunkley (1984) found optimum nutrient uptake and growth in *S. glomerata* from New South Wales, Australia occurred in the range 20–30°C.

The oysters grow best in salinities of ~26–36 but can tolerate the range ~15–45 (Nell & Dunkley 1984; reported as g l^{-1}) and possibly even up to ~50 (Nell & Gibbs 1986). *Saccostrea glomerata* generally take 2.5–3 years to reach a commercial sale size, which is usually shell length (from hinge to growth edge) of 85–100 mm (Malcolm 1971), and some cultivated oysters have reached 255 mm (Lamprell & Healy 1998). *Saccostrea glomerata* can live for up to 10 years (Kailola et al. 1993). *Saccostrea glomerata* was a commonly exploited species among Australia's indigenous population and is found in Aboriginal midden sites along the east coast of Australia (e.g. Bailey 1975; Sullivan 1982; Ulm 2002).

4.2.2. Field culturing experiments

In-situ culturing experiments were conducted at two locations on the east coast of Australia: Moreton Bay, Queensland and Pambula Lake, New South Wales (Figure 4.1). These two locations approximate the geographical extremes of *S. glomerata*'s occurrence in the Western Pacific. Commercial oyster farms at each location provided the samples for the experiments, and infrastructure such as trays, bags and suitable mooring sites for the oysters.

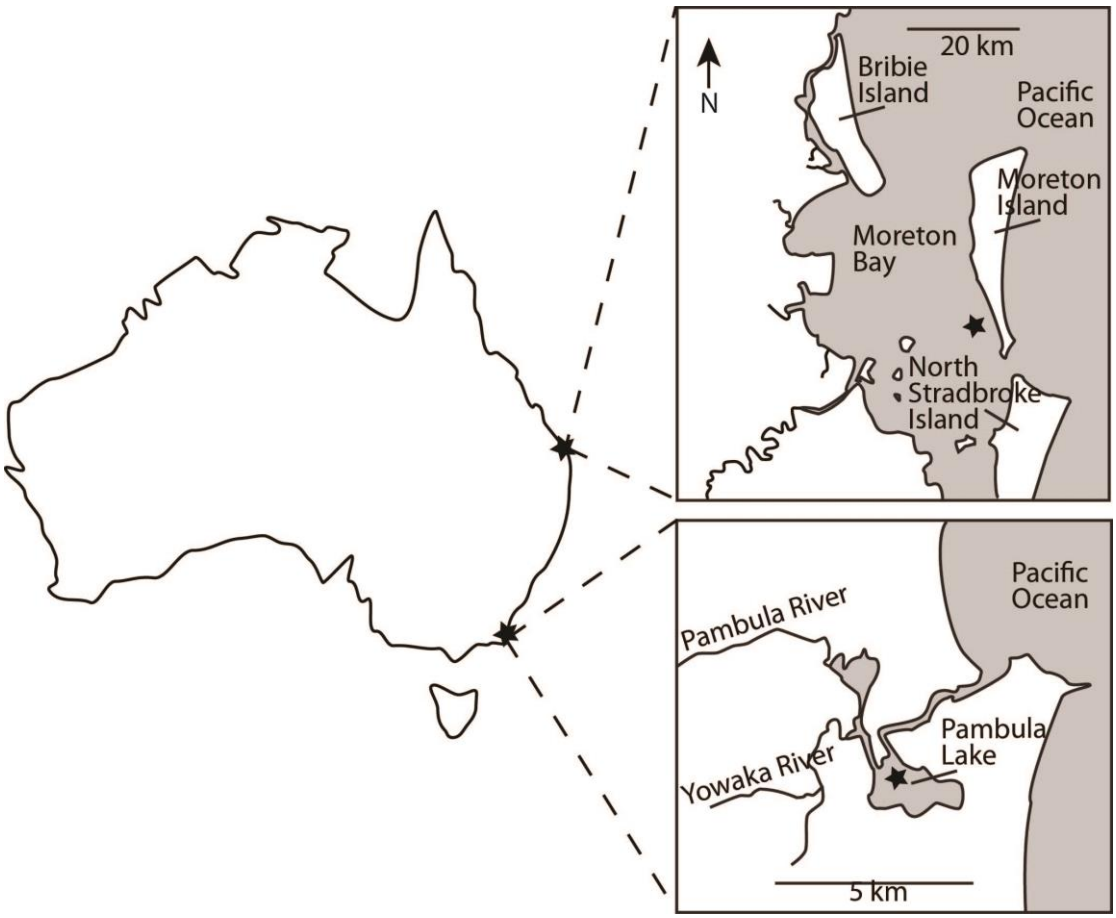

Figure 4.1. Maps showing locations of the field culturing experiment sites: Moreton Bay, southeast Queensland and Pambula Lake, southeast New South Wales.

4.2.2.1. Moreton Bay

Moreton Bay is located in the transitional subtropical/tropical climate zone of southeast Queensland. The bay is a wedge-shaped embayment, ~31 km at the widest point in the north and ~1 km wide at the southern end flanked on the eastern side by the North Stradbroke and Moreton sand barrier islands (Figure 1). The Moreton Bay Marine Park is a protected site under the Ramsar Convention, and covers an area of 1523 km^2. Its catchment area of 21,220 km^2 (Dennison and Abal 1999) encompasses the major metropolitan area of the city of Brisbane. The bay supports a variety of highly productive and diverse ecosystems, including wetlands, mangrove and coral communities, seagrass beds, swamps and barrier islands.

River discharge into the bay occurs primarily as response to rainfall, which occurs mainly in the summer months. Discharge into the northern part of the bay is derived from the Brisbane, North and South Pine, and Caboolture rivers. While freshwater plumes from the Brisbane River have been documented to cover areas of up to ~14 km^2, with a reach of ~3.6 km into Moreton Bay in times of extreme flooding, the influence of river discharge is generally restricted to a plume covering ~0.5–2 km^2 during summer months and 0.1–1.5km^2 during winter months (Yu 2011). Modeling of suspended sediment loads shows that riverine influences generally do not extend sufficiently far into the bay to affect the prevailing marine salinity conditions at the experiment site (Bell and Amghar 2000). Hydrodynamic transport modeling indicating residence times of waters in Moreton Bay ranging from 3–5 days near the oceanic entrances to up to >100 days in areas close to the mainland and river mouths. Overall residence time for water in the bay is ~45 days. Most exchange with ocean waters occurring through the northern entrance, with flow through the southern end more restricted (Dennison and Abal 1999).

4.2.2.2. Pambula Lake

Pambula Lake is a tidal lake located on the far south coast of New South Wales, and experiences a mild, temperate climate. Freshwater enters the lake from the Pambula and Yowaka rivers (Figure 4.1). The lake has a catchment area of 296.5 km^2, and the volume of the estuary is 9773.7 ML. This, divided by the mean tidal flux 2.96×10^6 m^3 gives a residence time for waters in the lake of ~3 tidal cycles, i.e. 1.5 days (data from NSW Government Office of Environment and Heritage; http://www.environment.nsw.gov.au/estuaries/stats/PambulaRiver.htm). The lake

narrows into the Pambula River which flows for a further ~5 km before reaching the ocean.

4.2.3. Experiment set-up

In each location, ~100 oysters were collected, measured along the shell length from hinge to the ventral margin using digital calipers (accuracy ±0.2 mm), and labelled using Hallprint® fish-tags. The oysters were then placed in floating plastic mesh bags such that they were submerged in the surface water at all times. Oysters at Pambula Lake were measured every 4–6 weeks, but logistical constraints prevented regular measurement of the Moreton Bay oysters.

HOBO® U22 Water Temp Pro v2 temperature loggers (accuracy ±0.2ºC)) were deployed with the oysters at each location, set to record water temperature every 30 minutes. The data was reduced to a record of mean daily temperatures. Water samples and salinity readings, using a TPS AQUA-CP handheld pH conductivity meter were taken fortnightly. Water samples for trace element analysis were collected fortnightly. Samples were filtered through Millipore 0.2 µm filters, acidified with 2% HNO_3 and kept refrigerated until analysis.

The experiments were conducted for 13 months at each location, from June 2006–July 2007 at Pambula Lake, and July 2006–August 2007 at Moreton Bay.

4.2.4. Analysis

4.2.4.1. Saccostrea glomerata shell trace element analysis

Sample preparation and analysis was carried out at the Australian National University. The hinge region was selected for analysis as it contains a full record

of growth increments and is the most consolidated region of carbonate suitable for sampling. The hinge regions from six oysters from each location were set in epoxy resin, then cut through the resilifer along the growth axis, exposing a cross section of the internal growth layers (Figure 4.2).

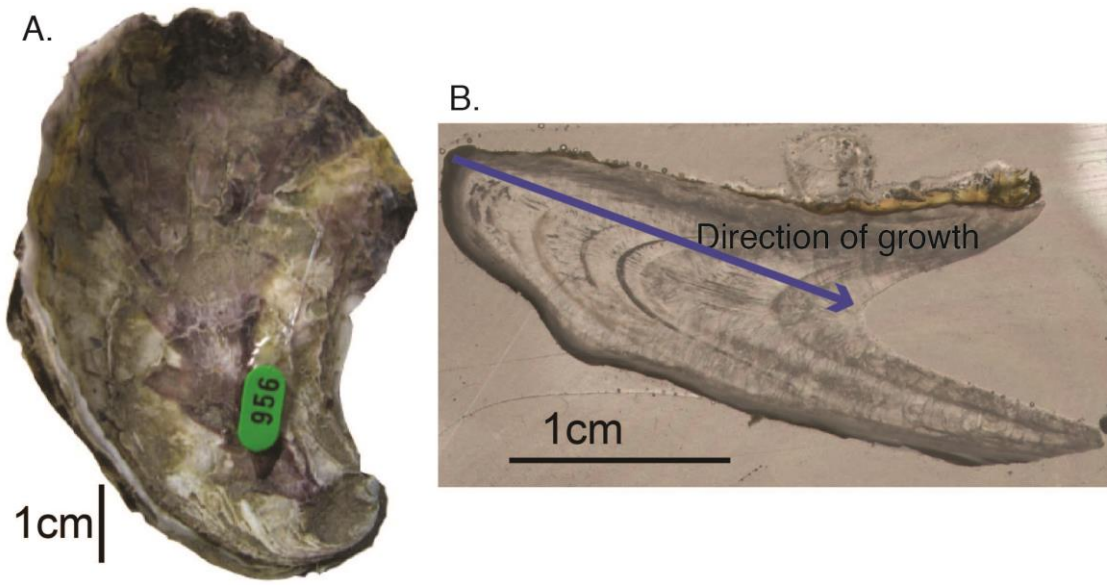

Figure 4.2. *Saccostrea glomerata*. A: Top view of the entire shell. B: Cross-section through the oyster resilifer region, showing growth increments perpendicular to the direction of growth.

The oysters were then sampled for Mg, Sr, Ba, Fe, Sn, Mn and Pb along the maximum growth axis via Laser Ablation Inductively Coupled Mass Spectrometry (LA-ICP-MS), using an excimer laser with 193 nm wavelength. Samples were pre-ablated with a spot size of 233 µm, at a speed of 6 mm/min. Analysis was conducted with a spot size of 50 µm, at a scan speed of 1.2 mm/min. The NIST 612 glass standard was analysed prior to and following each sample transect for calibration and to account for instrument drift. The ablated material was then analysed by a Varian 820-MS Inductively Coupled Plasma mass spectrometer.

4.2.4.2. Water trace element analysis

Water samples were measured at the Australian National University using a Varian Vista AX CCD Simultaneous Inductively Coupled Plasma Atomic Emission Spectrometer. Two repeats of standards of known concentrations of Mg, Ba, Mn, Ca and Sr were run in between each sample to account for instrument drift. The detection limits for Mg was 0.01 ppm.

4.2.5. Establishment of mean Mg/Ca_{shell} for each location

Based on the bulk of previous work regarding Mg/Ca in biogenic carbonate and the seasonal nature of the *S. glomerata* Mg/Ca profiles we expected that the Mg/Ca ratios in the *S. glomerata* shells would be influenced by the calcification temperature. Accordingly, the most recent annual cycles of the Mg/Ca profiles from the *S. glomerata* shells were taken to represent the most recent year of growth, i.e. growth that occurred during the ~1 year-long field culture experiments.

The shell Mg/Ca profiles were 'stacked' by averaging the last annual growth cycle of each shell to obtain a mean annual Mg/Ca profile for each location. This was accomplished by correcting for differences in shell growth rate between individual oysters via 'tuning' the last annual growth cycle to a reference shell profile. Moreton Bay shells were correlated to shell MBSg905 and all Pambula Lake shells were correlated to shell PLSg602, using the AnalySeries software (Version 2.0), a package designed for stratigraphic correlation in paleoclimate studies.

The records were correlated via consistent tie-points reflecting both the extreme and the transitional values of the seasonal Mg/Ca cycle. The tie-points were user-defined by identifying and matching significant features between the

shell Mg/Ca profiles. Given the variation between individuals, the same features were not readily identifiable in every individual shell record. As such, tie-points did not necessarily always match the same features in each shell record and their number was variable, numbering between 12 and 15 for the Moreton Bay *S. glomerata* shells and between 6 and 12 for the Pambula Lake shells. Tie-points were kept to a minimum, with more tie-points added only when necessary to improve correlation coefficients between the shell and reference shell records. Maximum correlation coefficients (R^2) between the Mg/Ca profile of shell PLsg602 and the other Pambula Lake *S. glomerata* were between 0.71 and 0.89. For the Moreton Bay shells, R^2 values were between 0.77 and 0.9.

After the shell Mg/Ca records has been correlated to the reference shell, the Mg/Ca values were averaged to obtain a 'mean' Mg/Ca signal that takes into account the variable growth rates of the oysters and also any inter-shell variability in Mg/Ca profiles.

4.2.6. Establishment of a temporal context for Mg/Ca_{shell}

The mean Mg/Ca records were then correlated with the temperature record from each location, again using AnalySeries. Tie-points between the mean Mg/Ca records and the temperature records were user-defined, and determined by identifying the corresponding extreme and transitional values within the temperature and Mg/Ca records, assuming a zero time-lag between ambient water temperature fluctuations and Mg/Ca variation in the shell. Thirteen tie-points were used for the Moreton Bay correlation and 14 for the Pambula Lake correlation. It is noted that this is a somewhat subjective approach and that the ultimate correlations may vary slightly between users. However, the strength of the relationship between the two records and the features chosen as tie points is

indicated by the high correlation coefficients (R^2) of 0.86 for Moreton Bay *S. glomerata* and 0.93 for the Pambula Lake *S. glomerata* for the Mg/Ca-temperature correlations. These correlations produced a 're-scaled' Mg/Ca profile for each location within the temporal context of the temperature record for the experiment period.

4.2.7. Investigation of shell Mg/Ca-temperature relationships

The re-scaled mean Mg/Ca datasets were then used to derive a linear Mg/Ca-temperature calibration. As the temperature datasets were of a higher resolution than the rescaled shell Mg/Ca datasets, the mean Mg/Ca records were interpolated (stretched) to match the resolution of the temperature datasets.

The data was then plotted with a least-squares linear regression to derive a calibration equation for the Mg/Ca-temperature relationship. Exponential regressions have been used to describe the Mg/Ca relationship in foraminifera (e.g. Lea et al. 1999; Elderfield and Ganssen 2000) and the bivalve *P. maximus* (Freitas et al. 2005) but we found that fitting an exponential curve to the data did not result in a stronger correlation.

As well as linear regressions of the Mg/Ca-temperature relationships, we also calculated partition coefficients for Mg incorporation (D_{Mg}) for the *S. glomerata* at each site. D_{Mg} values describe the partitioning of Mg between the ambient water and the shell, and are calculated:

$$D_{Mg} = Mg/Ca_{shell} / Mg/Ca_{water} \quad \text{(Eq. 4.1)}$$

The available water sample data allowed for calculation of D_{Mg} values at a ~monthly resolution for Moreton Bay, and a ~fortnightly resolution for Pambula

Lake. The Mg/Ca_{shell} values (as determined by the temporal constraint provided by the Mg/Ca_{shell}-temperature tuning) were compared to the Mg/Ca_{water} value for the corresponding date. In some instances there was no direct match between the assigned date of the Mg/Ca_{shell} value and the Mg/Ca water sample date. In these cases, Mg/Ca_{shell} values were derived by taking an average of the Mg/Ca_{shell} values on either side of the target date.

To assess the temperature dependence of D_{Mg}, linear regressions between temperature and D_{Mg} were calculated for the *S. glomerata* from each location.

4.2.8. Shell growth

Along with the measurements of overall shell length that were taken at the beginning and conclusion of the experiment period for the Moreton Bay *S. glomerata* and throughout the experiment period at the Pambula Lake location, an additional estimate of the shell growth rates was determined based on individual shell seasonal Mg/Ca cycles. This again relies on the assumption that the Mg/Ca signal contained within the oyster shells is influenced by temperature, and that a full cycle/oscillation/ represents a full year of shell growth.

Using AnalySeries, shell Mg/Ca-temperature correlations for the last annual cycle were conducted by manually defining tie-points between the growth axis of the individual oyster hinge and the logged temperature record. This provided a temporal context for the Mg/Ca profile of each shell. As the shell Mg/Ca values were then correlated with set time periods, growth rates were estimated by dividing the distance along the growth axis (mm) by the time represented by each discrete Mg/Ca value. Linear regressions were plotted between growth rates and Mg/Ca values for the *S. glomerata* from each location to assess the influence of growth rate upon Mg/Ca.

4.3. Results

4.3.1. Environmental conditions

The environmental parameters and *S. glomerata* growth rates for each location over the duration of the field culturing experiments are shown in Figure 4.3. The water temperature at Pambula Lake ranged from 11.6–24.7 ºC. A salinity of ~33–34 was generally maintained within the lake, except during periods of intense rainfall, when a minimum value of 1.8 was reached.

At Moreton Bay, temperature ranged from 11 to 30 ºC and salinity was 35.1–36.7. Rainfall data shown in Figure 3 are from Bureau of Meteorology rainfall records for the Redland Bay Golf Club site number 40853 (Moreton Bay) and the Pambula Post Office site number 69024 (Pambula Lake).

4.3.2. Shell growth

As with other oysters, (e.g. *C. virginica*, see Surge and Lohmann 2008) shell growth in *S. glomerata* is ecophenotypic, i.e. it is irregular and exhibits variation within and between individuals. Unfortunately no method of marking the shells at the commencement of the experiment period was conducted and so although visible growth increments can be seen in shell thin section (e.g. Figure 4.2) we are unable to constrain these increments/growth layers within a temporal context.

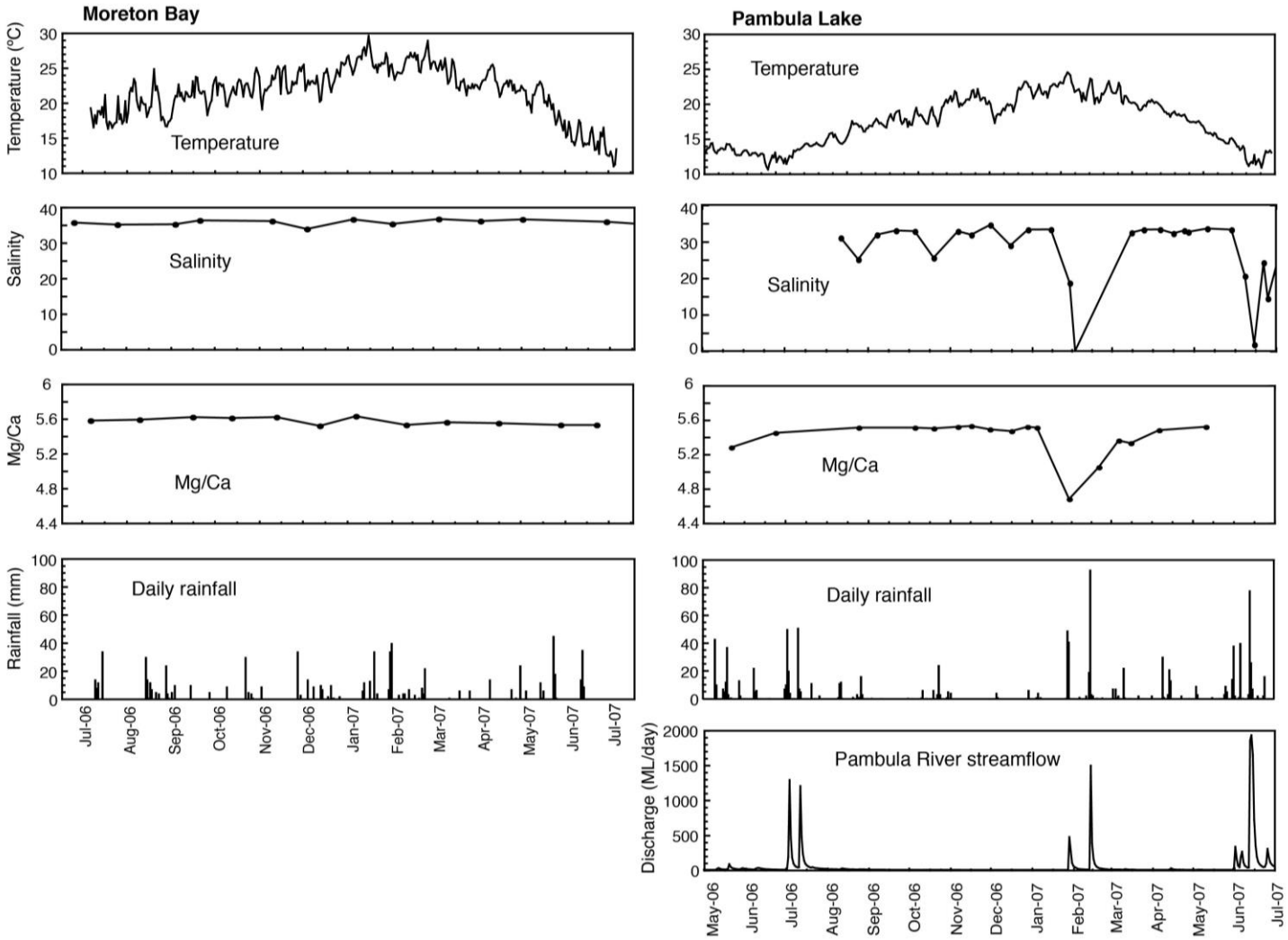

Figure 4.3. Environmental parameters during the field culturing experiments at Moreton Bay and Pambula Lake.

The growth data obtained at the beginning and end of the experiment at Moreton Bay, and throughout the experiment at Pambula Lake are shown in Table 4.2. The measurements are of the entire shell length, and while this gives an indication of overall shell growth during the experiment period, it cannot be directly related to the rate of growth along the growth axis through the umbo region, where the LA-ICP-MS transects were analysed. Furthermore, any breakage of the shell that resulted from tidal movements while in the water or during handling would result in measurements that are not representative of the full amount of growth. As such, these growth rates only provide a qualitative indication of the amount of growth that occurred over the experiment period.

The data do show that all *S. glomerata* shells at both locations exhibited growth during the experiment period and that overall growth rates were comparable between the two locations, varying from 0.10 mm/week (MBSg997) to 0.68 mm/week (MBSg909) at Moreton Bay, and 0.13 mm/week (PLSg705) to 0.60 mm/week (PLSg606) at Pambula Lake. Furthermore, although the sample size is limited, it can be seen that the younger (smaller at the beginning of the experiment period) oysters' shells exhibit faster growth rates than the older ones (larger at the beginning of the experiment period).

4.3.3. Saccostrea glomerata Mg/Ca

The Mg/Ca profiles for each of the *S. glomerata* are shown in Figure 4.4. There is good reproducibility between the individuals from each location, and the Mg/Ca of each shell exhibits clear seasonal cycles. This supports our assumption that the Mg incorporation into *S. glomerata* shell does exhibit a temperature dependence. The most recent seasonal Mg/Ca cycle (shown as the shaded regions in Figure 4.4) was taken to represent the most recent year of shell growth, i.e. that which occurred during the experiment period.

Table 4. 2. Shell lengths recorded during the experiment periods for *Saccostrea glomerata* at Moreton Bay and Pambula Lake.

	Pambula Lake Shell length (mm)								
	4-Jun-06	**8-Jul-06**	**25-Aug-06**	**6-Oct-06**	**30-Nov-06**	**9-Apr-07**	**9-Jul-07**	**Total growth (mm)**	**Mean growth rate (mm/week)**
PLSg602	53.9	53.4	54.0	55.0	59.4	72.2	80.8	26.9	0.47
PLSg606	59.5	59.5	58.5	62.1	67.2	81.6	93.8	34.3	0.60
PLSg607	57.5	57.2	56.0	61.4	64.9	76.1	82.1	24.6	0.43
PLSg646	69.1	69.0	66.0	65.2	67.0	79.9	83.2	14.1	0.25
PLSg705	68.2	66.2	69.0	74.7	69.1	73.3	75.5	7.3	0.13
PLSg720	81.3	81.6	81.5	80.9	82.4	86.7	90.5	9.2	0.16
	Moreton Bay Shell length (mm)								
	20-Jul-06	**15-Aug-07**	**Total growth (mm)**	**Mean growth rate (mm/week)**					
MBSg905	30.0	63.3	33.3	0.60					
MBSg909	37.2	75.4	38.2	0.68					
MBSg945	50.8	68.4	17.6	0.32					
MBSg960	65.4	82.5	17.1	0.31					
MBSg997	89.8	95.3	5.5	0.10					
MBSg981	94.7	-	-						

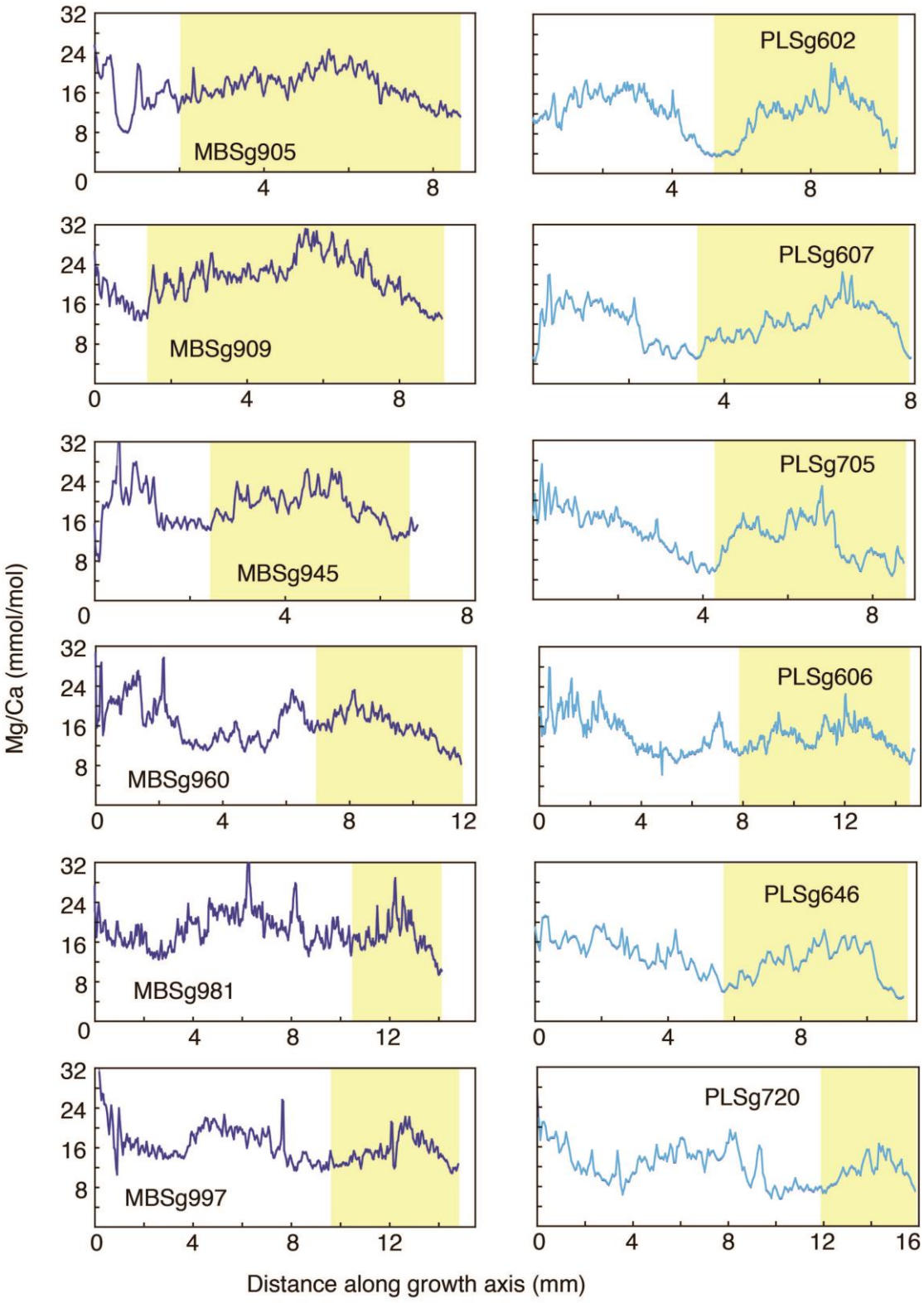

Figure 4.4. Entire shell Mg/Ca profiles from the Moreton Bay (sample name prefix MB) and Pambula Lake (sample name prefix PL) *S. glomerata*. Clear seasonal signals are apparent in all shells. Shaded area indicates most recent year of growth.

4.3.4. Mg/Ca-temperature relationships

The correlations between the mean Mg/Ca profiles for the *S. glomerata* from each location are shown in Figure 4.5.

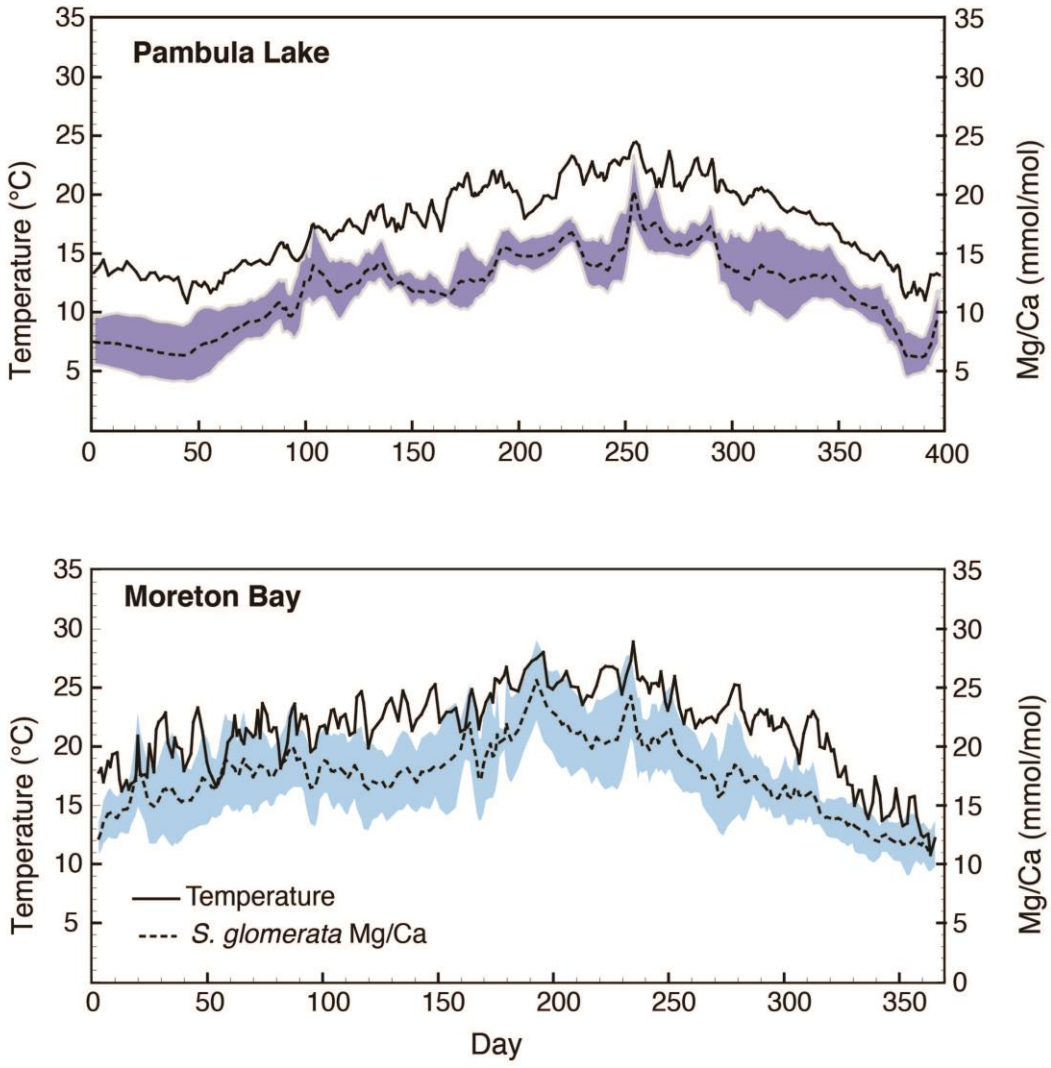

Figure 4.5. Correlations of 'mean' *S. glomerata* Mg/Ca profiles (dashed lines) and temperature records (solid lines) for each location. The shaded area represents one standard deviation around the mean (stacked) Mg/Ca values.

These correlations were used to derive the linear relationships (Figure 4.6) between Mg/Ca and temperature for the *S. glomerata* at each location. These relationships are defined by the equations (errors provided are 1σ):

Moreton Bay: $Mg/Ca = 0.71_{(\pm 0.02)} * T + 2.31_{(\pm 0.61)}$ (Eq. 4.2)

$R^2 = 0.72$, n = 243

Pambula Lake: $Mg/Ca = 0.81_{(\pm 0.02)} * T - 2.35_{(\pm 0.32)}$ (Eq. 4.3)

$R^2 = 0.85$, n = 373

N.B. The sample numbers (n) provided here refer to the number of data acquisition points, not the number of shells sampled.

The slopes on the two equations are similar, however, the y-intercepts of the calibration equations are markedly different.

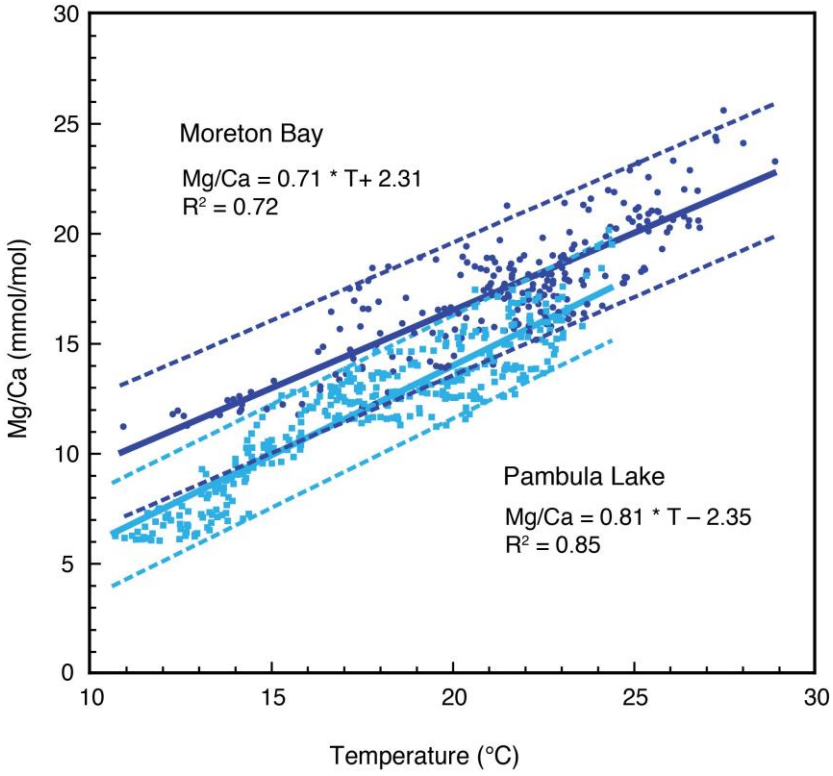

Figure 4.6. Linear regressions of Mg/Ca and temperature for the *S. glomerata* from each location. The slopes of the two regression equations are similar, but the marked difference in y-intercepts produces a clear distinction between the two populations.

4.3.5. Partition co-efficients (D_{Mg})

As the partition coefficient (D_{Mg}) is a description of the Mg/Ca within a shell compared to the Mg/Ca of the ambient water, it eliminates the potential influence of variation in the water Mg/Ca that may result from fluctuations in salinity.

Linear regressions between temperature and D_{Mg} for the two locations, shown in Figure 4.7, describe the temperature dependence of D_{Mg} as:

Moreton Bay: $D_{Mg} = 0.14_{(\pm 0.02)} * T - 0.02_{(0.46)}$ (Eq. 4.4)

$R^2 = 0.82$, n = 12

Pambula Lake $D_{Mg} = 0.14_{(\pm 0.02)} * T - 0.22_{(0.32)}$ (Eq. 4.5)

$R^2 = 0.77$, n = 22

The slopes of the two D_{Mg}-temperature equations are so similar as to be identical (within two decimal places reported here). Unlike the equations describing the Mg/Ca-temperature linear regressions, which have a clear discrepancy between their y-intercepts, the y-intercepts of the D_{Mg}-temperature equations are the same, within the reported uncertainty.

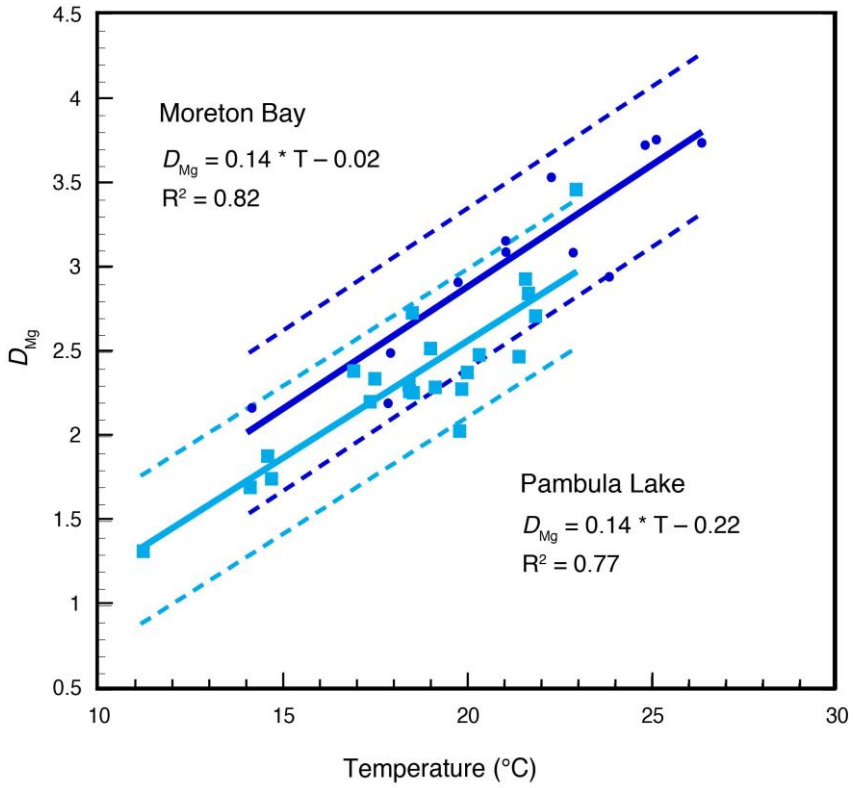

Figure 4.7. Comparison of the D_{Mg}-temperature relationships for the Moreton Bay and Pambula Lake *S. glomerata*.

4.4. Discussion

The results of this study show a clear temperature dependence of *S. glomerata* shell Mg/Ca, though there is a distinct difference in the Mg/Ca-temperature relationships derived for the two different study locations. According to our results, this difference is attributable to variations in salinity and thus water Mg/Ca ratios at the Pambula Lake site, as elaborated further below. Some geographically distinct populations of the same bivalve species have been found to exhibit genotypic differences, with subtle impacts upon growth and trace element incorporation. Genetic analysis of the oysters from each location would be required to rule out this possibility with regard to the *S. glomerata* of this study. However, this is perhaps unnecessary given that the apparent difference in Mg/Ca-temperature dependence in this case is entirely explained by accounting for the salinity of the ambient water.

4.4.1. Salinity and Mg/Ca_{water}

There is an oft-cited assumption of constant Mg/Ca in waters with salinity >10 (Dodd and Crisp 1982). However, Surge and Lohmann (2008) have cast doubt on the validity of this assumption with their observation that Mg/Ca ratios ranged from 3.5 to 5 across a salinity gradient of 10–37. Uncertainty on the lower salinity limit of constant dissolved Mg/Ca aside, the Pambula Lake salinity does briefly drop below 10, and it is evident from the data presented in Figure 4.3 that the Mg/Ca ratio of the Pambula Lake water fluctuates concurrently with the significant drop in salinity that occurred in Pambula Lake in February. Also, in general the Mg/Ca value of the water at Pambula Lake is slightly lower than that of Moreton Bay, due to the difference in salinity between the two sites.

4.4.2. Mg/Ca- and DMg-temperature relationships

The similarity between the slopes of the Mg/Ca temperature dependence equations (Equations 4.2 and 4.3) indicates that the *rate* at which Mg is incorporated into *S. glomerata* shell as temperature increases is the same, at the two locations. However, the disparity in the y-intercepts suggests a fundamental difference in the background value of Mg/Ca ratios in the oysters from the two sites. The Moreton Bay *S. glomerata*, with the higher y-intercept, have a higher baseline Mg/Ca ratio, as reflected in the average Mg/Ca values for the *S. glomerata* of each location: 17.40 for the Moreton Bay *S. glomerata*, 12.12 for the Pambula Lake *S. glomerata*. This lower baseline Mg/Ca ratio in the Pambula Lake *S. glomerata* shells could in part be accounted for by the variation in salinity at this site. Although it is reported that *S. glomerata* can tolerate salinities as low as 15, their preferred salinity range is ~26–36 (Nell & Dunkley 1984). As such, it is possible that during times of extremely high rainfall and surface water freshening the oysters may cease to precipitate their shell. Mg/Ca values corresponding to these periods will not be recorded in the *S. glomerata* shells.

However, no significant difference is apparent in the regressions derived for the temperature dependence of the *S. glomerata* D_{Mg} values from each location (Figure 4.7). These equations are the same for both locations within the reported uncertainties for the values of the intercepts. The D_{Mg} values reflect only the temperature dependence of the Mg/Ca value of the shell, since it independently accounts for the Mg/Ca value of the seawater. Because the D_{Mg} temperature dependence is the same at the two sites whereas the Mg/Ca ratio temperature dependence is not the same indicates that the Mg/Ca_{shell} signal is a convolved signal of both temperature and ambient Mg/Ca_{water}. The difference seen in the

direct Mg/Ca-temperature equations from the two locations can be accounted for by the variability of the Mg/Ca_{water} at the Pambula Lake site.

4.4.3. Growth rate

A number of studies have found correlations between high growth rate and increased trace element incorporation (e.g. Sr/Ca in *P. maximus*, Freitas et al. 2006, Sr/Ca in *Mesodesma donacium* and *Chione subrugosa*, Carré et al. 2006).

Mean overall shell growth rates for the *S. glomerata* from the two sites are slightly different: 0.40 mm/week at Moreton Bay, and 0.34 mm/week at Pambula Lake. However, variations between the y-intercepts in the calibration equations derived for individual *S. glomerata* within each location suggests this is not the reason behind the different baseline Mg/Ca ratios, as shells with higher growth rates do not consistently exhibit correspondingly higher y-intercept values. Furthermore, no significant correlation between growth rate and Mg/Ca ratios was seen in the linear regressions calculated for the individual *S. glomerata* from either location.

4.4.4. Application of *S. glomerata* shell Mg/Ca as a temperature tracer

The fact that variations in the Mg/Ca_{water} can influence the Mg/Ca_{shell} has direct implications for the use of Mg/Ca_{shell} as a temperature tracer in fossil shell samples. Firstly, the D_{Mg}-temperature relationship is clearly a more reliable method of extracting a temperature record from *S. glomerata* shells than the direct Mg/Ca-temperature relationship. Secondly, it places the same limitations upon the use of Mg/Ca ratios as a temperature tracer as those accompanying the use of $\delta^{18}O$—namely, the need to know the paleo-water chemistry in order to correctly interpret the Mg/Ca_{shell} signal.

However, this is not an insurmountable problem, as if Mg/Ca ratios are used in conjunction with $\delta^{18}O$ then the two records will simultaneously provide constraints upon each other that can help to deconvolve the combined temperature-salinity signal they each contain. This is because lower salinity (with a concurrent more negative $\delta^{18}O_{water}$) will manifest as more negative $\delta^{18}O_{shell}$, which would be interpreted (erroneously) as warmer temperature. However, lower salinity that leads to lower Mg/Ca ratios in the ambient water will manifest in the shell also as lower Mg/Ca ratios, which would be interpreted as lower temperature. Hence, the temperature records derived from the two proxies/tracers will diverge at the points of the record affected by the salinity/Mg/Ca_{water} variation. Furthermore, these points of divergence can then be interpreted as resulting from pulses of freshwater, and thus provide a record of precipitation. Unfortunately this study did not include analysis of the *S. glomerata* $\delta^{18}O$ to test this, but this would be a clear target for future research.

If a complementary $\delta^{18}O_{shell}$ record is not available, then paleo-temperature interpretations will be restricted to samples from environments that experienced little variation in salinity/Mg/Ca_{water}. It would be useful to test the threshold values of salinity before Mg/Ca_{water} is affected to ascertain if there exists a reasonable window of salinity under which the direct Mg/Ca-temperature relationship is still robust.

As the Moreton Bay site experienced a constant salinity and thus Mg/Ca_{water} throughout the experiment period, the direct Mg/Ca-temperature relationship derived for the *S. glomerata* from this location offers a more reliable temperature tracer than that of the Pambula Lake *S. glomerata*.

4.4.5. Comparison with other bivalve Mg/Ca-temperature equations

It is clear that there is variability between the bivalve Mg/Ca-temperature equations (Table 4.1; Figure 4.8) and that the nature of trace element incorporation in bivalve shells is variable among the various bivalve species. Equally noteworthy is the discrepancy between Mg/Ca-temperature relationships derived for the various *Mytilus* mussels, where even the same species exhibit different Mg/Ca-temperature relationships.

The species-specific nature of the Mg/Ca-temperature relationship is highlighted by the results of Mouchi et al. (2013), who concluded that despite the close relation of *C. virginica* and *C. gigas*, the Mg/Ca-temperature equation derived for the former by Surge and Lohmann (2008) could not be used to determine sea surface temperatures from *C. gigas* because of marked differences in the two oysters' local environments (*C. virginica*: estuarine, with higher temperatures and large fluctuations in salinity; *C. gigas*: marine). Similarly, in a paleotemperature reconstruction from a fossil specimen of the marine oyster *Sokolowia buhsii*, Bougeois et al. (2014) found that the Mg/Ca-temperature relationship derived by Surge and Lohmann (2008) for the estuarine *C. virginica* did not yield realistic temperatures, but rather, the Mouchi et al. (2013) equation for *C. gigas* from an open marine environment was more suitable.

Given these findings, and the results of this study, it is possible that some of this variability in Mg/Ca-temperature dependence might be caused by differences in the salinity (and thus the water Mg/Ca) of the bivalves' ambient environments. A cursory analysis of the Mg/Ca-temperature correlations presented in Figure 4.8 in the context of the bivalves' local environment does not reveal any definitive conclusions, although three of the four estuarine species (*C. virginica*, Surge and Lohmann 2008; *S. glomerata* (Pambula Lake), this study; *M.*

edulis, Vander Putten et al. 2000) cluster together within the broader set of Mg/Ca-temperature relationships.

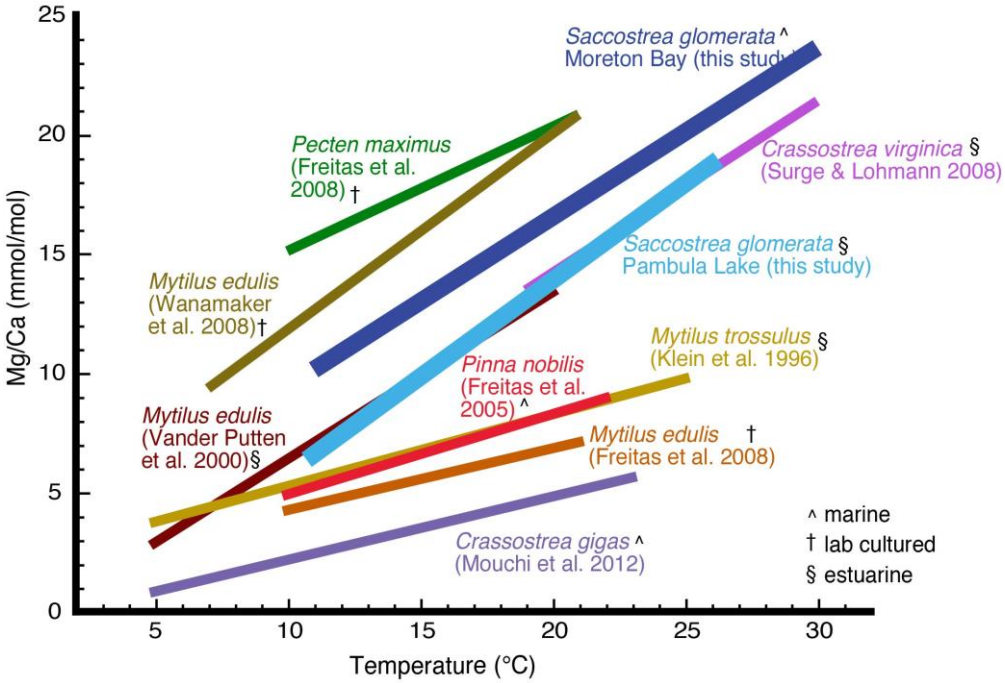

Figure 4.8. Comparison of various published bivalve Mg/Ca-temperature relationships. Clear variations between species, and even the same species, are evident.

Our ability to compare D_{Mg}-temperature dependence among other bivalves is more limited, as few studies have published this data. Surge and Lohmann (2008) published the following equation for *C. virginica*:

$$10^3 D_{Mg} = 0.16 * T - 0.33 \quad \text{(Eq. 4.6)}$$

$$R^2 = 0.33$$

As with the direct Mg/Ca-temperature relationship reported for *C. viginica* and the *S. glomerata* Mg/Ca-temperature relationships from this study, the temperature dependence of the D_{Mg} for *C. virginica* is identical to that of *S. glomerata* (Equations 4.4 and 4.5), within the reported uncertainties.

4.5. Conclusion

Two Mg/Ca-temperature equations have been developed for the shell of *S. glomerata*, using data from field culture experiments in estuarine and marine environments on the east coast of Australia. Results show that the Mg/Ca ratios of *S. glomerata* shell is a promising paleotemperature tracer, as the oysters show clear seasonal signals with a robust Mg/Ca-temperature dependence. However, significant variation/a distinct difference was seen in the y-intercept values of the equations derived for the *S. glomerata* from each site.

When the *S. glomerata* shell Mg/Ca temperature dependence was analysed with respect to D_{Mg} values, which take into account the Mg/Ca_{water} and thus eliminate the influence of salinity variations, the two sites exhibited a near-identical D_{Mg}-temperature dependence. This is an extremely significant finding, as it calls into question the prevailing paradigm that bivalve shell Mg/Ca offers a temperature tracer that is independent of salinity. Indeed, these findings show that like $\delta^{18}O$, to properly interpret a Mg/Ca_{shell} record from *S. glomerata*, and calculate absolute temperatures, the water chemistry must also be known. While the D_{Mg}-temperature relationship presents a more robust temperature tracer, provided salinity is constant, the direct Mg/Ca_{shell}-shell relationship still enables the determination of seasonal temperature ranges.

Furthermore, as $\delta^{18}O_{shell}$ and Mg/Ca_{shell} are both affected by variations in salinity but are driven in the opposite directions within temperature space then these two geochemical tracers could be used in conjunction to deconvolve the combined temperature-salinity signals in each of the record, and even potentially be used to simultaneously obtain a precipitation signal. This is an important observation that can potentially be applied more widely to other bivalve taxa to

improve the quality of paleotemperature reconstructions, even from existing datasets.

While the broad range of Mg/Ca-temperature equations published for bivalves has long supported the species-specific nature of bivalve shell Mg/Ca ratios, the disparity seen between the Mg/Ca-temperature equations for *S. glomerata* from estuarine and marine locations in this study emphasizes the additional influence of local environmental variations on trace element incorporation. This provides evidence that bivalve paleotemperature interpretations using Mg/Ca ratios should be conducted with caution, particularly if there is uncertainty about the provenance of the shell samples and their original environment.

Finally, given the scarcity of high-resolution Holocene climate records for the eastern Australia region and this species' prevalence in Aboriginal midden sites along the eastern coast of Australia, analysis of archaeological specimens using a combination of Mg/Ca and $\delta^{18}O$ analyses has the potential to provide useful information regarding Holocene climate variation in this currently understudied region.

Acknowledgements

Funding for this study was provided in the form of a CRC LEME PhD Scholarship. The authors would like to thank Chris and Ray Tynan and Jane and David Clout for providing both oysters and equipment for the field culturing experiments. We also extend our thanks to Les Kinsley for assistance with shell sampling and Linda McMorrow for assistance with water sampling. We also thank the editors for their efforts in compiling the special issue.

4.6. References

Bailey, G. N. (1975), The Role of Molluscs in Coastal Economies: The Results of Midden Analysis in Australia, *Journal of Archaeological Science*, *2*, 45–62.

Bell, S., and M. Amghar (2002), Modelling Scenarios for South East Queensland Regional Water Quality Management Strategy, Cooperative Research Centre for Coastal Zone, Estuary & Waterway Management.

Bougeois, L., M. de Rafelis, G. J. Reichart, L. J. de Nooijer, F. Nicollin, and G. Dupont-Nivet (2014), A high resolution study of trace elements and stable isotopes in oyster shells to estimate Central Asian Middle Eocene seasonality, *Chemical Geology*, *363*, 200–212.

Carré, M., I. Bentaleb, O. Bruguier, E. Ordinola, N. T. Barrett, and M. Fontugne (2006), Calcification rate influence on trace element concentrations in aragonitic bivalve shells: Evidences and mechanisms, *Geochimica Et Cosmochimica Acta*, *70*(19), 4906–4920.

Corrége, T. (2006), Sea surface temperature and salinity reconstruction from coral geochemical tracers, *Palaeogeography Palaeoclimatology Palaeoecology*, *232*(2-4), 408–428.

Dennison, W. C., and E. G. Abal (1999), *Moreton Bay Study: A Scientific Basis for the Healthy Waterways Campaign*, 246 pp., South East Queensland Regional Water Quality Management Strategy, Brisbane.

Dinamani, P. (1991), The Pacific oyster, *Crassotrea gigas* (Thunberg, 1793) in New Zealand., in *Estuarine and Marine Bivalve Mollusk Culture*, edited by W.

Menzel, pp. 315–318., CRC Press, Florida.

Dodd, J. R., and E. L. Crisp (1982), Non-linear variation with salinity of Sr/Ca and Mg/Ca ratios in water and aragonitic bivalve shells and implications for paleosalinity studies, *Palaeogeography Palaeoclimatology Palaeoecology*, *38*, 45–56.

Driscoll, R., M. Elliot, T. Russon (2014) ENSO reconstructions over the past 60 ka using giant clams (*Tridacna* sp.) from Papua New Guinea, *Geophysical Research Letters 41*(19), 6819–6825.

Dutton, A. L., K. C. Lohmann, and W. J. Zinsmeister (2002), Stable isotope and minor element proxies for Eocene climate of Seymour Island, Antarctica, *Paleoceanography*, *17*(2).

Elderfield, H., and G. Ganssen (2000), Past temperature and $\delta^{18}O$ of surface ocean waters inferred from foraminiferal Mg/Ca ratios, *Nature*, *405*(6785), 442–445.

Elliot, M., K. Welsh, C. Chilcott, M. McCulloch, J. Chappell, and B. Ayling (2009), Profiles of trace elements and stable isotopes derived from giant long-lived *Tridacna gigas* bivalves: Potential applications in paleoclimate studies, *Palaeogeography Palaeoclimatology Palaeoecology*, *280*(1–2), 13–22.

Elmore, A. C., S. Sosdian, Y. Rosenthal, and J. D. Wright (2012), A global evaluation of temperature and carbonate ion control on Mg/Ca ratios of ostracoda genus Krithe, *Geochemistry Geophysics Geosystems*, *13*.

Freitas, P., L. J. Clarke, H. Kennedy, C. Richardson, and F. Abrantes (2005), Mg/Ca, Sr/Ca, and stable-isotope ($\delta^{18}O$ and $\delta^{13}C$) ratio profiles from the fan mussel *Pinna nobilis*: Seasonal records and temperature relationships, *Geochemistry Geophysics Geosystems*, *6*.

Freitas, P. S., L. J. Clarke, H. A. Kennedy, and C. A. Richardson (2008), Inter- and intra-specimen variability masks reliable temperature control on shell Mg/Ca ratios in laboratory- and field-cultured *Mytilus edulis* and *Pecten maximus* (bivalvia), *Biogeosciences*, *5*(5), 1245–1258.

Freitas, P. S., L. J. Clarke, H. Kennedy, and C. A. Richardson (2009), Ion microprobe assessment of the heterogeneity of Mg/Ca, Sr/Ca and Mn/Ca ratios in *Pecten maximus* and *Mytilus edulis* (bivalvia) shell calcite precipitated at constant temperature, *Biogeosciences*, *6*(7), 1209–1227.

Freitas, P. S., L. J. Clarke, H. Kennedy, and C. A. Richardson (2012), The potential of combined Mg/Ca and $\delta^{18}O$ measurements within the shell of the

bivalve *Pecten maximus* to estimate seawater $\delta^{18}O$ composition, *Chemical Geology*, *291*, 286–293.

Freitas, P. S., L. J. Clarke, H. Kennedy, C. A. Richardson, and F. Abrantes (2006), Environmental and biological controls on elemental (Mg/Ca, Sr/Ca and Mn/Ca) ratios in shells of the king scallop *Pecten maximus*, *Geochimica Et Cosmochimica Acta*, *70*(20), 5119–5133.

Heinemann, A., C. Hiebenthal, J. Fietzke, A. Eisenhauer, and M. Wahl (2011), Disentangling the biological and environmental control of *M. edulis* shell chemistry, *Geochemistry Geophysics Geosystems*, *12*.

Ingram, B. L., P. De Deckker, A. R. Chivas, M. E. Conrad, and A. R. Byrne (1998), Stable isotopes, Sr/Ca, and Mg/Ca in biogenic carbonates from Petaluma Marsh, northern California, USA, *Geochimica Et Cosmochimica Acta*, *62*(19–20), 3229–3237.

Nell, J.A., and P.R. Dunkley (1984), Effects of temperature, nutritional factors and salinity on the uptake of L-methionine by the Sydney rock oyster (*Saccostrea commercialis*), *Marine Biology*, *80*, 335–339.

Kailola, P. (1993), *Australian fisheries resources*, Bureau of Resource Sciences and the Fisheries Research and Development Corporation, Canberra, Australia.

Lamprell, K., and J. Healy (1998), *Bivalves of Australia. Volume 2*, Backhuys, Leiden.

Lea, D. W., T. A. Mashiotta, and H. J. Spero (1999), Controls on magnesium and strontium uptake in planktonic foraminifera determined by live culturing, *Geochimica Et Cosmochimica Acta*, *63*(16), 2369–2379.

Malcolm, W. B. (1971), The Sydney rock oyster, *Australian Natural History*, *17*(2), 45–50.

Mouchi, V., M. de Rafélis, F. Lartaud, M. Fialin, and E. Verrecchia (2013), Chemical labelling of oyster shells used for time-calibrated high-resolution Mg/Ca ratios: A tool for estimation of past seasonal temperature variations, *Palaeogeography, Palaeoclimatology, Palaeoecology*, *373*(0), 66–74.

Nell, J. A. (2001), The history of oyster faming in Australia, *Marine Fisheries Review*, *63*(3), 14–25.

Nell, J. A., and P. J. Gibbs (1986), Salinity tolerance and absorption of L-methionine by some Australian bivalve mollusks, *Australian Journal of Marine and Freshwater Research*, *37*(6), 721–727.

Petherick, L., et al. (2013), Climatic records over the past 30 ka from temperate

Australia—a synthesis from the Oz-INTIMATE workgroup, *Quaternary Science Reviews*, *74*, 58–77.

Reeves, J. M., T. Barrows, T. Cohen, A. Kiem, H. Bostock, K. Fitzsimmons, J. Jansen, J Kemp, Claire Krause, Lynda Petherick, Steven J. Phipps, OZ-INTIMATE Members (2013), Climate variability over the last 35,000 years recorded in marine and terrestrial archives in the Australian region: an OZ-INTIMATE compilation, *Quaternary Science Reviews*, *74*, 21–34.

Rosenthal, Y, E.A. Boyle, N. Slowey (1997) Temperature control on the incorporation of magnesium, strontium, fluorine and cadmium into benthic foraminiferal shells from Little Bahama Bank: Prospects for thermocline paleoceanography, *Geochimica Et Cosmochimica Acta, 61*(17), 3633–3643.

Schöne, B. R., Z. J. Zhang, P. Radermacher, J. Thebault, D. E. Jacob, E. V. Nunn, and A. F. Maurer (2011), Sr/Ca and Mg/Ca ratios of ontogenetically old, long-lived bivalve shells (*Arctica islandica*) and their function as paleotemperature proxies, *Palaeogeography Palaeoclimatology Palaeoecology*, *302*(1–2), 52–64.

Schöne, B. R., Z. Zhang, D. Jacob, D. P. Gillikin, T. Tutken, D. Garbe-Schonberg, T. McConnaughey, and A. Soldati (2010), Effect of organic matrices on the determination of the trace element chemistry (Mg, Sr, Mg/Ca, Sr/Ca) of aragonitic bivalve shells (*Arctica islandica*)-Comparison of ICP-OES and LA-ICP-MS data, *Geochemical Journal*, *44*(1), 23–37.

Sisma-Ventura, G., B. Guzner, R. Yam, M. Fine, and A. Shemesh (2009), The reef builder gastropod *Dendropoma petreaum*—A proxy of short and long term climatic events in the Eastern Mediterranean, *Geochimica Et Cosmochimica Acta*, *73*(15), 4376–4383.

Strasser, C. A., L. S. Mullineaux, and B. D. Walther (2008), Growth rate and age effects on *Mya arenaria* shell chemistry: Implications for biogeochemical studies, *Journal of Experimental Marine Biology and Ecology*, *355*(2), 153–163.

Sullivan, M. (1982), *Aboriginal shell middens in the coastal landscape of New South Wales*, PhD Thesis, The Australian National University, Canberra.

Surge, D., and K. C. Lohmann (2008), Evaluating Mg/Ca ratios as a temperature proxy in the estuarine oyster, *Crassostrea virginica*, *Journal of Geophysical Research-Biogeosciences*, *113*(G2) Article number G02001.

Takesue, R. K., C. R. Bacon, and J. K. Thompson (2008), Influences of organic

matter and calcification rate on trace elements in aragonitic estuarine bivalve shells, *Geochimica Et Cosmochimica Acta*, *72*(22), 5431–5445.

Ullmann, C. V., F. Boehm, R. E. M. Rickaby, U. Wiechert, and C. Korte (2013), The Giant Pacific Oyster (*Crassostrea gigas*) as a modern analog for fossil ostreoids: Isotopic (Ca, O, C) and elemental (Mg/Ca, Sr/Ca, Mn/Ca) proxies, *Geochemistry Geophysics Geosystems*, *14*(10), 4109–4120.

Ulm, S. (2002), The Seven Mile Creek Mound: New Evidence for Mid-Holocene Aboriginal Marine Resource Exploitation in Central Queensland, *The Proceedings of the Royal Society of Queensland*, *110*, 121–126.

Vander Putten, E., F. Dehairs, E. Keppens, and W. Baeyens (2000), High resolution distribution of trace elements in the calcite shell layer of modern *Mytilus edulis*: Environmental and biological controls, *Geochimica Et Cosmochimica Acta*, *64*(6), 997–1011.

Wanamaker, A. D., K. J. Kreutz, T. Wilson, H. W. Borns, D. S. Introne, and S. Feindel (2008), Experimentally determined Mg/Ca and Sr/Ca ratios in juvenile bivalve calcite for *Mytilus edulis*: implications for paleotemperature reconstructions, *Geo-Marine Letters*, *28*(5–6), 359–368.

Yu, Y. (2011), *Numerical Study of the Brisbane River plume in Moreton Bay, Australia*, Masters Thesis, Griffith University, Queensland.

Chapter 5

Testing the viability of using Mg/Ca of archaeological *Saccostrea glomerata* shells as a paleotemperature archive

Authors and contributions:

Sarah Tynan: 80%: conceived study, conducted field work, sampling and data analysis

Bradley Opdyke 5%: overarching guidance and support, feedback on written drafts

Maureen Walczak 5%: overarching guidance and support, feedback on written drafts

Andrea Dutton 5%: overarching guidance and support, feedback on written drafts

Sean Ulm 5%: provision of shells and feedback on written drafts

ABSTRACT

Here we present the shell Mg/Ca ratio records of two archaeological specimens of the Sydney Rock oyster, *Saccostrea glomerata*, from the Sandstone Point midden site, in the Moreton Bay region of southeast Queensland, Australia. The Mg/Ca-temperature relationship derived for modern *S. glomerata* from Moreton Bay is used to infer seasonal sea-surface temperatures from the midden shells for the period ~1.6 ka cal BP.

An ontogenetic signal of declining amplitude in the Mg/Ca ratio profiles was evident in both midden shells. This has implications for the application of an appropriate Mg/Ca-temperature relationship, as a modern calibration derived for the early years of growth will be inappropriate for calculating temperatures from the later years of growth of archaeological specimens.

The temperatures derived from the early growth of the midden *S. glomerata* shells indicated similar summer maximum temperatures, cooler winter minima and cooler annual average temperatures for Moreton Bay region during the late Holocene. This study confirms the potential of using Mg/Ca ratios of *S. glomerata* found in Aboriginal midden sites to infer temperatures for the late Holocene period in Australia and also highlights the need for careful application of an appropriate Mg/Ca-temperature calibration.

Key words

Saccostrea glomerata, shell, midden, Mg/Ca, temperature, late Holocene climate

5.1. Introduction

Compared to the Northern Hemisphere, Holocene climate records for the Southern Hemisphere are scarce. In particular, there are very few spanning the late Holocene, i.e. the period from ~5 ka cal. BP to present (PAGES 2k Consortium 2013). Augmenting this record is crucial to understanding the Holocene climate dynamics of the Australian continent. The OZ-INTIMATE synthesis (Reeves et al. 2013) provides a thorough overview of existing climate records for the Australian region for the past 30 000 years, along with the complexities of compiling a picture of Holocene climate variability over such a large and diverse continent. Here we focus on understanding the potential contribution that can be made to knowledge of Late Holocene climate in southeast Queensland through the use of geochemical proxies in archaeological bivalve shells.

5.1.1. Eastern Queensland during the Holocene

Sea level

The size and variation in the continental shelf off the coast of Queensland leads to localised geographical variations in sea level over time. As such, caution must be exercised when attempting to extrapolate local records of sea-level change (and other climatic variability) to a regional scale (Lewis et al. 2013; Moss et al. 2013). Woodroffe (2009) presents evidence from Cleveland Bay in northern Queensland of a Holocene sea level highstand at ca. 5 ka cal. BP of ~2.8 m higher than modern sea level, and Lewis et al. (2015) found that prior to 1.2 ka cal. BP in the Cleveland Bay area, sea level was ~1 m higher than present, dropping until ca. 800 cal. yrs BP when it stabilised at the present level.

Studies of the northern New South Wales and Moreton Bay regions reviewed in Gontz et al. (2014) indicated a highstand of ~1.5–2 m higher than current sea level at ca. 6 ka cal. BP (Gontz et al. 2014 and references therein). Leonard et al. (2013) present evidence of coral reef growth in Moreton Bay indicating a sea-level highstand at ~6.6 ka cal. BP of at least 1.1 m greater than present sea level.

Whether the regression in sea level from the mid-Holocene highstand to current sea level occurred as a steady declining trend or in an oscillating fashion is unclear (Gontz et al. 2014; Lewis et al. 2013 and references therein). In the Moreton Bay area, Leonard et al. (2013) inferred that a rapid cessation of reef growth at ~5.7 ka cal. BP was possibly caused by a rapid drop in sea level at that time. In a discussion of the evolution of Moreton Bay since the Pleistocene, Robins et al. (2015) suggests that sea level reached current level ca. 2 ka cal. yrs BP. In general, the pattern of a mid-Holocene sea-level highstand followed by a gradual regression is consistent with glacial isostatic modelling of the region (e.g. Nakada and Lambeck 1989).

Holocene climate variability

Using pollen records from North Stradbroke Island to assess changes in vegetation through the Quaternary, Moss et al. (2013) found evidence for wetter conditions during the early Holocene (~10–5 ka cal BP) and drier conditions since 5 ka cal BP. These trends are consistent with the OZ-INTIMATE climate synthesis, wherein warmer and wetter conditions are implicated for the early Holocene, followed by drier, more variable conditions for the late Holocene (5 ka cal BP to present). Regionally, the climate regime for eastern Queensland that has persisted to the present was essentially in place by ~5 ka cal BP (Reeves et al.

2013). Shulmeister and Lees (1995) determined the onset of ENSO-like conditions at ~4 ka cal BP, while Donders et al. (2008) place the onset of a ENSO-dominated climate regime around 5 ka cal BP, with an increase in ENSO activity around 3 ka cal BP. A sclerochronological analysis of mollusc shells from an Aboriginal midden in the tropics of northern Australia suggests a shift to drier conditions 2–0.5 ka cal BP (Brockwell et al. 2013). However, these records focus on the equatorial Pacific and records that examine late-Holocene climate in the eastern Queensland region are scarce.

The scarcity of high-resolution records spanning the mid to late Holocene, along with the uncertainties and geographical sparseness of existing records limits the robustness of the paleoenvironmental record that can be inferred for eastern Queensland. There is a need to develop additional proxies of Holocene climate variability in the Queensland region to complement existing records, as well as expand the areal coverage of reconstructions, as the disparities evident between the studies referenced above emphasise the potentially localised nature of many records, meaning they may be inappropriate for interpreting regional scale environmental change.

5.1.2. Climate information from bivalves

A currently under-explored potential source of paleoclimate information for this region is the abundant bivalve shells in the numerous Aboriginal midden sites found along Australian coastlines (there are also several complementary inland midden sites containing freshwater bivalve shells). Sclerochronological techniques—analysis of growth increment widths and stable isotope (predominantly $\delta^{18}O$) and trace element geochemistry (predominantly Mg/Ca, Sr/Ca ratios) of internal shell structures—are yet to be used to their full potential.

There are few published sclerochronology studies pertaining to Australian shell species (e.g. Brockwell et al. 2013; Tynan et al. 2014; Twaddle et al. 2016; Tynan et al. 2016). This is despite the existence of numerous well-preserved midden sites along the Queensland coastline, and indeed, the entire coastline of eastern Australia (Ulm and Reid 2000; Ulm 2011). More than 1500 sites have been documented on the Queensland and northern New South Wales coasts (Aitken et al. 1992), Sullivan (1982) documents ~800 sites on the New South Wales coast, and there are 6325 midden sites recorded in the New South Wales Aboriginal Heritage Information Management System maintained by the New South Wales Department of Environment (http://www.environment.nsw.gov.au/licences/AboriginalHeritageInformationManagementSystem.htm). Shells found in midden sites are predominantly the remains of shellfish collected as a food resource and can represent centuries of continuous (or seasonal) habitation of an area. With their direct connection to the human occupation of the landscape, shells from midden sites can also provide unique insights into human-environment interactions.

Climate records have been interpreted from the sclerochronological analysis of fossil and archaeological bivalves from various regions of the globe (see reviews by Andrus 2011 and Twaddle et al. 2016). As bivalve carbonate is secreted incrementally throughout the organism's lifetime, they provide a high-resolution record of seasonal environmental variability. The life-spans of different bivalve species is variable, and although some bivalves are extremely long-lived (e.g. a specimen of the bivalve *Arctica islandica* from the north Atlantic Ocean has been documented as being 507 years old (Butler et al. 2013)) other bivalves, such as *S. glomerata,* offer only a short record of several years (e.g. Tynan et al. 2016). However, some studies have used large numbers of comparatively short-

lived species to construct longer climate records, such as the work of Carré et al. (2014) who used the $\delta^{18}O$ of 180 shells of the Peruvian surf clam, *Mesodesma donacium,* to compile a climate record of ENSO variability in western Peru during the Holocene.

A compensation for any lack of longevity in the temporal record obtained from bivalve shells is the record's high resolution. While this also varies among different bivalve species, it is possible to obtain annually-resolved records (e.g. Jones and Quitmyer 1996), seasonal signals (e.g. Tynan et al. 2014; Tynan et al. 2016) and even fortnightly, daily- and even diurnally- (tidal) resolved records (Schöne and Surge 2014 and references therein).

As well as the variation evident in the lifespans and the temporal nature of the growth patterns of different bivalve taxa, there is also strong evidence that controls upon the incorporation of trace elements into the carbonate of bivalve shell vary from species to species (e.g. Schöne et al. 2011) and even within the same species (e.g. Tynan et al. 2016). As such, trace element proxies within bivalve shells must be carefully calibrated within modern specimens and the impact of local environmental dynamics understood.

Several studies have examined fossil and/or archaeological oyster specimens to infer changes in climatic conditions or human-landscape interactions (e.g. Hong et al. 1995; Kirby et al. 1998; Kirby 2000; Surge et al. 2003; Brigaud et al. 2008; Mouchi et al. 2013; Bougeois et al. 2014; Bougeois et al. 2016). This study seeks to test the viability of using the Mg/Ca of the shell of an Australian bivalve species, *Saccostrea glomerata* (Sydney Rock oyster) sourced from the Sandstone Point midden site in southeast Queensland as a record of paleotemperature.

5.1.3. Sandstone Point midden

The coast of southeast Queensland has been extensively studied with respect to archaeological deposits, with more than 1500 coastal midden sites documented (Atiken et al. 1992). Exploitation of marine resources in this region during the late Holocene is well-documented, as discussed by Ulm (2002). Sandstone Point midden is located within a series of beach ridges on the mainland of southeast Queensland on the shore of Moreton Bay (Figure 5.1). Moreton Bay is fed by the Brisbane, North Pine and Logan Rivers, with the sand islands of Moreton Island and North and South Stradbroke Island acting as barrier islands that restrict the flow of coastal currents into the bay.

Sandstone Point midden covers an area of ~25 000 m^2 and forms a triangle bounded by mudflats to the east, Godwin Beach township to the south-west, and a wave-cut cliff that represents the mid-Holocene sea-level highstand on the north-west. The site is comprised of a series of sand ridges, parallel to the shore. These represent paleo-shorelines throughout the period of sea-level variation since the mid-Holocene highstand. Densely packed shell material is found within these ridges, indicating close occupation of the changing shoreline (Walton 2012).

Various sections of the deposit have been excavated since initial work carried out by Haglund (1974). This initial excavation identified several species of shells: *Anadara trapezia* (cockles), *S. glomerata* (classified as *Sassostrea commercialis*) *Trichomya hirsuta* (hairy mussel) and *Pyrazus ebenius* (mud whelks). These shell deposits were found to extend to depths of 60–90 cm throughout the midden. Cow bones were also excavated from the top of these deposits, located within a layer of powdery compacted shell material. This layer was attributed to European lime-burning activities and indicates potential disturbance to the site.

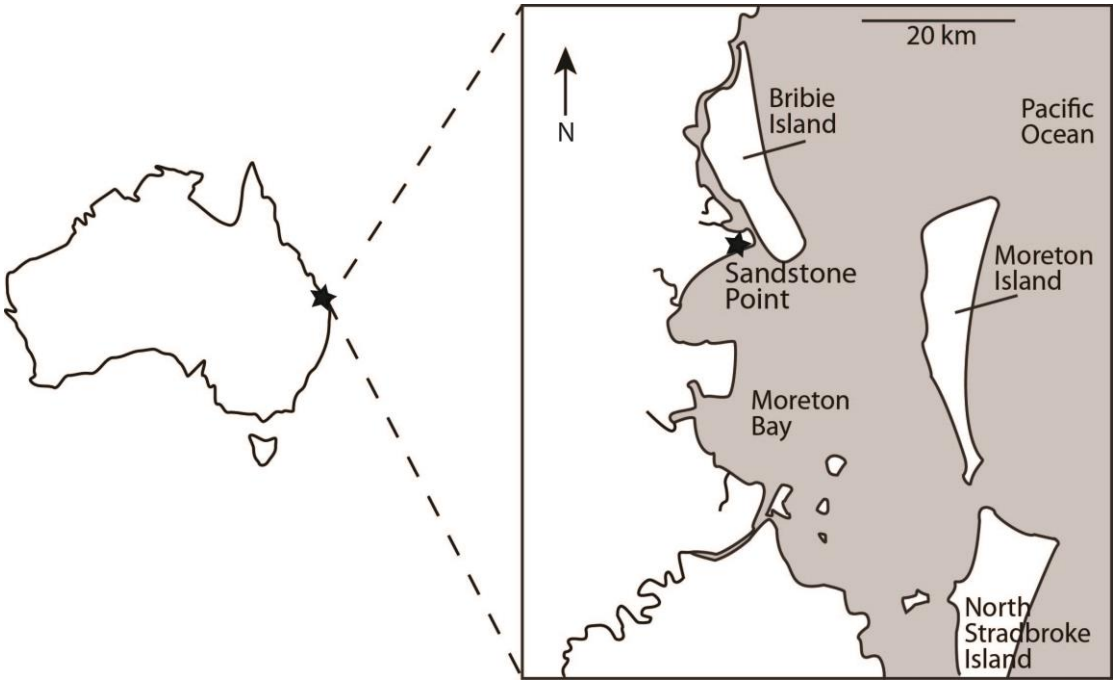

Figure 5.1. The location of the Sandstone Point midden within the Moreton Bay region.

Charcoal samples from this initial excavation were dated at 620 +/-95 years BP (Crooks 1982, in Nolan 1986). Further work carried out in 1985 by Nolan found a very high density of fish bone remains. Other 'non-economic' (shells that were not specifically collected for their food value) shells were found in the midden, along with a small number of crustacean claws and some bird and mammal bones. Small stone artifacts are present throughout the midden site, with variable density of distribution (Nolan 1986). Overall, this excavation included 38 sample locations throughout the midden complex, which exhibited high variability in both age and distribution of material.

Radiocarbon dates obtained by Nolan (1986) for charcoal samples from various locations within the midden complex range from 320 +/-50 years BP to 2,290 +/- 100 years BP. These dates indicate the Sandstone Point midden complex was formed during the late Holocene, with a significant lag time between the mid-

Holocene sea-level highstand to the current sea level and occupation of the coastal site.

Just as these archaeological sites can provide a rich source of paleoenvironmental information, these same paleoenvironmental interpretations can help inform archaeological and anthropological investigations of human-environment interactions (e.g. Brockwell et al. 2013; Twaddle et al. 2016). Nolan (1986) provides a discussion of the anthropological history of the Toorbul region, highlighting the uncertainty resulting from conflicting ethnographical accounts of the boundaries of the various Aboriginal groups that lived in the broader area. Ethnographical accounts also indicate that as the region was rich in food sources, Aboriginal groups inhabited the area throughout the year, with no need to travel in search of alternate subsistence resources. These accounts can vary depending on their ultimate source, and geochemical analysis of shells from middens can contribute to understanding of site usage by offering objective insights regarding the season of collection of shellfish—whether they were collected and consumed predominantly only during particular seasons, or all year round.

Another aspect of sclerochronological analysis that could prove useful is the ability to assess the age of shellfish at the time of their collection, which can contribute to understandings of exploitation rates. Walton (2012) investigated material from Sandstone Point midden, using morphometrical analysis of shells and shell fragments to assess the exploitation rates of shellfish during the time of site occupation. With respect to interpreting the changes in shellfish species and density throughout the stratigraphy of midden sites, geochemical analysis of shells can elucidate climatic conditions and help decouple the impacts of human harvesting and environmental controls upon shellfish abundance (Brockwell et al. 2013).

The two archaeological shell specimens used in this study were part of Nolan's 1985 excavation. The shells came from a section of the midden containing charcoal samples that were dated at 1600 ±80 ka BP (Nolan 1986). Although the exact provenance of the two Sandstone Point midden *S. glomerata* shells can not be definitively determined, it is assumed that they were sourced locally. Foraging ranges documented for coastal people in Australia have shown that shellfish are generally sourced no more than 1500 m from the midden site location, and generally within 500 m (Meehan 1982). This indicates that the environmental information inferred from midden shells is relevant to the local area.

5.2. Methods

5.2.1. *Saccostrea glomerata* shell trace element analysis

Shell trace element analysis was conducted at the Research School of Earth Sciences, the Australian National University. The hinge region was cut from the rest of the shell using a diamond rock saw, and embedded within epoxy resin. When set, the shells were cut through the resilifer along the growth axis to expose a cross section of the internal growth layers within the hinge (Figure 5.2).

The shells were prepared into thick sections (~100µm) affixed to glass microscope slides. Sampling for Mg, Sr, Ba, Fe, Sn, Mn and Pb along the maximum growth axis was conducted via Laser Ablation Inductively Coupled Mass Spectrometry (LA-ICP-MS), using an Excimer laser with 193 nm wavelength. Samples were pre-ablated with a spot size of 233 µm, at a speed of 6 mm/min. Continuous line analysis was conducted with a spot size of 50 µm, at a scan speed of 1.2 mm/min. The NIST 612 glass standard was analysed prior to and following each sample transect for calibration and to account for instrument

drift. The ablated material was then analysed by a Varian 820-MS Inductively Coupled Plasma mass spectrometer.

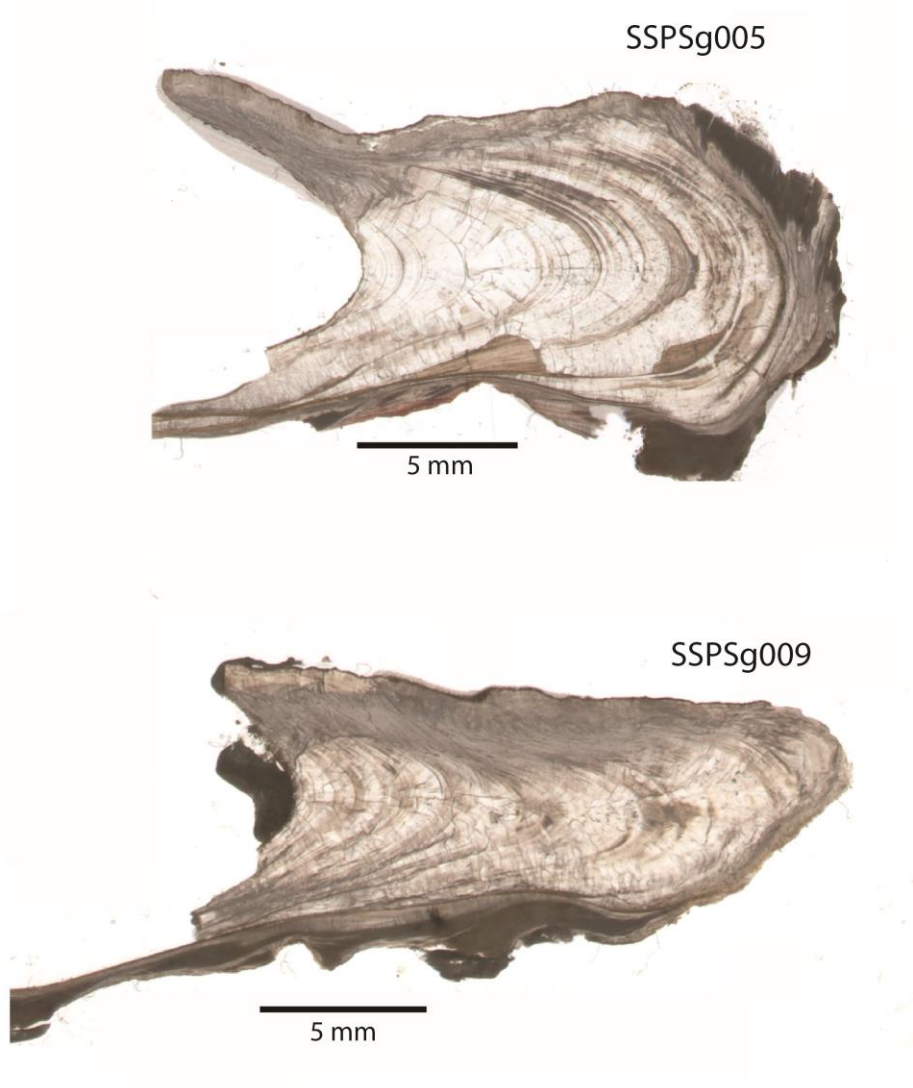

Figure 5.2. Thin-section photographs of cross-sections the hinge region of the two midden shells used in this study.

A data reduction process was carried out on the ICP-MS data whereby values were normalised to Ca and anomalously high amplitude peaks were removed from the dataset through visual inspection of the plotted data. Comparison of the standard values analysed prior and following each shell transect enabled correction of the data for instrumental drift. The data were then smoothed to obtain a more consistent signal.

5.2.2. Temperature reconstruction from Sandstone Point midden S. glomerata Mg/Ca

The Mg/Ca-temperature equation derived for modern-day *S. glomerata* grown in Moreton Bay by Tynan et al. (2016) was used to reconstruct temperature records from selected portions of the Mg/Ca profiles of each of the Sandstone Point midden *S. glomerata*. The calibration study examined *S. glomerata* from both estuarine and marine environments, and found that there was a marked difference between the Mg/Ca-temperature relationships for the *S. glomerata* from each location. As the two *S. glomerata* populations showed consistent D_{Mg}-temperature relationships, authors concluded that this value is a more reliable proxy for calcification temperature. D_{Mg} values describe the partitioning of Mg between the ambient water and the shell, and thus requires that the ambient water Mg/Ca be known. This is a significant finding as the application of an inappropriate calibration equation can seriously impact upon the integrity of a paleoclimate interpretation, and is compelling evidence that interpretation of paleotemperature records derived from *S. glomerata* Mg/Ca must be approached with caution, and ideally with supplementary knowledge that can place the archaeological shells within the context of their paleoenvironment.

However, use of this parameter requires that the Mg/Ca of the ambient water is also known. As we have no means of determining paleo-Mg/Ca ratio of the water, we used the Mg/Ca-temperature relationship derived for modern *S. glomerata*, with the fundamental assumption that the Sandstone Point midden shells grew in a marine environment analogous to that of the modern-day Moreton Bay *S. glomerata*. Given the indications that sea level had stabilised by this period of the late Holocene (Woodroffe 2009; Lewis et al. 2013; Moss et al. 2013;

Leonard et al. 2013; Gontz et al. 2014) this is an acceptable assumption, however the associated uncertainties are discussed in more detail in the Discussion section.

The Mg/Ca-temperature relationship derived by Tynan et al. (2016) for *S. glomerata* is described by the equation:

$$Mg/Ca = 0.71_{(\pm 0.02)} * T + 2.31_{(\pm 0.61)} \quad \text{(Eq 5.1)}$$

$$R^2 = 0.72, n = 243$$

Re-arranging this equation to derive a temperature record from shell Mg/Ca gives the following equation:

$$T = 1.41_{(\pm 0.06)} * Mg/Ca - 3.25_{(\pm 0.10)} \quad \text{(Eq 5.2)}$$

The RMSE for Equation 5.3 is 2.14 ºC. Errors on the equation coefficients were propagated by deriving the maximum and minimum values using errors on Equation 5.2, then inverting these values to derive errors for the coefficients within Equation 5.3.

To enable the use of the Mg/Ca-temperature equation derived from the modern Moreton Bay *S. glomerata*, for which only juvenile growth was available for analysis and thus derivation of the calibration relationship, only the early years of growth were used to create the temperature reconstructions: the first year of shell SSPSg005, and the first three years of shell SSPSg009. We acknowledge that it is possible that these early years of growth potentially exhibit some disequilibrium of trace metal incorporation due to faster growth rates, which makes this portion of the shell less preferred for temperature reconstructions, but

only juvenile shells were available for the Moreton Bay *S. glomerata* calibration study so the paleo-temperature reconstruction focussed on this region.

The very early growth of each shell Mg/Ca profile exhibited Mg/Ca values lower than the mean minimum values of the rest of the shell. The reasons for these low values are unclear and so this portion of the Mg/Ca record was not included in the temperature reconstruction. This is further discussed in Section 5.4.2.

5.3. Results

5.3.1. *Saccostrea glomerata* Mg/Ca

The two Sandstone Point midden shells' Mg/Ca profiles (Figure 5.3) show clear seasonal variation, each representing multi-year records that likely span the transition from juvenile to adult growth. A feature within both shells is a difference in the Mg/Ca ratio profile of the early years of growth compared to the later years, with more variable and higher amplitude Mg/Ca ratios during the juvenile years of growth. This higher amplitude and more variable pattern is evident during the first year of growth in shell SSPSg005 and the first three years of growth in shell SSPSg009. The reason underlying this discrepancy in the duration of the juvenile Mg/Ca regime is unclear.

The two shells show good reproducibility in their maximum and minimum Mg/Ca values, and the overall shape of the Mg/Ca ratio profiles. The maximum Mg/Ca value during the juvenile growth in shell SSPSg005 is 24.7 with a mean maximum value of 18.7 for the later years. Shell SSP009 exhibits a mean maximum Mg/Ca of 25.6 during the juvenile growth years, and 18.1 during the later years. The Mg/Ca maxima show broad peaks, while the Mg/Ca minima are more truncated, indicating the precipitation of less carbonate this time, and slower

growth. The intra-shell minimum Mg/Ca values are consistent throughout the duration of shell growth within each specimen. The mean minimum Mg/Ca value for shell SSPSg005 is 8.9 and 10.4 for shell SSPSg009.

The mean annual Mg/Ca values, calculated by averaging all Mg/Ca for each year-long period, are 12.6 for the first year of shell SSPSg005, and 14.2, 12.9 and 13.4 (mean value 13.5) for the later years. In shell SSPSg009, the mean annual Mg/Ca values for the three juvenile years are 17.1, 16.2 and 14.9 (mean value 16.7) and 13.7, 14.6 and 14.5 (mean value 14.3) for the later years of growth. It should be noted that as a result of increased precipitation of carbonate during the warmer months (as indicated by the broader peaks in the Mg/Ca maxima as compared to the more cuspate minima), mean annual Mg/Ca values may be biased towards higher values.

5.3.2. Mg/Ca-derived temperature record

The temperature records derived from the Sandstone Point midden shells Mg/Ca from the first year of growth from shell SSPSg005 and the first three years of growth of shell SSPSg009 are shown in Figure 5.4. The mean annual temperature, calculated using Equation 5.2, derived from the first year of growth in shell SSPSg005 Mg/Ca is 19.6 ºC. Mean annual temperatures derived for the first three years of growth in shell SSPSg009 are 20.9, 19 and 16.7 ºC. As mentioned above, it must be noted that the increased precipitation of carbonate during the warmer months likely biases mean annual temperatures towards warmer temperatures.

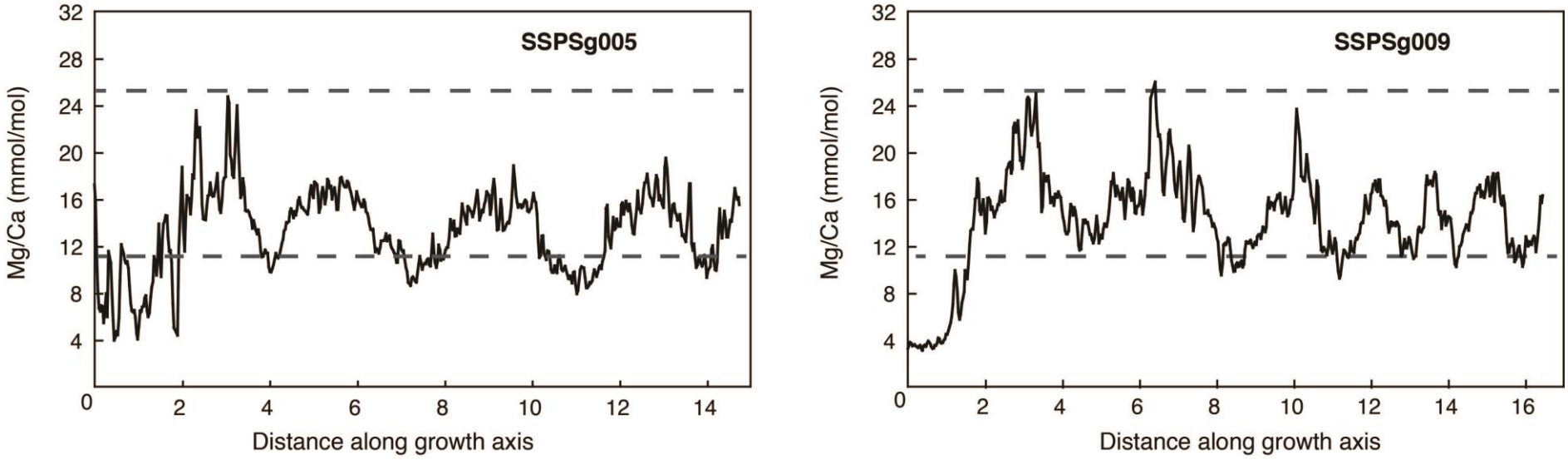

Figure 5.3. Mg/Ca profiles of shells SSP005 and SSP009. Clear seasonal signals are evident in both shell profiles.

The dashed lines indicate the seasonal amplitude of the Mg/Ca ratios within modern *S. glomerata* shells.

As the decreased amplitude in the Mg/Ca signal during the later years of growth is the result of lower maximum Mg/Ca values only, the modern Mg/Ca-temperature calibration can also be applied to the midden *S. glomerata* shells to obtain winter minimum temperatures. Mg/Ca values in shell SSPSg009 indicate a mean winter minimum of 10.4 ºC, whereas values in shell SSPSg009 indicate a mean winter minimum of 8.9 ºC.

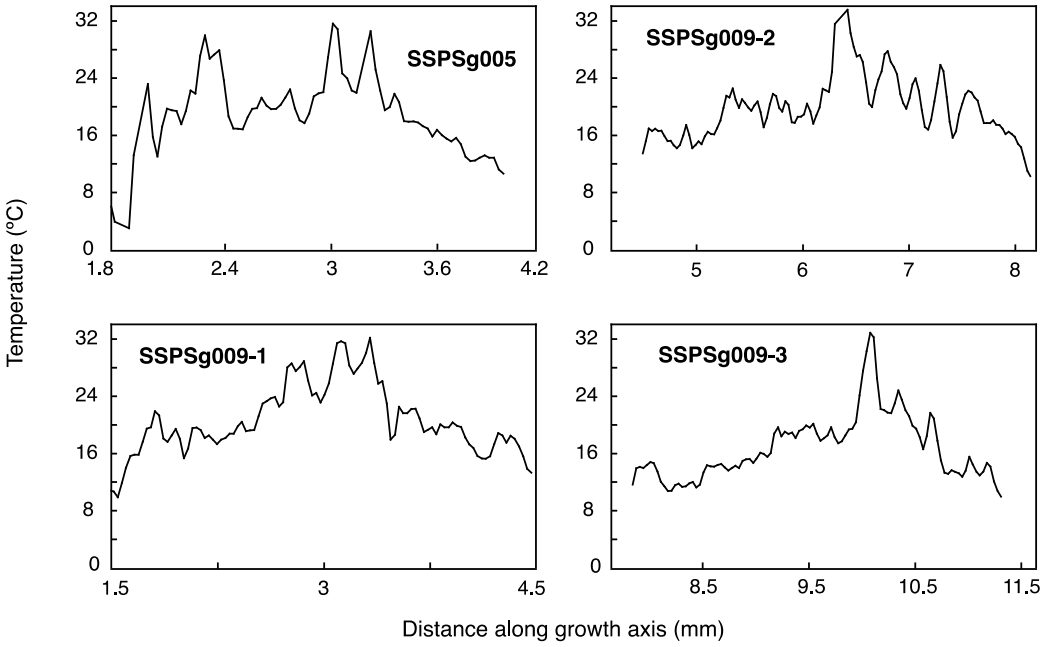

Figure 5.4. Temperature profiles reconstructed from the Mg/Ca ratios of shells SSP005 and SSP009. Clear seasonal signals are evident in both shell profiles.

5.4. Discussion

5.4.1. Reproducibility and integrity of *S. glomerata* Mg/Ca records

The similarity between the two shell Mg/Ca profiles is encouraging, however, this sample size is insufficient for a definitive assessment of consistent reproducibility between *S. glomerata* Mg/Ca. Sampling of a greater number of shells is needed to properly test Mg/Ca reproducibility within *S. glomerata* shells. Furthermore,

repeat samples individual shells should be carried out to ensure reproducibility in Mg/Ca ratios within individual shells.

It also cannot be determined if the shells grew contemporaneously, or indeed if their lifespans overlapped at all. Again, analysis of a greater number of shells, particularly from various locations throughout the midden stratigraphy to assess the consistency of the Mg/Ca-temperature record over time would add confidence to the reliability and robustness of the climate signal being recorded in the *S. glomerata* shells.

Another important consideration is the quality of the shell samples and the integrity of the geochemical record they contain. If the shells have undergone diagenesis or degradation over time then the Mg/Ca-temperature record they hold will be compromised. This study relies on the assumption that the region of the shell used for sampling is well-protected from external environmental influences and has thus remained unaltered following deposition in the midden site, however more stringent analysis to assess sample quality or potential diagenesis should be undertaken in any further studies.

5.4.2. Ontogenetic variation

An ontogenetic influence upon trace element incorporation has been reported for several bivalves (e.g. Freitas 2005; Strasser et al. 2008; Eliot et al. 2009; Schöne 2011; Mouchi et al. 2013) and a clear ontogenetic transition, marked by a decrease in maximum Mg/Ca values, in the shell of both the midden *S. glomerata*. This is accompanied by a decrease in growth rate, as evidenced by the smaller distance along the growth axis represented by a complete Mg/Ca in the later years of shell growth. A possible explanation for this slower growth could be a

diversion of the animal's energy to spawning and reproductive activities during the summer months.

Apart from the first year of growth in each shell, the minimum Mg/Ca values are consistent, with the decrease in Mg/Ca amplitude being accounted for solely by a decrease in the maximum Mg/Ca values. A similar trend of decreasing maximum Mg/Ca values with increasing age was also documented by Freitas et al. (2005) for *Pinna nobilis*. However, this trend is not consistent across various other bivalve species. Several bivalves show an opposite trend: Mouchi et al. (2013) reported a slight increase in mean Mg/Ca values in adult *Crassostrea gigas* compared to juveniles; an ontogenetic trend of increasing Mg/Ca ratios was reported for *Arctica islandica* by Shöne et al. (2011) and also in the inner layer of the (aragonite) shell of *Tridacna gigas* (Elliot et al. 2009). Bougeois et al (2014) did not observe any difference in the Mg/Ca ratios of the long-lived oyster *Sokolowia buhsii* over a period of 21 years. These differences are most likely attributable to variations in the different bivalves' thermal tolerances and preferred breeding seasons.

This distinct change in Mg incorporation in the later years of *S. glomerata* growth has significant implications for the use of Mg/Ca as a temperature tracer. Although this is essentially the result of decreased growth rate leading to a lower Mg/Ca amplitude, rather than a fundamental difference in the D_{Mg}-temperature relationship, a calibration of the Mg/Ca-temperature relationship for these earlier, high-Mg/Ca, years of growth will be different to that calculated for the later years of growth: a single calibration will not be applicable to both regions of the shell. This observation of a shift in the Mg/Ca-temperature relationship exclusively during the course of a bivalve's lifetime is not unique; a number of studies identify correlations between Mg/Ca and temperature only during specific periods

of growth. Some studies report temperature dependence of Mg/Ca exclusively during the juvenile years (*Crassostrea gigas*, Mouchi et al. 2013: *Pinna nobilis*, Freitas et al. 2005) while others found that only carbonate precipitated in maturity exhibited an identifiable Mg/Ca-temperature relationship: *Crassostrea virginica*, (Surge and Lohmann 2008); *Tridacna gigas* (Batenburg et al. 2011).

The Mg/Ca-temperature calibration obtained for *S. glomerata* by Tynan et al. (2016) was derived from the data collected over one year of juvenile shell growth. As such, it is appropriate to apply this calibration to only the juvenile years of shell growth of these two longer-lived midden shells. Longer-term calibration experiments with modern *S. glomerata* need to be conducted to assess the Mg/Ca-temperature relationship throughout the later years of *S. glomerata* growth and potentially derive a Mg/Ca-temperature calibration for this period.

5.4.3. Comparison of midden S. glomerata Mg/Ca to modern records

The Sandstone Point midden *S. glomerata* shell Mg/Ca profiles are shown in Figure 5.3, along with an indication of the mean maximum and minimum Mg/Ca values recorded in modern-day *S. glomerata* from the Moreton Bay calibration experiment documented in Tynan et al. (2016). The amplitude of the Mg/Ca signal of the juvenile years of the midden *S. glomerata* falls within the range of the modern, also juvenile, *S. glomerata*.

The maximum Mg/Ca values of the later years of the midden shells are of lower amplitude than those recorded in the juvenile modern shells (Figure 5.3). Analysis of longer-lived modern *S. glomerata* specimens is needed to systematically compare this part of the midden shells' records. Overall, for the period of juvenile growth for which a comparison with the modern *S. glomerata* is

possible, the midden shells' Mg/Ca profiles show a seasonal amplitude consistent with that of the modern *S. glomerata* Mg/Ca.

The minimum Mg/Ca value recorded in the modern *S. glomerata* was 11.8. This is higher than the minimum Mg/Ca of both the midden *S. glomerata*, which show minimum Mg/Ca values of 10.37 (shell SSPSg009) and 8.90 (shell SSPSg005).

5.4.4. Temperature record derived from midden *S. glomerata*

The mean annual water temperature recorded by Tynan et al. (2016) for Moreton Bay for the period of July 2006–July 2007 was 21.6 ºC. A longer-term record from the Queensland Department of Environment and Heritage Protection Crab Island monitoring station from the period August 2003–August 2010 provides a mean annual water temperature of 22.8 ºC.

The mean annual temperatures derived from the juvenile region of the *S. glomerata* midden shells range from ~1 to ~5 ºC lower than the temperature recorded by Tynan et al. (2016), with mean annual temperatures of 19.6 ºC from shell SSPSg005 and 20.9, 19 and 16.7 ºC from the first three years of shell SSPSg009. Given that the RMSE on the temperature-Mg/Ca equation is 2.14 ºC, more data from a greater number of shells will be needed to build a robust and reliable temperature signal. Nonetheless, the two midden shells analysed here consistently indicate cooler mean annual temperatures for the Moreton Bay region ca. 1600 ka cal BP.

The modern minimum winter temperature for the two winters recorded by Tynan et al. (2016) was 11 ºC, while the mean winter minimum temperature from the Crab Island field station during 2003–2010 was 16.93 ºC. Shell SSPSg009 exhibits a mean winter minimum of 10.4 ºC, and shell SSPSg005 exhibits a mean

winter minimum of 8.9 ºC, 2.1 ºC lower than the modern value recorded by Tynan et al. (2016). While these values are again within error of the value recorded by Tynan et al. (2016), the consistency of the apparently lower winter minima reiterates the trend of lower mean annual temperatures exhibited by the midden *S. glomerata* compared to the modern recorded temperature.

A potential complicating factor is identifying the exact provenance of the midden shells. As we can not be certain that the midden shells grew in a marine environment analogous to the modern *S. glomerata* used for the Mg/Ca-temperature calibration, it is possible that the application of the calibration derived in Tynan et al. (2016) is not appropriate. Ideally, an additional proxy should be employed to constrain this uncertainty, and determine whether the shell grew in an estuarine or marine environment. As discussed in Tynan et al. (2016), a combined Mg/Ca and $\delta^{18}O_{shell}$ analysis could help in identifying potential influences upon shell Mg/Ca caused by fluctuations in the ambient water salinity and Mg/Ca. Points of divergence of the two signals could be interpreted as the result of pulses of freshwater input typical of an estuarine environment: the lower salinity water, with a more negative $\delta^{18}O$, would drive the $\delta^{18}O_{shell}$ to more negative values (which would translate to apparently warmer temperatures), while having the opposite impact upon the temperature record constructed from Mg/Ca ratios—a dilution of the water Mg/Ca ratio would result in a lower Mg/Ca values within the shell, which would translate into apparently cooler temperatures.

Additionally, larger sample sizes are needed to expand upon the 'snapshots' of paleoclimate information afforded by individual *S. glomerata* shells. While analysis of more shells will improve the confidence of any paleoenvironmental interpretation, the two shells analysed here show an encouraging similarity in their Mg/Ca-derived temperature records. Another

obvious area for further investigation is the examination of other trace element ratios within *S. glomerata* shells.

5.4.5. Potential archaeological interpretations

The Mg/Ca profiles of each of the Sandstone Point midden *S. glomerata* terminate at values that are close to the Mg/Ca maxima for the later years of shell growth. This indicates the season of death (and therefore collection) for both shells was likely early summer.

Analysis of a greater number of shells to determine if this is a consistent pattern throughout the midden site would make a valuable contribution to the other archaeological evidence discussed in Nolan (1986) and Walton (2012) in further investigating human-environment interactions at the Sandstone Point midden site.

5.5. Conclusion

While Mg/Ca of *S. glomerata* shell has been shown to be an effective tracer of temperature, interpretations of paleotemperature are not necessarily straightforward. Evidence from these multi-year shell profiles shows a more variable Mg/Ca signal during the early years of growth, with an abrupt regime shift to lower amplitude Mg/Ca ratios with lower maximum values in later years of growth. This inconsistency of Mg/Ca ratios from the juvenile to later years of growth means that a Mg/Ca-temperature relationship derived for the early years of growth will likely not give reliable results if applied to carbonate precipitated in later years of growth. Further calibrations of the Mg/Ca-temperature relationship will be required to fully assess the ontogenetic changes in *S. glomerata* shell

Mg/Ca ratios and to enable the construction of temperature records from the entire shell Mg/Ca profile.

The Mg/Ca-derived temperature records derived from the juvenile years of growth of the *S. glomerata* shells evaluated in this study indicate summer maximum temperatures for the period ~1600 years BP consistent with the modern Moreton Bay region. However, mean annual temperatures recorded by the midden shells were potentially ~1–5 ºC cooler, largely driven by winter minimum temperatures up to ~2 ºC cooler than modern.

While greater numbers of shells must be analysed to obtain a robust paleoclimate signal, this study has shown that the application of Mg/Ca ratios within *S. glomerata* shells as a temperature proxy clearly has potential to yield useful records of paleo-sea surface temperatures. The prevalence of Aboriginal midden sites along the east coast of Australia, combined with the dominance of *S. glomerata* within those sites offers a valuable source of climate information that could help inform understanding of mid to late Holocene climate in Australia.

Acknowledgements

This work was funded by a CRC LEME PhD Scholarship. Thanks to Jay Hall (School of Social Science, The University of Queensland) for providing archaeological specimens for this study. Thanks also to Les Kinsley for assistance with LA-ICP-MS analysis. SU is the recipient of an Australian Research Council Future Fellowship (project number FT120100656).

5.6. References

Aiken, G., Nicholson, A., & Cane, S. (1992). *North Coast Middens: A Report on the Distribution, Type and Representation of Middens in Northern New South Wales and South East Queensland.* Unpublished report to the Australian Heritage Commission, Canberra.

Barr, C., Tibby, J., Marshall, J. C., McGregor, G. B., Moss, P. T., Halverson, G. P., & Fluin, J. (2013). Combining monitoring, models and palaeolimnology to assess ecosystem response to environmental change at monthly to millennial timescales: the stability of Blue Lake, North Stradbroke Island, Australia. *Freshwater Biology*, 58(8), 1614-1630. doi:10.1111/fwb.12154

Batenburg, S. J., Reichart, G. J., Jilbert, T., Janse, M., Wesselingh, F. P., & Renema, W. (2011). Interannual climate variability in the Miocene: High resolution trace element and stable isotope ratios in giant clams. *Palaeogeography Palaeoclimatology Palaeoecology*, 306(1-2), 75-81. doi:10.1016/j.palaeo.2011.03.031

Bougeois, L., de Rafelis, M., Reichart, G. J., de Nooijer, L. J., & Dupont-Nivet, G. (2016). Mg/Ca in fossil oyster shells as palaeotemperature proxy, an example from the Palaeogene of Central Asia. *Palaeogeography Palaeoclimatology Palaeoecology*, 441, 611-626. doi:10.1016/j.palaeo.2015.09.052

Bougeois, L., de Rafelis, M., Reichart, G. J., de Nooijer, L. J., Nicollin, F., & Dupont-Nivet, G. (2014). A high resolution study of trace elements and stable isotopes in oyster shells to estimate Central Asian Middle Eocene seasonality. *Chemical Geology*, 363, 200-212. doi:10.1016/j.chemgeo.2013.10.037

Brigaud, B., Puceat, E., Pellenard, P., Vincent, B., & Joachimski, M. M. (2008). Climatic fluctuations and seasonality during the Late Jurassic (Oxfordian-Early Kimmeridgian) inferred from delta O-18 of Paris Basin oyster shells. *Earth and*

Planetary Science Letters, 273(1-2), 58-67. doi:10.1016/j.epsl.2008.06.015

Brockwell, S., Marwick, B., Bourke, P., Faulkner, P., & Willan, R. (2013). Late Holocene Climate Change and Human Behavioural Variability in the Coastal Wet-Dry Tropics of Northern Australia: Evidence from a pilot study of oxygen isotopes in marine bivalve shells from archaeological sites. *Australian Archaeology* 76, 21-33.

Butler, P. G., Wanamaker, A. D., Scourse, J. D., Richardson, C. A., & Reynolds, D. J. (2013). Variability of marine climate on the North Icelandic Shelf in a 1357-year proxy archive based on growth increments in the bivalve *Arctica islandica*. *Palaeogeography Palaeoclimatology Palaeoecology, 373*, 141-151. doi:10.1016/j.palaeo.2012.01.016

Carré, M., Sachs, J. P., Purca, S., Schauer, A. J., Braconnot, P., Falcon, R. A., Julien, M. & Lavallee, D. (2014). Holocene history of ENSO variance and asymmetry in the eastern tropical Pacific. *Science,* 345(6200), 1045-1048. doi:10.1126/science.1252220

Donders, T. H., Wagner, F., & Visscher, H. (2006). Late Pleistocene and Holocene subtropical vegetation dynamics recorded in perched lake deposits on Fraser Island, Queensland, Australia. *Palaeogeography Palaeoclimatology Palaeoecology,* 241(3-4), 417-439.

Donders, T. H., Wagner-Cremer, F., & Visscher, H. (2008). Integration of proxy data and model scenarios for the mid-Holocene onset of modern ENSO variability. *Quaternary Science Reviews*, 27(5-6), 571-579. doi:10.1016/j.quascirev.2007.11.010

Elliot, M., Welsh, K., Chilcott, C., McCulloch, M., Chappell, J., & Ayling, B. (2009). Profiles of trace elements and stable isotopes derived from giant long-lived *Tridacna gigas* bivalves: Potential applications in paleoclimate studies. *Palaeogeography Palaeoclimatology Palaeoecology,* 280(1-2), 132-142. doi:10.1016/j.palaeo.2009.06.007

Freitas, P., Clarke, L. J., Kennedy, H., Richardson, C., & Abrantes, F. (2005). Mg/Ca,Sr/Ca, and stable-isotope (delta O-18 and delta C-13) ratio profiles from the fan mussel *Pinna nobilis*: Seasonal records and temperature relationships. *Geochemistry Geophysics Geosystems,* 6. doi:10.1029/2004gc000872

Gontz, A. M., Moss, P. T., Sloss, C. R., Petherick, L. M., McCallum, A., & Shapland, F. (2015). Understanding past climate variation and environmental change for the future of an iconic landscape - K'gari Fraser Island, Queensland,

Australia. *Australasian Journal of Environmental Management,* 22(2), 105-123. doi:10.1080/14486563.2014.1002120

Gontz, A. M., Moss, P. T., & Wagenknecht, E. K. (2014). Stratigraphic Architecture of a Regressive Strand Plain, Flinders Beach, North Stradbroke Island, Queensland, Australia. *Journal of Coastal Research,* 30(3), 575-585. doi:10.2112/jcoastres-d-12-00234.1

Hong, W., Keppens, E., Nielsen, P., & Vanriet, A. (1995). Oxygen and carbon-isotope study of the Holocene oyster reefs and paleoenvironmental reconstruction on the northwest coast of Bohai Bay, China. *Marine Geology,* 124(1-4), 289-302. doi:10.1016/0025-3227(95)00046-2

Jones, D. S., & Quitmyer, I. R. (1996). Marking time with bivalve shells: Oxygen isotopes and season of annual increment formation. *Palaios,* 11(4), 340-346. doi:10.2307/3515244

Kirby, M. X. (2000). Paleoecological differences between tertiary and Quaternary *Crassostrea* oysters, as revealed by stable isotope sclerochronology. *Palaios,* 15(2), 132-141.

Kirby, M. X., Soniat, T. M., & Spero, H. J. (1998). Stable isotope sclerochronology of pleistocene and recent oyster shells (*Crassostrea virginica*). *Palaios,* 13(6), 560-569.

Leonard, N. D., Welsh, K. J., Zhao, J. X., Nothdurft, L. D., Webb, G. E., Major, J., Feng, Y. X., & Price, G. J. (2013). Mid-Holocene sea-level and coral reef demise: U-Th dating of subfossil corals in Moreton Bay, Australia. *Holocene,* 23(12), 1841-1852. doi:10.1177/0959683613508156

Lewis, S. E., Sloss, C. R., Murray-Wallace, C. V., Woodroffe, C. D., & Smithers, S. G. (2013). Post-glacial sea-level changes around the Australian margin: a review. *Quaternary Science Reviews,* 74, 115-138. doi:10.1016/j.quascirev. 2012.09.006

Meehan, B. (1982). *Shell bed to shell midden*. Canberra: Australian Institute of Aboriginal Studies.

Moss, P. T., Tibby, J., Petherick, L., McGowan, H., & Barr, C. (2013). Late Quaternary vegetation history of North Stradbroke Island, Queensland, eastern Australia. *Quaternary Science Reviews,* 74, 257-272 doi:10.1016/j.quascirev.2 013.02.019

Mouchi, V., de Rafélis, M., Lartaud, F., Fialin, M., & Verrecchia, E. (2013). Chemical labelling of oyster shells used for time-calibrated high-resolution

Mg/Ca ratios: A tool for estimation of past seasonal temperature variations. *Palaeogeography, Palaeoclimatology, Palaeoecology,* 373(0), 66-74. doi:http://dx.doi.org/10.1016/j.palaeo.2012.05.023

Nakada, M., & Lambeck, K. (1989) Late Pleistocene and Holocene sea-level change in the Australian region and mantle rheology. *Geophysical Journal-Oxford* 96(3):497-517.

Neukom, R., & Gergis, J. (2012). Southern Hemisphere high-resolution palaeoclimate records of the last 2000 years. *Holocene,* 22(5), 501-524. doi:10.1177/0959683611427335

Nolan, A. (1986). *Sandstone Point: temporal and spatial patterns of Aboriginal site use at a midden complex, south-east Queensland.* (B Arts (Hons)), The University of Queensland, Queensland.

PAGES 2k Consortium (2013). Continental-scale temperature variability during the past two millennia. *Nature Geoscience,* 6(5), 339-346. doi:10.1038/ngeo1797

Reeves, J. M., Bostock, H. C., Ayliffe, L. K., Barrows, T. T., De Deckker, P., Devriendt, L. S., Dunbar, G. B., Drysdale, R. N., Fitzsimmons, K. E., Gagan, M. K., Griffiths, M. L., Haberle, S. G., Jansen, J. D., Krause, C., Lewis, S., McGregor, H. V., Mooney, S. D., Moss, P., Nanson, G. C., Purcell, A., & van der Kaars, S. (2013). Palaeoenvironmental change in tropical Australasia over the last 30,000 years - a synthesis by the OZ-INTIMATE group. Quaternary Science Reviews, 74, 97-114. doi:10.1016/j.quascirev.2012.11.027

Robins, R., Hall, J., & Stock, E. (2015). Geoarchaeology and the archaeological record in the coastal Moreton Region, Queensland, Australia. *Quaternary International,* 385, 191-205. doi:10.1016/j.quaint.2015.02.060

Schone, B. R., Zhang, Z. J., Radermacher, P., Thebault, J., Jacob, D. E., Nunn, E. V., & Maurer, A. F. (2011). Sr/Ca and Mg/Ca ratios of ontogenetically old, long-lived bivalve shells (Arctica islandica) and their function as paleotemperature proxies. *Palaeogeography Palaeoclimatology Palaeoecology,* 302(1-2), 52-64. doi:10.1016/j.palaeo.2010.03.016

Schöne, B., & Surge, D. (2014). Bivalve shells: ultra-high resolution paleoclimate archives. *PAGES Magazine,* 22(1), 20-21.

Shulmeister, J., & Lees, B. G. (1995). Pollen evidence from tropical Australia for the onset of an ENSO-dominated climate at c. 4000 BP. *Holocene,* 5(1), 10-18.

Strasser, C. A., Mullineaux, L. S., & Walther, B. D. (2008). Growth rate and age

effects on *Mya arenaria* shell chemistry: Implications for biogeochemical studies. *Journal of Experimental Marine Biology and Ecology,* 355(2), 153-163. doi:10.1016/j.jembe.2007.12.022

Sullivan, M. (1982). *Aboriginal shell middens in the coastal landscape of New South Wales.* (PhD), The Australian National University, Canberra.

Surge, D., & Lohmann, K. C. (2008). Evaluating Mg/Ca ratios as a temperature proxy in the estuarine oyster, *Crassostrea virginica*. *Journal of Geophysical Research-Biogeosciences,* 113(G2). doi:G02001 10.1029/2007jg000623

Surge, D. M., Lohmann, K. C., & Goodfriend, G. A. (2003). Reconstructing estuarine conditions: oyster shells as recorders of environmental change, Southwest Florida. *Estuarine Coastal and Shelf Science,* 57(5-6), 737-756.

Twaddle, R. W., Ulm, S., Hinton, J., Wurster, C. M., & Bird, M. I. (2016). Sclerochronological analysis of archaeological mollusc assemblages: methods, applications and future prospects. *Archaeological and Anthropological Sciences,* 8(2), 359-379. doi:10.1007/s12520-015-0228-5

Tynan, S., Dutton, A., Opdyke, B. N., & Eggins, S. M. (2014). Oxygen isotope records of the Australian flat oyster (*Ostrea angasi*) as a potential temperature archive. *Marine Geology*, 357, 195-209. doi:10.1016/j.margeo.2014.07.009

Tynan, S., Opdyke, B. N., Walczak, M., Eggins, S., & Dutton, A. (2017). Assessment of Mg/Ca in Saccostrea glomerata (the Sydney rock oyster) shell as a potential temperature record. *Palaeogeography Palaeoclimatology Palaeoecology*, 484, 79-88. doi:10.1016/j.palaeo.2016.08.009

Ulm, S., & Reid, J. (2000). Index of Dates from Archaeological Sites in Queensland. *Queensland Archaeological Research* 12, 1-129.

Ulm, S. (2002). Reassessing Marine Fishery Intensification in Southeast Queensland. *Queensland Archaeological Research*, 13, 79-96.

Ulm, S. (2011). Coastal foragers on southern shores: Marine resource use in northeast Australia since the late Pleistocene. In *Trekking the Shore: Changing Coastlines and the Antiquity of Coastal Settlement* (pp.441-461). New York: Springer.

Walton, R. C. (2012). *Sucking the Shell Beds Dry? The morphometric analysis of oyster (Saccostrea glomerata), cockle (Anadara trapezia) and whelk (Pyrazus ebeninus) to interpret the intensity of human exploitation of molluscs at the Sandstone Point shell midden complex, southeast Queensland.* (Bachelor of Social Science (Hons)), The University of Queensland, Queensland.

Woodroffe, S. A. (2009). Testing models of mid to late Holocene sea-level change, North Queensland, Australia. *Quaternary Science Reviews,* 28(23-24), 2474-2488. doi:10.1016/j.quascirev.2009.05.004

Chapter 6

An investigation of Mg/Ca-temperature relationship in the shell of *Mytilus galloprovincialis*

This manuscript is yet to be submitted for publication.

ABSTRACT

Samples of *Mytilus galloprovincialis* from two eastern Australia locations, Pambula Lake, New South Wales, and Little Swanport, Tasmania, were cultured in their natural environment, along with temperature loggers for approximately 1 year. Mg/Ca ratio profiles were then obtained for three shells from each location via LA-ICP-MS.

Two of the three Pambula Lake shells showed a clear seasonal signal in their Mg/Ca ratios, while the third Pambula Lake shell exhibited much greater variability. The Little Swanport *M. galloprovincialis* showed no strong seasonal signals in their shell Mg/Ca. A Mg/Ca-temperature relationship was determined for the two Pambula Lake *M. galloprovincialis* shells of Mg/Ca = 0.38 (±0.01) * T + 1.62 (±0.20) (n = 384, R^2 = 0.76).

These results suggest that the Mg/Ca ratios of *M. galloprovincialis* can be employed as a temperature proxy. However, the variation evident between individuals from the same location and between the geographically distinct *M. galloprovincialis* populations detracts from the reliability of the temperature record contained with any one single shell. Multiple shells should be analysed to ensure the robustness of any paleotemperature interpretations conducted with *M. galloprovincialis* Mg/Ca ratios.

6.1. Introduction

Trace element ratios (primarily Mg/Ca, Sr/Ca, Ba/Ca) in the carbonate shells of various species of bivalve have been widely investigated to determine if and how they are controlled by ambient environmental conditions (e.g. Arias-Ruiz et al. 2017; Vihtakari et al. 2017; Schöne et al. 2011; Freitas et al. 2005). The ultimate goal is to establish robust geochemical proxies that can be used to analyse paleo-specimens in order to investigate past environmental conditions, such as water temperatures or salinity. These would provide a valuable complement to the proxies offered by other biogenic carbonates, such as corals (e.g. Corrége 2006), foraminifera (e.g. Lea et al. 1999; Elderfield and Ganssen 2000), ostracods and (e.g. Elmore et al. 2012; Ingram et al. 1998) and gastropods (e.g. Ingram et al. 1998). Elemental ratio temperature proxies are particularly useful as they are generally thought to be independent of other climatic variables, such as salinity, unlike other geochemical proxies such as $\delta^{18}O$ (e.g. Eisma et al. 1976; Dodd and Crisp 1982; Surge and Lohmann 2008; Wanamaker et al. 2008).

However, bivalves appear to present a more complex story, and while a number studies have found that some correlations can be drawn between trace element incorporation and environmental conditions, there is also evidence to the contrary, with several studies reporting that biological effects such as growth rate (Carré et al. 2006), developmental and ontogenetic changes (e.g. Vander Putten et al. 2000; Freitas et al. 2005; Gillikin et al. 2005; Strasser et al. 2008; Schöne et al. 2011) and the presence of organic matter within the shell can obfuscate environmental signals seen in the trace element ratios in bivalve shells (e.g. Schöne et al. 2010), limiting the use of this aspect of bivalve shell chemistry as a climate proxy. Other studies have reported variation in trace element

incorporation between contemporaneous individuals of some bivalve species (e.g. Freitas et al. 2008; Freitas et al. 2009; Schöne et al. 2010; Lazareth et al. 2013; Schöne et al. 2013). Schöne and Surge (2012) also provide a comprehensive overview of bivalve sclerochronology, and the associated issues and complications.

This case study focuses on the Mg/Ca-temperature relationship in the shell of the common blue mussel endemic to Australian waters, *Mytilus galloprovincialis*. We place the results within the context of results from other *Mytilus spp.* investigations, probing the potential temperature proxy that can be obtained from the Mg/Ca ratios of shells of this mussel genus.

6.1.1. Mg/Ca ratios in *Mytilus* shell

With a virtually global distribution (barring warm equatorial waters) (Gosling 2002) mussels of the *Mytilus* genus have the potential to offer a useful environmental archive. It is generally accepted that increasing calcification temperature correlates with an increased amount of Mg incorporated into carbonate lattice, with a resultant increase in Mg/Ca values (Schöne and Surge 2012).

Various species of the *Mytilus* genus of mussels have been studied, producing a diverse range of results (Dodd 1965; Lorens and Bender 1977; Klein et al. 1996; Vander Putten et al. 2000; Freitas et al. 2008; Wanamaker et al. 2008; Ford et al. 2010). Early work by Dodd (1965) found that the mol % $MgCO_3$ followed a seasonal pattern in shells of *M. edulis diegensis*, with higher $MgCO_3$ in the warmer months. He also found that concentrations of Mg were generally lower in the larger (older) mussels as compared to smaller (younger) specimens.

Klein et al. (1996) reported a strong dependence of Mg/Ca ratios in the outer calcitic region of shell of *M. trossulus* upon calcification temperature. However, work on other species of *Mytilus* has not found such solid relationships between the shells' Mg/Ca ratios and temperature. Vander Putten et al. (2000) described how Mg/Ca ratios in *M. edulis* closely tracked temperature for a limited time, but the relationship was abruptly disturbed, and was not subsequently re-established.

Freitas et al. (2008) cultured *M. edulis* specimens in both laboratory and field environments and found that any temperature dependence the shell Mg/Ca ratios exhibited ranged from very weak to non-existent (Freitas et al. 2008). Similarly, only a very weak correlation between Mg/Ca and temperature was reported by Wanamaker et al. (2008) from a well-constrained laboratory experiment also using *M. edulis*. Ford et al. (2010) examined *M. californianus* and while they did derive an Mg/Ca-temperature calibration for this species, their overall conclusion was that the predominant control upon Mg/Ca was growth rate, rather than temperature.

These studies reiterate the now well-established instances of species-specific behaviour in bivalves with regard to trace element incorporation. Dodd's 1965 study also documented distinct differences in the trace element concentrations with the shells of *M. californianus* and *M. edulis*. Additionally, the widespread distribution of the *Mytilus* genus, along with its many hybrid species, and the complications of local adaptations may also serve to prevent effective comparison of different *Mytilus* species.

Early classifications denoted the *Mytilus* mussels found in Australia as *M. edulis planulatus*, (Kailola et al. 1993), M. *planulatus* (Lamprell and Healy 1998) and also as *M. edulis* (Yearsley et al. 1999). A genetic study conducted in

1991 provides the most definitive classification of *M. galloprovincialis*, although the mussels share only some, not all, the genetic markers with the northern hemisphere *M. galloprovincialis*, and do share some features with *M. edulis* (McDonald et al. 1991).

In Australia, *M. galloprovincialis* occurs throughout Western Australia, South Australia, Tasmania, Victoria and New South Wales. *M. galloprovincialis* prefers sheltered, brackish environments (Gosling 1992). Nell and Gibbs (1986) give a salinity tolerance of 14–45 for *M. galloprovincialis* specimens from Jervis Bay, New South Wales (their classification: *Mytilus edulis planulatus*).

6.2. Methods

6.2.1. Field experiments

Field experiments were conducted at Pambula Lake, located on the far south coast of New South Wales, and at Little Swanport, an estuary on the east coast of Tasmania (Figure 6.1). Commercial oyster farms are located at both sites, which provided the infrastructure for the experiments.

6.2.1.1. Pambula Lake

Pambula Lake is a tidal lake, located ~5 km up-river from the ocean. It receives freshwater input from the Pambula and Yowaka Rivers, but a salinity of 33.35 is generally maintained. Intense rainfall events result in significant ephemeral freshening of the lake waters, with salinities approaching that of freshwater. Residence time of the water in the estuary is ~1.5 days (3 tidal cycles).

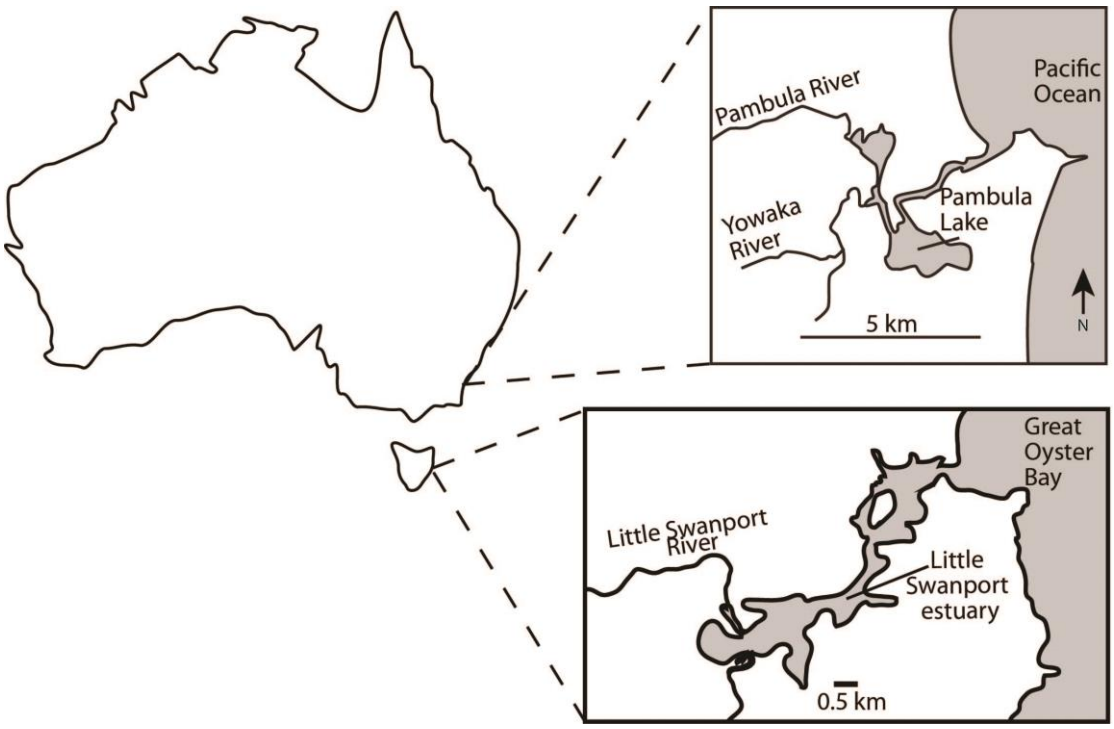

Figure 6.1. Location of the two field-culturing experiment locations in eastern Australia: Pambula Lake, New South Wales, and Little Swanport, Tasmania.

A selection of wild mussels were collected, measured along the maximum growth axis using digital calipers (accuracy ±0.2 mm) and labelled with a plastic fish tag (Hallprint labels) glued to a clean and dry section of the shell with either Araldite® or Selleys Supa Glue®. The mussels were placed in plastic mesh bags with flotation devices attached, and secured to a post in the middle of the lake, near the main channel. As such, the mussels were immersed in the surface water at all times. The water depth was typically ~2 m at high tide and ~0.5 m at low tide. The mussels were measured every 4–6 weeks to obtain a basic record of growth rates.

HOBO® U22 Water Temp Pro v2 temperature loggers (accuracy ±0.2 ºC) were deployed with the mussels and temperature was recorded every 30 minutes. Water samples and salinity readings were taken fortnightly. Water samples were collected from the lake at the location of the monitoring experiment, brought back

to shore and filtered through a 0.2 µm filter. Samples for trace metal analysis were acidified with ~10 % HNO_3. All samples were kept refrigerated. The duration of the experiment at Pambula Lake was 13 months.

6.2.1.2. Little Swanport

The Little Swanport estuary is a marine dominated system. Freshwater from the Little Swanport river does not significantly affect the salinity of the estuary except in some localised areas, and care was taken to place the mussels for the monitoring experiment well clear of these locations.

As at Pambula Lake, several wild specimens were collected, measured and labeled, then placed in closed baskets and suspended below the oyster racks on a rope strung between two posts, to ensure the mussels were constantly submerged. HOBO® U22 Water Temp Pro v2 temperature loggers (accuracy ±0.2 ºC) were deployed with the mussels and temperature was recorded every 30 minutes.

Water samples were collected fortnightly, following the same method as described for Pambula Lake. The duration of the field experiment at Little Swanport was 9 months.

6.2.2. Shell analysis

6.2.2.1. Sample preparation

The mussels for analysis were steamed open and the soft tissue discarded. One valve of the shell was embedded within resin (a 10:1 ratio of Araldite M Bisphenol A epoxy resin (70-82%) and Hardener HY 951, containing >60% Triethylenetetramine). The shell was cut along the axis of maximum growth, and

one portion of the shell impregnated with resin to be made into a thick section (~100 µm) mounted on a glass petrographic slide. Following impregnation, shell sections were sanded down to ensure a flat sample surface using 180 and ten 280 Norton Tufbak Waterproof Sanding Sheets. A secondary resin impregnation was performed at this stage. Samples were then sanded further, using Norton Tufbak Waterproof Sanding Sheets, stepping through 320, 400, then 800. The sample block was then affixed to a glass petrographic slide using Loctite. The samples were polished was performed in two stages, using 3 µm diamond paste, followed by 1 µm diamond paste.

6.2.2.2. Trace element analysis

Mytilus spp. shells are comprised of an outer calcitic layer with a prismatic structure, and an inner nacreous layer of aragonite. This study focused on the outer calcitic layer only. The trace element concentrations of this layer were measured via Laser Ablation Inductively Coupled Plasma Mass Spectrometry, at The Australian National University, using an ArF Excimer laser (wavelength = 193 nm). The sampling transect was mapped out along the growth axis, keeping to the centre of the calcitic layer. The transect was pre-ablated using a spot size of 233 µm, at a speed of 6 mm/min. Analysis was conducted with a spot size of 50 µm, and a scan speed of 1.2 mm/min. The ablated material was then analysed by a Varian 820-MS Inductively Coupled Plasma mass spectrometer. The standard NIST 612 glass was analysed prior to and following every sample to account for standard drift.

A data reduction process was carried out on the ICP-MS data whereby values were normalised to Ca and anomalously high amplitude peaks were

removed from the dataset through visual inspection of the plotted data. The data were smoothed to obtain a more consistent seasonal signal.

6.3. Results

6.3.1. Water data

The environmental data collected during the experiment period is shown in Figure 6.2 and reported in Tynan et al. (2014) and Tynan et al. (2017). At Pambula Lake, the water temperature ranged from 11.57 ºC to 24.68 ºC, and the salinity ranged from 1.76 to 34. Mg/Ca between 5.2 and 6.0 was maintained throughout the experiment period, with the exception of markedly lower values following freshwater input to the estuary during an intense rainfall in February 2007.

The water temperature at Little Swanport during the monitoring experiment period ranged from 9.38 ºC to 12.22 ºC. Salinity ranged from 34.64 to 37.12, with an average of 36.1, slightly higher than average marine salinity, most likely due to evaporation in the estuary.

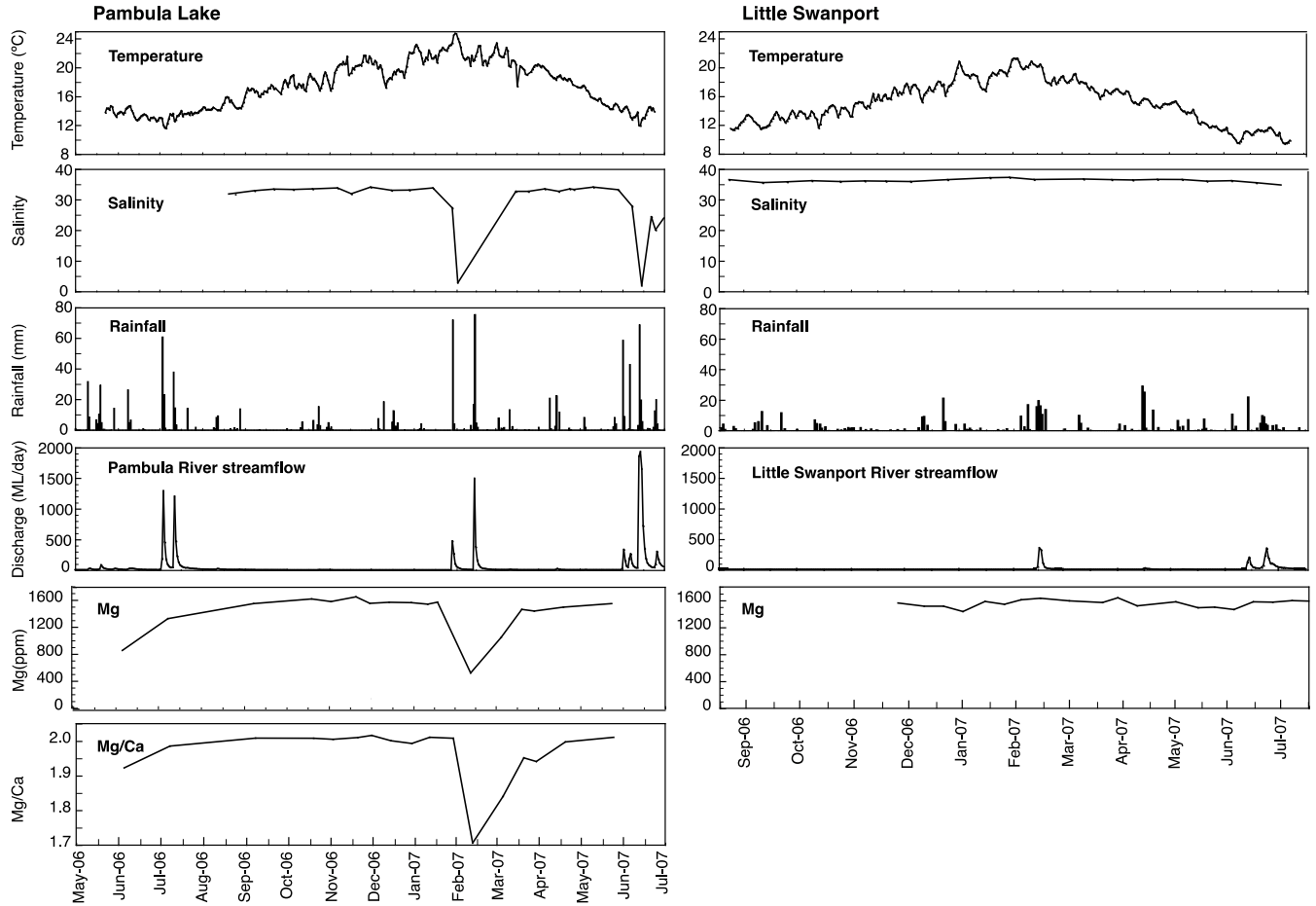

Figure 6.2. Water parameters in Pambula Lake and the Little Swanport estuary during the field-culturing experiment period.

6.3.2. Growth rates

Growth data obtained from the Pambula Lake and Little Swanport *M. galloprovincialis* (Figure 6.3) indicate that the mussels at the Pambula Lake site grew steadily throughout the year, exhibiting a similar growth rate to that reported for *M. galloprovincialis* specimens from Galacia, Spain (Sunila 2004). Unfortunately, it was not possible to measure the Little Swanport mussels periodically throughout the experiment period, so the only data available is total growth over the experiment period.

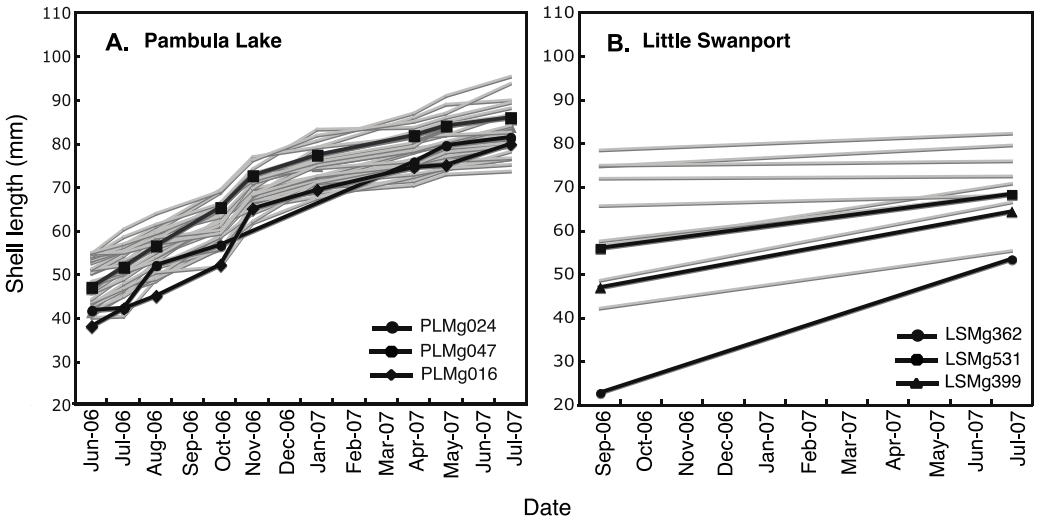

Figure 6.3. Growth data for Pambula Lake and Little Swanport *M. galloprovincialis* shells.

Despite the fact that the Little Swanport *M. galloprovincialis* were of a similar starting size to the Pambula Lake samples, they exhibited a slower growth rate. It can be assumed that the environmental conditions at this site, most likely the lower temperature, result in the *M. galloprovincialis* in this location growing more slowly and thus reaching greater ages at smaller sizes. Thus, the Little Swanport *M. galloprovincialis* are most likely older than their Pambula Lake counterparts.

6.3.3. *M. galloprovincialis* Mg/Ca

The Mg/Ca ratio profiles from the *M. galloprovincialis* shells are shown in Figure 6.3. Two of the three Pambula Lake *M. galloprovincialis* shells (PLMg024, PLMg047) show a consistent seasonal pattern in their Mg/Ca profiles, with two distinct peaks of high Mg/Ca. If the most recent complete Mg/Ca ratio cycle is taken to represent the most recent year of growth, this indicates that the shell approximately doubled in length during the field-culturing period. This agrees with the growth records, with shell PLMg024 increasing from 41.7 mm to 81.4 mm and PLMg047 from 47 mm to 85.9 mm, however it must be noted that owing to the curvature of the shells, increase in shell length can not be directly relate to the increase in distance along the growth axis through the centre of the shell. Shell PLMg016 exhibited a similar increase in length from 38 mm to 79.8, however, this is not reflected in the Mg/Ca ratio profile of this shell as with the other shells. Approximately halfway through this shell's growth a period of increased Mg/Ca ratios is evident, rather than the winter minimum that would correspond to the winter of the beginning of the field culture experiment. This shell lacks the clear seasonal signal in the Mg/Ca ratio present in the other two Pambula Lake *M. galloprovincialis* shells.

With the possible exception of shell LSMg399, seasonal signals are also absent in the Little Swanport *M. galloprovincialis* Mg/Ca ratio profiles. There is a possible weak seasonal signal evident in shell LSMg399l. The Little Swanport shells show more variable Mg/Ca ratios in the mussels' earlier years of growth, then a shift to lower average Mg/Ca ratios with less variability in the more recent (older ontogenetic age) shell growth (Figure 6.4).

6.3.4. Mg/Ca-temperature relationship

Based on the assumption that Mg/Ca ratios in bivalve shell does in fact co-vary with calcification temperature, the most recent full seasonal Mg/Ca cycle was taken to correspond to the temperature record obtained during the year-long culturing experiments.

Given the lack of a seasonal signal in the Pambula Lake shell PLMg016, this shell was not considered in the Pambula Lake *M. galloprovincialis* Mg/Ca-temperature calibration. Similarly, no attempt was made to establish an Mg/Ca-temperature relationship from the Little Swanport *M. galloprovincialis* shells.

The most recent cycle of growth in shells PLMg024 and PLMg047 were correlated together using the stratigraphic correlation program AnalySeries. This program enables comparison and correlation of records using manually identified 'tie-points' to tie the records together. Correlating the records using this process is important in accounting for the variable growth rate between different individuals. Shells PLMg024 and PLMg047 Mg/Ca ratio records were correlated using 18 distinct tie-points, with a correlation coefficient of 0.61. Following this, the larger record of shell PLMg024 was smoothed to obtain a constant resolution with that of PLMg047, then the two records were averaged to give a 'mean' Mg/Ca signal for the two shells.

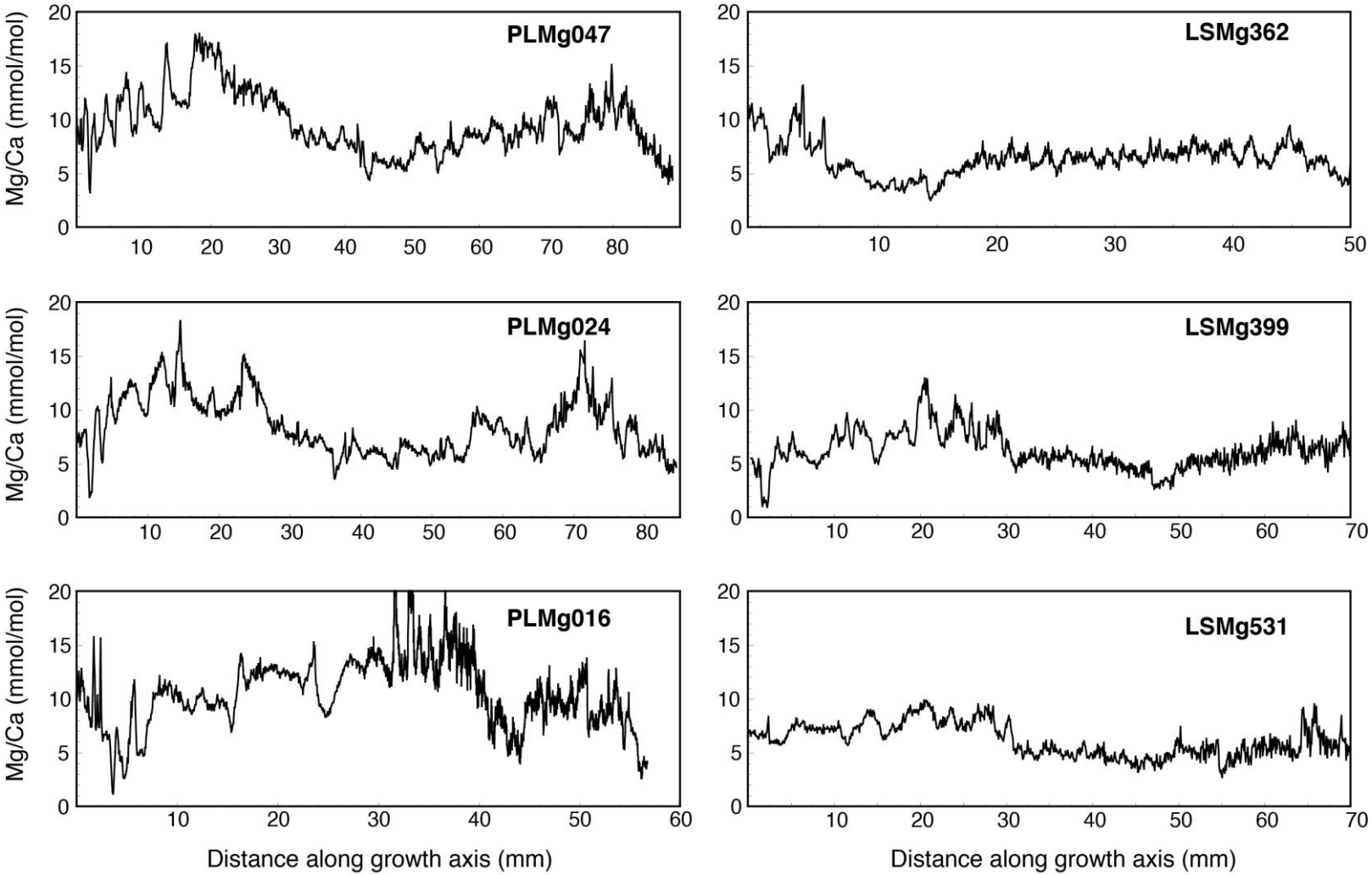

Figure 6.4. Entire shell Mg/Ca profiles from the Pambula Lake and Little Swanport *M. galloprovincialis*.

This mean Mg/Ca signal was then correlated with the Pambula Lake temperature record, again using the AnalySeries program, obtaining a correlation coefficient of 0.85. A comparison of the rescaled mean Mg/Ca profile and the Pambula Lake temperature record is shown in Figure 6.5. It must be noted that the use of this method imposes a degree of subjectivity upon the correlation relationship, as the choice of tie-points between the records influences the strength of the correlation.

The mean Mg/Ca ratio dataset was then smoothed to obtain a consistent resolution with the temperature record (Figure 6.5), then the two were plotted in order to perform a linear regression to establish the Mg/Ca-temperature calibration relationship for the Pambula Lake *M. galloprovincialis* (Figure 6.6).

6.4. Discussion

6.4.1. Entire shell Mg/Ca profiles

6.4.1.1. Little Swanport

No clear seasonal pattern is evident in the *M. galloprovincialis* Mg/Ca ratios from the Little Swanport site. The differences between the shell profiles signals at the two locations are too great to be the result of subtle location-specific adaptation alone; there must be other environmental or biological factors also influencing (or confounding) the shells' Mg/Ca ratios. It is possible that the slower overall growth rate of the Little Swanport *M. galloprovincialis*, although itself a result of the environmental conditions at the site, affects the Mg/Ca ratio of the shells such that they no longer reflect the ambient temperature or Mg/Ca ratio of the water.

Additionally, a shift in the Mg/Ca ratio profiles of each of the Little Swanport shells from more variable Mg/Ca ratios to more consistent, lower levels

is evident, indicating some sort of disruptive event after which the original pattern of Mg incorporation into the shell is not re-established. Assuming the three mussels were of a similar age and shared a consistent growth rate, this shift occurred at nearly exactly the same time in each shell. A possible explanation for this is the onset of gameteogenesis and the animal's first spawning event. *Mytilus* mussels generally reach sexual maturity in 1–2 years (Wilson and Hodgkin 1967; Seed 1968), but this timeframe can be very variable, with one study reporting sexual maturity in M. *edulis* within 6 months (Sunila et al. 2004). Wilson and Hodgkin described the reproductive cycles of *M. galloprovincialis* (their classification: *Mytilus edulis planulatus*) in Western Australian waters, and found that most individuals first spawn when they are ~11 months old. The factors controlling this variable rate of sexual maturity can be both physiological and environmental, so it would not necessarily be expected that *M. galloprovincialis* from the locations of this study follow the same behavioural patterns as those from Western Australia.

However, it can be assumed that the first spawning most likely occurs in *M. galloprovincialis* at both Pambula Lake and Little Swanport around the age of 1–2 years. This process can be very energy-intensive and could well serve to disrupt the process of carbonate secretion and trace element incorporation. As such, the onset of spawning could account for the abrupt shift in the Mg/Ca ratio profile seen in both the Little Swanport shells and also explain the absence of such a shift in the Mg/Ca of the younger Pambula Lake shells, as these mussels had likely not yet reached that stage of development.

Vander Putten et al. (2000) described a similarly inconsistent Mg/Ca-temperature relationship in *M. edulis*, where Mg/Ca ratios covaried closely with temperature until a sharp breakdown occurred, following which the Mg/Ca-

temperature relationship was not resumed. It is possible that any Mg/Ca-temperature relationships present in *Mytilus* species are robust only for the early, faster growing years of the animal's life, or up until the time of gametogenesis, after which other biological or developmental/ontogenetic factors play a more dominant role in regulating (or disrupting) the Mg incorporation into the shell. This could also indicate that growth rate plays a role in Mg incorporation, as concluded by Ford et al. (2010).

6.4.1.2. Pambula Lake

Mussels PLMg024 and PLMg047 from the Pambula Lake site show a good seasonal signal in their Mg/Ca profiles, with two distinct summer-time peaks of higher Mg/Ca (Figure 6.4). Why shell PLMg016 does not show a similarly consistent seasonal pattern is unclear. This highlights the variability in trace element incorporation that can be present between individuals of the same bivalve species, and emphasises the need to perform trace element analysis on several samples to obtain a 'consensus' record.

Comparison of the 'mean' Pambula Lake *M. galloprovincialis* Mg/Ca ratios and Pambula Lake water temperature shows a good correlation between the two records (Figure 6.4), indicating that temperature does exert a control over Mg/Ca ratios in these shells. There is some mismatch evident around the months of November–December, where although the shape of the profiles is still similar, the shell Mg/Ca ratios lag an increase in ambient temperature until February, where again the records align more closely. The underlying cause/s of this lag are unclear.

Salinity has been found to influence Mg incorporation into *M. edulis* shells. Wanamaker et al. (2008) report that in their laboratory-cultured *M. edulis*

specimens Mg/Ca and temperature showed a (weak) positive correlation only in their 'low salinity' treatment (salinity = 23). Heinemann et al. (2011) found that the Mg/Ca ratios in the shell of *M. edulis* specimens cultured at higher salinities (salinity = 29, 34) showed a positive correlation with temperature, but no correlation was evident at lower salinity. Pambula Lake experienced a major rain event during late February, which significantly affected the salinity and Mg/Ca ratios of the ambient lake water. Salinity in the lake dropped to ~0, with a significant decrease in the Mg/Ca ratios (Figure 6.2). Interestingly, this does not appear to have any impact upon the Mg/Ca-temperature relationship as the correlation remains robust during this time (Figure 6.5).

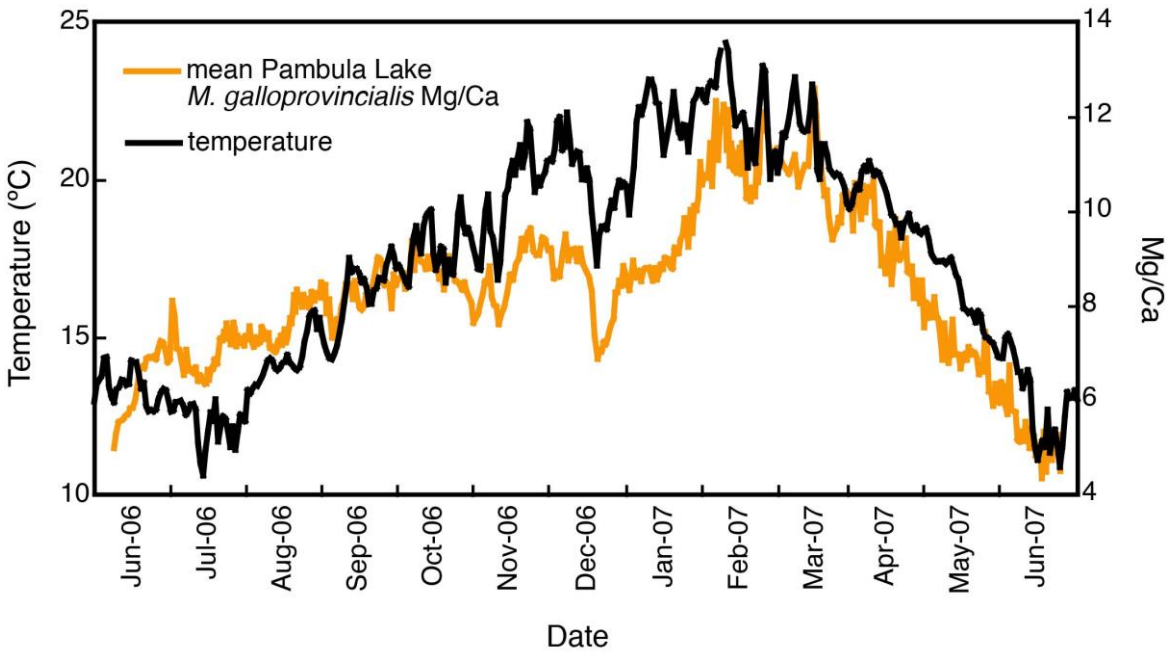

Figure 6.5. Comparison of the 'mean' Pambula Lake *M. galloprovincialis* Mg/Ca profile with the recorded temperature in Pambula Lake during the experiment period.

6.4.2. Pambula Lake *M. galloprovincialis* Mg/Ca-temperature calibration

The Mg/Ca-temperature relationship derived for the two Pambula Lake *M. galloprovincialis* is shown in Figure 6.6 and described by the equation (the errors given are 1σ):

$$Mg/Ca = 0.38_{(\pm 0.01)} * T + 1.62_{(\pm 0.20)} \quad \text{(Eq 6.1)}$$

$$n = 384, R^2 = 0.76$$

This indicates a positive correlation exists between *M. galloprovincialis* shell Mg/Ca ratios and ambient water temperature. Further work is required to ascertain if this relationship holds true throughout the lifetime of older *M. galloprovincialis* specimens, and to further investigate geographical variation that may exist in *M. galloprovincialis* from different locations.

Table 6.1. Published Mg/Ca-temperature relationships for *Mytilus* spp.

Species	Mg/Ca-temperature calibration	Temperature range (ºC)	Citation
M. edulis	Mg/Ca = 0.70T – 0.63	5-20	Vander Putten et al. 2000
M. edulis	Mg/Ca = 0.26(±0.06)T + 1.56(±0.84)	10-20	Freitas et al. 2008
M. edulis	Mg/Ca = 0.82(±0.24)T + 3.6(±3.24)	7-20	Wanamaker et al. 2008
M. trossulus	Mg/Ca = 0.30(±0.04)T + 2.25(±0.63)	5-25	Klein et al. 1996
M. californianus	Mg/Ca = (T-2.962)/4.209	12-25	Ford et al. 2010
M. galloprovincialis	Mg/Ca = 0.38T + 1.62	10-25	This study

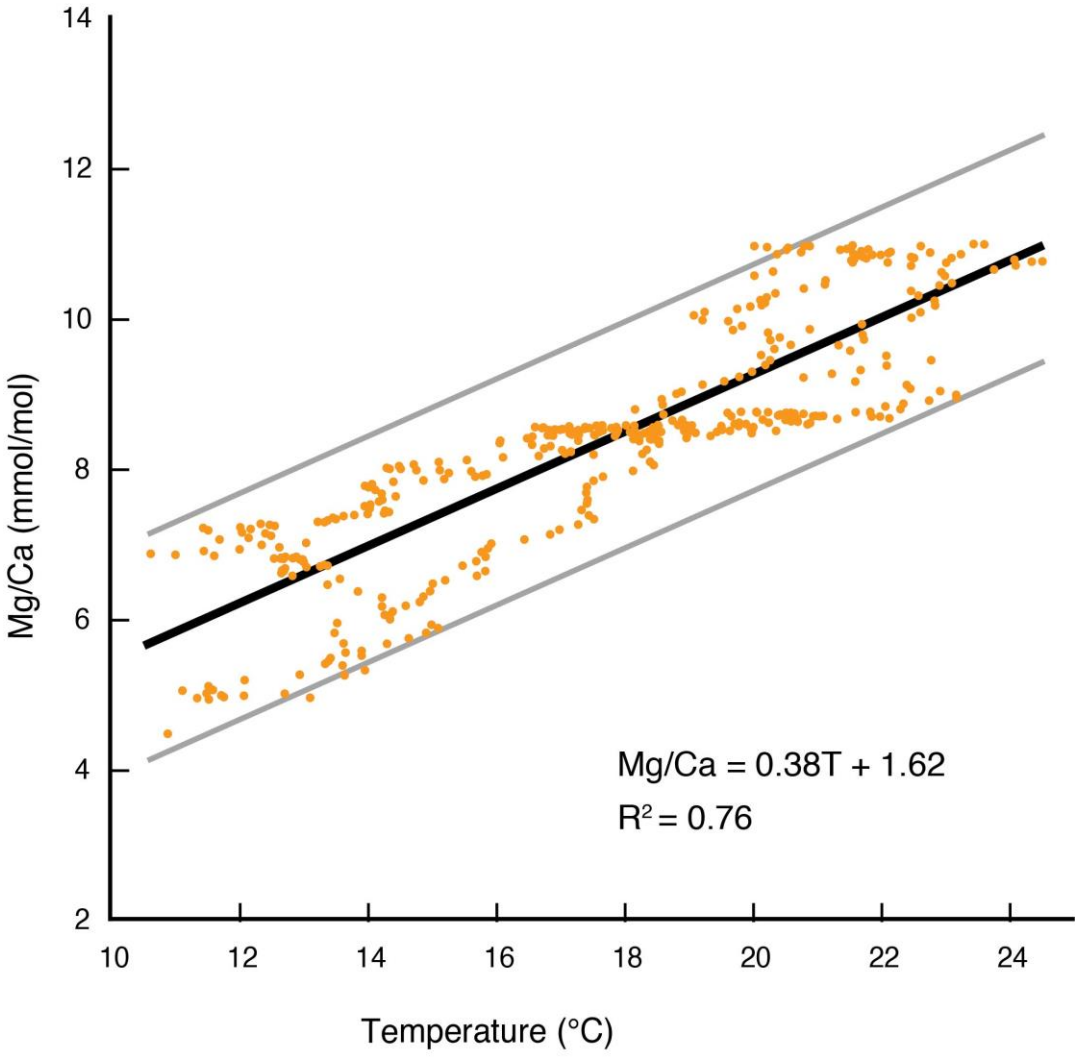

Figure 6.6. Linear regression of the Pambula Lake *M. galloprovincialis* Mg/Ca and temperature. A significant positive correlation between shell Mg/Ca and temperature is evident. Grey lines indicate a 95% (2σ) confidence interval.

Despite the numerous caveats and limitations discussed by other researchers, several have published (qualified) Mg/Ca-temperature relationship calibration equations, presented in Table 6.1 and Figure 6.7. The Mg/Ca-temperature relationship derived for the Pambula Lake *M. galloprovincialis* fits well within the range of these published *Mytilus* Mg/Ca-temperature equations.

The relationship derived for the Pambula Lake *M. galloprovincialis* is closest to the Mg/Ca-temperature equation from Klein et al. (1996) for *M. trossulus*. Despite the difference in species, the mussels of that study and the

Pambula Lake *M. galloprovincialis* both grew in estuarine habitats with varying salinity throughout the period pertaining to the region of shell growth analysed. Further, the Klein et al (1996) study also examined mussels grown *in situ* in a natural habitat, rather than in controlled laboratory conditions. This too could contribute to the similarity seen between the *M. trossulus* and *M. galloprovincialis* Mg/Ca-temperature relationships. However, both the Ford et al. (2010) and Vander Putten et al (2000) studies also examined *Mytilus* species within intertidal environments, and the resulting Mg/Ca-temperature relationships do not exhibit such a close similarity with the Pambula Lake *M. galloprovincialis*.

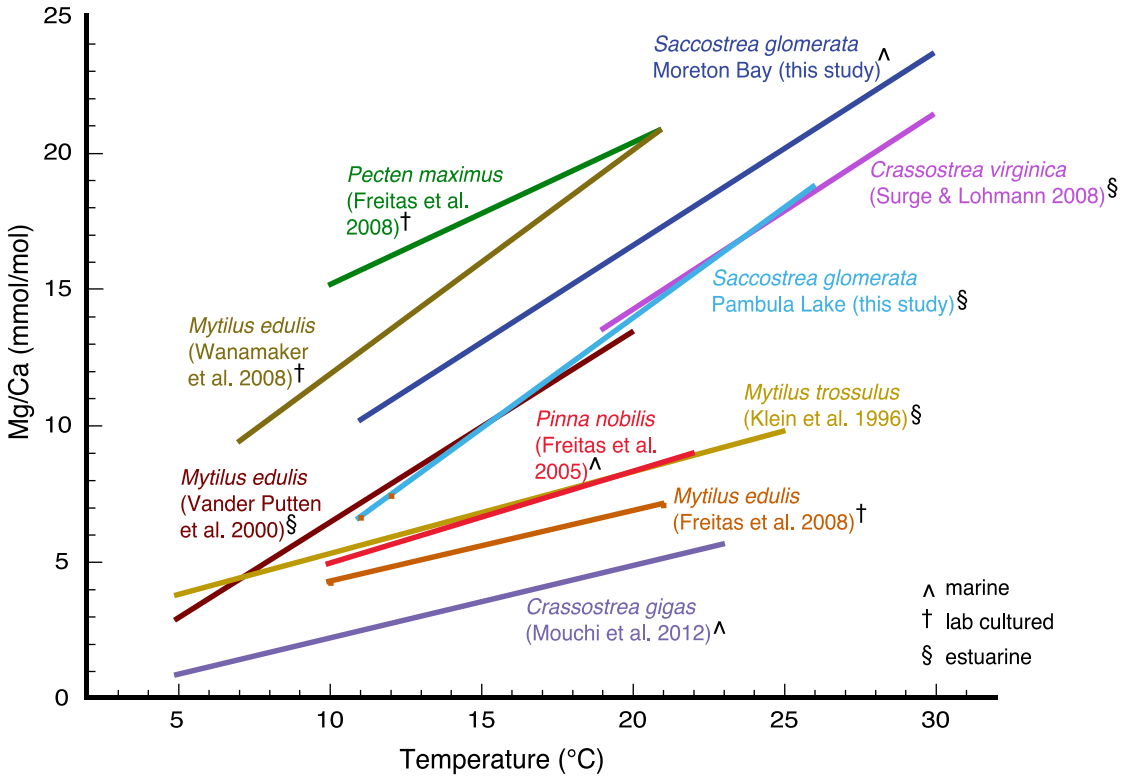

Figure 6.7. Comparison of published Mg/Ca-temperature relationships for various *Mytilus* species.

6.5. Conclusion—*M. galloprovincialis* Mg/Ca ratios as a temperature proxy

While the shells from Little Swanport did not contain a clear seasonal signal in their Mg/Ca ratios, the potential shown by the Pambula Lake *M. galloprovincialis* shells to act as climate archives is promising. Further calibration to obtain a more comprehensive understanding of the effects of growth rate and other biological aspects, such as gametogenesis, that may affect shell growth and Mg/Ca ratios would be desirable to develop this relationship into a more robust and reliable paleotemperature proxy. Further study is also required to pin down the effects of changes in the ambient water chemistry, such as salinity, Mg/Ca ratios and overall Mg concentration.

It is readily apparent from the published data and this study that any Mg/Ca-temperature relationship in the *Mytilus* genus of mussels is species-specific. Furthermore, this study found significant variability in *M. galloprovincialis* Mg/Ca ratios between different locations, and between individuals from the same location. Analysis of several shells is required to obtain a robust mean signal that could then be used to make paleotemperature interpretations. Combination of Mg/Ca ratio data with $\delta^{18}O$ data from *M. galloprovincialis* would also be beneficial in any future studies, to further elucidate the relationship between shell chemistry and environmental influences.

Geographical differences in the Mg/Ca-temperature relationships further indicate that any paleotemperature reconstructions should be conducted using a calibration equation derived from modern specimens from the same or similar location. However, uncertainty regarding the exact provenance of any palaeo-specimens could still potentially complicate the reconstruction of

palaeotemperature records. Extensive genetic studies of *Mytilus* species from a range of locations would also assist in ruling out genetic or species variation as a cause of different Mg/Ca-temperature relationships between geographically distinct populations.

6.6. References

Arias-Ruiz, C., Elliot, M., Bezos, A., Pedoja, K., Husson, L., Cahyarini, S. Y., Cariou, E., Michel, E., La, C., Manssouri, F. (2017). Geochemical fingerprints of climate variation and the extreme La Nina 2010-11 as recorded in a *Tridacna squamosa* shell from Sulawesi, Indonesia. *Palaeogeography Palaeoclimatology Palaeoecology,* 487, 216-228. doi:10.1016/j.palaeo.2017.08.037

Carré, M., Bentaleb, I., Bruguier, O., Ordinola, E., Barrett, N. T., & Fontugne, M. (2006). Calcification rate influence on trace element concentrations in aragonitic bivalve shells: Evidences and mechanisms. *Geochimica Et Cosmochimica Acta*, 70(19), 4906-4920.

Correge, T. (2006). Sea surface temperature and salinity reconstruction from coral geochemical tracers. *Palaeogeography Palaeoclimatology Palaeoecology,* 232(2-4), 408-428. doi:10.1016/j.palaeo.2005.10.014

Dodd, J. R. (1965). Environmental control of strontium and magnesium in *Mytilus*. *Geochimica Et Cosmochimica Acta,* 29(5), 385. Dodd, J. R., & Crisp, E. L. (1982). Non-linear variation with salinity of Sr/Ca and Mg/Ca ratios in water and aragonitic bivalve shells and implications for paleosalinity studies. *Palaeogeography Palaeoclimatology Palaeoecology,* 38(1-2), 45-56. doi:10.1016/0031-0182(82)90063-3

Eisma, D., Mook, W. G., & Das, H. A. (1976). Shell characteristics, isotopic composition and trace-element contents of some euryhaline mollusks as indicators of salinity. *Palaeogeography Palaeoclimatology Palaeoecology, 19*(1), 39-62. doi:10.1016/0031-0182(76)90041-9

Elderfield, H., & Ganssen, G. (2000). Past temperature and delta O-18 of surface ocean waters inferred from foraminiferal Mg/Ca ratios. *Nature,* 405(6785), 442-445. doi:10.1038/35013033

Elmore, A. C., S. Sosdian, Y. Rosenthal, and J. D. Wright (2012), A global evaluation of temperature and carbonate ion control on Mg/Ca ratios of ostracoda genus Krithe, Geochemistry Geophysics Geosystems, 13. doi: 10.1029/2012GC004073

Ford, H. L., Schellenberg, S. A., Becker, B. J., Deutschman, D. L., Dyck, K. A., & Koch, P. L. (2010). Evaluating the skeletal chemistry of *Mytilus californianus* as a temperature proxy: Effects of microenvironment and ontogeny. *Paleoceanography,* 25. doi:10.1029/2008pa001677

Freitas, P., Clarke, L. J., Kennedy, H., Richardson, C., & Abrantes, F. (2005). Mg/Ca,Sr/Ca, and stable-isotope (delta O-18 and delta C-13) ratio profiles from the fan mussel *Pinna nobilis*: Seasonal records and temperature relationships. *Geochemistry Geophysics Geosystems,* 6. doi:10.1029/2004gc000872

Freitas, P. S., Clarke, L. J., Kennedy, H. A., & Richardson, C. A. (2008). Inter- and intra-specimen variability masks reliable temperature control on shell Mg/Ca ratios in laboratory- and field-cultured *Mytilus edulis* and *Pecten maximus* (bivalvia). *Biogeosciences,* 5(5), 1245-1258.

Freitas, P. S., Clarke, L. J., Kennedy, H., & Richardson, C. A. (2009). Ion microprobe assessment of the heterogeneity of Mg/Ca, Sr/Ca and Mn/Ca ratios in *Pecten maximus* and *Mytilus edulis* (bivalvia) shell calcite precipitated at constant temperature. *Biogeosciences,* 6(7), 1209-1227.

Gosling, E. (2003). *Bivalve Molluscs: Biology, Ecology and Culture Fishing*. Oxford: Fishing News Books.

Heinemann, A., Hiebenthal, C., Fietzke, J., Eisenhauer, A., & Wahl, M. (2011). Disentangling the biological and environmental control of M. edulis shell chemistry. *Geochemistry Geophysics Geosystems,*12. doi:10.1029/2010gc003340

Ingram, B. L., P. De Deckker, A. R. Chivas, M. E. Conrad, and A. R. Byrne (1998), Stable isotopes, Sr/Ca, and Mg/Ca in biogenic carbonates from Petaluma Marsh, northern California, USA, *Geochimica Et Cosmochimica Acta*, *62*(19–20), 3229–3237.

Kailola, P. (1993). *Australian fisheries resources*. Canberra, Australia: Bureau of Resource Sciences and the Fisheries Research and Development Corporation.

Klein, R. T., Lohmann, K. C., & Thayer, C. W. (1996). Bivalve skeletons record sea-surface temperature and delta O-18 via Mg/Ca and O-18/O-16 ratios. *Geology,* 24(5), 415-418.

Lamprell, K., & Healy, J. (1998). *Bivalves of Australia. Volume 2*. Leiden: Backhuys.

Lazareth, C. E., Le Cornec, F., Candaudap, F., & Freydier, R. (2013). Trace element heterogeneity along isochronous growth layers in bivalve shell: Consequences for environmental reconstruction. *Palaeogeography Palaeoclimatology Palaeoecology,* 373, 39-49. doi:10.1016/j.palaeo. 2011.04.024

Lea, D. W., Mashiotta, T. A., & Spero, H. J. (1999). Controls on magnesium and strontium uptake in planktonic foraminifera determined by live culturing.

Geochimica Et Cosmochimica Acta, 63(16), 2369-2379. doi:10.1016/s0016-7037(99)00197-0

Lorens, R. B., & Bender, M. L. (1977). Physiological exclusion of magnesium from *Mytilus-edulis* calcite. *Nature, 269*(5631), 793-794. doi:10.1038/269793a0

McDonald, J. H., Seed, R., & Koehn, R. K. (1991). Allozymes and morphometric characters of 3 species of *Mytilus* in the northern and southern hemispheres. *Marine Biology,* 111(3), 323-333.

Nell, J. A., & Gibbs, P. J. (1986). Salinity tolerance and absorption of L-methionine by some Australian bivalve mollusks. *Australian Journal of Marine and Freshwater Research,* 37(6), 721-727. Schöne, B. R., Zhang, Z. J., Radermacher, P., Thebault, J., Jacob, D. E., Nunn, E. V., & Maurer, A. F. (2011). Sr/Ca and Mg/Ca ratios of ontogenetically old, long-lived bivalve shells (Arctica islandica) and their function as paleotemperature proxies. *Palaeogeography Palaeoclimatology Palaeoecology,* 302(1-2), 52-64. doi:10.1016/j.palaeo.2010.03.016

Schöne, B., & Surge, D. (2012). Bivalve sclerochronology and geochemistry. In P. Sheldon & J. Hardesty (Eds.), *Part N, Bivalvia, Revised, Treatise Online* (Vol. 1, pp. 1-24): Paleontological Institute. Schöne, B. R., & Gillikin, D. P. (2013). Unraveling environmental histories from skeletal diaries — Advances in sclerochronology. *Palaeogeography, Palaeoclimatology, Palaeoecology,* 373(0), 1-5. doi:http://dx.doi.org/10.1016/

j.palaeo.2012.11.026

Seed, R. (1968). Factors influencing shell shape in mussel *Mytilus edulis*. *Journal of the Marine Biological Association of the United Kingdom,* 48(3), 561-&.

Sunila, I., Williams, L., Russo, S., & Getchis, T. (2004). Reproduction and pathology of blue mussels, *Mytilus edulis* (L) in an experimental longline in Long Island Sound, Connecticut. *Journal of Shellfish Research,* 23(3), 731-740.

Strasser, C. A., Mullineaux, L. S., & Walther, B. D. (2008). Growth rate and age effects on *Mya arenaria* shell chemistry: Implications for biogeochemical studies. *Journal of Experimental Marine Biology and Ecology,* 355(2), 153-163. doi:10.1016/j.jembe.2007.12.022

Surge, D., & Lohmann, K. C. (2008). Evaluating Mg/Ca ratios as a temperature proxy in the estuarine oyster, *Crassostrea virginica*. *Journal of Geophysical Research-Biogeosciences,* 113(G2). doi:G02001 10.1029/2007jg000623

Tynan, S., Dutton, A., Opdyke, B. N., & Eggins, S. M. (2014). Oxygen isotope

records of the Australian flat oyster (Ostrea angasi) as a potential temperature archive. *Marine Geology*, 195-209. doi:10.1016/j.margeo.2014.07.009

Tynan, S., Opdyke, B. N., Walczak, M., Eggins, S., & Dutton, A. (2017). Assessment of Mg/Ca in Saccostrea glomerata (the Sydney rock oyster) shell as a potential temperature record. *Palaeogeography Palaeoclimatology Palaeoecology,* 484, 79-88. doi:10.1016/j.palaeo.2016.08.009

Vander Putten, E., Dehairs, F., Keppens, E., & Baeyens, W. (2000). High resolution distribution of trace elements in the calcite shell layer of modern *Mytilus edulis*: Environmental and biological controls. *Geochimica Et Cosmochimica Acta,* 64(6), 997-1011.

Vihtakari, M., Ambrose, W. G., Renaud, P. E., Locke, W. L., Carroll, M. L., Berge, J., Clarke, L. J., Cottier, F., Hop, H. (2017). A key to the past? Element ratios as environmental proxies in two Arctic bivalves. *Palaeogeography Palaeoclimatology Palaeoecology,* 465, 316-332. doi:10.1016/j.palaeo.2016.10.020

Wanamaker, A. D., Kreutz, K. J., Wilson, T., Borns, H. W., Introne, D. S., & Feindel, S. (2008). Experimentally determined Mg/Ca and Sr/Ca ratios in juvenile bivalve calcite for *Mytilus edulis*: implications for paleotemperature reconstructions. *Geo-Marine Letters,* 28(5-6), 359-368. doi:10.1007/s00367-008-0112-8

Wilson, B. R., & Hodgkin, E. P. (1967). A comparative account of reproductive cycles of 5 species of marine mussels (Bivalvia – Mytilidae) in vicinity of Freemantle Western Australia. *Australian Journal of Marine and Freshwater Research,* 18(2), 175.

Yearsley, G. K., Last, P. R., & Ward, R. D. (1999). *Australian Seafood Handbook*: CSIRO.

Chapter 7

Conclusion

The goal of this thesis was to begin to fill the gap in the sclerochronological literature as regards studies of Australian bivalve species, and test the viability of using these species to investigate climate variability during the Holocene in the Australian region. To this end, *in situ* field culturing experiments were conducted to calibrate the $\delta^{18}O_{shell}$-temperature relationship in modern specimens of *O. angasi*, and the Mg/Ca-temperature relationship in *S. glomerata* and *M. galloprovincialis*. All these bivalves are estuarine species, although they can also inhabit marine environments. The field culturing experiments were conducted at Pambula Lake, New South Wales, Little Swanport, Tasmania, and Moreton Bay, Queensland. Pambula Lake and Little Swanport are estuarine sites, while the Moreton Bay site was within a sheltered bay marine environment.

The *O. angasi* $\delta^{18}O_{shell}$ and the *S. glomerata* Mg/Ca ratios produced high-resolution seasonal records that were both found to reflected the ambient calcification temperature. However, the hydrological dynamics of the estuarine sites also exerted an influence upon the relationship of these proxies to temperature. Inflow of freshwater, with a more negative $\delta^{18}O$, tended to bias the O. *angasi* $\delta^{18}O_{shell}$ towards more negative values, and thus warmer inferred temperatures. The Mg/Ca-temperature relationship within *S. glomerata* shell was also affected by the estuarine hydrodynamics, as evidenced by a disparity found between the Mg/Ca-temperature relationships derived for the Pambula Lake *S. glomerata* compared to that derived for the Moreton Bay *S. glomerata*. However, it was found that the D_{Mg}-temperature relationship was consistent between the two sites. This suggests that Mg/Ca ratios do not necessarily offer a salinity-independent temperature proxy, as previously believed. Rather, like $\delta^{18}O_{shell}$, it is a convolved signal between temperature and ambient water chemistry.

Taking this into account, the two calibrated relationships were applied to archaeological specimens of *O. angasi* from an Aboriginal midden on the far south coast of New South Wales, and of *S. glomerata* from a midden on Moreton Bay, Queensland, to test their potential to contribute to paleoclimate records for the southeastern Australian region. Two shells from each midden site were analysed, and all shells presented high-resolution, multi-year records of seasonal temperature variation. The small sample sizes provided only a 'snapshot' of late Holocene sea surface temperatures, but these initial applications of the calibrated temperature proxies confirmed the potential of sclerochronological analysis of archaeological oyster specimens to make a valuable contribution to palaeoclimate records, for a time period and region for which records are currently scarce. Further, the seasonal nature of the records these shells can yield provides a level of detail unobtainable from other climate proxies. From an archaeological perspective, these records offer valuable insights into human-environment interactions.

The *M. galloprovincialis* calibration experiment showed geographical variation between Little Swanport and Pambula Lake populations of *M. galloprovincialis* shell Mg/Ca ratios. Mussels from Pambula Lake were found to show a temperature dependence in the shell Mg/Ca ratios, while no seasonal signals were identified in the Little Swanport *M. galloprovincialis* shell Mg/Ca ratios.

7.1. Avenues for further work

While this work provides a solid base from which to develop further sclerochronological studies of Australian species, the gap we set out to fill is but

partially filled: this initial foray into the sclerochronology of Australian oyster species and its application within a Holocene paleoclimate context has shown just how much more untapped potential (and work) lies in sclerochronological studies of Australian species. There are several avenues worthy of pursuit in further studies.

While no obvious connections between growth structures and shell chemical profiles were found in this project, a thorough and focussed investigation of the shell growth patterns and micro-structures of *O. angasi*, *S. glomerata* and *M. galloprovincialis* is warranted. This would be a valuable addition to any further geochemical analysis.

While the integrity of $\delta^{18}O$ ratios as a temperature proxy in the shell of *O. angasi* has been tested and proven, additional calibration studies would be useful to comprehensively disentangle the convolved signal of temperature and salinity within the oyster's estuarine habitat. Further long-term calibration studies would also enable the ontogenetic controls evidenced in the midden specimens of *S. glomerata* to be teased out and their implications for palaeoclimate interpretations properly understood. Controlled experiments within a laboratory setting could potentially further refine any environmental proxies.

Logistical constraints prevented $\delta^{18}O_{shell}$ analysis of *S. glomerata* within this study. Given the promising potential of Mg/Ca ratios within this species as a paleotemperature tracer, the investigation of $\delta^{18}O$ ratios as a complementary proxy to Mg/Ca ratios should be a priority and can only make any paleotemperature interpretations using *S. glomerata* more robust and reliable.

Examination of trace element ratios other than Mg/Ca should also be pursued. Sr/Ca, Ba/Ca, Li/Ca are all promising proxies within biogenic carbonates and could add valuable insights into salinity, hydrological dynamics and shell

growth. Additionally, further investigation of novel methods to decouple the combined temperature-salinity signal of $\delta^{18}O_{shell}$ in *O. angasi* and Mg/Ca ratios in *S. glomerata* is clearly necessary. Combined trace element and isotopic studies that include clumped isotopes are an obvious candidate for this.

Analysis of $\delta^{18}O$ in *M. galloprovincialis* shells would also make a valuable addition to further sclerochronological studies of this species, along with complementary analysis of the aragonitic nacreous layer. As *M. galloprovincialis* is also commonly found in Aboriginal midden sites, a more robust calibration of the geochemical proxies it can offer would be useful.

Any future studies on these species could also be complemented by studies of other marine bivalve or gastropod species from the same or neighbouring localities. As different species inhabit different hydrologic environments and have different temperature and salinity thresholds, compilation of records from a variety of species would help provide a more comprehensive picture of climatic and environmental change.

The geographical and chronological extent of Aboriginal midden sites along the eastern Australian coast clearly offer an extensive and rich repository of palaeoclimate information. Combined with appropriate geomorphological and sedimentary studies to elucidate the regional hydrological and physical environmental dynamics, shells from these archaeological sites have the potential to provide paleoclimate information for both a time period and a region where current records are both limited in number and geographically scattered. As well as the seasonal nature of the shell records, of particular significance is the marine perspective they offer, as the majority of the existing records are from inland environments. Compilations of multiple shells from midden sites would potentially provide a more robust picture of Holocene climate. The depth of the

temporal record that could be sourced from Aboriginal midden shells will of course be dependent on midden preservation and occurrence. Investigations that persist further back in time will rely on obtaining well-preserved fossil samples.

Further investigations building upon the foundation provided within this thesis will enable the future study of a range of bivalve shells from modern, midden and fossil contexts to help elucidate climate dynamics in the Australian region, and also make a valuable contribution to understanding the human-climate interactions of our country's original inhabitants.

Appendix 1

An overview of bivalve shell formation

When analysing the shells of bivalves with the aim of obtaining an environmental record, it is essential to have at least a basic understanding of where and how the animals live, and even more importantly, how they grow their shells. Indeed, without this information, it is impossible to place the record offered by the shell's geochemistry into any sort of temporal or environmental context, and the record loses its relevance and usefulness.

All bivalves belong to the class Bivalvia, within the phylum Mollusca. The Mollusca are a very diverse group of invertebrates. The phylum includes sea slugs, octopuses and squid, and animals with shells, such as gastropod snails, nautiloids and of course, the bivalves such as clams, oysters and mussels.

Bivalves generally have an anterior head, ventral foot, and a visceral mass, which is covered by folds of tissue called the mantle. They also possess adductor muscles, which are responsible for pulling the shell valves shut, and the elastic ligament connecting the two valves opens the shell upon relaxation of the adductor muscle. All bivalves have a foot in their larval stage, to enable movement, but some species of oysters, which cement themselves to a suitable substrate, lose this foot lost as they grow.

Most bivalves are ciliary suspension feeders, which means they take in water and the suspended material within from their environment and extract the nutrients necessary for their growth. The gills, which lie laterally on the side of the body as two deep folds, contain the ctenidia, which make a filtering structure with a very large surface area. The animal opens its shell slightly while submerged, and the gills create a current, which pushes water through the ctenidia, where particles are sieved out and then transported to the labial palps in the head. Here it is sorted and either rejected or consumed (Korringa 1952; Winter 1978).

Varieties of the genus *Mytilus* have been found to retain particles down to colloid size (roughly less than or equal to 1μm), and other work has found effective retention in many other bivalves of particles down to the size of 7μm, with a limited ability to retain particles down to 1μm. *Mytilus* proved to be proficient in retaining particles the size of 2μm (Winter 1978 and references therein).

It has generally been assumed that bivalves discriminate between the material they ingest and that which they expel as pseudofeces, rejecting material that is too large or irregularly shaped (Korringa 1952; Winter 1978). However, some studies have shown that this assumption does not necessarily always hold true. Animals were fed combinations of normal food and metals, and it was found that each were ingested and rejected in the same proportions. This has implications for bivalves in polluted environments, as they will possibly consume large amounts of potentially toxic material.

Bivalves can occupy a wide variety of marine, estuarine and freshwater environments. As estuarine species comprise the bulk of this study, it is worth outlining some of the physical features of estuarine environments that can have the most significant effect on bivalves' and other molluscs' growth and survival.

Salinity in estuaries can vary greatly, depending upon the amount of freshwater flow into the estuary, and whether or not the estuary is permanently connected to the sea. High fluctuations in temperature, salinity and oxygen availability can develop in estuaries with only intermittent freshwater flow and/or sporadic connection to the ocean, which can be very demanding on the bivalves present. Extreme conditions can lead to the dominance of one hardy species of bivalve, with the widest variety of species seen in estuaries with close to marine conditions (Peterson & Wells 1998).

The suspension feeding nature of most bivalves results in a preference for cleaner waters, with sandy bottoms. Too much turbidity and in the water can lead to their gills becoming clogged with fine particles. Generally, sediments in estuaries are coarser towards the opening of the estuary to the ocean, with a fining of sediments up towards the top of the estuary. Higher flows and rapid currents lead to the frequent replenishment of food stocks and mixing of water masses, which are factors contributing to optimal growth (Peterson & Wells 1998).

It is at the high tide mark in an estuary, where water coverage would be minimal, that diversity and density of molluscan and bivalve species is often lowest. Some species are vulnerable to exposure to air, and prefer to be continually submerged. Highest density is reached in the upper regions of the intertidal zone, with density declining, but diversity of species increasing, with depth (Peterson & Wells 1998).

Many bivalves bore or burrow into sediments, and are relatively mobile, while others, such as mussels and oysters attach themselves to a hard substrate, where they will remain unless dislodged by some outside force.

Shell formation

Every bivalve has two parts to its shell—a left and right valve joined by a ligament. With mussels, these valves are basically identical. With oysters however, the two valves differ in both size and shape, with the right valves usually being much more convex, or cup-shaped, with the left valves being much flatter, forming a ‘lid’ to the cupped right valve.

Shells are comprised of calcium carbonate, $CaCO_3$, which can exist in a number of different polymorphs, the two dominant forms being calcite and aragonite. They differ in terms of structure, and in abiogenic/inorganic systems,

are found in environments with significantly different pressure-temperature regimes. Calcite is rhombohedral in structure, with each Ca^{2+}atom bonded to six O^{2-} atoms from different CO_3 groups, resulting in a slightly distorted octahedron formation. Each O^{2-} from the CO_3 group is bonded to one C and two Ca^{2+}atoms from adjacent layers in the crystal structure. In the orthorhombic aragonite, the Ca^{2+} atoms are arranged in pseudo-hexagonal layers, and each Ca^{2+} atom is bonded to nine O atoms (Milliman et al. 1974).

The $CaCO_3$ of bivalve shells can be in the form of either calcite or aragonite, or a combination of both. Usually, about 10% of the shell is comprised of an organic matrix. Shell structure is generally in the form of an organic layer covering the exterior surface of the shell, known as the periostracum, which is underlain by a prismatic carbonate layer, then a denser nacreous carbonate layer.

Wilbur (1972) describes the process of shell formation as consisting of four ‘compartments’:

- The medium, i.e., the seawater or freshwater environment where the animal lives
- the soft tissue, in particular the mantle region of the animal, which is responsible for secreting the extrapallial fluid (EPF)
- the EPF, the fluid that fills the fills the space between the shell surface and the outer mantle edge of the animal and from which the shell is deposited
- the shell itself

The chemical composition of each of these compartments is dependent upon that of its direct predecessor, i.e., the composition of the shell itself is obviously controlled by the composition of the EPF, which is in turn regulated by

the soft tissues and blood of the animal, which are dependent upon intake from food and the ambient water.

Shell formation occurs in two main phases: the accumulation of the necessary elements for shell formation from the ambient water, with the subsequent secretion of the EPF, and then the production of the organic matrix and nucleation and growth of $CaCO_3$.

It is generally accepted that the primary source of Ca^{2+} for bivalve shell comes from the ambient water of the animal's environment, with stores of $CaCO_3$ within the animal's soft tissue providing a secondary source. Carbon can either be obtained from the dissolved inorganic carbon (DIC) of the ambient water, or from metabolic/respiratory CO_2.

While the extremely complex process of ionic transport to the EPF and biomineralisation is not fully understood, it is assumed by many authors that at least Ca^{2+}, and probably the other ingredients necessary for shell formation are diffused through the mantle epithelium to and from the EPF. It has been found that the mantle membrane is far more permeable with regard to Ca^{2+} than any other ions, and an approximate calculation from Wheeler (1992) shows that the flux of Ca^{2+} from the hemolymph (tissue on the edge of the mantle from which the EPF is secreted) to shell in a freshwater clam provided sufficient Ca^{2+} to satisfy the calcification rate of the oyster *Crassostrea virginica*. Other authors suggest that Ca^{2+} transport could be both an intercellular and intracellular process, with intracellular pathways being more likely to be Ca-specific (Watabe and Kingsley 1989 in Klein et al. 1996). In a metabolically controlled process, Ca^{2+} can also bind with proteins and then travel to the EPF (Wilbur 1972; Klein et al. 1996).

The Ca^{2+} concentration of the EPF is usually very close to that of seawater, and the DIC concentration generally around double that of seawater. The EPF usually is supersaturated with respect to $CaCO_3$, at roughly the same degree as seawater, with a pH of around 7.3-7.6. Interestingly, the EPF chemical composition of freshwater bivalves is very similar, meaning the animal is able to concentrate Ca^{2+} significantly as compared to the ambient water (Wheeler 1992).

The organic matrix is generally a mixture of proteins, mucopolysaccharides, glycoprotein and organic acids, and plays a very important part in shell formation. Not only does it provide the basis for crystal nucleation and growth, it has been suggested that the content of the organic matrix exerts some control over the mineralogy of the shell (Wilbur 1972; Wheeler 1992). Shells of aragonite composition have been found to contain a wider range of proteins and mucopolysaccharides within the organic matrix than those comprised of calcite. It is also assumed that it is the organic matrix that enables the highly ordered growth of $CaCO_3$ crystals in the various different structures found in bivalve shells, and also the precipitation of individual crystal layers.

There are two processes occurring simultaneously during shell growth—the addition of $CaCO_3$ at the ventral growing edge, contributing to the shell's length, and also the thickening of the shell through the addition of dense nacreous $CaCO_3$ on the inner shell surface (Jones and Quitmyer 1996). In some bivalves, these two processes produce $CaCO_3$ of different mineralogy—calcite at the growth edge, and aragonite in the inner nacreous layers.

The prismatic layer can contain various microstructures—simple, fibrous, composite and spherulitic prisms, which generally form perpendicular to the shell's surface. The nacre is comprised of thin sheets of flat tablets, tall pyramidal columns or stacked elongate tablets that form parallel to the shell's surface. The

nacre is almost always made of aragonite, and is the lustrous inner shell surface seen in many bivalves. Its composition is similar to pearl. Also present in some bivalve shells is a foliated calcite layer, where flat elongate laths or blades of calcite overlap each other, similar to roof shingles.

This accretionary style of growth offers enables the interpretation of the geochemistry of the shells within a temporal context. Crucial to this understanding is the fact that the shells exhibit distinct growth bands, or increments, usually attributed to regular hiatuses in growth, such as a 'shut-down' resulting from extreme summer or winter temperatures. The animal withdraws its mantle from the edge of the shell, and carbonate secretion ceases (Richardson 2001). If growth increments are in fact interpreted to be occurring in a regular fashion, their periodicity can facilitate age determination of the shell.

These increments are often visible on the outer surface of the shell in many species, however a more reliable record is generally found in the internal growth structures. This is especially true with regard to the shells of oysters and mussels, where growth bands can be non-existent or difficult to distinguish from other features on the exterior surface of the shell (Gosling 2003).

However, many studies have shown that interpretation of these growth increments is not necessarily as straightforward as simply assigning an annual periodicity. Growth banding can occur with a tidal or lunar periodicity, or can be related to spawning events, whereby energy is diverted to reproduction rather than shell growth. Other forms of environmental stress can also cause cessations in shell growth, wherein a 'disturbance ring' rather than a regular growth increment is formed (Richardson 2001).

Kirby et al. (1998) found that the morphology of the growth increments found in the hinge region of the oyster *Crassostrea virginica* exhibited a seasonal

pattern, with the convex top of a band representing the summer and concave bottoms winter. However, Surge et al. (2001) in a study of the same species, found no such relationship between the morphology of the growth increments and seasonal changes.

Other studies have also highlighted the dangers of making assumptions regarding the growth increment patterns within bivalve shells. Jones and Quitmeyer (1996) found that in shells of *Mercenaria mercenaria*, shells collected from the northern limits of the species' distribution exhibited a pattern that was the direct opposite of that shown in the shells collected from the southern limits of the distribution. The northern shells showed a growth hiatus in the cold winter months, while the southern shells shut down during the hottest months of summer.

As the shell grows, other elements can substitute for Ca in the carbonate crystal lattice (e.g. Schöne et al 2011). Mg^{2+} and Sr^{2+} can be incorporated into the calcium carbonate crystals in varying proportions depending on temperature and/or salinity of the ambient water, giving us information regarding the climatic conditions at the time of shell formation.

Toxic heavy metals can also become incorporated in the carbonate crystal lattice (e.g. McFarlane et al. 2005). It can be assumed that via this process, any metals found incorporated into the calcium carbonate structure have been actively metabolised by the organism, thus providing an indication of the degree of bioavailable metal present in the environment.

Shell growth rates

Not only is it important to understand how the bivalve shell grows, but also the rate at which this process occurs. A number of studies have pointed out that

growth rate can affect the formation of $CaCO_3$ and trace element incorporation into the shell (e.g. Owen et al. 2002).

Although there are many different factors that affect bivalve growth rates, and growth patterns vary from species, there are some characteristics of growth that are common to most bivalves. Growth is generally more rapid in younger animals and then slows as the animal gets older (Gosling 2003). This tendency is best described by the von Bertalanffy growth equation (von Bertalanffy 1938), which many subsequent studies have used to describe bivalve growth:

$$l_t = L_\infty(1 - \exp[-k(t - t_0)] \qquad \text{(Eq. A1)}$$

This equation relates the length of the animal at any given age (l_t), and the theoretical maximum size (L_∞) of the animal with a growth constant (k). It assumes that there is a definite maximum age attainable for any given bivalve population. This assumption does not necessarily apply to all bivalves, as some can keep growing throughout their entire lifespan. Also, the equation does not take into account seasonal variations in growth, nor the major part that external factors, such as food availability, temperature, salinity, exposure to air, water flow and depth and population density play in governing growth rates.

Of these environmental factors, food supply exhibits the greatest control upon growth. Without sufficient food and energy, no animal can grow, or indeed, survive. Nearly all of the other factors can also be related back to this fundamental requirement, as all the environmental conditions that can affect bivalve growth and prosperity will also affect the growth and abundance of the bivalves' food, such as plankton and algae.

Generally, higher temperatures result in faster growth rates. It has been found that with comparable species growth is enhanced at higher latitudes as compared to lower latitudes. This relationship between temperature and growth is not a linear function, however, as each species has a maximum temperature threshold above which they are no longer comfortable. Extreme temperatures will lead to death of the animal. While temperature tolerances differ greatly from species to species, it can also have a geographical factor, as tolerances often relate to the ambient conditions to which the animal is acclimated.

The effects of salinity upon growth again differ from species to species, with most exhibiting a distinct salinity range for optimum growth. As with temperature, some studies have suggested that salinity tolerances can vary geographically, depending on the ambient salinity the animal is accustomed to (Gosling 2003).

As the animals can only feed when they are immersed in water, exposure to air at low tides can also play a part in their growth. The animals can only feed when immersed in water, and although some species have higher tolerances, for most bivalves zero growth results when the animal is subjected to exposure out of the water for around 50% of the time. Other factors related to exposure out of water such as heat shock and desiccation can also impair growth and survival (Gosling 2003).

The effects of water depth upon bivalve growth are most likely directly related to temperature and again, food availability. Shallow waters are generally warmer and more productive and so bivalves in these environments exhibit enhanced growth. In general, bivalves grow better in rapid flowing water, but there is an upper limit on the strength of the current (Gosling 2003).

Again, the observed decline in bivalve growth rates with increased population density is also a direct function of food availability. More individuals competing for the same amount of food will obviously result in less food for each animal, thus inhibiting their growth (Gosling 2003).

The most important aspect of growth rate variation with regard to this study is the effect of increasing age upon an individual's growth rate. Numerous studies have pointed out that ontogenetic (developmental) influences upon growth rate can strongly influence an animal's growth, with many animals growing much faster in their early years, with a decline or complete cessation in growth in later years. Obviously this can complicate an interpretation of the growth patterns and must be taken into account during geochemical analysis of growth increments.

References

Gosling, E. (2003). *Bivalve Molluscs: Biology, Ecology and Culture Fishing*. Oxford: Fishing News Books.

Jones, D. S., & Quitmyer, I. R. (1996). Marking time with bivalve shells: Oxygen isotopes and season of annual increment formation. *Palaios, 11*(4), 340-346. doi:10.2307/3515244

Kirby, M. X., Soniat, T. M., & Spero, H. J. (1998). Stable isotope sclerochronology of pleistocene and recent oyster shells *(Crassostrea virginica*). *Palaios, 13*(6), 560-569.

Klein, R. T., Lohmann, K. C., & Thayer, C. W. (1996). Sr/Ca and C-13/C-12 ratios in skeletal calcite of *Mytilus trossulus*: Covariation with metabolic rate, salinity, and carbon isotopic composition of seawater. *Geochimica Et Cosmochimica Acta, 60*(21), 4207-4221.

Korringa, P. (1952). Recent advances in oyster biology. *Quarterly Review Biology, 27*, 266-365.

MacFarlane, G. R., Markich, S. J., Linz, K., Gifford, S., Dunstan, R. H., O'Connor, W., & Russell, R. A. (2006). The Akoya pearl oyster shell as an

archival monitor of lead exposure. *Environmental Pollution, 143*(1), 166-173. doi:10.1016/j.envpol.2005.10.042

Milliman, J. D., Müller, G., & Förstner, U. (1974). *Recent sedimentary carbonates*. *Part 1 Marine Carbonates*. Berlin: Springer.

Owen, R., Kennedy, H., & Richardson, C. (2002). Isotopic partitioning between scallop shell calcite and seawater: Effect of shell growth rate. *Geochimica Et Cosmochimica Acta, 66*(10), 1727-1737.

Peterson, C. H., & Wells, F. E. (1998). Molluscs in Marine and Estuarine Sediments. In *Mollusca: The Southern Synthesis. Part A.* (pp. 36-46). Melbourne: CSIRO Publishing.

Richardson, C. A. (2001). Molluscs as archives of environmental change. In *Oceanography and Marine Biology, Vol 39* (Vol. 39, pp. 103-164).

Schone, B. R., Zhang, Z. J., Radermacher, P., Thebault, J., Jacob, D. E., Nunn, E. V., & Maurer, A. F. (2011). Sr/Ca and Mg/Ca ratios of ontogenetically old, long-lived bivalve shells (*Arctica islandica*) and their function as paleotemperature proxies. *Palaeogeography Palaeoclimatology Palaeoecology, 302*(1-2), 52-64. doi:10.1016/j.palaeo.2010.03.016

Surge, D., Lohmann, K. C., & Dettman, D. L. (2001). Controls on isotopic chemistry of the American oyster, *Crassostrea virginica*: implications for growth patterns. *Palaeogeography Palaeoclimatology Palaeoecology, 172*(3-4), 283-296.

Wilbur. (1972). Shell formation in molluscs. In M. Florkin & B. T. Scheer (Eds.), *Chemical Zoology Vol VII: Mollusca* (pp. 243-282). New York: Academic Press.

Wheeler, A. P. (1992) Mechanisms of molluscan shell formation, In E. Bonucci (Ed.), Calcification in Biological Systems (pp179–216). Florida, USA: CRC Press.

Winter, J. E. (1978). A review of the knowledge of suspension feeding in lamellibranch bivalves, with special reference to artificial aquaculture systems. *Aquaculture, 13*, 1-33.

Appendix 2

The bivalves of this study

There are three estuarine species examined in this work—two species of oyster, *Ostrea angasi* (flat or native or mud oyster) and *Saccostrea glomerata* (Sydney Rock oyster), and one species of mussel, *Mytilus galloprovincialis.* The scientific classification of the species examined in this work is shown in Table A2.1:

Table A2.1. Classification of the bivalves used in this study

	O. angasi	***S. glomerata***	***M. galloprovincialis***
Phylum	Mollusca	Mollusca	Mollusca
Class	Bivalvia	Bivalvia	Bivalvia
Order	Ostreoida	Ostreoida	Mytiloida
Family	Ostreidae	Ostreidae	Mytilidae
Subfamily	Ostreinae	Ostreinae	
Genus	*Ostrea*	*Saccostrea*	*Mytilus*
Species	*O. angasi*	*S. glomerata*	*M. galloprovincialis*

All the species examined in this study belong to the class Bivalvia within the phylum Mollusca. All the estuarine species examined also belong to the subclass Pteriomorphia. Members of this subclass are usually epifaunal, that is, they are either byssally attached (via byssal threads, sometimes known as beards in mussels) or cemented to a hard substrate.

It is when the level of Order is reached that the various bivalves begin to diverge. The matter of classification is extremely complicated, as various morphological, anatomical, genetic and evolutionary features all contribute to the final specific classification. Rather than trying to understand the somewhat convoluted science and intricacies of the taxonomic process, brief descriptions of the relevant taxonomic levels are given below, leading to a description of each species of interest in this study.

A2.1. Order Ostreoida

Oysters of the order Ostreoida have highly variable shell shapes, both between and even within species. Most possess valves that are unequal in size and shape, but are usually generally roughly symmetrical in the top view. The left valve is usually cemented to a hard substrate. Shell composition is calcitic, and the right valve usually has simple foliated and prismatic layers, while the left valve has thick outer foliated layers. The shells are quite weak and brittle.

A2.2. Family Ostreidae, subfamily Ostreinae

Oysters within the family Ostreidae usually have rounded or elongate oval shaped shells. Within the subfamily Ostreinae, the left valve is usually only shallowly cupped below the hinge line. The shells are thick, friable, lamellose structures, often with cavities between the layers, particularly in the left valve. These cavities can become filled with fluid or a chalky deposit. These oysters generally prefer to live in a clear-water, subtidal environment, with marine salinity. There can be a large degree of variation in shell shapes amongst this subfamily.

Within the subfamily Crassostreinae, again there is a large degree of variation in shell shape. The left valve is significantly more cupped, with the right valve essentially forming a lid for the left valve. The left valve is cemented to a hard substrate and the shells often develop fluid or chalk-filled cavities.

The main difference between oysters of the *Ostrea* and *Crassostrea* genera is that of the method of reproduction. In *Ostrea*, the female oyster takes in sperm

and the eggs are fertilised while still in the female's shell, and the eggs further develop in place for up to three weeks, after which they are expelled into the water column. In *Crassostrea*, both male and female oysters expel their sperm and eggs into the water, and so all fertilisation and development occurs externally.

A2.3. *Saccostrea glomerata* (Sydney Rock oyster)

This oyster is found along the east coast of Australia, from Wingan Inlet in Victoria, up through Queensland and through the tropics to Shark Bay in Western Australia (Malcolm 1971; Kailola et al. 1993; Nell 2001). *S. glomerata* is almost always cemented to a hard substrate, and while it prefers an estuarine intertidal habitat, can be found up to 3m deep, surviving completely submerged conditions (Malcolm 1971; Kailola et al. 1993).

S. glomerata reported temperature tolerance ranges from 12°C in winter to 25°C in summer. *S. glomerata* in New Zealand exhibit the greatest growth between temperatures of 17°C - 20°C (Dinamani 1991). Nell and Dunkley (1984) found optimum nutrient uptake and growth occurred between 20°C and 30°C.

The oysters grow best in salinities of 25–35g/l but can tolerate the range 15 - 45g/l (Nell & Dunkley 1984 and possibly even up to 50g/l (Nell & Gibbs 1986). This is significantly higher than the range given for optimum growth of *S. glomerata* in New Zealand of 12 - 16 parts per thousand (Dinamani 1991).

Commercially cultivated *Saccostrea glomerata* generally take 2.5–3 years to reach "market" size, which is usually 85–100mm (Malcolm 1971). Some cultivated shells have been known to reach 255mm (Lamprell & Healy 1998). They have been known to live for up to 10 years (Kailola et al. 1993).

A2.4. *Ostrea angasi* (flat/native/mud oyster)

The distribution of this oyster extends along the southern coast of Australia, from New South Wales, through Victoria and South Australia to Western Australia, and it is also found in Tasmania (Nell 2001; Lamprell & Healy 1998). Some recent studies have carried out genetic analyses on stocks of what was thought to be solely *O. angasi* from Albany, Western Australia, and found that there was an approximate 30% occurrence of *Ostrea edulis*, a morphologically very similar species that is native to European waters. It was previously assumed that *O. edulis* was not present in Australia, and as visible differentiation between the two species is very difficult this could have implications for the other Australian populations of *O. angasi* (Morton et al. 2003). While this does create some uncertainty about the exact species of oyster we may be dealing with, it does offer the advantage of the fact that there is a much broader range of published literature regarding *O. edulis*. Furthermore, if their morphological similarity is such that for the purposes of this study, the two are comparable, then the possibility that a calibration curve obtained for the trace element and isotopic information with *O. angasi* shells could also be used to interpret shells of *O. edulis* and vice versa certainly warrants further investigation.

O. angasi generally grow in sub-tidal regions, and are usually found in shallow waters, up to around 20m deep (Nell 2001). They often start out their life cemented to a hard substrate but then separate themselves and lie on top of the sediment.

Their preferred salinity range is 25–35g/l, but can tolerate a range of 20 - 45g/l (Nell & Gibbs 1986). It is difficult to find a published thermal tolerance range for *O. angasi*, but it has been reported that *O. edulis* can tolerate

temperatures of 4°C–22°C, but grow best at 15°C–20°C and can not tolerate temperatures above 26°C (Aquaculture guide). Judging from the distribution patterns of *O. angasi* it is evident that this species is not capable of tolerating temperatures as high as *S. glomerata*.

Shells of *O. angasi* can grow up to 190mm (Lamprell & Healy 1998). It has been suggested that growth rate is strongly related to temperature. Mitchell et al. (2000) found that wild *O. angasi* oysters in Georges Bay, Tasmania, exhibited little to no growth over the winter period, but there was a marked increase in shell length over the summer. Similar patterns have been reported for *O. edulis*, where monitoring experiments showed that growth only occurred over the summer, once water temperatures had reached around 12°C (Walne 1972) A similar lower limit for shell growth was found to be 50° Fahrenheit (10°C) (Orton 1928). Growth of *O. edulis* was also found to be sensitive to changes in water temperature over periods as shorts as one week (Grant et al.1990). Both *O. angasi* and *O. edulis* are also more susceptible to exposure to air than *S. glomerata.*

A2.5. Mytilus galloprovincialis (blue mussel)

There is some debate regarding the species of *Mytilus* that occurs in Australia. Different publications give the classifications of *Mytilus edulis planulatus* (Kailola et al. 1993) *Mytilus planulatus* (Lamprell & Healy 1998) and *Mytilus edulis* (Yearsley et al. 1999). A study in 1991 analysed the allozymes (a genetic marker) of *Mytilus* mussels from both the northern and southern hemisphere, including mussels collected from the Huon River estuary in Tasmania and Albany, Western Australia. These Australian mussels, while containing some genetic features common to northern hemisphere *Mytilus edulis,* they were in fact

closest to the species *Mytilus galloprovincialis* (McDonald et al. 1991). Thus, based on this study, it will be assumed that the mussels under scrutiny in this project are indeed *Mytilus galloprovincialis*.

The uncertainty of specific classification is not unique to the mussels occurring in Australia. The genus *Mytilus* enjoys an extremely wide distribution worldwide, one of the broadest distributions of all the marine genera (Koehn 1991). Early classifications were generally based upon morphological features. Further studies regarding geographic and inter-specific shell plasticity, and more advanced genetic techniques have revealed that many early classifications and species distribution patterns are indeed erroneous and needed to be revised (Gosling 1992; Koehn 1991). This uncertainty further complicates comparison of the results of this study with other published work on various species of *Mytilus*.

It is currently accepted that the distribution of *M. galloprovincialis* extends from temperate latitudes into warmer waters in both the northern and southern hemisphere (Gosling 1992). In Australia, *M. galloprovincialis* occurs throughout Western Australia, South Australia, Tasmania, Victoria and New South Wales.

M. galloprovincialis prefers sheltered, brackish environments, though it is unsure whether it is the lower salinity of these environments from which this preference arises, or the comparative abundance of food (Gosling 1992).

Published information regarding the temperature tolerance of *M. galloprovincialis* could not be found, with the best estimate of its thermal tolerance to be inferred from its distribution patterns. It is also known as the Mediterranean mussel, and is found on the southern European coastline, the mid-western coast of the USA, the Chinese and Japanese coastlines, the north-eastern coast of New Zealand and the southern coasts of Australia. It can be surmised that *M. galloprovincialis* prefers warmer and temperate waters, and is generally

supplanted by other species at higher latitudes (Gosling 1992). Its presence in Australia, particularly Tasmanian waters, is perhaps somewhat anomalous.

Nell and Gibbs (1986) give a salinity tolerance for *M. edulis planulatus* specimens from Jervis Bay, New South Wales, of 14–45g/l. It will be assumed that due to the aforementioned confusion in *Mytilus* taxonomy, they were in fact referring to specimens of *Mytilus galloprovincialis*.

Mytilus shells can reach 100–130mm in length (Gosling 2003), and *M. galloprovincialis* can keep growing at around 80% of the rate of submerged mussels even at 50% aerial exposure (Gosling 2003).

References

Dinamani, P. (1991). The Pacific oyster, *Crassotrea gigas* (Thunberg, 1793) in New Zealand. In W. Menzel (Ed.), *Estuarine and Marine Bivalve Mollusk Culture* (pp. 315-318.). Florida: CRC Press.

Gosling, E. (1992). The mussel *Mytilus*: ecology, physiology, genetics and culture. *Developments in Aquaculture and Fisheries Science, 25*.

Gosling, E. (2003). *Bivalve Molluscs: Biology, Ecology and Culture Fishing*. Oxford: Fishing News Books.

J.A., N., & P.R., D. (1984). Effects of temperature, nutritional factors and salinity on the uptake of L-methionine by the Sydney rock oyster (*Saccostrea commercialis*). *Marine Biology, 80*, 335–339.

Kailola, P. (1993). *Australian fisheries resources*. Canberra, Australia: Bureau of Resource Sciences and the Fisheries Research and Development Corporation.

Koehn, R. (1991). The genetics and taxonomy of species in the genus *Mytilus*. *Aquaculture, 94*, 125-145.

Lamprell, K., & Healy, J. (1998). *Bivalves of Australia. Volume 2*. Leiden: Backhuys.

Malcolm, W. B. (1971). The Sydney rock oyster. *Australian Natural History*, *17*(2), 45–50.

McDonald, J. H., Seed, R., & Koehn, R. K. (1991). Allozymes and morphometric

characters of 3 species of *Mytilus* in the northern and southern hemispheres. *Marine Biology, 111*(3), 323-333.

Mitchell, I. M., Crawford, C. M., & Rushton, M. J. (2000). Flat oyster (*Ostrea angasi*) growth and survival rates at Georges Bay, Tasmania (Australia). *Aquaculture, 191*(4), 309-321.

Morton, B., Lam, K., & Slack-Smith, S. (2003). First report of the European flat oyster *Ostrea edulis*, identified genetically, from Oyster Harbour, Albany, south-western Western Australia. *Molluscan Research, 23*(3), 199-208.

Nell, J. A. (2001). The history of oyster faming in Australia. *Marine Fisheries Review, 63*(3), 14-25.

Nell, J. A., & Gibbs, P. J. (1986). Salinity tolerance and absorption of L-methionine by some Australian bivalve mollusks. *Australian Journal of Marine and Freshwater Research, 37*(6), 721-727.

Orton, J. H. (1928). On rhythmic periods in shell growth in *Ostrea edulis* with a note on fattening. *Journal of Marine Biology, 15*, 365-427.

Walne, P. R. (1958). Growth of Oysters (Ostrea Edulis L.). *Journal of the Marine Biology Association, 37*, 591-602.

Yearsley, G. K., Last, P. R., & Ward, R. D. (1999). *Australian Seafood Handbook*: CSIRO.

Appendix 3

Late Holocene inter-annual temperature variability reconstructed from the $\delta^{18}O$ of archaeological *Ostrea angasi* shells—published version

Appendix 4

Data tables

Table A4.1. Logger temperature records for Pambula Lake, Little Swanport, and Moreton Bay.

Pambula Lake Date	Pambula Lake surface temperature (°C)	Pambula Lake Date	Pambula Lake bottom temperature (°C)	Little Swanport Date	Little Swanport temperature (°C)	Moreton Bay Date	Moreton Bay temperature (°C)
6/6/06	12.94	6/6/06	13.74	8/9/06	11.46	22/7/06	20.90
7/6/06	13.50	7/6/06	14.32	9/9/06	11.29	23/7/06	17.35
8/6/06	13.62	8/6/06	14.31	10/9/06	11.30	24/7/06	16.07
9/6/06	13.76	9/6/06	14.12	11/9/06	11.57	25/7/06	17.60
10/6/06	14.32	10/6/06	14.65	12/9/06	11.53	26/7/06	16.54
11/6/06	14.36	11/6/06	14.54	13/9/06	12.00	27/7/06	18.31
12/6/06	13.41	12/6/06	13.73	14/9/06	12.30	28/7/06	18.03
13/6/06	13.08	13/6/06	13.40	15/9/06	12.49	29/7/06	18.58
14/6/06	12.92	14/6/06	13.13	16/9/06	12.83	30/7/06	18.04
15/6/06	13.32	15/6/06	13.61	17/9/06	13.29	31/7/06	19.26
16/6/06	13.40	16/6/06	13.74	18/9/06	13.38	1/8/06	20.87
17/6/06	13.64	17/6/06	13.86	19/9/06	13.18	2/8/06	17.64
18/6/06	13.60	18/6/06	13.74	20/9/06	12.97	3/8/06	20.11
19/6/06	13.47	19/6/06	13.51	21/9/06	12.50	4/8/06	20.47
20/6/06	13.51	20/6/06	13.74	22/9/06	12.33	5/8/06	18.76
21/6/06	14.25	21/6/06	14.28	23/9/06	12.05	6/8/06	19.24
22/6/06	14.20	22/6/06	14.43	24/9/06	11.92	7/8/06	18.94
23/6/06	14.20	23/6/06	14.60	25/9/06	11.42	8/8/06	18.13
24/6/06	13.83	24/6/06	14.66	26/9/06	11.55	9/8/06	17.83
25/6/06	13.36	25/6/06	14.05	27/9/06	11.63	10/8/06	18.37
26/6/06	13.55	26/6/06	13.68	28/9/06	11.68	11/8/06	16.61
27/6/06	12.81	27/6/06	13.14	29/9/06	11.83	12/8/06	16.11
28/6/06	12.64	28/6/06	12.79	30/9/06	11.96	13/8/06	17.16
29/6/06	12.68	29/6/06	12.65	1/10/06	12.53	14/8/06	17.65
30/6/06	12.64	30/6/06	12.82	2/10/06	12.89	15/8/06	18.10
1/7/06	12.70	1/7/06	13.01	3/10/06	13.42	16/8/06	17.72
2/7/06	13.03	2/7/06	13.26	4/10/06	13.80	17/8/06	18.96
3/7/06	13.24	3/7/06	13.40	5/10/06	13.39	18/8/06	21.11
4/7/06	13.35	4/7/06	13.51	6/10/06	12.72	19/8/06	20.60
5/7/06	13.30	5/7/06	13.43	7/10/06	13.01	20/8/06	22.59
6/7/06	12.98	6/7/06	13.25	8/10/06	12.79	21/8/06	21.99
7/7/06	12.63	7/7/06	12.80	9/10/06	12.30	22/8/06	21.32
8/7/06	12.67	8/7/06	12.68	10/10/06	12.53	23/8/06	21.24
9/7/06	12.93	9/7/06	13.01	11/10/06	12.93	24/8/06	20.06
10/7/06	12.95	10/7/06	13.01	12/10/06	13.55	25/8/06	19.61
11/7/06	12.97	11/7/06	13.07	13/10/06	13.99	26/8/06	20.41
12/7/06	12.81	12/7/06	12.86	14/10/06	13.65	27/8/06	20.11
13/7/06	12.53	13/7/06	12.52	15/10/06	12.99	28/8/06	19.80
14/7/06	12.64	14/7/06	12.66	16/10/06	13.29	29/8/06	20.19
15/7/06	12.85	15/7/06	13.00	17/10/06	13.85	30/8/06	18.28
16/7/06	12.87	16/7/06	13.01	18/10/06	13.85	31/8/06	18.59
17/7/06	12.70	17/7/06	12.93	19/10/06	13.57	1/9/06	19.26
18/7/06	11.59	18/7/06	11.96	20/10/06	13.56	2/9/06	19.22
19/7/06	10.99	19/7/06	11.63	21/10/06	12.87	3/9/06	21.70
20/7/06	10.60	20/7/06	11.57	22/10/06	12.95	4/9/06	25.05
21/7/06	11.43	21/7/06	12.24	23/10/06	13.28	5/9/06	23.16
22/7/06	11.99	22/7/06	12.89	24/10/06	13.87	6/9/06	21.83
23/7/06	12.60	23/7/06	13.54	25/10/06	13.59	7/9/06	22.01
24/7/06	12.33	24/7/06	13.35	26/10/06	13.02	8/9/06	19.60
25/7/06	13.02	25/7/06	13.60	27/10/06	12.79	9/9/06	17.84
26/7/06	11.68	26/7/06	12.54	28/10/06	11.57	10/9/06	18.31
27/7/06	12.13	27/7/06	12.73	29/10/06	12.11	11/9/06	17.66
28/7/06	12.47	28/7/06	13.27	30/10/06	13.38	12/9/06	16.52

29/7/06	12.39	29/7/06	13.37	31/10/06	13.44	13/9/06	16.58
30/7/06	12.02	30/7/06	13.59	1/11/06	13.97	14/9/06	17.29
31/7/06	11.50	31/7/06	13.98	2/11/06	13.78	15/9/06	17.62
1/8/06	12.16	1/8/06	13.22	3/11/06	14.42	16/9/06	18.10
2/8/06	11.42	2/8/06	13.58	4/11/06	14.63	17/9/06	20.54
3/8/06	12.00	3/8/06	13.56	5/11/06	14.74	18/9/06	23.00
4/8/06	12.53	4/8/06	13.59	6/11/06	14.51	19/9/06	21.65
5/8/06	12.46	5/8/06	13.71	7/11/06	13.99	20/9/06	21.72
6/8/06	12.32	6/8/06	13.40	8/11/06	13.05	21/9/06	21.42
7/8/06	13.31	7/8/06	13.82	9/11/06	13.52	22/9/06	21.37
8/8/06	13.20	8/8/06	13.45	10/11/06	14.36	23/9/06	21.63
9/8/06	13.36	9/8/06	13.62	11/11/06	14.27	24/9/06	21.47
10/8/06	13.48	10/8/06	13.73	12/11/06	14.39	25/9/06	20.75
11/8/06	13.44	11/8/06	13.70	13/11/06	14.05	26/9/06	21.72
12/8/06	13.61	12/8/06	13.72	14/11/06	13.76	27/9/06	21.29
13/8/06	13.77	13/8/06	13.94	15/11/06	13.17	28/9/06	21.23
14/8/06	13.98	14/8/06	14.07	16/11/06	13.17	29/9/06	21.02
15/8/06	14.24	15/8/06	14.23	17/11/06	14.61	30/9/06	21.41
16/8/06	14.32	16/8/06	14.47	18/11/06	15.00	1/10/06	22.48
17/8/06	14.25	17/8/06	14.46	19/11/06	15.01	2/10/06	21.39
18/8/06	14.01	18/8/06	14.12	20/11/06	15.17	3/10/06	23.45
19/8/06	13.94	19/8/06	14.14	21/11/06	15.09	4/10/06	25.00
20/8/06	14.02	20/8/06	14.14	22/11/06	15.12	5/10/06	22.11
21/8/06	14.16	21/8/06	14.14	23/11/06	14.50	6/10/06	21.80
22/8/06	14.21	22/8/06	14.24	24/11/06	14.27	7/10/06	21.97
23/8/06	14.42	23/8/06	14.46	25/11/06	14.64	8/10/06	21.38
24/8/06	14.20	26/8/06	14.06	26/11/06	14.37	9/10/06	21.93
25/8/06	14.10	27/8/06	14.09	27/11/06	15.22	10/10/06	19.28
26/8/06	14.00	28/8/06	14.05	28/11/06	16.31	11/10/06	18.08
27/8/06	13.94	29/8/06	14.38	29/11/06	15.34	12/10/06	19.26
28/8/06	14.05	30/8/06	14.84	30/11/06	15.52	13/10/06	21.09
29/8/06	14.38	31/8/06	15.12	1/12/06	16.17	14/10/06	22.44
30/8/06	14.85	1/9/06	15.79	2/12/06	15.39	15/10/06	22.33
31/8/06	15.18	2/9/06	15.90	3/12/06	15.38	16/10/06	23.64
1/9/06	15.66	3/9/06	15.81	4/12/06	16.02	17/10/06	25.88
2/9/06	15.78	4/9/06	15.20	5/12/06	16.23	18/10/06	21.91
3/9/06	15.83	5/9/06	15.47	6/12/06	15.60	19/10/06	23.82
4/9/06	15.25	6/9/06	15.06	7/12/06	15.68	20/10/06	23.28
5/9/06	15.60	7/9/06	14.73	8/12/06	15.56	21/10/06	22.68
6/9/06	15.11	8/9/06	14.48	9/12/06	16.49	22/10/06	23.52
7/9/06	14.74	9/9/06	14.32	10/12/06	17.20	23/10/06	21.27
8/9/06	14.49	10/9/06	14.31	11/12/06	16.91	24/10/06	19.09
9/9/06	14.32	11/9/06	14.40	12/12/06	16.07	25/10/06	19.77
10/9/06	14.28	12/9/06	14.33	13/12/06	16.55	26/10/06	20.14
11/9/06	14.47	13/9/06	14.65	14/12/06	16.25	27/10/06	21.11
12/9/06	14.70	14/9/06	15.18	15/12/06	16.48	28/10/06	21.92
13/9/06	15.09	15/9/06	15.88	16/12/06	17.40	29/10/06	22.55
14/9/06	15.53	16/9/06	16.52	17/12/06	17.74	30/10/06	21.71
15/9/06	16.09	17/9/06	17.13	18/12/06	17.30	31/10/06	21.39
16/9/06	16.65	18/9/06	16.79	19/12/06	16.34	1/11/06	23.92
17/9/06	17.50	19/9/06	16.86	20/12/06	17.30	2/11/06	24.39
18/9/06	17.06	20/9/06	17.07	21/12/06	17.54	3/11/06	25.04
19/9/06	17.15	21/9/06	16.98	22/12/06	17.56	4/11/06	22.49
20/9/06	17.15	22/9/06	16.56	23/12/06	17.07	5/11/06	21.99
21/9/06	17.01	23/9/06	16.73	24/12/06	16.84	6/11/06	23.23
22/9/06	16.73	24/9/06	16.55	25/12/06	15.70	7/11/06	23.66
23/9/06	16.83	25/9/06	15.96	26/12/06	15.15	8/11/06	22.88
24/9/06	16.54	26/9/06	15.93	27/12/06	16.17	9/11/06	22.48
25/9/06	16.04	27/9/06	16.33	28/12/06	16.47	10/11/06	21.72
26/9/06	16.05	28/9/06	16.33	29/12/06	16.77	11/11/06	21.54

27/9/06	16.47	29/9/06	16.69	30/12/06	17.26	12/11/06	23.15
28/9/06	16.55	30/9/06	16.63	31/12/06	16.76	13/11/06	24.24
29/9/06	16.87	1/10/06	16.56	1/1/07	16.64	14/11/06	25.06
30/9/06	16.84	2/10/06	17.12	2/1/07	17.05	15/11/06	25.77
1/10/06	16.79	3/10/06	17.10	3/1/07	17.65	16/11/06	25.07
2/10/06	17.27	4/10/06	17.57	4/1/07	18.01	17/11/06	20.67
3/10/06	17.51	5/10/06	17.39	5/1/07	17.97	18/11/06	19.05
4/10/06	17.86	6/10/06	17.00	6/1/07	17.42	19/11/06	21.08
5/10/06	17.58	7/10/06	17.11	7/1/07	17.62	20/11/06	22.37
6/10/06	17.18	11/10/06	16.32	8/1/07	16.03	21/11/06	22.27
7/10/06	17.26	12/10/06	17.10	9/1/07	16.69	22/11/06	22.69
8/10/06	17.10	13/10/06	17.95	10/1/07	17.35	23/11/06	22.73
9/10/06	16.90	14/10/06	18.24	11/1/07	17.53	24/11/06	22.66
10/10/06	16.70	15/10/06	17.89	12/1/07	17.76	25/11/06	24.08
11/10/06	16.59	16/10/06	17.28	13/1/07	18.26	26/11/06	23.70
12/10/06	17.54	17/10/06	17.89	14/1/07	19.12	27/11/06	23.87
13/10/06	18.14	18/10/06	18.65	15/1/07	19.95	28/11/06	25.88
14/10/06	18.51	19/10/06	18.81	16/1/07	20.78	29/11/06	25.62
15/10/06	18.01	20/10/06	18.93	17/1/07	20.18	30/11/06	24.26
16/10/06	17.64	21/10/06	17.44	18/1/07	19.48	1/12/06	21.40
17/10/06	18.51	22/10/06	17.07	19/1/07	19.02	2/12/06	25.33
18/10/06	18.82	23/10/06	17.28	20/1/07	18.93	3/12/06	25.09
19/10/06	18.95	24/10/06	17.71	21/1/07	18.90	4/12/06	25.98
20/10/06	19.03	25/10/06	17.51	22/1/07	18.48	5/12/06	22.21
21/10/06	17.64	26/10/06	17.19	23/1/07	18.95	6/12/06	21.87
22/10/06	17.12	27/10/06	17.66	24/1/07	19.01	7/12/06	21.20
23/10/06	17.37	28/10/06	16.88	25/1/07	18.85	8/12/06	21.69
24/10/06	17.86	29/10/06	16.71	26/1/07	18.78	9/12/06	23.49
25/10/06	17.78	30/10/06	17.68	27/1/07	17.94	10/12/06	22.64
26/10/06	16.72	31/10/06	18.70	28/1/07	17.24	11/12/06	23.95
27/10/06	17.44	1/11/06	19.12	29/1/07	16.94	12/12/06	23.68
28/10/06	17.02	2/11/06	18.73	30/1/07	16.94	13/12/06	24.62
29/10/06	16.97	3/11/06	18.31	31/1/07	16.67	14/12/06	25.62
30/10/06	17.88	4/11/06	18.46	1/2/07	17.74	15/12/06	24.75
31/10/06	18.91	5/11/06	18.12	2/2/07	18.59	16/12/06	25.83
1/11/06	19.42	6/11/06	17.78	3/2/07	18.86	17/12/06	25.50
2/11/06	18.55	7/11/06	17.48	4/2/07	19.26	18/12/06	22.77
3/11/06	18.28	8/11/06	16.80	5/2/07	19.04	19/12/06	22.82
4/11/06	18.45	9/11/06	17.14	6/2/07	18.91	20/12/06	23.24
5/11/06	18.23	10/11/06	17.79	7/2/07	19.17	21/12/06	23.40
6/11/06	17.84	11/11/06	18.85	8/2/07	19.60	22/12/06	23.94
7/11/06	17.53	12/11/06	19.32	9/2/07	19.54	23/12/06	23.25
8/11/06	17.16	13/11/06	18.90	10/2/07	19.34	24/12/06	23.12
9/11/06	17.13	14/11/06	18.25	11/2/07	19.26	25/12/06	22.84
10/11/06	18.07	15/11/06	17.58	12/2/07	18.79	26/12/06	24.00
11/11/06	18.99	16/11/06	16.79	13/2/07	19.49	27/12/06	22.54
12/11/06	19.51	17/11/06	17.12	14/2/07	20.10	28/12/06	20.27
13/11/06	18.37	18/11/06	18.01	15/2/07	21.04	29/12/06	20.49
14/11/06	18.14	19/11/06	19.23	16/2/07	21.22	30/12/06	23.16
15/11/06	17.65	20/11/06	19.67	17/2/07	21.17	31/12/06	24.22
16/11/06	16.81	21/11/06	20.07	18/2/07	21.22	1/1/07	24.33
17/11/06	17.36	22/11/06	20.28	19/2/07	20.73	2/1/07	25.02
18/11/06	18.43	23/11/06	20.46	20/2/07	20.05	3/1/07	24.16
19/11/06	19.49	24/11/06	20.39	21/2/07	19.75	4/1/07	22.76
20/11/06	19.70	25/11/06	20.78	22/2/07	19.79	5/1/07	22.06
21/11/06	20.23	26/11/06	20.43	23/2/07	20.13	6/1/07	22.75
22/11/06	20.58	27/11/06	20.52	24/2/07	19.96	7/1/07	23.21
23/11/06	20.14	28/11/06	21.51	25/2/07	20.39	8/1/07	24.22
24/11/06	20.67	29/11/06	18.93	26/2/07	20.81	9/1/07	25.34
25/11/06	21.08	1/12/06	19.22	27/2/07	20.44	10/1/07	24.62

26/11/06	20.38	2/12/06	19.92	28/2/07	20.29	11/1/07	24.11
27/11/06	20.77	3/12/06	19.72	1/3/07	20.09	12/1/07	26.15
28/11/06	21.81	4/12/06	20.18	2/3/07	20.14	13/1/07	25.75
29/11/06	21.59	5/12/06	20.20	3/3/07	20.41	14/1/07	26.23
30/11/06	20.50	6/12/06	20.27	4/3/07	19.99	15/1/07	26.45
1/12/06	19.59	7/12/06	20.35	5/3/07	19.13	16/1/07	27.24
2/12/06	20.05	8/12/06	20.25	6/3/07	18.05	17/1/07	27.19
3/12/06	19.80	9/12/06	20.76	7/3/07	17.85	18/1/07	26.06
4/12/06	20.04	10/12/06	21.63	8/3/07	17.83	19/1/07	25.77
5/12/06	20.22	11/12/06	21.64	9/3/07	17.52	20/1/07	25.01
6/12/06	20.57	12/12/06	20.80	10/3/07	18.15	21/1/07	25.05
7/12/06	20.63	13/12/06	20.68	11/3/07	18.56	22/1/07	25.67
8/12/06	20.57	14/12/06	21.55	12/3/07	17.67	23/1/07	26.39
9/12/06	20.96	15/12/06	21.25	13/3/07	17.87	24/1/07	26.78
10/12/06	21.84	16/12/06	20.46	14/3/07	18.28	25/1/07	27.05
11/12/06	21.96	17/12/06	20.44	15/3/07	18.62	26/1/07	26.55
12/12/06	20.93	18/12/06	20.92	16/3/07	18.77	27/1/07	28.08
13/12/06	21.02	19/12/06	20.70	17/3/07	18.13	28/1/07	28.01
14/12/06	22.11	20/12/06	19.84	18/3/07	17.86	29/1/07	27.68
15/12/06	21.30	21/12/06	20.03	19/3/07	17.88	30/1/07	29.40
16/12/06	20.49	22/12/06	20.32	20/3/07	18.14	31/1/07	29.96
17/12/06	20.68	23/12/06	19.74	21/3/07	18.35	1/2/07	28.54
18/12/06	20.88	24/12/06	18.70	22/3/07	18.95	2/2/07	26.64
19/12/06	20.83	25/12/06	17.84	23/3/07	19.08	3/2/07	25.29
20/12/06	19.99	26/12/06	17.19	24/3/07	18.24	4/2/07	24.75
21/12/06	19.98	27/12/06	18.11	25/3/07	17.79	5/2/07	25.40
22/12/06	20.35	28/12/06	18.41	26/3/07	17.97	6/2/07	24.24
23/12/06	19.97	29/12/06	18.54	27/3/07	17.91	7/2/07	25.89
24/12/06	18.96	30/12/06	18.37	28/3/07	17.78	8/2/07	25.78
25/12/06	18.12	31/12/06	19.04	29/3/07	17.78	9/2/07	26.71
26/12/06	17.26	1/1/07	19.40	30/3/07	17.21	10/2/07	26.89
27/12/06	18.21	2/1/07	19.06	31/3/07	16.88	11/2/07	26.86
28/12/06	18.50	3/1/07	19.58	1/4/07	17.30	12/2/07	27.45
29/12/06	18.52	4/1/07	19.73	2/4/07	17.07	13/2/07	27.63
30/12/06	18.40	5/1/07	19.42	3/4/07	16.61	14/2/07	24.37
31/12/06	18.95	6/1/07	19.44	4/4/07	16.52	15/2/07	26.21
1/1/07	19.32	7/1/07	19.41	5/4/07	16.32	16/2/07	25.69
2/1/07	19.09	8/1/07	18.57	6/4/07	15.59	17/2/07	24.61
3/1/07	19.63	9/1/07	19.38	7/4/07	16.01	18/2/07	23.45
4/1/07	19.95	10/1/07	20.12	8/4/07	16.11	19/2/07	24.32
5/1/07	19.76	11/1/07	21.29	9/4/07	16.85	20/2/07	24.85
6/1/07	19.88	12/1/07	22.11	10/4/07	16.72	21/2/07	24.62
7/1/07	19.77	13/1/07	21.95	11/4/07	16.41	22/2/07	24.42
8/1/07	18.88	14/1/07	21.98	12/4/07	16.30	23/2/07	24.62
9/1/07	19.65	15/1/07	22.10	13/4/07	16.56	24/2/07	24.97
10/1/07	20.41	16/1/07	22.90	14/4/07	16.77	25/2/07	25.86
11/1/07	21.81	17/1/07	23.15	15/4/07	16.96	26/2/07	27.26
12/1/07	22.28	18/1/07	22.73	16/4/07	16.97	27/2/07	27.24
13/1/07	22.05	19/1/07	22.29	17/4/07	16.61	28/2/07	27.90
14/1/07	22.33	20/1/07	22.07	18/4/07	16.44	1/3/07	27.58
15/1/07	22.73	21/1/07	21.27	19/4/07	16.27	2/3/07	27.16
16/1/07	23.16	22/1/07	20.43	20/4/07	16.34	3/3/07	27.17
17/1/07	23.15	23/1/07	20.89	21/4/07	16.68	4/3/07	27.55
18/1/07	22.91	24/1/07	21.38	22/4/07	16.56	5/3/07	26.90
19/1/07	22.44	25/1/07	21.06	23/4/07	16.06	6/3/07	27.26
20/1/07	22.38	26/1/07	22.36	24/4/07	15.32	7/3/07	24.90
21/1/07	21.58	27/1/07	21.89	25/4/07	15.05	8/3/07	24.60
22/1/07	20.77	28/1/07	21.23	26/4/07	15.13	9/3/07	26.04
23/1/07	21.21	29/1/07	21.24	27/4/07	14.88	10/3/07	26.86
24/1/07	21.66	30/1/07	21.41	28/4/07	14.80	11/3/07	26.78

25/1/07	22.07	31/1/07	21.64	29/4/07	15.08	12/3/07	27.83
26/1/07	22.76	1/2/07	20.67	30/4/07	15.43	13/3/07	28.92
27/1/07	22.07	2/2/07	21.72	1/5/07	15.64	14/3/07	26.67
28/1/07	21.50	3/2/07	22.27	2/5/07	15.59	15/3/07	24.90
29/1/07	21.32	4/2/07	22.41	3/5/07	15.54	16/3/07	25.71
30/1/07	21.72	5/2/07	22.75	4/5/07	15.29	17/3/07	27.45
31/1/07	21.69	6/2/07	22.48	5/5/07	14.95	18/3/07	26.10
1/2/07	20.87	7/2/07	22.38	6/5/07	14.58	19/3/07	25.52
2/2/07	21.69	8/2/07	22.31	7/5/07	14.41	20/3/07	25.15
3/2/07	22.46	9/2/07	22.73	8/5/07	14.70	21/3/07	25.55
4/2/07	22.60	10/2/07	23.03	9/5/07	14.45	22/3/07	26.24
5/2/07	22.82	11/2/07	23.14	10/5/07	14.34	23/3/07	25.24
6/2/07	22.82	12/2/07	23.37	11/5/07	14.52	24/3/07	25.73
7/2/07	22.56	13/2/07	24.44	12/5/07	14.83	25/3/07	26.83
8/2/07	22.45	14/2/07	24.68	13/5/07	14.93	26/3/07	25.52
9/2/07	22.89	15/2/07	24.61	14/5/07	14.85	27/3/07	23.08
10/2/07	23.08	16/2/07	23.98	15/5/07	14.86	28/3/07	23.13
11/2/07	22.98	17/2/07	23.49	16/5/07	14.94	29/3/07	23.84
12/2/07	22.92	18/2/07	22.82	17/5/07	15.08	30/3/07	26.30
13/2/07	23.74	19/2/07	21.86	18/5/07	15.18	31/3/07	26.92
14/2/07	24.08	20/2/07	21.30	19/5/07	15.28	1/4/07	25.17
15/2/07	24.50	21/2/07	21.04	20/5/07	14.89	2/4/07	22.00
16/2/07	24.33	22/2/07	21.18	21/5/07	14.58	3/4/07	23.31
17/2/07	24.06	23/2/07	21.40	22/5/07	14.14	4/4/07	23.47
18/2/07	23.08	24/2/07	21.30	23/5/07	13.89	5/4/07	23.78
19/2/07	22.50	25/2/07	20.20	24/5/07	13.87	6/4/07	23.77
20/2/07	21.70	26/2/07	21.62	25/5/07	13.53	7/4/07	23.49
21/2/07	21.85	27/2/07	20.91	26/5/07	13.76	8/4/07	22.48
22/2/07	21.98	28/2/07	21.02	27/5/07	13.67	9/4/07	22.10
23/2/07	22.09	1/3/07	21.55	28/5/07	13.71	10/4/07	22.49
24/2/07	21.64	2/3/07	22.19	29/5/07	14.11	11/4/07	22.19
25/2/07	20.36	3/3/07	22.93	30/5/07	13.45	12/4/07	22.17
26/2/07	21.55	4/3/07	23.00	31/5/07	13.14	13/4/07	23.47
27/2/07	20.74	5/3/07	21.68	1/6/07	12.23	14/4/07	22.99
28/2/07	20.51	6/3/07	20.30	2/6/07	12.09	15/4/07	22.87
1/3/07	21.78	7/3/07	20.88	3/6/07	12.37	16/4/07	22.71
2/3/07	22.60	8/3/07	20.92	4/6/07	12.28	17/4/07	22.61
3/3/07	23.59	9/3/07	20.25	5/6/07	12.16	18/4/07	22.44
4/3/07	23.43	10/3/07	20.60	6/6/07	11.98	19/4/07	23.09
5/3/07	21.54	11/3/07	21.45	7/6/07	11.63	20/4/07	23.44
6/3/07	20.01	12/3/07	21.48	8/6/07	11.66	21/4/07	23.49
7/3/07	20.78	13/3/07	21.72	9/6/07	11.82	22/4/07	23.57
8/3/07	20.87	14/3/07	22.06	10/6/07	11.72	23/4/07	24.55
9/3/07	20.20	15/3/07	22.80	11/6/07	11.80	24/4/07	24.73
10/3/07	20.53	16/3/07	23.35	12/6/07	11.47	25/4/07	24.85
11/3/07	21.45	17/3/07	22.51	13/6/07	11.29	26/4/07	25.34
12/3/07	21.35	18/3/07	21.67	14/6/07	11.14	27/4/07	25.53
13/3/07	21.67	19/3/07	21.50	15/6/07	11.29	28/4/07	25.43
14/3/07	22.13	20/3/07	21.44	16/6/07	11.33	29/4/07	23.28
15/3/07	22.74	21/3/07	21.44	17/6/07	11.61	30/4/07	24.12
16/3/07	23.23	22/3/07	21.91	18/6/07	10.80	1/5/07	22.77
17/3/07	22.45	23/3/07	22.74	19/6/07	10.74	2/5/07	22.27
18/3/07	21.75	24/3/07	22.31	20/6/07	10.62	3/5/07	23.01
19/3/07	21.57	25/3/07	20.20	21/6/07	10.21	4/5/07	22.97
20/3/07	21.52	26/3/07	20.08	22/6/07	9.93	5/5/07	23.37
21/3/07	21.54	27/3/07	20.95	23/6/07	9.50	6/5/07	23.69
22/3/07	22.09	28/3/07	20.96	24/6/07	9.47	7/5/07	23.16
23/3/07	23.00	29/3/07	20.82	25/6/07	9.70	8/5/07	22.94
24/3/07	22.45	30/3/07	20.40	26/6/07	10.12	9/5/07	24.16
25/3/07	20.30	31/3/07	17.39	27/6/07	10.91	10/5/07	23.69

26/3/07	20.01	2/4/07	20.19	28/6/07	11.13	11/5/07	22.41
27/3/07	21.12	3/4/07	20.05	29/6/07	11.05	12/5/07	22.86
28/3/07	21.11	4/4/07	19.82	30/6/07	10.87	13/5/07	21.98
29/3/07	20.78	5/4/07	19.65	1/7/07	10.57	14/5/07	22.56
30/3/07	20.34	6/4/07	19.05	2/7/07	10.65	15/5/07	22.83
31/3/07	20.20	7/4/07	18.98	3/7/07	10.97	16/5/07	22.49
1/4/07	20.10	10/4/07	19.37	4/7/07	11.15	17/5/07	23.06
2/4/07	20.18	11/4/07	19.76	5/7/07	11.34	18/5/07	22.81
3/4/07	20.12	12/4/07	20.08	6/7/07	11.16	19/5/07	22.06
4/4/07	19.94	13/4/07	20.29	7/7/07	11.21	20/5/07	22.26
5/4/07	19.74	14/4/07	20.25	8/7/07	11.05	21/5/07	20.24
6/4/07	19.23	15/4/07	20.44	9/7/07	11.18	22/5/07	21.33
7/4/07	19.06	16/4/07	20.27	10/7/07	11.24	23/5/07	21.07
8/4/07	19.20	17/4/07	20.02	11/7/07	11.57	24/5/07	20.07
9/4/07	19.60	18/4/07	20.20	12/7/07	11.63	25/5/07	22.05
10/4/07	19.82	19/4/07	20.08	13/7/07	11.31	26/5/07	22.21
11/4/07	19.67	20/4/07	19.83	14/7/07	10.98	27/5/07	22.63
12/4/07	20.22	21/4/07	19.63	15/7/07	10.57	28/5/07	22.75
13/4/07	20.40	22/4/07	19.50	16/7/07	10.51	29/5/07	22.89
14/4/07	20.26	23/4/07	19.15	17/7/07	10.92	30/5/07	23.16
15/4/07	20.57	24/4/07	18.89	18/7/07	10.04	31/5/07	23.73
16/4/07	20.32	25/4/07	18.74	19/7/07	9.48	1/6/07	23.32
17/4/07	20.11	26/4/07	18.51	20/7/07	9.38	2/6/07	21.62
18/4/07	20.25	27/4/07	18.52	21/7/07	9.47	3/6/07	20.28
19/4/07	20.18	28/4/07	18.28	22/7/07	9.56	4/6/07	19.95
20/4/07	19.97	29/4/07	18.67	23/7/07	9.85	5/6/07	21.14
21/4/07	19.77	30/4/07	18.77			6/6/07	20.11
22/4/07	19.54	1/5/07	18.90			7/6/07	19.08
23/4/07	19.20	2/5/07	18.52			8/6/07	19.60
24/4/07	18.87	3/5/07	18.33			9/6/07	18.13
25/4/07	18.79	4/5/07	18.51			10/6/07	16.53
26/4/07	18.57	5/5/07	18.32			11/6/07	18.65
27/4/07	18.58	6/5/07	18.16			12/6/07	20.07
28/4/07	18.15	7/5/07	18.38			13/6/07	18.66
29/4/07	18.59	8/5/07	18.41			14/6/07	17.16
30/4/07	18.73	9/5/07	18.10			15/6/07	16.90
1/5/07	18.90	10/5/07	17.60			16/6/07	17.78
2/5/07	18.53	13/5/07	17.30			17/6/07	15.65
3/5/07	18.39	14/5/07	17.24			18/6/07	15.46
4/5/07	18.52	15/5/07	17.21			19/6/07	16.89
5/5/07	18.33	16/5/07	17.24			20/6/07	16.24
6/5/07	18.26	17/5/07	17.40			21/6/07	13.83
7/5/07	18.39	18/5/07	17.49			22/6/07	14.43
8/5/07	18.44	19/5/07	17.24			23/6/07	13.97
9/5/07	18.12	20/5/07	16.82			24/6/07	14.37
10/5/07	17.65	21/5/07	16.74			25/6/07	15.96
11/5/07	17.50	22/5/07	16.37			26/6/07	17.52
12/5/07	17.40	23/5/07	15.89			27/6/07	17.05
13/5/07	17.39	24/5/07	15.82			28/6/07	15.30
14/5/07	17.41	25/5/07	15.69			29/6/07	15.13
15/5/07	17.40	26/5/07	15.66			30/6/07	14.95
16/5/07	17.32	27/5/07	15.52			1/7/07	15.76
17/5/07	17.43	28/5/07	15.39			2/7/07	16.16
18/5/07	17.51	29/5/07	15.63			3/7/07	15.68
19/5/07	17.26	30/5/07	15.68			4/7/07	16.73
20/5/07	16.97	31/5/07	15.07			5/7/07	16.70
21/5/07	16.82	1/6/07	14.89			6/7/07	15.63
22/5/07	16.42	2/6/07	14.87			7/7/07	13.70
23/5/07	15.91	3/6/07	14.68			8/7/07	13.77
24/5/07	15.86	4/6/07	14.66			9/7/07	14.98

25/5/07	15.76	5/6/07	14.51	10/7/07	13.93
26/5/07	15.82	6/6/07	14.24	11/7/07	16.50
27/5/07	15.68	7/6/07	14.23	12/7/07	16.46
28/5/07	15.46	8/6/07	14.25	13/7/07	17.00
29/5/07	15.81	9/6/07	14.77	14/7/07	15.34
30/5/07	15.69	10/6/07	14.96	15/7/07	14.22
31/5/07	15.19	11/6/07	14.82	16/7/07	13.20
1/6/07	14.99	12/6/07	14.53	17/7/07	13.16
2/6/07	14.95	13/6/07	14.09	18/7/07	13.53
3/6/07	14.85	14/6/07	13.86	19/7/07	12.98
4/6/07	14.79	15/6/07	13.96	20/7/07	11.12
5/6/07	14.57	16/6/07	14.28	21/7/07	11.55
6/6/07	14.37	17/6/07	14.47	22/7/07	14.16
7/6/07	14.33	18/6/07	14.58	23/7/07	16.02
8/6/07	14.33	19/6/07	14.17	24/7/07	16.10
9/6/07	14.98	20/6/07	13.73	25/7/07	18.40
10/6/07	15.08	21/6/07	13.09	26/7/07	17.81
11/6/07	14.89	22/6/07	12.77	27/7/07	18.70
12/6/07	14.62	23/6/07	13.09	28/7/07	18.34
13/6/07	14.28	24/6/07	13.14	29/7/07	17.81
14/6/07	13.89	25/6/07	13.36	30/7/07	16.18
15/6/07	13.89	26/6/07	13.78	31/7/07	15.53
16/6/07	13.37	27/6/07	11.97	1/8/07	15.91
17/6/07	13.59	28/6/07	11.93	2/8/07	16.21
18/6/07	13.94	29/6/07	12.78	3/8/07	17.53
19/6/07	13.62	30/6/07	12.99	4/8/07	17.63
20/6/07	12.07	1/7/07	12.93	5/8/07	15.92
21/6/07	11.50	2/7/07	13.46	6/8/07	13.79
22/6/07	11.10	3/7/07	13.97	7/8/07	14.52
23/6/07	11.47	4/7/07	14.45	8/8/07	16.08
24/6/07	11.70	5/7/07	14.54	9/8/07	18.57
25/6/07	11.50	6/7/07	14.06	10/8/07	18.55
26/6/07	12.69	7/7/07	14.35	11/8/07	19.39
27/6/07	11.32	8/7/07	13.91	12/8/07	18.25
28/6/07	11.74			13/8/07	15.56
29/6/07	12.06			14/8/07	14.86
30/6/07	11.57			15/8/07	12.22
1/7/07	10.86			16/8/07	17.21
2/7/07	11.52			17/8/07	19.38
3/7/07	12.49				
4/7/07	13.25				
5/7/07	13.05				
6/7/07	13.07				
7/7/07	13.30				
8/7/07	13.01				

Table A4.2. Pambula Lake growth records for *Ostrea angasi*, *Saccostrea glomerata* and *Mytilus galloprovincialis*.

***Ostrea angasi*: length (mm)**

PLOa \ Date	02-Jun-06	08-Jul-06	25-Aug-06	09-Oct-06	30-Nov-06	26-Jan-07	09-Apr-07	11-May-07	09-Jul-07
401	55.5	61.1	63.0	69.8	81.5	85.4	85.5	93.5	101
402	54.5	62.7	63.0	65.5	69.8	76.7	80	82	90.9
403	52.0	58.4	61.0	62.6	69.4	81.7	80.4	78.5	83.7
404	44.0	54.6	55.0	58.2	68.6	75.5	76.5	82.5	92
405	50.6	54.4	58.0	71.5	79.5	84.8	90.9	97	104.3
406	53.5	57.1	60.0	70.5	75.5	86.0	81.5	89	94.9
407	52.8	60.9	63.0	71.2	71.7	81.1	80.9	83	85.1
408	50.2	57.6	57.5	63.3	67.4	77.0	75.6	77.5	86
409	57.1	62.3	63.5	67.3	72.1	81.4	81.4	84.5	92.8
410	53.9	63.3	63.0	67.8	69.0	80.3	83.3	86	88.2
411	48.9	58.1	58.0	66.2	71.9	83.2	81.5	81	90.5
412	49.2	57.6	58.0	64.4	68.6	78.3	78.1	78	86.1
413	52.8	59.7	63.0	68.5	72.5	85.0	86.6	91.5	102.8
414	52.2	60.5	61.0	71.2	76.0	87.1	86.3	89.5	94.9
415	56.8	61.9	64.0	73.9	78.7	82.7	85	85	87
416	54.3	63.8	64.0	76.8	80.3	85.2	82.2	94	88.3
417	49.7	55.1	55.0	60.9	70.3	82.2	85.8	91	95.8
418	54.5	57.2	62.5	66.1	72.8	80.5	86.4	92.5	98.5
419	56.3		60.5	64.2	68.1	85.4	82.4	87.5	94.4
420	51.4	58.7	61.0	62.2	71.1	77.7	84.3	91.5	91.5
421	51.9	57.5	62.0	69.1	76.0	83.6	83.7	82	98.2

422	54.3	62.7	64.0	78.5	80.1	93.1	91.4	95	95.1
423	49.7	54.4	58.0	61.7	70.3	78.4			
424	53.9	58.4	60.5	65.9	70.8	80.2	82.9	82	83.3
425	50.6	57.9	59.0	57.7	66.3	78.8	82.2	90	90.9
426	48.6	55.4	56.0	63.5	61.4	64.0	65.8	66	95.6
427	54.2	58.5	61.0	72.8	71.9	87.2			
428	48.0	54.1	58.0	66.2	60.9	76.7			
429	53.8	57.8	60.5	63.6	66.2	76.7			
430	46.8	52.7	53.5	54.6	63.1	70.4	79.6	88	87
431	60.9	65.1	65.5	69.9	73.5	80.5	82.9	91	92.1
432	56.6	61.8	67.0	71.7	81.1	87.6	89.7	94	100
433	62.7	73.8	73.5	80.1		94.9	98.1	104.5	106
434	65.3	72.6	74.5	82.6	90.9	96.3	95.6	102	98.4
435	58.1	61.5	63.5	72.5	78.2	78.3	79.5	79.5	84.4
436	63.1	68.6	72.0	80.7	83.5	88.4	85.7	90.5	93.5
437	56.1	63.7	65.0	68.3	80.3	79.3	80.2	83.5	84.8
438	60.3	67.4	69.5	77.7	79.7	81.7	82.2	91	99.7
439	61.9	66.2	66.0	76.2	79.1	89.4	87.1	100	103
440	64.3	69.7	71.0	75.7	76.8	82.1	87	90.5	89.3
441	62.3	68.6	69.0	75.0	76.8	85.8	85.8	86	91
442	62.7	69.6	69.0	73.0	74.9	86.1	83.3	89.5	98.8
443	63.0		74.0	78.2	81.5	89.1	89.4	89	88.3
444	63.8	71.7	73.0	79.9	80.5	92.7	87.7	91	91.8
445	63.8	71.3	74.0	85.7	84.6	95.7	98	97	99.3
446	62.3	66.7	67.0	70.7	68.5	80.5	80.2	85.5	93.4
447	61.1	65.7	67.0	74.8	76.1	84.6	84.9	85.5	83.7
448	57.2	59.6	65.0	71.5	78.5	82.5	86.9	89	91
449	61.3	66.6	68.5	75.3	82.2	86.0	86.1	89	97

450	64.2	67.7	72.0	78.0	82.7	87.2	87.9	89.5	99.1
451	60.2	66.2	67.0	74.4	72.2	84.5	83.5	87.5	87.3
452	62.0	66.3	68.0	73.5	76.8	76.7	83.6	88.5	91.4
453	58.3	64.6	68.5	70.5	87.3	76.0			
454	59.5	65.3	65.5	70.9		84.5	87.2	93	92.4
455	62.9	71.1	72.5	85.5		88.1	89.9	97	100
456	56.5	63.1	69.0	78.3	79.8	90.0			
457	57.8	63.6	65.0	74.5	74.8	85.5	87.3	94	90.1
458	57.2	63.1	69.0	78.0	81.2	87.5	90.7	97	98.2
459	59.4	62.9	63.0	70.4	71.7	83.1			
460	58.9	62.5	64.0	69.2	70.2	76.7	79.1	88	89.5
461	69.4	76.4	77.0	81.7	89.9	95.9	90.7	95	105.3
462	70.3	76.6	78.0	77.6	86.6	93.3	86.6	95.5	101.7
463	67.4	67.8	74.0	80.4		91.0	92.4	95	99.7
464	67.1	71.2	72.5	76.2	76.3	77.9	79.4	87	91.8
465	66.0	6837.0	71.5	71.8	76.1	82.5	81.9	82.5	83.2
466	69.8	73.3	74.0	81.7	81.5	87.9		87.5	86.2
467	68.9	72.6	75.0	74.2	84.9	84.9	88.6	99	99.4
468	67.9	72.6	73.0	79.9		89.1	95.7	95.5	100.3
469	82.9	92.0	93.5	92.7	101.4	103.4	105	105	107.5
470	77.4	82.1	82.0	89.7	92.7	103.7	100.4	97	96.7
471	70.1	76.2	77.5	76.5	86.2	87.4	88.8	96	93.5
472	71.0	74.6	80.5	88.1	88.6	91.1	94.1	97	95.3
473	68.8	75.8	76.5	83.6	85.3	88.9	90.2	97	105.1
474	64.3	72.7	73.5	85.4	84.4	93.1	90.7	99	105.9
475	76.3	84.0	86.0	90.2	90.4	92.5	95.9	101	104.5
476	73.5	79.6	80.0	79.2	82.8	90.9	93.3	97	95.7
477	75.2	84.9	84.5	83.5	93.5	96.3	98.6	99	101.4

478	66.1	73.8	79.5	79.3	85.5	92.7	93.5	96	98.1
479	75.7	80.7	82.0	87.4	88.7	93.7	94.1	102	101
480	80.4	85.7	87.5	89.5	98.9	106.8			
481	72.5	79.1	82.5	84.2	89.8	89.5	91.3	93.5	94.5
482	68.1	72.3	76.0	75.5	82.7	83.7			
483	69.2	74.5	75.5	74.7	78.7	87.2	90.5	91	96.3
484	68.5	76.0	78.5	87.5	90.0	102.7	95.3	109	111.4
485	64.9								
486	69.5	72.7	75.0	74.9	79.1	88.3			
487	68.4	76.8	76.0	76.7	88.1	87.9	90.5	93.5	97.3
488	67.1	76.3	76.0	79.8	80.7	88.4	88.1		94.5
489	64.7	68.0	68.5	77.3	82.5	93.7	86.6	88	96
490	72.2	79.5	79.0	86.9	87.7	87.8			
491	88.2	93.5	95.0	97.4	103.0	113.1	111	112	114.3
492	80.5	91.7	92.0	93.2	93.1	92.8	90.2	91.5	96.6
493	88.8	93.8	94.0	98.5	102.6	105.2	105.4	110	113.9
494	86.1	91.1	95.0	100.2	100.3	106.7	107.3	112	111.7
495	88.3	95.1	95.5	95.4	100.1	104.1	103	102	113.7
496	83.5	86.3	90.0	94.0	94.0	97.0	97.8	101.2	100.1
497	83.0	87.5	90.0	92.0	93.7	96.7	93.9	97.5	103.9
498	90.2	92.1	92.5	97.3	100.6	108.4	107.4	105	105.8
499	84.4	93.0	95.0	94.0	96.4	105.6	100.3	101	110
500	91.0	98.9	104.0	109.3	106.1	108.3	105.6	113.5	117.9
501	89.9	96.4	97.5	101.4	111.3	110.9	104.3	107.5	109.2
502	78.2	81.3	84.0	85.9	83.1	93.2	92	93	90.9
503	85.0	88.3	89.0	91.0	94.6	97.2	95.7	97	103.4
504	87.0	94.2	95.0	94.6	99.0	100.5	101	101	106.2
505	81.1	84.2	87.5	89.5	95.6	96.0	96.6	96.5	99.9

506	87.0	87.2	95.0	100.6	108.5	112.8	111.3	110	113
507	87.9	97.5	97.5	106.3					
508	82.2	84.1	88.0	90.8	92.6	104.8	98.5	96.5	101.4
509	88.9	97.8	97.5	96.6	107.6	106.0	105.9	104.5	110.6
510	86.0	92.4	93.5	93.6	97.6	98.1	98	99	104
511	82.4	84.4	84.5	84.6	90.8	96.7	102.2	dead	
512	91.2	96.7	97.5	100.6	103.4	103.4	102.3	107	112.1
513	78.8	86.5	87.5	88.8	88.4	92.4	94.9	94.9	98
514	81.9	89.4	91.5	96.7	98.2	103.5	99.6	103	101.7
515	93.0	100.4	101.0	106.5					
516	83.9	89.2	92.0	98.2	97.8	97.9	97.2	100.5	107.6
517	83.1	88.4	88.5	96.4	94.5	96.8			
518	86.2	93.8	94.0	100.4	102.5	108.6			107.6
519	87.6	90.3	91.5	95.6	96.1	97.1			
520	83.5	90.2	92.5	97.4	95.2	96.8	94.9	96	101.7

***Saccostrea glomerata*: length (mm)**

PLSg \ Date	04-Jun-06	08-Jul-06	25-Aug-06	09-Oct-06	30-Nov-06	26-Jan-07	01-Apr-07	11-May-07	09-Jul-07
201	55.8	55.9	55.5	55.9	56.9	58.4	62.2	66	67.3
202	58.1	dead							
203	61.8	62.5	62.5	61.7	61.7	62.3			
204	48.9	49.1	50.0	49.9	51.1	56.9	62.9	64.5	64.5
205	50.8	51.8	57.0	52.2	55.0	61.6	72.7	78.5	80.3
206	59.6	58.6	58.0	57.9	61.1	61.9	62.8	69	70.9
207	47.6	48.3	48.0	47.6	48.6	52.6	61.2	70	69.9
208	52.0	50.9	51.5	51.4	52.7	55.2			
209	54.4	55.2	54.0	55.4	55.1	57.7	61.2	67	67.5
210	54.2	53.5	54.0	53.6	56.5	61.3	69.8	73	75.7
211	56.5	56.7	57.0	55.4	55.4	54.7			
212	58.7	56.6	58.5	59.2	61.3	62.2	65.6	71	72.3
213	56.0	56.0	57.0	56.7	58.8	62.2	68	73.5	74.9
214	56.1	56.0	58.5	55.5	55.1	55.5	57.8	62	63.7
215	49.9	49.2	49.0	48.5	49.2	51.9	60.6	65	63.5
216	64.4	63.6	65.5	64.1	64.3	69.5	75.5		
217	46.9	44.9	45.0	46.0	47.7	50.9	57.7	65	64.7
218	50.1	49.1	49.0	58.4	52.2	56.1			
219	51.0	51.0	51.0	50.7	50.8	52.1			
220	48.4	50.3	50.5	50.8	52.9	54.6	58.7		61.2
221	45.0	46.1	46.0	46.2	44.5	46.9	48.4	44	
222	41.6	41.5	43.0	dead					
223	47.2	48.4	48.0	46.9	47.2	47.4	46.4		46.5

224	50.4	50.8	50.5	49.1	49.3	49.2	47.2	47	47.7
225	45.6	45.0	45.5	45.9	45.9	46.2	46.3	49.5	51.2
226	49.0	49.5	49.5	49.5	49.2	49.9	49.9	53	50.9
227	41.2	41.6	41.5	42.3	40.6	39.2			
228	41.3	42.0	41.5	41.6	41.5	40.4	40.5		
229	50.5	49.0	49.5	49.1	47.9	49.5	dead		
230	45.2	45.4	46.5	45.8	45.5	45.2		45	dead
231	42.1	42.0	dead						
232	52.0	dead							
233	46.7	47.2	47.0	dead					
234	40.3	40.8	40.5	40.7	dead				
235	40.2	39.4	40.5	40.1	40.1	39.6	40.9	42	
236	45.1	45.2							
237	38.5	39.3	39.0	38.8	38.9	38.2			
238	47.2	47.9	47.5	46.8	46.4	45.8	46.3	47	48.6
239	37.0	38.8	38.0	37.2	38.3	39.3			
240	38.2	39.4	38.5	38.5	38.6	39.6		38.5	
241	71.7	71.5	71.0	70.8	70.8	dead			
242	62.1	62.3	62.5	61.8	61.9	61.8	66.4	70	68
243	66.2	66.4	67.0	66.4	66.9	69.7	70.6	75	75.3
244	59.5	57.8	58.0	57.1	57.1	56.2	60.9	67.5	65.9
245	66.2	65.5	65.5	65.4	70.7	66.6	69.1	75	72.6
246	74.8	74.5	75.0	74.5	74.5	74.2	75.1	83	81.6
247	71.5	dead							
248	66.3	66.4	65.0	65.2	64.6	68.5	76.6	82	81.9
249	71.5	71.3	72.0	71.7	72.9	71.4	72.2	80	80.7
250	69.5	69.4	69.0	69.3	69.3	72.4	76.6	80.5	83
251	66.5	66.4	66.5	67.0	68.8	71.2	77.8	85	82.3

252	70.7	69.8	70.5	70.5	70.3	dead			
253	67.9	68.9	69.0	68.5	70.1	72.5	77.6	86	85.8
254	77.2	78.1	78.0	77.5	77.6	77.0	79.7	83	81.8
255	61.4	61.1	62.0	61.7	61.4	61.6	65.3	68	67.5
256	59.8	59.4	59.0	59.7	61.3	61.2	62.7	67	68.6
257	64.5	61.8	62.5	61.7	62.2	66.3	72.5	76	78.6
258	64.2	63.6	63.5	64.1	64.0	62.5	62.4	63	62.6
259	64.7	64.4	64.5	65.7	65.5	65.0	69.6	72	73.2
260	62.9	62.3	62.0	61.8	62.2	62.3	64.5	67	69.3
261	62.6	62.1	63.0		56.7	dead			
262	64.7	64.3	65.0	64.4	69.2	63.8	62.8	65	66.3
263	61.0	61.2	61.0	60.4	61.2	60.3	61.9	66	66.4
264	52.6	52.3	53.5	51.8	51.8	51.7	51.3	52	52.8
265	67.3	66.9	67.0	66.1	65.4	62.8	61.3		62.8
266	56.5	56.5	57.5	59.0	61.8	62.9	62.3	66	67.4
267	67.4	65.4	64.5	63.6	61.7	61.5		62	62
268	54.6	56.0	55.5	56.6	57.2	56.6	57.6	60	61
269	63.2	61.3	61.5	61.6	61.6	61.5	63	67	66.4
270	62.2	61.8	62.0	62.0	57.4	54.6	55.4		58.4
271	56.6	56.4	55.5	55.5	55.3	53.9	53.7		57.4
272	59.0	61.1	61.5	61.1		63.5	63.8		
273	55.2	55.7	55.0	55.4	55.2	55.3	54.2	55	56.5
274	62.8	64.1	63.5	62.8	63.0	65.8	65.6	71	70.2
275	52.0	51.5	51.5	50.6	50.4	49.3	50.8		50.6
276	58.8	59.3	59.5	59.6	59.6				
277	65.0	63.8	63.0	63.5	61.2	60.9	61.1		64.3
278	57.3	56.9	57.0	56.5	56.1	55.8			
279	58.6	59.8	58.5	57.5					

280	59.0	58.3	54.5	56.5	56.2	54.3			
281	88.6	90.1	92.0	92.8	94.3	96.0	97.1	101	99.9
282	88.8	88.9	88.5	89.5	90.2	90.7	92.5	93	93.2
283	87.7	87.6	87.0	86.9	86.9	88.7	91	92	91.6
284	82.4	80.2	83.0	82.6	81.4	80.9	81.8		dead
285	76.3	76.8	77.0	77.2	76.7	77.0			
286	89.0	89.3	90.0	89.9					
287	80.2	81.5	81.5	81.7	82.9	83.1	80.1	83	83.1
288	84.9	85.2	84.5	84.9	85.0	83.6	84.8	89.5	87.7
289	85.5	85.5	86.0	85.4					
290	90.8	90.9	91.5	91.3	91.8	91.7	90.9		95.6
291	91.6	89.8	90.0	90.6	90.1	89.8	93.2	97	
292	74.8	74.7	75.0	74.3	74.6	73.2	74.2		
293	79.7	79.4	80.0	79.3	79.5	79.1	79.2		84.2
294	78.0	75.8	75.5	76.3	75.6	76.7	77.2		
295	76.7	76.9	76.0	76.8	76.0	77.7	83.1	84	89
296	76.6	76.4	77.5	77.8	78.3	82.0	80.4		87.4
297	81.5	82.2	82.5	82.2	dead				
298	80.9	81.3	82.5	81.5	81.4	82.5			
299	80.5	80.7	81.0	81.5	81.7	81.3			
300	91.1	89.1	89.0	89.3	89.2	88.9	88.1	96	95.1
301	64.4	63.7	64.0	64.2	63.1	63.7	64.2	62.5	62.8
302	69.6	68.9	69.0	69.3	69.0	67.8	67.8	65	64.2
303	62.9	63.4	63.5	62.8	63.3	63.0			
304	64.2	63.3	63.5	64.5	64.9	65.5	64.7	66	
305	82.4	82.0	82.0	82.3	81.6	81.7	82	81	
306	65.8	65.0	65.0	64.5	64.5	64.4	64.1	64.5	64
307	70.7	71.0	70.5	67.3	63.0	64.0	62.7	62	59.2

308	71.9	72.6	73.0	72.9	70.0	69.9	69.3	72	74.3
309	67.3	66.7	67.0	67.0	67.0	66.6	66.8	67	65.6
310	65.0	62.7	63.0	62.3	63.0	63.1	63	66	66.3
311	73.1	73.4	73.5						
312	72.5	72.9	72.0	72.2					
313	70.4	70.5	70.0	69.7					
314	74.1	74.3	74.0	74.0	72.0	70.2	69.5	76	
315	72.5	72.9	72.5	72.5					
316	71.8	70.7	69.0	68.6	69.5	69.5	68.4	70	
317	80.8	79.9	81.0	80.6					
318	69.6	68.2	68.0						
319	72.3	71.9	72.0	71.4					
320	70.1	67.2	67.0	66.9					

***Saccostrea glomerata*: length (mm)**

PLSg \ Date	04-Jun-06	08-Jul-06	25-Aug-06	06-Oct-06	30-Nov-06	09-Apr-07			09-Jul-07
601	58.9	58.7	58.5	62.5	70.1	89.7	-	-	97.3
602	53.9	53.4	54.0	55.0	59.4	72.2	-	-	80.8
603	59.7	61.2	59.5	61.6	68.3		-	-	
604	54.7	54.9	54.0	56.9	57.9	68.1	-	-	74.1
605	52.6	52.5	52.0	57.4	61.7	60.8	-	-	61
606	59.5	59.5	58.5	62.1	67.2	81.6	-	-	93.8
607	57.5	57.2	56.0	61.4	64.9	76.1	-	-	82.1
608	65.6	63.5	64.0	65.9	70.5		-	-	
609	64.9	66.9	66.0	67.9	59.4	84.2	-	-	88.5
610	42.6	42.5	42.5	42.1	41.8	76.8	-	-	46.3
611	48.4	50.6	49.0	54.0	57.4	73.1	-	-	85.9

612	61.4	61.7	62.0	64.5	66.6	79.5	-	-	84
613	54.8	57.5	57.5	62.7	69.8	99.5	-	-	105.7
614	54.8	54.6	55.0	55.9	57.1	69.4	-	-	
615	53.7	52.6	53.5	54.9	58.6	72.5	-	-	76.1
616	43.0	42.9	44.0	42.4	42.8	45.3	-	-	54.4
617	57.2	56.9	56.5	59.2	63.2	65.5	-	-	65.5
618	60.8	60.7	61.0	61.8	65.3	73.4	-	-	78
619	49.2	48.1	48.5	52.7	54.4	67.8	-	-	69.4
620	54.2	54.4	54.0	57.3	59.9	83.7	-	-	87.5
621	47.3	45.3	45.5	45.3	45.3	44.7	-	-	dead
622	48.7	48.7	49.0	49.7			-	-	
623	52.5	51.3	51.0	52.0	52.4		-	-	
624	46.5	45.5	dead				-	-	
625	45.6	45.8	45.5	50.7	53.8		-	-	
626	42.1	43.9	42.0	41.5	41.2		-	-	
627	40.4	dead					-	-	
628	47.0	47.2	47.5	46.9	dead		-	-	
629	44.6	44.0	43.5	44.3	43.0	42.7	-	-	dead
630	47.6	48.0	47.0	48.6	46.3	50.3	-	-	49.1
631	44.6	44.3	44.0				-	-	
632	42.7	43.7	44.0	43.8	43.6	43.4	-	-	dead
633	41.2	40.5	40.5	39.4	38.5	39.8	-	-	40.4
634	47.6	46.8	47.5	46.5	46.4	48.2	-	-	48.3
635	54.6	54.2	54.0	53.1	53.1	52.4	-	-	52.7
636	44.8	44.8	45.0				-	-	
637	45.6	44.8	45.0	43.1			-	-	
638	51.1	49.5	49.0				-	-	
639	40.8	40.4	41.5	43.6	44.1		-	-	

640	42.6	42.7	42.5	46.6	45.6	46.9	-	-	dead
641	65.7	67.0	66.5	66.4	67.7	81	-	-	80.8
642	68.6	68.4	69.0	68.2	68.1	75.7	-	-	80
643	64.0	63.9	63.5	64.2	64.8	73.9	-	-	81.8
644	65.6	66.1	67.0	68.8	69.0	70.6	-	-	74.4
645	70.8	70.4	69.5	69.1	70.7	71.2	-	-	dead
646	69.1	69.0	66.0	65.2	67.0	79.9	-	-	83.2
647	64.4	62.4	63.0	64.8	66.0	68.6	-	-	dead
648	66.3	66.2	66.0	69.3	67.1		-	-	
649	66.7	65.6	65.0	69.4	64.9	76.4	-	-	75.2
650	76.8	76.2	76.0	75.9	76.9	86.2	-	-	91.1
651	69.2	69.4	67.0	67.2	70.3	84	-	-	dead
652	61.6	64.2	62.0	66.0	68.7	74.6	-	-	83.7
653	67.3	66.6	66.5	66.5	66.5	71.9	-	-	74.7
654	57.7	57.8	58.0	62.2			-	-	
655	65.1	65.7	64.0	66.2	67.6	72.4	-	-	dead
656	66.0	66.4	66.5	66.0	67.7	80.6	-	-	83.8
657	71.4	70.5	69.0	70.3	71.7	76.8	-	-	85.1
658	70.0	71.0	70.0	71.1			-	-	
659	70.0	65.5	66.0	70.2	69.3	69.1	-	-	dead
660	65.4	65.5	65.5	64.0	67.9		-	-	
661	57.2	57.4	58.0	59.1	57.8	60.4	-	-	dead
662	54.7	54.2	54.0	54.8	54.6	53	-	-	56.4
663	55.4	53.9	53.0	54.3	53.2	56.2	-	-	
664	58.7	59.5	59.5	62.0	62.5	65.8	-	-	68
665	63.1	63.2	63.0	63.6	66.9	71.5	-	-	75.5
666	50.1	50.0	49.0	51.6	53.0	54.4	-	-	59.5
667	62.6	62.7	63.0	61.3	62.5	70.1	-	-	71.5

668	57.7	56.3	55.5	54.3	54.5	55.7	-	-	56.1
669	57.2	55.9	56.0	58.3	58.7	65.7	-	-	66.7
670	59.9	58.3	58.0	58.0	57.6	59.9	-	-	60.4
671	57.4	59.1	59.0	61.2	61.6	67.5	-	-	67.3
672	58.6	59.3	59.5	60.2			-	-	
673	51.9	52.6	52.5	57.3	59.0	64.9	-	-	69.5
674	63.2	62.8	63.0	62.1	61.2	58.6	-	-	59.1
675	65.7	65.7	65.5	70.6	69.7	72.6	-	-	dead
676	54.4	55.9	55.5	56.4	54.4	56.5	-	-	62.9
677	59.5	59.6	62.0	61.9	63.5	76.4	-	-	74.2
678	53.7	56.0	55.0	55.9	55.1	57.3	-	-	label lost
679	57.6	53.1	55.5	57.0	55.8	54.5	-	-	57.6
680	68.2	67.4	66.5	66.5	65.7	66.9	-	-	70.3
681	83.2						-	-	
682	85.2	83.8	83.0	84.0	83.6	94.1	-	-	94.1
683	83.9	82.3	82.0	87.2	88.9		-	-	
684	90.9	88.3					-	-	
685	85.4						-	-	
686	76.5	76.0	75.5	76.2			-	-	
687	80.5	79.8	80.0	79.0	79.4	82.5	-	-	84.4
688	80.8						-	-	
689	73.7	76.5					-	-	
690	81.3	82.8	82.5	81.4	82.4	88.6	-	-	91.4
691	81.1	81.2	81.0				-	-	
692	86.7	87.4	88.0				-	-	
693	97.1	98.2	97.5	100.9	100.5	dead	-	-	
694	76.8	79.1	77.0	76.5	dead		-	-	
695	78.7	77.7	76.0	76.8	78.6	82.9	-	-	82.9

696	76.9	76.8	77.0	81.0	81.1	dead	-	-	
697	82.3	81.7	82.0	82.6	81.6	91.5	-	-	93.4
698	88.1	89.1	89.0	91.2			-	-	
699	81.1	81.2	80.0	88.6	81.7	83.9	-	-	86.7
700	85.6	85.7	85.0	88.9	90.4	94.9	-	-	101.7
701	81.7	81.3	80.0	dead			-	-	
702	74.7	73.4	73.5	73.4	72.2	77.3	-	-	85.9
703	72.1	71.4	67.0	72.3	66.5	73.8	-	-	74.8
704	76.3	74.7	74.5	74.1	71.7	77.7	-	-	81.9
705	68.2	66.2	69.0	74.7	69.1	73.3	-	-	75.5
706	75.9	78.2	74.5	77.5	75.4	77.7	-	-	82.1
707	83.6	82.5	82.5	84.0	84.3	87.6	-	-	92
708	73.5	73.2	73.0	72.8	72.6	74.4	-	-	79.5
709	69.6	69.9	70.0	69.8	70.6		-	-	
710	71.0	69.5	70.0	65.5			-	-	
711	67.8						-	-	
712	62.9	66.1	66.0		66.5	66.4	-	-	dead
713	70.0	69.7	70.0	66.2			-	-	
714	74.2	74.0	74.0	70.7	74.1	72.7	-	-	72.5
715	71.8	71.8	72.0	73.9	70.5	74.3	-	-	79.5
716	66.0	64.3		70.9			-	-	
717	68.0	66.7					-	-	
718	67.4	67.9	67.5	dead			-	-	
719	67.1	67.6	68.5	71.2	70.6		-	-	
720	81.3	81.6	81.5	80.9	82.4	86.7	-	-	90.5

***Mytilus galloprovincialis*: length (mm)**

PLMg \ Date	2-Jun-06	8-Jul-06	25-Aug-06	9-Oct-06	30-Nov-06	26-Jan-07	1/04/07	11/05/07	9/07/07
120	58.5	61.0	65.0	73.0	77.1	80.5	84.5	87.5	88.7
121	52.7	58.8	62.5	63.8	76.0	80.8			
001	38.9	41.3	47.5	55.0	66.3	69.1	69.5	72.5	75.7
002	41.6	45.0	49.5	59.2	66.8	68.8	70.5	73	73.7
003	37.7	38.9	44.5	50.6	59.5	69.3	75	77	81.1
004	39.7	46.1	53.5	63.8	72.2	77.9	80.5	84.5	90
005	34.9	36.0	39.0	45.5	53.9	55.2			
006	41.9	47.5	49.0	56.0	65.3	67.8	72.5	74.5	76.5
007	38.8	39.3	42.0	51.3	60.9	66.2	69	74	75.8
008	35.9	39.7	45.5	52.6	60.7	69.1	73.8	76	76.9
009	35.1	40.6	47.0	57.4	64.4	68.4	75.5	78	81.7
010	44.3	49.8	56.0	66.6	71.9	80.0	89.7	80	dead
011	44.3	49.6	54.5	60.1	67.8	77.1	82.7	85	88.2
012	42.6	46.4	53.0	63.0	67.4	71.6	78	80	82.4
013	38.5	42.4	47.5	51.4	63.2	72.6	76.2	78.5	80.4
014	41.6	47.4	53.0	61.8	70.8	75.1	80.5	83.3	84.1
015	34.8	41.9	49.0	54.4	62.9	67.3	72	73.5	81
016	38.0	42.1	45.0	52.1	65.0	69.3	74.5	75	79.8
017	42.2	49.3	53.0	63.5	64.5	72.8	81.4	86.5	87
018	36.7	42.8	48.5	52.8	59.2	62.2	69.6	72	73.1
019	35.4	dead							
020	36.8	43.1	47.0	57.0	64.0	70.0	74	76	77.8
021	36.6	40.8	48.0	56.6		66.8	dead		
022	43.2	47.9	52.0	58.7	64.0	69.9	71.5	74	78.2
023	43.6	46.8	50.5	51.8	61.8	67.5	72.4	74.5	76.5

024	41.7	42.2	52.0	56.7			75.7	79.5	81.4
025	40.4	46.0	48.5	58.4	69.7	70.4	74.8	76.5	79.7
026	40.7	45.1	51.5	55.7	66.3	71.0	74.2	76.5	79.8
027	40.1	40.4	49.0	56.0	64.7	71.3	76.5	78.5	80.1
028	36.6	40.4	46.0	52.2	57.9	63.9	70	75	78.2
029	45.7	48.9	54.0	61.7	65.1	71.0	73	74.3	75.2
030	44.9	48.9	54.0	55.0	57.9	60.4	63.5	66	69.5
031	59.2	60.9	62.0	63.6	69.2	72.6	74.9	77	78.5
032	55.1	58.7	60.0	62.8	67.9	71.7	77.7	81	83.1
033	53.8	56.3	60.0	65.1	72.3	74.4	76	79	80.1
034	55.0	57.0	59.5	65.5	73.1	77.5	81.5	82	82.6
035	50.3	54.3	60.0	68.8	76.6	80.7	87	91	95.4
036	47.5	50.1	54.0	62.4	69.7	79.2	86	89	90
037	54.2	55.4	58.5	60.1	68.4	75.0	78.4	80.5	84.1
038	61.1	61.2	62.5	62.7	68.0	72.8	75	75.3	76.2
039	53.2	55.5	57.0	64.8	73.4	75.5	78.9	80	83.7
040	52.9	57.3	63.5	71.4	74.2				
041	51.1	52.1	56.0	61.2	71.3	76.5	80.2	82	86.9
042	53.1	56.8	61.0	69.5	77.0	79.2	81.6	84	86.2
043	50.2	53.2	56.5	61.9	71.2	74.9	78.4	80.5	82.1
044	56.6	58.2	59.0	62.1	66.1	70.9	75	78	79.7
045	46.0	50.6	55.0	62.4	68.6	72.3	75.5	76	76.7
046	54.2	58.6	61.5	66.3	71.6	75.8	79.4	84.5	86.5
047	47.0	51.6	56.5	65.3	72.6	77.3	81.8	84	85.9
048	48.4	50.5	53.0	55.9	62.2	71.1	75.4	77	79.4
049	46.2	52.6	59.0	63.5	69.7	72.5	78.4	79.8	81
050	58.9	59.8	59.5	60.4	62.8	65.2	67.6	68.5	68.8
051	53.0	dead							

052	57.1	60.1	62.5	66.2		75.5	77.3	78.5	80.6
053	57.1	58.9	61.5	68.0	74.3	77.6	81.5	82	83
054	55.5	58.4	63.0	65.6	70.1	75.1	78	80	82.5
055	55.6	57.7	61.5	69.2		76.5	82	83.5	84.4
056	52.6	55.4	58.0	66.5	74.2	83.3	83.7	86	89.4
057	51.3	55.3	59.5	63.2	71.0	75.3	78.4	79.5	81.1
058	54.8	60.4	64.0	69.1	76.2	81.9	85.1	87	93.8
059	58.0	60.8	63.0	66.6	71.0	dead			
060	53.9	dead							
061	61.5	64.0	66.5	69.6	76.6	82.4	86.9	90	93.4
062	61.2	68.3	65.0	71.4	77.9	83.4	86.7	88	89.5
063	60.2	63.9	66.0	67.1	75.0	80.0	81.3	82.5	85.4
064	59.3	62.2	65.0	64.7	73.9	79.3	81	83.5	84.8
065	62.3	64.5	67.0	dead					
066	57.2	60.8	62.5	65.1	70.3	74.0	76	80	79.3
067	56.9	61.6	64.5	68.1	72.7	85.0	82.5	84	84.8
068	65.4		66.0	66.3	69.8	71.0	72.6	73.8	74.7
069	62.1	63.2	64.0	68.4	71.3	73.9	77.7	80.8	81.1
070	60.8	61.7	62.0	62.9	64.5	69.8	73.3	76	76
071	57.7	59.5	61.5	66.2		75.9	79.2	81.3	83.8
072	54.2	55.2	57.5	62.0	dead				
073	60.7	61.7	62.5	64.9	66.2	71.4	73.5	75.5	75.8
074	60.1	61.4	62.0	64.8	66.4	68.7	72.7	75	77.4
075	55.8	59.4	62.5	64.5	67.1	69.5	75.5	80	80.2
076	65.7	65.6	65.5	67.5	74.0	77.4	80.4	82	83.2
077	54.8	55.0	57.0	59.4	68.2	72.6	75.1	78	79.5
078	57.7	60.9	64.0	68.7	77.5	80.7	83.4	85	86
079	58.8	61.9	63.0	70.0	75.1	79.1	81.1	82.3	86.3

080	64.3	66.1	66.5	71.2		74.5	76.5	79.5	80.5
081	61.8	62.8	65.0	68.1	72.5	76.3	78.9	80.2	83.1
082	62.2	65.2	68.5	71.6	78.6	83.9	86.2	89	93.4
083	64.7	67.9	69.0	70.5	72.5	74.6	75.6	77.2	87.4
084	57.3	62.6	68.0	87.7	84.2	86.5	94	90	99.3
085	62.8	65.8	67.0	70.1		78.2	79.7	81.5	86.6
086	56.2	59.8	63.5	68.7	74.5	81.9	84.4	87	89.1
087	59.8	63.0	64.0	65.7	72.9	76.3	78.7	89.8	82
088	64.5	66.4	67.5	71.0	76.9	80.4	83.2	84.8	87.2
089	65.5	67.8	71.0	75.8	81.2	86.9	89.5	91.2	93.5
090	61.1	61.6	62.0	62.1	64.4	66.0	67.1	68.5	70.4
091	68.1	69.0	69.5	69.8	72.7	76.5			
092	72.8	75.4	76.0	76.0	80.9	85.5	90	90.2	90.6
093	70.0	71.9	73.0	76.8	79.6	83.6	85.5	86.5	
094	67.4	69.8	73.0	76.8	81.6	82.7	84	86.5	90.2
095	67.3	69.8	72.5	77.6	83.3	88.4	90.6		
096	79.1	81.5	82.0	84.2	87.0	88.4	89.7	91	92.4
097	72.6	75.5	77.5	81.7	85.1	86.1	90.1	92.5	93.4
098	73.5	75.9	76.0	78.0	81.6				
099	70.5	72.0	74.0	78.0	81.5	83.9	84.5	86	85.7
100	77.8	78.6	80.0	80.5	81.0	82.4	82.9	85	85
101	68.5	70.9	71.5	73.4					
102	66.7	68.3	69.5	72.2	76.3	78.3	81	82.5	84.3
103	76.7	77.3	79.5	82.5	87.0	89.1	91.7	93.5	95
104	73.6	74.5	76.0	79.3	82.7	84.5			
105	73.0	73.2	75.0	76.2	81.8	85.2	87.4	89	91.7
106	73.4	73.3	73.0	73.0	74.9	79.1	82.6	84	85.3
107	72.4	73.6	75.5	78.5	81.9	87.9	84.3	86.5	87.6

108	63.9	71.6	73.5	76.2	83.3	87.5	89.2	90.2	92.2
109	67.3	74.8	73.0	77.1	84.0	86.8	87.9	90	89.7
110	71.3	72.7	73.5	76.4	81.5	82.3	82.5	83.5	83.5
111	70.4	71.4	72.0	72.4		81.3	83.4	85.5	85.5
112	65.6	67.4	67.5	68.4	68.9	76.3	77.4	78.8	81.8
113	65.6	66.1	66.0	66.9	68.1	68.4	68.5	70	70.5
114	68.5	69.4	70.0	72.6	76.6	79.1	81.6	83.2	84.1
115	72.0	73.4	73.5	75.2	78.1	79.4	80.6	81.3	83.4
116	74.6	74.7	75.5	76.6		82.1	85.4	86.2	88.1
117	69.0	70.8	73.0	73.1	77.7	79.4	81.9	85	87.1
118	74.9	76.7	78.5	81.3	83.9	85.3	87.8	88.8	88.5
119	71.2	72.2	72.5	73.5	77.5	79.1	80.4	83.2	84.6

Table A4.3. Growth records for Moreton Bay *Saccostrea glomerata*

Saccostrea glomerata: length (mm)	Date		
	MBSg	20-Jul-06	15-Aug-07
	903	37.6	dead
	905	30.0	63.3
	906	36.7	62.5
	907	33.0	66.5
	908	39.8	68.0
	909	37.2	75.4
	910	35.7	46.9
	919	32.7	56.2
	924	35.2	60.1
	925	32.5	62.8
	940	51.2	72.5
	944	47.5	73.3
	945	50.8	68.4
	960	65.4	82.5
	976	91.7	93.1
	981	94.7	92.5
	994	87.9	88.9
	997	89.8	95.3

Table A4.4. Growth records from Little Swanport *Ostrea angasi* and *Mytilus galloprovincialis*

Ostrea angasi: length (mm)	Date		
LSOa		06-Sep-06	24-Jul-07
	744	50.9	67.3
	743	52.5	71.1
	765	52.6	62
	736	53.8	67.3
	773	58.7	72.3
	780	63.9	74.9
	735	64.1	79.5
	781	66.6	80.8
	793	70.6	85
	756	72.5	85.9
	739	73.3	74.9
	746	74.3	88.5
	741	74.8	78.1
	785	76.1	99.5
	758	76.3	91.9
	789	76.3	83.2
	768	77.6	92.1
	764	79	90.8
	782	81.2	96.6
	796	82.7	84.3
	774	84.5	92.9
	727	86	101.4
	788	86.8	98.1
	734	87	103.3
	797	90.6	100.5
	754	91.1	104.3
	770	95.2	95.4

Mytilus galloprovincialis: length (mm)	Date		
LSMg		06-Sep-06	24-Jul-07
	369	20.5	22.2
	359	22.3	24.5
	362	22.7	53.4
	360	27.7	45.6
	385	42.2	55.4
	399	46.9	64.3
	382	48.6	66.5
	531	55.9	68.3
	537	56.4	70.8
	533	56.6	68.7
	530	57.6	68.4
	567	65.7	68.1

	559	72	72.5
	560	74.8	79.6
	563	75	76
	553	78.5	82.3

Table A4.5. Pambula Lake and Little Swanport *Ostrea angasi* $\delta^{18}O$.

PLOa 410 Distance along growth axis (mm)	PLOa410 $\delta^{18}O$ (VPDB)	PLOa421 Distance along growth axis (mm)	PLOa421 $\delta^{18}O$ (VPDB)	PLOa440 Distance along growth axis (mm)	PLOa440 $\delta^{18}O$ (VPDB)	PLOa472 Distance along growth axis (mm)	PLOa 472 $\delta^{18}O$ (VPDB)	LSOa754 Distance along growth axis (mm)	LSOa754 $\delta^{18}O$ (VPDB)	LSOa756 Distance along growth axis (mm)	LSOa756 $\delta^{18}O$ (VPDB)	LSOa793 Distance along growth axis (mm)	LSOa793 $\delta^{18}O$ (VPDB)
0	-0.74	0	-0.79	0	-0.78	0.000	-0.798	0.00	0.85	0.00	0.44	0.00	0.02
1.197	-0.88	-0.9	-0.78	1.345	-1.03	0.393	-0.755	0.21	-0.58	0.34	0.16	0.56	0.03
2.169	-0.34	-1.8	-0.27	1.983	-0.94	0.786	-1.047	0.43	-0.54	0.68	0.01	1.11	0.11
3.141	0.08	-2.128	-0.08	2.621	0.01	1.179	-0.997	0.64	-0.17	1.03	-0.27	1.11	0.05
3.653	0.06	-2.456	-0.02	3.259	0.26	1.572	-0.889	0.86	-0.08	1.41	-0.17	1.30	1.17
3.909	-0.19	-2.784	0.00	3.911	-0.11	1.965	-0.863	1.07	-0.09	1.79	-0.23	1.49	1.18
4.826	-0.30	-3.112	0.19	4.559	-0.03	2.358	-0.996	1.32	0.04	2.17	0.19	1.73	0.94
5.096	-0.22	-3.393	0.11	5.207	-0.07	3.058	-0.886	1.57	-0.04	2.47	0.38	1.96	1.22
5.366	-0.73	-3.674	0.31	5.697	-0.55	3.269	-0.989	1.82	0.06	2.77	0.56	2.20	1.46
5.636	-0.88	-3.955	-0.22	6.187	-0.49	3.480	-0.911	2.07	0.19	3.08	0.63	2.44	1.28
6.176	-1.87	-4.236	0.01	6.677	-1.01	3.691	-0.749	2.31	0.28	3.38	0.89	2.67	1.35
6.311	-1.67	-4.517	0.01	7.198	-1.41	3.902	-0.600	2.56	0.48	3.68	1.05	2.91	1.06
6.446	-1.04	-4.798	0.08	7.75	-0.59	4.113	-0.206	2.81	0.78	4.01	1.08	3.15	0.63
6.716	-0.34	-5.079	0.03	8.267	-0.09	4.324	-0.409	3.06	0.98	4.34	0.71	3.38	-0.18
6.986	-0.26	-5.36	0.10	8.508	0.34	4.535	0.229	3.31	1.03	4.66	0.82	3.38	0.01
7.256	-0.21	-5.641	-0.24			4.957	0.099	3.56	1.03	4.99	0.39	3.98	-0.47
		-5.928	-0.09			5.168	0.219	3.81	0.96	5.32	-0.04	4.57	-0.41
		-6.215	-0.17			5.379	0.134	4.06	1.01	5.65	-0.31	5.16	-0.30
		-6.502	-0.17			5.590	0.246	4.31	1.04	5.99	0.07	5.75	-0.62
		-6.789	-0.36			5.801	0.170	4.56	0.91	6.34	0.34	5.96	-0.46
		-7.076	-0.35			6.012	0.184	4.80	0.67	6.68	0.69	6.18	-0.20
		-7.363	-0.52			6.223	0.162	5.53	-0.37	7.02	1.06	6.39	-0.54
		-7.65	-0.27			6.434	-0.018	5.76	-0.49	7.37	1.28	6.61	-0.40
		-7.907	-0.70			6.645	0.036	5.99	-0.51	7.71	1.28	6.82	-0.05

-8.164	-1.10
-8.421	-1.03
-8.678	-0.93
-8.935	-1.51
-9.192	-1.32
-9.449	-1.56
-9.718	-0.96
-9.987	-0.61
-10.256	-0.36
-10.525	-0.06
-10.794	0.39
-11.063	0.36
	-0.47

7.048	0.006
7.240	-0.092
7.432	0.059
7.624	-0.092
7.816	0.037
8.008	0.026
8.200	0.018
8.392	-0.194
8.584	-0.332
8.776	-0.343
8.968	-0.464
9.160	-0.345
9.352	-0.676
9.544	-0.938
9.736	-1.605
9.928	-1.301
10.120	-0.993
10.312	-0.385
10.504	-0.131
10.696	-0.013
10.888	0.501
11.080	0.519

6.21	-0.35
6.44	-0.35
6.67	-0.28
6.90	-0.42
7.35	-0.08
7.58	0.09
7.81	0.18
8.49	0.82
8.72	0.92
9.41	1.24
10.47	0.46
10.64	0.67
10.80	0.86
10.97	1.31
11.14	1.32
11.31	1.29
11.47	1.09
11.64	0.88
11.81	0.49
11.97	0.41
12.14	0.65
12.30	0.82
12.63	1.21
12.96	1.06
13.12	0.62
13.28	0.50
13.61	-0.07
13.77	-0.04
14.75	1.04
15.06	1.15
15.21	0.94
15.52	0.62
15.67	0.39

8.04	0.89
8.36	0.49
8.69	0.08
9.01	0.85
9.34	1.40
9.70	1.48
10.05	0.24
10.41	0.17
10.76	0.16
11.48	1.38
11.83	1.21
12.19	0.68
12.54	0.67
12.85	-0.11
13.15	0.48
13.45	1.66

7.04	0.19
7.25	0.27
7.47	0.47
7.68	0.87
7.90	0.80
8.11	1.05
8.33	1.18
8.54	1.07
8.76	1.21
8.97	1.15
9.19	1.17
9.40	0.95
9.62	0.88
9.82	0.66
10.02	0.17
10.23	-0.03
10.43	0.00
10.63	-0.19
10.84	-0.21
11.04	-0.40
11.24	-0.50
11.45	-0.21
11.65	-0.07
11.85	-0.02
12.05	0.42
12.26	0.69
12.46	1.08
12.66	1.72

15.83	0.27
15.98	0.12
16.29	0.43
16.49	0.59
16.70	0.78
16.90	1.01
17.10	1.15
17.31	1.14
17.51	1.03
17.92	0.24
18.27	-0.11
18.42	0.02
18.57	0.02
19.32	0.93
19.47	0.85
19.62	0.40
19.77	0.39
19.92	0.06
20.14	0.33

Table A4.6. Severs Beach midden *Ostrea angasi* $\delta^{18}O$.

SBOa001 Distance along growth axis (mm)	SBOa001 $\delta^{18}O$ (VPDB)	SBOa004 Distance along growth axis (mm)	SBOa004 $\delta^{18}O$ (VPDB)
0.00	-0.64	0.00	-0.34
0.57	0.01	0.60	0.08
1.14	0.15	1.20	0.66
1.70	0.88	1.81	0.68
2.27	0.90	2.41	0.44
2.93	0.37	3.01	0.23
3.59	-0.17	3.61	-0.43
4.24	0.03	4.20	-0.39
4.89	-0.37	4.78	-0.49
5.54	-0.56	5.37	-0.53
6.10	-0.49	5.96	-0.35
6.65	-0.86	6.49	0.56
7.21	-0.42	6.96	1.28
7.76	0.80	7.44	0.91
8.31	1.23	7.92	0.20
8.87	0.45	8.39	-0.56
9.66	0.06	8.98	-0.68
10.44	-0.51	9.68	-0.29
11.00	0.36	10.13	0.34
11.56	1.26	10.57	0.99
12.12	0.08	11.02	0.47
12.60	-0.19	11.47	-0.02
13.07	0.53	11.91	-0.33
13.54	1.07	12.37	-0.48
14.01	0.44	12.84	-0.88
14.49	-0.17	13.31	0.01
14.97	0.61	13.81	1.07
15.45	1.03	14.33	0.06
15.93	-0.44	14.81	0.58
16.41	-0.36	15.26	0.96
16.91	-0.15		
17.40	0.52		
17.90	1.05		
18.40	-0.19		
18.86	-0.79		
19.29	-0.44		
19.72	0.32		
19.86	1.03		

Table A4.7. Pambula Lake *Saccostrea glomerata* Mg/Ca ratios.

PLSg602 Distance along growth axis (mm)	PLSg602 Mg/Ca (mmol/mol)	PLSg606 Distance along growth axis (mm)	PLSg606 Mg/Ca (mmol/mol)	PLSg607 Distance along growth axis (mm)	PLSg607 Mg/Ca (mmol/mol)	PLSg646 Distance along growth axis (mm)	PLSg646 Mg/Ca (mmol/mol)	PLSg705 Distance along growth axis (mm)	PLSg705 Mg/Ca (mmol/mol)	PLSg720 Distance along growth axis (mm)	PLSg720 Mg/Ca (mmol/mol)
0.00	10.86	0.00	18.10	0.00	4.91	0.00	0.02	0.00	16.75	0.00	30.15
0.02	10.38	0.03	17.89	0.03	4.66	0.08	0.02	0.02	17.56	0.07	21.38
0.04	9.82	0.05	19.46	0.05	4.34	0.15	0.01	0.04	20.98	0.14	17.20
0.07	10.26	0.08	18.17	0.08	5.63	0.23	0.02	0.07	18.22	0.22	20.63
0.10	10.07	0.11	13.98	0.11	6.73	0.31	0.02	0.10	15.13	0.29	20.70
0.12	10.04	0.13	14.19	0.13	9.36	0.39	0.02	0.12	15.33	0.36	19.77
0.15	10.42	0.16	15.43	0.16	13.69	0.46	0.02	0.15	18.04	0.43	17.30
0.18	10.51	0.19	15.43	0.19	14.69	0.54	0.02	0.18	23.87	0.50	17.12
0.20	10.91	0.21	14.34	0.21	12.72	0.62	0.02	0.21	26.93	0.57	17.56
0.23	11.17	0.24	14.50	0.24	11.49	0.69	0.01	0.23	23.62	0.65	17.62
0.26	11.30	0.27	16.81	0.27	12.51	0.77	0.01	0.26	19.42	0.72	17.58
0.28	10.89	0.29	17.13	0.30	16.59	0.85	0.02	0.29	15.96	0.79	18.71
0.31	11.62	0.32	17.01	0.32	21.48	0.93	0.02	0.31	17.89	0.86	17.48
0.34	11.70	0.35	17.54	0.35	21.60	1.00	0.02	0.34	21.24	0.93	14.70
0.36	12.26	0.37	22.28	0.38	16.58	1.08	0.02	0.37	23.12	1.00	15.03
0.39	11.89	0.40	27.81	0.40	11.87	1.16	0.02	0.39	20.26	1.08	16.12
0.42	10.71	0.43	27.62	0.43	12.18	1.23	0.02	0.42	17.09	1.15	16.50
0.44	10.71	0.45	22.77	0.46	13.96	1.31	0.02	0.45	17.96	1.22	18.62
0.47	11.02	0.48	19.28	0.48	15.62	1.39	0.01	0.48	19.63	1.29	16.70
0.50	11.57	0.51	18.66	0.51	16.21	1.47	0.02	0.50	20.80	1.36	15.03
0.52	12.40	0.53	17.58	0.54	16.78	1.54	0.01	0.53	22.23	1.43	12.89
0.55	13.59	0.56	15.86	0.56	16.99	1.62	0.01	0.56	20.32	1.51	12.01
0.58	15.27	0.59	15.07	0.59	15.53	1.70	0.02	0.58	18.66	1.58	11.12
0.60	15.76	0.61	14.42	0.62	14.97	1.78	0.02	0.61	18.52	1.65	11.35
0.63	14.19	0.64	14.85	0.64	15.01	1.85	0.02	0.64	18.33	1.72	12.69
0.66	10.87	0.67	15.98	0.67	17.08	1.93	0.02	0.66	17.91	1.79	11.85
0.68	9.55	0.69	17.43	0.70	18.44	2.01	0.02	0.69	17.40	1.86	10.35

0.71	9.18	0.72	18.48	0.72	17.77	2.08	0.02	0.72	17.51	1.94	11.35
0.74	9.24	0.75	20.21	0.75	17.02	2.16	0.02	0.75	18.93	2.01	10.92
0.76	9.91	0.77	19.08	0.78	17.08	2.24	0.02	0.77	19.03	2.08	10.19
0.79	8.92	0.80	19.53	0.80	17.23	2.32	0.02	0.80	19.68	2.15	11.76
0.82	8.65	0.83	20.09	0.83	16.24	2.39	0.01	0.83	19.80	2.22	12.52
0.84	10.31	0.86	21.54	0.86	15.05	2.47	0.01	0.85	18.22	2.30	14.93
0.87	11.81	0.88	20.23	0.89	14.15	2.55	0.02	0.88	17.88	2.37	11.45
0.90	12.89	0.91	20.57	0.91	14.36	2.62	0.02	0.91	17.38	2.44	9.97
0.92	12.61	0.94	17.39	0.94	14.78	2.70	0.01	0.93	16.70	2.51	10.44
0.95	12.39	0.96	17.64	0.97	14.66	2.78	0.02	0.96	18.74	2.58	10.35
0.98	13.31	0.99	17.52	0.99	14.65	2.86	0.01	0.99	20.36	2.65	9.83
1.01	14.25	1.02	18.77	1.02	13.13	2.93	0.01	1.01	19.46	2.73	9.10
1.03	14.77	1.04	19.72	1.05	12.57	3.01	0.01	1.04	18.01	2.80	9.12
1.06	15.29	1.07	20.74	1.07	14.91	3.09	0.01	1.07	17.19	2.87	8.92
1.09	15.66	1.10	20.60	1.10	16.11	3.16	0.01	1.10	14.65	2.94	8.41
1.11	15.46	1.12	20.23	1.13	16.99	3.24	0.01	1.12	14.43	3.01	8.10
1.14	14.85	1.15	17.83	1.15	18.10	3.32	0.01	1.15	14.46	3.08	8.82
1.17	14.97	1.18	22.26	1.18	16.96	3.40	0.01	1.18	14.69	3.16	10.09
1.19	17.04	1.20	22.45	1.21	15.55	3.47	0.01	1.20	15.24	3.23	9.78
1.22	16.42	1.23	22.77	1.23	15.58	3.55	0.01	1.23	16.29	3.30	10.17
1.25	16.06	1.26	24.70	1.26	16.27	3.63	0.01	1.26	16.82	3.37	14.84
1.27	15.06	1.28	25.31	1.29	16.36	3.70	0.02	1.28	17.10	3.44	12.08
1.30	13.40	1.31	19.72	1.31	16.53	3.78	0.01	1.31	17.42	3.51	7.96
1.33	13.29	1.34	17.82	1.34	16.61	3.86	0.01	1.34	16.35	3.59	6.20
1.35	13.18	1.36	18.17	1.37	16.10	3.94	0.01	1.37	15.06	3.66	7.28
1.38	13.28	1.39	19.99	1.40	16.37	4.01	0.01	1.39	15.15	3.73	9.11
1.41	13.99	1.42	19.64	1.42	16.81	4.09	0.01	1.42	16.14	3.80	8.77
1.43	15.64	1.44	19.04	1.45	16.23	4.17	0.01	1.45	17.26	3.87	8.82
1.46	16.87	1.47	21.07	1.48	14.81	4.24	0.02	1.47	16.68	3.94	9.79
1.49	17.53	1.50	22.54	1.50	14.34	4.32	0.01	1.50	16.52	4.02	10.52
1.51	18.17	1.52	22.15	1.53	14.63	4.40	0.01	1.53	17.28	4.09	10.35
1.54	18.41	1.55	20.17	1.56	15.23	4.48	0.01	1.55	16.19	4.16	10.67
1.57	17.29	1.58	18.73	1.58	14.60	4.55	0.01	1.58	16.39	4.23	13.01
1.59	15.89	1.60	17.97	1.61	13.55	4.63	0.01	1.61	16.26	4.30	13.76

1.62	15.65	1.63	17.23	1.64	15.37	4.71	0.01	1.64	17.38	4.37	12.80
1.65	15.00	1.66	16.64	1.66	15.75	4.79	0.01	1.66	17.50	4.45	13.15
1.67	14.82	1.68	16.30	1.69	14.40	4.86	0.01	1.69	16.34	4.52	13.61
1.70	15.15	1.71	15.93	1.72	14.06	4.94	0.01	1.72	15.84	4.59	12.89
1.73	15.12	1.74	13.84	1.74	14.57	5.02	0.01	1.74	15.09	4.66	11.64
1.75	15.89	1.76	14.26	1.77	14.65	5.09	0.01	1.77	14.53	4.73	11.04
1.78	16.61	1.79	15.97	1.80	13.81	5.17	0.01	1.80	14.91	4.81	11.63
1.81	16.45	1.82	16.04	1.82	13.36	5.25	0.01	1.82	16.20	4.88	11.16
1.83	16.01	1.84	14.47	1.85	13.21	5.33	0.01	1.85	16.90	4.95	13.83
1.86	15.65	1.87	13.64	1.88	14.13	5.40	0.01	1.88	15.60	5.02	16.09
1.89	16.33	1.90	15.99	1.90	13.61	5.48	0.01	1.91	15.84	5.09	13.88
1.91	16.93	1.92	17.02	1.93	12.71	5.56	0.01	1.93	17.09	5.16	13.44
1.94	17.75	1.95	15.28	1.96	13.10	5.63	0.01	1.96	18.32	5.24	13.60
1.97	17.00	1.98	15.38	1.99	11.82	5.71	0.01	1.99	18.03	5.31	13.25
1.99	16.03	2.00	15.38	2.01	12.25	5.79	0.01	2.01	16.48	5.38	14.26
2.02	15.11	2.03	14.74	2.04	13.29	5.87	0.01	2.04	16.24	5.45	12.88
2.05	14.71	2.06	15.44	2.07	13.43	5.94	0.01	2.07	16.07	5.52	14.08
2.07	14.53	2.08	18.24	2.09	14.04	6.02	0.01	2.09	14.49	5.59	16.16
2.10	14.32	2.11	20.64	2.12	16.91	6.10	0.01	2.12	14.66	5.67	15.26
2.13	14.44	2.14	20.64	2.15	14.60	6.17	0.01	2.15	15.46	5.74	12.65
2.15	15.00	2.16	19.22	2.17	12.78	6.25	0.01	2.18	15.34	5.81	12.70
2.18	15.19	2.19	17.93	2.20	11.69	6.33	0.01	2.20	15.01	5.88	15.67
2.21	14.95	2.22	17.25	2.23	11.28	6.41	0.01	2.23	15.23	5.95	16.02
2.23	13.75	2.24	17.80	2.25	9.73	6.48	0.01	2.26	15.12	6.02	17.42
2.26	14.64	2.27	17.51	2.28	8.37	6.56	0.01	2.28	14.71	6.10	17.49
2.29	15.14	2.30	16.76	2.31	6.87	6.64	0.01	2.31	14.95	6.17	17.08
2.31	15.82	2.32	19.01	2.33	6.04	6.72	0.01	2.34	13.87	6.24	15.65
2.34	15.78	2.35	21.35	2.36	6.10	6.79	0.01	2.36	13.38	6.31	13.66
2.37	15.41	2.38	22.77	2.39	6.38	6.87	0.01	2.39	14.27	6.38	14.30
2.39	16.31	2.40	22.82	2.41	6.88	6.95	0.01	2.42	14.31	6.46	13.41
2.42	17.35	2.43	21.51	2.44	7.60	7.02	0.01	2.45	13.74	6.53	14.14
2.45	16.03	2.46	19.83	2.47	7.70	7.10	0.01	2.47	12.76	6.60	13.76
2.47	16.16	2.49	19.41	2.50	7.84	7.18	0.01	2.50	13.07	6.67	13.35
2.50	16.10	2.51	20.07	2.52	7.78	7.26	0.01	2.53	13.39	6.74	14.81

2.53	16.52	2.54	19.15	2.55	8.13	7.33	0.01	2.55	12.94	6.81	14.81
2.56	16.52	2.57	17.85	2.58	8.65	7.41	0.01	2.58	11.73	6.89	14.51
2.58	16.49	2.59	17.42	2.60	8.50	7.49	0.01	2.61	12.04	6.96	12.42
2.61	17.48	2.62	17.82	2.63	8.38	7.56	0.01	2.63	12.21	7.03	10.70
2.64	17.94	2.65	18.58	2.66	7.92	7.64	0.01	2.66	12.39	7.10	12.55
2.66	16.82	2.67	18.19	2.68	6.76	7.72	0.01	2.69	12.33	7.17	15.16
2.69	16.56	2.70	16.71	2.71	5.78	7.80	0.01	2.72	11.75	7.24	14.06
2.72	18.03	2.73	17.09	2.74	5.76	7.87	0.01	2.74	12.46	7.32	14.78
2.74	17.38	2.75	16.07	2.76	6.60	7.95	0.01	2.77	13.07	7.39	14.87
2.77	16.60	2.78	15.86	2.79	7.21	8.03	0.01	2.80	12.19	7.46	14.12
2.80	17.31	2.81	15.77	2.82	7.26	8.10	0.01	2.82	12.07	7.53	13.42
2.82	16.81	2.83	15.36	2.84	7.15	8.18	0.01	2.85	12.70	7.60	13.09
2.85	17.56	2.86	15.73	2.87	6.06	8.26	0.01	2.88	13.26	7.67	13.19
2.88	17.46	2.89	16.16	2.90	5.19	8.34	0.01	2.90	15.56	7.75	13.51
2.90	16.29	2.91	16.33	2.92	4.98	8.41	0.02	2.93	15.83	7.82	13.98
2.93	14.68	2.94	16.83	2.95	4.95	8.49	0.02	2.96	12.45	7.89	14.75
2.96	14.21	2.97	18.19	2.98	4.86	8.57	0.02	2.99	11.53	7.96	16.49
2.98	14.55	2.99	17.59	3.01	5.13	8.64	0.02	3.01	11.70	8.03	16.65
3.01	15.67	3.02	16.88	3.03	5.80	8.72	0.02	3.04	11.49	8.10	19.05
3.04	16.29	3.05	15.33	3.06	6.13	8.80	0.02	3.07	11.07	8.18	17.28
3.06	17.69	3.07	15.18	3.09	6.55	8.88	0.01	3.09	11.03	8.25	17.51
3.09	16.78	3.10	16.78	3.11	7.15	8.95	0.01	3.12	10.45	8.32	18.46
3.12	16.20	3.13	17.21	3.14	7.38	9.03	0.01	3.15	10.32	8.39	16.26
3.14	16.18	3.15	17.05	3.17	7.52	9.11	0.01	3.17	9.99	8.46	14.72
3.17	16.75	3.18	15.72	3.19	7.71	9.18	0.02	3.20	9.69	8.54	12.93
3.20	17.75	3.21	16.47	3.22	6.94	9.26	0.02	3.23	9.39	8.61	11.13
3.22	15.90	3.23	16.57	3.25	6.26	9.34	0.02	3.26	9.46	8.68	11.54
3.25	15.40	3.26	16.27	3.27	6.05	9.42	0.01	3.28	9.32	8.75	10.11
3.28	15.86	3.29	16.89	3.30	5.80	9.49	0.01	3.31	9.76	8.82	8.87
3.30	14.38	3.31	15.03	3.33	5.61	9.57	0.02	3.34	10.39	8.89	8.10
3.33	14.46	3.34	15.87	3.35	5.49	9.65	0.02	3.36	11.08	8.97	7.63
3.36	14.39	3.37	15.38	3.38	5.15	9.73	0.01	3.39	10.20	9.04	9.05
3.38	13.49	3.39	14.27	3.41	4.89	9.80	0.01	3.42	8.92	9.11	9.79
3.41	12.79	3.42	14.22	3.43	4.92	9.88	0.01	3.44	8.04	9.18	11.59

3.44	14.54	3.45	14.04	3.46	5.02	9.96	0.02	3.47	7.91	9.25	14.38
3.46	13.78	3.47	14.20	3.49	5.17	10.03	0.02	3.50	8.07	9.32	15.92
3.49	12.10	3.50	14.41	3.52	5.46	10.11	0.02	3.53	8.23	9.40	15.12
3.52	11.86	3.53	13.52	3.54	6.13	10.19	0.01	3.55	7.93	9.47	10.39
3.54	12.70	3.55	13.68	3.57	6.70	10.27	0.01	3.58	7.66	9.54	9.22
3.57	11.87	3.58	13.51	3.60	7.81	10.34	0.01	3.61	7.36	9.61	7.03
3.60	11.42	3.61	13.51	3.62	9.02	10.42	0.01	3.63	7.20	9.68	6.70
3.62	11.99	3.63	13.76	3.65	9.11	10.50	0.01	3.66	7.02	9.75	6.25
3.65	13.09	3.66	13.62	3.68	9.10	10.57	0.01	3.69	7.41	9.83	5.49
3.68	13.41	3.69	12.48	3.70	8.76	10.65	0.01	3.71	8.98	9.90	7.24
3.70	13.39	3.71	12.12	3.73	8.39	10.73	0.01	3.74	9.24	9.97	7.80
3.73	12.98	3.74	12.11	3.76	8.75	10.81	0.01	3.77	7.57	10.04	7.17
3.76	11.87	3.77	12.23	3.78	8.58	10.88	0.00	3.80	6.53	10.11	5.92
3.78	12.62	3.79	11.77	3.81	8.72	10.96	0.00	3.82	6.00	10.18	5.32
3.81	12.41	3.82	10.66	3.84	9.09	11.04	0.00	3.85	5.45	10.26	5.44
3.84	11.32	3.85	10.95	3.86	10.06	11.10	0.00	3.88	5.32	10.33	6.34
3.86	11.02	3.87	10.15	3.89	10.67			3.90	5.74	10.40	7.59
3.89	10.83	3.90	10.73	3.92	10.86			3.93	6.36	10.47	7.21
3.92	11.06	3.93	11.58	3.94	9.40			3.96	6.83	10.54	6.70
3.95	11.99	3.95	11.54	3.97	8.60			3.98	6.96	10.61	7.37
3.97	11.35	3.98	11.36	4.00	8.40			4.01	6.77	10.69	7.12
4.00	12.83	4.01	11.37	4.02	8.03			4.04	6.90	10.76	8.27
4.03	16.40	4.03	11.46	4.05	8.37			4.07	6.71	10.83	9.32
4.05	14.39	4.06	12.17	4.08	9.02			4.09	6.20	10.90	8.31
4.08	12.33	4.09	11.77	4.11	8.93			4.12	5.52	10.97	7.37
4.11	11.24	4.11	10.96	4.13	8.48			4.15	5.15	11.05	7.71
4.13	11.74	4.14	10.93	4.16	8.25			4.17	5.10	11.12	7.18
4.16	12.33	4.17	11.12	4.19	8.31			4.20	5.69	11.19	6.85
4.19	12.53	4.20	10.80	4.21	8.13			4.23	6.07	11.26	7.26
4.21	11.36	4.22	10.94	4.24	8.88			4.25	5.81	11.33	8.02
4.24	9.79	4.25	12.15	4.27	10.50			4.28	5.52	11.40	7.16
4.27	9.11	4.28	11.51	4.29	10.48			4.31	5.70	11.48	7.14
4.29	8.11	4.30	10.50	4.32	10.30			4.34	6.08	11.55	6.83
4.32	7.52	4.33	10.84	4.35	10.62			4.36	6.56	11.62	6.74

4.35	7.28	4.36	11.29	4.37	8.90
4.37	7.03	4.38	11.61	4.40	8.98
4.40	6.57	4.41	11.68	4.43	9.30
4.43	6.49	4.44	10.73	4.45	9.86
4.45	6.50	4.46	9.75	4.48	10.29
4.48	6.79	4.49	9.74	4.51	10.59
4.51	7.43	4.52	9.71	4.53	10.72
4.53	7.24	4.54	10.02	4.56	10.26
4.56	7.48	4.57	10.08	4.59	9.76
4.59	6.96	4.60	9.99	4.62	8.98
4.61	7.19	4.62	9.87	4.64	8.19
4.64	7.54	4.65	9.98	4.67	8.05
4.67	6.95	4.68	9.72	4.70	8.41
4.69	6.18	4.70	9.68	4.72	9.07
4.72	5.56	4.73	9.90	4.75	9.79
4.75	5.30	4.76	10.44	4.78	10.63
4.77	5.20	4.78	12.52	4.80	11.27
4.80	5.31	4.81	8.18	4.83	11.37
4.83	4.90	4.84	6.14	4.86	12.36
4.85	4.57	4.86	10.69	4.88	14.26
4.88	4.35	4.89	10.94	4.91	14.14
4.91	4.20	4.92	11.18	4.94	13.41
4.93	3.91	4.94	11.29	4.96	13.23
4.96	3.73	4.97	11.32	4.99	13.07
4.99	3.74	5.00	11.43	5.02	12.77
5.01	3.96	5.02	11.12	5.04	11.54
5.04	3.92	5.05	10.96	5.07	11.11
5.07	3.77	5.08	10.31	5.10	11.41
5.09	3.60	5.10	10.13	5.12	12.35
5.12	3.50	5.13	10.16	5.15	12.31
5.15	3.34	5.16	10.19	5.18	11.72
5.17	3.33	5.18	10.01	5.21	11.88
5.20	3.58	5.21	9.71	5.23	11.30
5.23	3.69	5.24	9.51	5.26	11.47
4.39	6.78	11.69	7.54		
4.42	7.44	11.76	7.14		
4.44	8.70	11.83	7.61		
4.47	10.52	11.91	7.67		
4.50	9.81	11.98	6.53		
4.52	9.54	12.05	6.85		
4.55	9.43	12.12	6.50		
4.58	9.83	12.19	7.48		
4.61	11.14	12.26	7.68		
4.63	11.98	12.34	8.13		
4.66	12.24	12.41	8.02		
4.69	12.36	12.48	8.26		
4.71	12.65	12.55	8.36		
4.74	12.67	12.62	8.89		
4.77	13.50	12.70	9.75		
4.79	13.84	12.77	10.55		
4.82	14.56	12.84	11.52		
4.85	14.37	12.91	10.55		
4.88	14.90	12.98	9.96		
4.90	14.25	13.05	10.48		
4.93	15.62	13.13	11.42		
4.96	17.06	13.20	11.83		
4.98	15.98	13.27	11.43		
5.01	15.28	13.34	11.29		
5.04	14.35	13.41	10.21		
5.06	14.52	13.48	10.87		
5.09	14.49	13.56	10.05		
5.12	14.01	13.63	11.86		
5.15	14.07	13.70	13.03		
5.17	14.01	13.77	14.07		
5.20	15.02	13.84	15.11		
5.23	14.28	13.91	15.07		
5.25	15.17	13.99	12.89		
5.28	16.25	14.06	11.05		

5.25	3.56	5.26	9.35	5.29	11.75
5.28	3.32	5.29	9.30	5.31	12.76
5.31	3.26	5.32	9.00	5.34	13.99
5.33	3.43	5.34	8.55	5.37	13.58
5.36	3.53	5.37	8.81	5.39	12.40
5.39	3.40	5.40	8.57	5.42	11.85
5.42	3.37	5.42	8.46	5.45	11.76
5.44	3.56	5.45	8.67	5.47	10.66
5.47	3.87	5.48	9.10	5.50	10.52
5.50	3.96	5.50	9.20	5.53	10.68
5.52	4.10	5.53	9.34	5.55	10.98
5.55	4.20	5.56	9.69	5.58	11.10
5.58	4.20	5.58	10.93	5.61	10.90
5.60	4.17	5.61	10.78	5.63	11.30
5.63	4.07	5.64	10.65	5.66	11.68
5.66	3.85	5.66	10.04	5.69	11.72
5.68	3.93	5.69	9.64	5.72	11.53
5.71	3.67	5.72	9.57	5.74	11.01
5.74	3.64	5.74	9.69	5.77	11.33
5.76	3.62	5.77	9.69	5.80	12.55
5.79	3.63	5.80	9.95	5.82	13.78
5.82	3.74	5.82	9.90	5.85	13.89
5.84	4.26	5.85	9.76	5.88	15.02
5.87	4.32	5.88	10.33	5.90	15.37
5.90	4.28	5.91	10.50	5.93	15.50
5.92	4.43	5.93	10.23	5.96	14.63
5.95	4.71	5.96	10.31	5.98	14.57
5.98	5.40	5.99	10.28	6.01	13.42
6.00	5.83	6.01	10.66	6.04	13.09
6.03	6.47	6.04	10.54	6.06	13.80
6.06	6.61	6.07	10.48	6.09	14.44
6.08	6.56	6.09	10.32	6.12	16.41
6.11	6.91	6.12	10.22	6.14	17.34
6.14	7.06	6.15	10.29	6.17	16.63
5.31	16.39	14.13	10.38		
5.33	15.31	14.20	11.43		
5.36	13.42	14.27	11.32		
5.39	12.83	14.34	16.26		
5.42	13.39	14.42	14.88		
5.44	12.95	14.49	15.79		
5.47	12.58	14.56	14.07		
5.50	12.86	14.63	13.21		
5.52	13.72	14.70	15.19		
5.55	13.14	14.78	15.14		
5.58	12.31	14.85	13.01		
5.60	12.08	14.92	12.35		
5.63	12.44	14.99	11.74		
5.66	12.30	15.06	10.79		
5.69	11.91	15.13	11.99		
5.71	11.52	15.21	12.26		
5.74	11.50	15.28	13.12		
5.77	11.57	15.35	10.53		
5.79	11.51	15.42	10.18		
5.82	12.56	15.49	10.55		
5.85	12.31	15.56	10.14		
5.87	12.33	15.64	9.39		
5.90	11.96	15.71	8.30		
5.93	12.68	15.78	7.72		
5.96	14.23	15.85	6.94		
5.98	15.42				
6.01	16.94				
6.04	17.68				
6.06	17.22				
6.09	18.00				
6.12	17.15				
6.14	16.13				
6.17	15.25				
6.20	13.92				

6.16	8.06	6.17	10.64	6.20	15.94	6.23	15.11
6.19	9.80	6.20	10.71	6.23	15.67	6.25	15.91
6.22	10.71	6.23	10.93	6.25	15.13	6.28	16.64
6.24	9.96	6.25	10.79	6.28	15.29	6.31	18.10
6.27	9.79	6.28	10.74	6.31	16.24	6.33	16.57
6.30	8.84	6.31	10.91	6.33	16.71	6.36	17.46
6.32	8.15	6.33	11.06	6.36	16.87	6.39	16.55
6.35	8.28	6.36	11.18	6.39	17.19	6.41	16.75
6.38	8.86	6.39	10.83	6.41	17.92	6.44	16.12
6.40	9.27	6.41	11.52	6.44	16.98	6.47	15.80
6.43	10.63	6.44	12.51	6.47	19.95	6.50	15.58
6.46	12.58	6.47	13.23	6.49	22.11	6.52	16.15
6.48	12.87	6.49	13.55	6.52	20.12	6.55	16.33
6.51	13.28	6.52	12.46	6.55	17.81	6.58	16.49
6.54	14.11	6.55	12.25	6.57	16.19	6.60	15.46
6.56	13.71	6.57	12.34	6.60	16.00	6.63	14.85
6.59	13.04	6.60	12.01	6.63	16.85	6.66	15.00
6.62	13.47	6.63	12.17	6.65	19.83	6.68	15.60
6.64	13.39	6.65	12.28	6.68	21.34	6.71	18.42
6.67	12.27	6.68	11.61	6.71	17.45	6.74	19.46
6.70	11.85	6.71	11.49	6.73	15.25	6.77	19.44
6.72	11.46	6.73	11.95	6.76	15.29	6.79	21.35
6.75	11.13	6.76	12.63	6.79	15.56	6.82	22.51
6.78	11.32	6.79	12.95	6.82	16.35	6.85	18.23
6.80	11.81	6.81	14.00	6.84	15.65	6.87	15.98
6.83	12.25	6.84	14.83	6.87	14.82	6.90	14.85
6.86	12.43	6.87	14.95	6.90	15.55	6.93	15.30
6.88	12.09	6.89	15.73	6.92	15.85	6.95	16.08
6.91	12.81	6.92	15.54	6.95	15.47	6.98	16.54
6.94	13.91	6.95	16.34	6.98	15.14	7.01	17.15
6.97	13.75	6.97	16.12	7.00	15.58	7.04	17.35
6.99	12.46	7.00	15.82	7.03	14.95	7.06	17.56
7.02	12.40	7.03	17.00	7.06	15.17	7.09	17.07
7.05	14.07	7.05	17.61	7.08	16.23	7.12	14.73

7.07	14.11	7.08	18.47	7.11	16.24	7.14	10.35
7.10	13.50	7.11	17.28	7.14	16.04	7.17	10.54
7.13	12.21	7.13	16.15	7.16	15.70	7.20	10.65
7.15	12.07	7.16	15.94	7.19	15.21	7.22	10.20
7.18	12.78	7.19	16.48	7.22	14.55	7.25	8.74
7.21	12.41	7.21	15.41	7.24	14.05	7.28	8.28
7.23	10.95	7.24	14.10	7.27	14.24	7.31	8.41
7.26	10.92	7.27	12.86	7.30	14.23	7.33	8.51
7.29	11.44	7.29	11.70	7.33	13.94	7.36	7.95
7.31	11.04	7.32	12.03	7.35	13.68	7.39	7.56
7.34	10.96	7.35	12.74	7.38	13.63	7.41	7.33
7.37	11.44	7.37	12.42	7.41	13.74	7.44	7.47
7.39	12.26	7.40	11.67	7.43	12.98	7.47	7.26
7.42	11.82	7.43	11.27	7.46	13.18	7.49	7.69
7.45	11.22	7.45	11.54	7.49	12.63	7.52	8.64
7.47	10.52	7.48	12.08	7.51	12.22	7.55	8.63
7.50	10.82	7.51	12.42	7.54	11.91	7.58	8.47
7.53	11.87	7.53	12.51	7.57	11.31	7.60	7.74
7.55	12.34	7.56	11.75	7.59	11.69	7.63	7.12
7.58	13.61	7.59	11.01	7.62	11.99	7.66	6.82
7.61	13.43	7.61	10.89	7.65	11.32	7.68	6.23
7.63	12.56	7.64	11.02	7.67	10.11	7.71	5.62
7.66	12.41	7.67	10.84	7.70	9.09	7.74	5.55
7.69	11.78	7.70	10.64	7.73	7.99	7.76	6.13
7.71	12.33	7.72	11.08	7.75	7.27	7.79	6.80
7.74	11.95	7.75	11.14	7.78	6.53	7.82	7.91
7.77	12.16	7.78	11.23	7.81	6.09	7.85	8.52
7.79	12.81	7.80	10.90	7.84	5.59	7.87	9.01
7.82	13.33	7.83	10.20	7.86	5.36	7.90	9.47
7.85	14.23	7.86	10.06	7.89	4.97	7.93	9.39
7.87	15.24	7.88	10.06	7.92	4.98	7.95	9.59
7.90	15.08	7.91	10.11			7.98	10.05
7.93	14.29	7.94	10.29			8.01	9.32
7.95	13.82	7.96	10.53			8.03	8.90

7.98	13.51	7.99	10.42
8.01	13.31	8.02	10.54
8.03	13.37	8.04	10.80
8.06	14.27	8.07	11.49
8.09	16.35	8.10	11.40
8.11	16.60	8.12	11.65
8.14	15.46	8.15	10.96
8.17	14.88	8.18	10.87
8.19	14.23	8.20	10.49
8.22	13.17	8.23	11.20
8.25	12.38	8.26	12.27
8.27	12.48	8.28	12.72
8.30	13.03	8.31	12.80
8.33	12.88	8.34	12.50
8.36	12.55	8.36	11.87
8.38	12.32	8.39	10.90
8.41	12.02	8.42	11.27
8.44	12.24	8.44	11.48
8.46	12.21	8.47	11.29
8.49	12.80	8.50	11.43
8.52	13.32	8.52	11.33
8.54	14.53	8.55	11.24
8.57	18.50	8.58	11.35
8.60	21.84	8.60	12.15
8.62	18.65	8.63	12.39
8.65	18.30	8.66	13.11
8.68	20.65	8.68	13.48
8.70	20.77	8.71	13.80
8.73	19.39	8.74	13.29
8.76	18.00	8.76	13.47
8.78	17.53	8.79	13.80
8.81	17.08	8.82	13.43
8.84	17.37	8.84	13.60
8.86	15.87	8.87	11.77
8.06	9.31		
8.09	9.18		
8.12	8.81		
8.14	8.84		
8.17	8.75		
8.20	8.32		
8.22	8.77		
8.25	8.46		
8.28	8.94		
8.30	8.53		
8.33	7.27		
8.36	6.20		
8.39	5.72		
8.41	5.30		
8.44	4.90		
8.47	4.61		
8.49	4.88		
8.52	5.39		
8.55	6.71		
8.57	9.20		
8.60	10.34		
8.63	9.03		
8.66	8.29		
8.68	8.11		
8.71	8.02		
8.74	7.22		

8.89	17.80	8.90	10.87
8.92	17.85	8.92	10.32
8.94	16.85	8.95	10.49
8.97	18.01	8.98	11.43
9.00	19.08	9.00	12.61
9.02	18.87	9.03	12.45
9.05	17.83	9.06	12.83
9.08	17.28	9.08	13.47
9.10	16.69	9.11	14.35
9.13	15.47	9.14	14.87
9.16	14.26	9.16	15.10
9.18	14.37	9.19	15.04
9.21	15.73	9.22	14.94
9.24	14.45	9.24	15.81
9.26	13.81	9.27	15.92
9.29	14.00	9.30	16.47
9.32	14.19	9.33	15.11
9.34	13.38	9.35	14.55
9.37	13.19	9.38	15.33
9.40	12.76	9.41	18.45
9.42	13.45	9.43	18.29
9.45	14.87	9.46	16.80
9.48	14.55	9.49	16.00
9.50	14.85	9.51	14.97
9.53	14.41	9.54	14.46
9.56	14.27	9.57	14.13
9.58	14.59	9.59	14.75
9.61	13.65	9.62	14.16
9.64	13.35	9.65	14.44
9.66	12.87	9.67	14.85
9.69	12.45	9.70	14.31
9.72	13.03	9.73	14.49
9.75	12.69	9.75	14.53
9.77	14.17	9.78	14.10

9.80	14.16	9.81	13.88
9.83	12.75	9.83	14.19
9.85	11.65	9.86	14.41
9.88	11.48	9.89	14.86
9.91	11.16	9.91	15.38
9.93	11.16	9.94	14.33
9.96	10.94	9.97	14.19
9.99	10.87	9.99	14.34
10.01	10.85	10.02	15.24
10.04	10.44	10.05	15.07
10.07	8.52	10.07	14.96
10.09	7.52	10.10	13.83
10.12	7.63	10.13	12.60
10.15	8.02	10.15	13.34
10.17	8.20	10.18	12.89
10.20	8.51	10.21	13.98
10.23	8.25	10.23	14.29
10.25	7.37	10.26	13.18
10.28	6.30	10.29	13.13
10.31	5.12	10.31	12.78
10.33	4.91	10.34	12.99
10.36	5.43	10.37	12.83
10.39	5.50	10.39	12.53
10.41	5.18	10.42	12.00
10.44	5.12	10.45	11.32
10.47	5.92	10.47	11.35
10.49	6.82	10.50	11.63
		10.53	12.08
		10.55	11.96
		10.58	11.83
		10.61	11.60
		10.63	11.74
		10.66	11.48
		10.69	11.66

10.71	11.55
10.74	11.88
10.77	11.34
10.79	11.74
10.82	11.78
10.85	11.81
10.87	11.57
10.90	12.45
10.93	13.79
10.96	14.49
10.98	13.81
11.01	13.32
11.04	13.74
11.06	13.84
11.09	14.00
11.12	15.31
11.14	16.04
11.17	15.94
11.20	17.24
11.22	17.88
11.25	17.96
11.28	17.53
11.30	17.58
11.33	16.82
11.36	16.54
11.38	15.96
11.41	15.19
11.44	14.95
11.46	14.95
11.49	14.95
11.52	15.48
11.54	15.14
11.57	14.37
11.60	15.61

11.62	16.21
11.65	15.52
11.68	13.83
11.70	12.19
11.73	13.06
11.76	15.84
11.78	17.04
11.81	16.46
11.84	15.58
11.86	14.84
11.89	14.02
11.92	14.27
11.94	14.02
11.97	15.68
12.00	16.72
12.02	21.52
12.05	22.19
12.08	19.32
12.10	17.98
12.13	18.23
12.16	18.28
12.18	16.48
12.21	16.16
12.24	16.13
12.26	15.81
12.29	15.48
12.32	15.26
12.34	14.76
12.37	16.07
12.40	18.75
12.42	17.72
12.45	14.66
12.48	14.81
12.50	14.95

12.53	14.94
12.56	16.73
12.59	16.19
12.61	16.49
12.64	17.06
12.67	15.99
12.69	15.91
12.72	15.62
12.75	15.95
12.77	16.79
12.80	17.36
12.83	17.10
12.85	16.15
12.88	17.47
12.91	17.21
12.93	15.53
12.96	15.61
12.99	15.75
13.01	16.52
13.04	15.87
13.07	15.64
13.09	14.91
13.12	13.75
13.15	13.75
13.17	14.07
13.20	13.76
13.23	13.34
13.25	13.91
13.28	13.55
13.31	13.18
13.33	14.10
13.36	14.34
13.39	14.44
13.41	13.43

13.44	13.28
13.47	14.73
13.49	14.52
13.52	13.95
13.55	13.16
13.57	12.98
13.60	13.63
13.63	12.36
13.65	11.95
13.68	12.01
13.71	11.57
13.73	12.15
13.76	12.29
13.79	11.94
13.81	11.95
13.84	12.13
13.87	12.00
13.89	11.05
13.92	10.72
13.95	10.32
13.97	10.84
14.00	11.87
14.03	11.85
14.05	11.24
14.08	11.05
14.11	11.04
14.13	10.80
14.16	10.71
14.19	9.84
14.22	9.75
14.24	9.80
14.27	9.57
14.30	10.41
14.32	10.19

14.35	10.35
14.38	10.11
14.40	9.79
14.43	9.01
14.46	9.32
14.48	9.13
14.51	8.80
14.54	8.72
14.56	8.31
14.59	8.35
14.62	8.65
14.64	9.04
14.67	10.33
14.70	10.94
14.72	11.20
14.75	10.91

Table A4.8. Moreton Bay *Saccostrea glomerata* Mg/Ca ratios.

MBSg905 Distance along growth axis (mm)	MBSg905 Mg/Ca (mmol/mol)	MBSg909 Distance along growth axis (mm)	MBSg909 Mg/Ca (mmol/mol)	MBSg945 Distance along growth axis (mm)	MBSg945 Mg/Ca (mmol/mol)	MBSg960 Distance along growth axis (mm)	MBSg960 Mg/Ca (mmol/mol)	MBSg981 Distance along growth axis (mm)	MBSg981 Mg/Ca (mmol/mol)	MBSg997 Distance along growth axis (mm)	MBSg997 Mg/Ca (mmol/mol)
0.00	25.17	0.00	26.23	0.00	15.01	0.00	30.25	0.00	26.89	0.00	48.77
0.02	24.07	0.02	23.24	0.02	10.95	0.03	18.98	0.02	22.03	0.04	52.15
0.05	22.49	0.05	21.64	0.04	9.03	0.05	15.45	0.05	19.60	0.08	41.65
0.08	20.08	0.07	23.12	0.07	9.08	0.08	16.90	0.08	16.77	0.12	37.14
0.11	19.50	0.10	22.06	0.10	7.76	0.11	16.85	0.10	18.08	0.16	37.09
0.13	18.94	0.13	18.79	0.12	9.64	0.13	18.46	0.13	21.38	0.20	30.81
0.16	18.66	0.15	17.64	0.15	15.62	0.16	27.40	0.16	22.82	0.24	28.33
0.19	19.17	0.18	17.09	0.18	18.94	0.19	28.41	0.18	23.37	0.28	25.37
0.21	21.32	0.21	19.27	0.20	18.41	0.22	18.36	0.21	21.69	0.32	26.55
0.24	21.40	0.23	21.08	0.23	18.79	0.24	13.93	0.24	20.02	0.36	26.37
0.27	21.46	0.26	20.91	0.26	19.43	0.27	15.00	0.26	17.67	0.40	24.55
0.30	22.76	0.29	20.72	0.29	18.57	0.30	17.06	0.29	17.91	0.44	24.36
0.32	22.72	0.32	20.51	0.31	19.14	0.32	18.06	0.32	17.92	0.48	23.82
0.35	22.64	0.34	19.61	0.34	19.83	0.35	18.70	0.34	17.95	0.52	22.55
0.38	23.16	0.37	17.67	0.37	20.89	0.38	19.35	0.37	19.58	0.56	20.28
0.41	21.28	0.40	15.45	0.39	23.78	0.40	20.25	0.40	19.62	0.60	18.53
0.43	20.39	0.42	17.22	0.42	23.80	0.43	20.70	0.43	20.04	0.64	21.55
0.46	16.91	0.45	17.72	0.45	23.45	0.46	20.61	0.45	19.30	0.68	24.18
0.49	13.66	0.48	18.56	0.47	26.71	0.49	21.60	0.48	17.16	0.72	22.36
0.51	11.61	0.50	18.85	0.50	32.32	0.51	20.27	0.51	16.17	0.76	19.90
0.54	10.58	0.53	19.96	0.53	31.29	0.54	21.13	0.53	17.10	0.80	15.71
0.57	9.25	0.56	18.40	0.55	23.17	0.57	21.06	0.56	17.97	0.84	15.34
0.60	8.83	0.58	15.93	0.58	20.24	0.59	20.37	0.59	16.80	0.88	11.67
0.62	8.52	0.61	16.94	0.61	19.27	0.62	20.22	0.61	16.39	0.92	10.37
0.65	8.31	0.64	16.74	0.63	20.35	0.65	20.48	0.64	16.48	0.96	19.25
0.68	8.03	0.67	15.96	0.66	22.41	0.67	20.87	0.67	16.22	1.00	23.64
0.70	7.95	0.69	17.08	0.69	21.04	0.70	20.12	0.69	15.97	1.04	20.85

0.73	7.95	0.72	17.41	0.72	19.14	0.73	21.64	0.72	15.15	1.08	18.35
0.76	7.82	0.75	17.25	0.74	19.56	0.75	21.33	0.75	15.89	1.12	16.13
0.79	7.80	0.77	16.01	0.77	21.33	0.78	18.27	0.78	15.91	1.16	14.40
0.81	8.08	0.80	14.41	0.80	25.36	0.81	18.15	0.80	15.85	1.20	16.71
0.84	8.61	0.83	15.22	0.82	27.35	0.84	20.99	0.83	14.97	1.24	16.00
0.87	9.86	0.85	16.38	0.85	27.10	0.86	21.03	0.86	16.71	1.28	17.29
0.90	11.24	0.88	15.83	0.88	27.60	0.89	22.64	0.88	18.14	1.32	18.42
0.92	11.45	0.91	13.91	0.90	26.17	0.92	23.84	0.91	19.76	1.36	17.27
0.95	12.64	0.93	14.64	0.93	24.24	0.94	24.48	0.94	19.82	1.40	16.96
0.98	15.04	0.96	15.01	0.96	22.24	0.97	22.83	0.96	18.74	1.44	17.59
1.00	18.32	0.99	16.09	0.98	21.70	1.00	21.84	0.99	17.33	1.48	15.42
1.03	21.43	1.02	15.07	1.01	21.70	1.02	22.97	1.02	16.87	1.52	15.90
1.06	21.03	1.04	12.74	1.04	23.27	1.05	24.06	1.05	17.55	1.56	16.39
1.09	20.01	1.07	12.65	1.07	23.41	1.08	23.15	1.07	16.63	1.60	15.86
1.11	16.66	1.10	13.45	1.09	24.80	1.10	23.53	1.10	16.17	1.64	16.43
1.14	13.04	1.12	14.17	1.12	23.06	1.13	23.19	1.13	15.23	1.68	17.28
1.17	12.57	1.15	14.44	1.15	19.45	1.16	24.86	1.15	15.58	1.72	16.92
1.19	12.51	1.18	13.76	1.17	19.58	1.19	25.72	1.18	14.96	1.76	17.59
1.22	13.28	1.20	12.64	1.20	20.87	1.21	23.92	1.21	15.67	1.80	14.36
1.25	14.63	1.23	12.56	1.23	24.16	1.24	24.59	1.23	16.51	1.84	14.54
1.28	14.60	1.26	13.77	1.25	24.50	1.27	24.12	1.26	15.14	1.88	15.56
1.30	13.56	1.29	14.42	1.28	19.54	1.29	23.88	1.29	15.15	1.92	16.00
1.33	12.51	1.31	13.84	1.31	17.08	1.32	26.41	1.31	14.72	1.96	16.08
1.36	13.20	1.34	14.02	1.33	15.26	1.35	26.74	1.34	14.84	2.00	15.22
1.39	13.21	1.37	13.71	1.36	14.70	1.37	25.05	1.37	15.20	2.04	14.85
1.41	12.89	1.39	13.04	1.39	16.13	1.40	25.61	1.40	15.72	2.08	15.17
1.44	13.56	1.42	15.19	1.41	17.28	1.43	22.63	1.42	15.49	2.12	16.91
1.47	15.57	1.45	17.09	1.44	14.39	1.46	20.12	1.45	16.33	2.16	15.73
1.49	15.61	1.47	17.60	1.47	14.01	1.48	17.44	1.48	17.69	2.20	14.15
1.52	15.66	1.50	19.16	1.50	16.14	1.51	15.90	1.50	17.63	2.24	14.09
1.55	15.82	1.53	22.40	1.52	16.82	1.54	16.02	1.53	15.49	2.28	14.61
1.58	16.07	1.55	23.53	1.55	16.03	1.56	15.81	1.56	14.54	2.32	14.67
1.60	16.20	1.58	20.93	1.58	15.50	1.59	15.66	1.58	15.13	2.36	16.19
1.63	15.89	1.61	18.56	1.60	15.50	1.62	17.14	1.61	15.55	2.40	15.59

1.66	16.87	1.64	18.58	1.63	14.42	1.64	18.07	1.64	16.31	2.44	15.03
1.68	17.67	1.66	17.31	1.66	14.79	1.67	18.52	1.66	17.66	2.48	14.02
1.71	18.00	1.69	16.10	1.68	15.46	1.70	18.25	1.69	19.05	2.52	13.61
1.74	18.25	1.72	16.26	1.71	15.54	1.72	17.23	1.72	17.11	2.56	14.64
1.77	17.09	1.74	16.94	1.74	16.44	1.75	17.03	1.75	18.97	2.60	15.62
1.79	15.96	1.77	17.39	1.76	15.50	1.78	16.34	1.77	19.18	2.64	16.01
1.82	15.20	1.80	18.42	1.79	15.09	1.81	16.65	1.80	18.96	2.68	15.03
1.85	14.82	1.82	18.94	1.82	14.33	1.83	19.21	1.83	17.37	2.72	15.40
1.88	14.71	1.85	21.76	1.84	14.71	1.86	21.11	1.85	15.08	2.76	14.70
1.90	15.26	1.88	19.99	1.87	15.84	1.89	20.68	1.88	16.18	2.80	13.56
1.93	14.59	1.90	22.00	1.90	16.57	1.91	18.22	1.91	19.28	2.84	13.78
1.96	12.96	1.93	20.39	1.93	15.25	1.94	17.98	1.93	18.06	2.88	14.51
1.98	11.81	1.96	20.40	1.95	14.11	1.97	19.17	1.96	15.41	2.92	13.82
2.01	12.55	1.99	20.68	1.98	15.34	1.99	19.97	1.99	15.58	2.96	13.78
2.04	13.69	2.01	19.79	2.01	15.62	2.02	20.58	2.01	16.47	3.00	13.57
2.07	14.82	2.04	19.26	2.03	16.06	2.05	21.52	2.04	17.56	3.04	14.01
2.09	14.93	2.07	19.58	2.06	15.98	2.07	21.11	2.07	17.66	3.08	13.84
2.12	13.69	2.09	17.86	2.09	15.91	2.10	22.64	2.10	17.49	3.12	14.30
2.15	14.21	2.12	16.78	2.11	15.44	2.13	29.11	2.12	15.26	3.16	14.32
2.17	15.37	2.15	17.69	2.14	14.41	2.16	29.40	2.15	13.58	3.20	14.08
2.20	14.64	2.17	18.41	2.17	15.18	2.18	21.22	2.18	13.81	3.24	14.97
2.23	14.78	2.20	18.32	2.19	16.24	2.21	18.71	2.20	14.08	3.28	15.01
2.26	14.35	2.23	20.17	2.22	16.08	2.24	19.95	2.23	14.31	3.32	14.99
2.28	13.94	2.26	23.00	2.25	15.09	2.26	18.25	2.26	13.50	3.36	14.79
2.31	15.66	2.28	20.58	2.28	14.42	2.29	17.40	2.28	13.16	3.40	13.99
2.34	20.67	2.31	21.85	2.30	14.69	2.32	17.52	2.31	13.55	3.44	14.08
2.37	18.02	2.34	19.97	2.33	14.19	2.34	17.56	2.34	13.66	3.48	14.29
2.39	15.09	2.36	16.67	2.36	13.99	2.37	17.16	2.37	13.12	3.52	13.83
2.42	14.04	2.39	16.40	2.38	14.67	2.40	15.86	2.39	12.46	3.56	13.80
2.45	13.81	2.42	16.47	2.41	14.35	2.43	15.90	2.42	13.43	3.60	13.94
2.47	13.93	2.44	16.99	2.44	14.05	2.45	16.62	2.45	13.52	3.64	13.65
2.50	14.16	2.47	18.85	2.46	15.06	2.48	15.53	2.47	12.74	3.68	13.97
2.53	15.61	2.50	19.08	2.49	15.95	2.51	15.64	2.50	13.47	3.72	14.62
2.56	17.14	2.52	20.21	2.52	16.66	2.53	17.05	2.53	13.60	3.76	15.09

2.58	16.29	2.55	20.93	2.54	17.63	2.56	17.33	2.55	13.83	3.80	15.81
2.61	16.58	2.58	21.45	2.57	18.24	2.59	17.53	2.58	13.02	3.84	16.06
2.64	16.06	2.61	22.13	2.60	17.97	2.61	16.55	2.61	12.29	3.88	16.25
2.66	15.72	2.63	21.06	2.63	17.23	2.64	15.81	2.63	12.28	3.92	18.38
2.69	15.18	2.66	22.57	2.65	17.11	2.67	14.92	2.66	12.98	3.96	18.87
2.72	15.21	2.69	24.19	2.68	16.61	2.69	14.06	2.69	14.69	4.00	18.26
2.75	15.53	2.71	22.95	2.71	15.85	2.72	13.19	2.72	15.94	4.04	18.32
2.77	14.79	2.74	22.52	2.73	16.75	2.75	12.30	2.74	14.94	4.08	17.34
2.80	15.09	2.77	21.65	2.76	17.48	2.78	12.26	2.77	12.42	4.12	16.68
2.83	15.52	2.79	22.26	2.79	16.77	2.80	12.80	2.80	12.97	4.16	18.58
2.86	16.15	2.82	24.46	2.81	16.27	2.83	12.45	2.82	13.03	4.20	18.57
2.88	16.34	2.85	23.66	2.84	16.09	2.86	12.23	2.85	13.63	4.24	19.74
2.91	16.41	2.87	20.96	2.87	16.15	2.88	12.28	2.88	13.35	4.28	19.70
2.94	15.81	2.90	20.52	2.89	15.69	2.91	12.42	2.90	12.62	4.32	19.05
2.96	15.69	2.93	18.37	2.92	16.35	2.94	12.49	2.93	13.02	4.36	19.74
2.99	16.29	2.96	18.76	2.95	20.03	2.96	12.81	2.96	13.52	4.40	20.21
3.02	14.91	2.98	21.25	2.97	21.75	2.99	11.99	2.98	13.64	4.44	19.71
3.05	15.07	3.01	22.76	3.00	23.62	3.02	12.21	3.01	14.53	4.48	20.95
3.07	16.56	3.04	24.47	3.03	21.95	3.05	11.64	3.04	14.82	4.52	21.73
3.10	18.47	3.06	25.92	3.06	20.26	3.07	11.13	3.07	14.90	4.56	21.29
3.13	18.90	3.09	26.01	3.08	21.10	3.10	11.62	3.09	15.93	4.60	21.53
3.15	18.83	3.12	24.07	3.11	19.84	3.13	12.13	3.12	14.83	4.64	20.54
3.18	18.35	3.14	21.32	3.14	20.21	3.15	12.76	3.15	13.83	4.68	19.19
3.21	17.30	3.17	22.84	3.16	20.32	3.18	12.88	3.17	13.80	4.72	19.49
3.24	17.08	3.20	22.86	3.19	19.94	3.21	12.28	3.20	14.09	4.76	20.90
3.26	15.45	3.23	21.50	3.22	22.86	3.23	11.89	3.23	13.87	4.80	20.77
3.29	16.21	3.25	20.81	3.24	21.28	3.26	11.83	3.25	13.82	4.84	21.46
3.32	17.83	3.28	21.13	3.27	18.63	3.29	11.58	3.28	15.60	4.88	21.49
3.35	17.65	3.31	22.27	3.30	18.53	3.31	11.33	3.31	16.75	4.92	21.06
3.37	16.62	3.33	22.33	3.32	18.99	3.34	11.40	3.33	17.38	4.96	20.65
3.40	16.67	3.36	22.36	3.35	18.87	3.37	11.42	3.36	18.25	5.00	19.96
3.43	17.70	3.39	21.93	3.38	19.13	3.40	10.97	3.39	20.29	5.04	19.95
3.45	18.09	3.41	21.41	3.41	19.47	3.42	11.44	3.42	18.85	5.08	19.48
3.48	19.24	3.44	21.36	3.43	19.63	3.45	11.85	3.44	17.19	5.12	19.35

3.51	18.17	3.47	20.40	3.46	19.71	3.48	11.58	3.47	17.60	5.16	18.76
3.54	17.06	3.49	19.87	3.49	20.17	3.50	10.97	3.50	17.44	5.20	18.15
3.56	16.49	3.52	22.15	3.51	21.24	3.53	10.84	3.52	18.17	5.24	20.07
3.59	17.62	3.55	22.07	3.54	21.92	3.56	11.05	3.55	18.79	5.28	22.34
3.62	18.16	3.58	20.94	3.57	22.51	3.58	11.13	3.58	17.42	5.32	21.10
3.64	18.95	3.60	20.17	3.59	20.99	3.61	11.37	3.60	16.28	5.36	19.01
3.67	18.85	3.63	21.29	3.62	21.53	3.64	11.67	3.63	15.77	5.40	18.12
3.70	19.66	3.66	21.68	3.65	22.66	3.66	11.82	3.66	16.22	5.44	18.87
3.73	19.30	3.68	21.31	3.67	21.39	3.69	12.36	3.69	18.21	5.48	19.21
3.75	19.94	3.71	21.27	3.70	20.33	3.72	13.30	3.71	19.62	5.52	19.78
3.78	20.83	3.74	20.23	3.73	20.00	3.75	13.23	3.74	17.75	5.56	19.96
3.81	20.71	3.76	20.94	3.75	20.31	3.77	14.20	3.77	17.70	5.60	19.23
3.84	19.97	3.79	20.72	3.78	20.20	3.80	13.57	3.79	20.91	5.64	18.14
3.86	17.86	3.82	21.23	3.81	18.87	3.83	12.66	3.82	23.41	5.68	17.47
3.89	18.02	3.84	20.25	3.84	17.54	3.85	12.62	3.85	20.71	5.72	19.75
3.92	19.38	3.87	21.25	3.86	18.62	3.88	13.56	3.87	20.28	5.76	19.87
3.94	18.04	3.90	22.86	3.89	20.32	3.91	14.56	3.90	20.08	5.80	19.94
3.97	16.07	3.93	22.82	3.92	21.76	3.93	15.11	3.93	20.68	5.84	18.86
4.00	15.13	3.95	22.32	3.94	21.93	3.96	15.20	3.95	19.76	5.88	19.16
4.03	15.92	3.98	21.46	3.97	21.36	3.99	14.42	3.98	19.43	5.92	19.83
4.05	17.04	4.01	22.71	4.00	20.00	4.02	14.49	4.01	19.63	5.97	19.44
4.08	17.89	4.03	23.92	4.02	19.06	4.04	14.21	4.04	19.51	6.01	19.37
4.11	19.05	4.06	23.70	4.05	18.30	4.07	13.36	4.06	19.50	6.05	18.51
4.13	19.04	4.09	22.54	4.08	17.29	4.10	12.94	4.09	19.53	6.09	18.71
4.16	18.56	4.11	20.92	4.10	18.62	4.12	13.03	4.12	20.43	6.13	18.47
4.19	19.25	4.14	21.16	4.13	19.41	4.15	12.84	4.14	19.44	6.17	16.99
4.22	18.63	4.17	21.45	4.16	19.55	4.18	12.56	4.17	20.14	6.21	15.71
4.24	18.50	4.20	21.14	4.18	19.65	4.20	12.71	4.20	19.93	6.25	16.63
4.27	18.51	4.22	20.89	4.21	20.42	4.23	13.68	4.22	20.63	6.29	17.87
4.30	17.57	4.25	20.67	4.24	20.48	4.26	14.14	4.25	19.69	6.33	19.23
4.33	18.10	4.28	20.45	4.27	19.61	4.28	13.80	4.28	17.93	6.37	19.58
4.35	18.93	4.30	20.49	4.29	18.46	4.31	14.09	4.30	16.41	6.41	19.36
4.38	18.38	4.33	21.81	4.32	19.26	4.34	14.67	4.33	15.28	6.45	19.11
4.41	17.46	4.36	22.72	4.35	20.80	4.37	14.53	4.36	15.51	6.49	18.28

4.43	16.85	4.38	22.81	4.37	21.98	4.39	16.36	4.39	16.45	6.53	17.40
4.46	16.95	4.41	22.78	4.40	22.78	4.42	16.56	4.41	16.55	6.57	17.80
4.49	17.13	4.44	22.58	4.43	25.39	4.45	16.31	4.44	15.57	6.61	18.16
4.52	16.01	4.46	23.09	4.45	25.68	4.47	15.47	4.47	17.20	6.65	17.54
4.54	15.05	4.49	22.67	4.48	26.14	4.50	15.05	4.49	18.11	6.69	16.62
4.57	14.31	4.52	23.42	4.51	24.78	4.53	14.78	4.52	16.92	6.73	16.09
4.60	16.68	4.55	22.59	4.53	22.48	4.55	13.67	4.55	17.29	6.77	16.53
4.62	18.66	4.57	22.07	4.56	20.78	4.58	12.49	4.57	17.04	6.81	18.16
4.65	18.80	4.60	22.63	4.59	20.97	4.61	12.57	4.60	18.03	6.85	19.54
4.68	17.72	4.63	23.45	4.62	21.62	4.63	11.39	4.63	17.89	6.89	18.71
4.71	16.66	4.65	24.49	4.64	21.16	4.66	11.34	4.65	22.91	6.93	18.16
4.73	16.02	4.68	23.08	4.67	22.85	4.69	10.71	4.68	24.46	6.97	18.07
4.76	16.93	4.71	21.98	4.70	25.11	4.72	10.63	4.71	23.35	7.01	18.08
4.79	17.99	4.73	22.01	4.72	24.34	4.74	11.18	4.74	22.44	7.05	18.65
4.82	18.79	4.76	21.28	4.75	21.25	4.77	11.85	4.76	23.38	7.09	19.92
4.84	19.48	4.79	20.28	4.78	20.99	4.80	12.51	4.79	23.27	7.13	18.93
4.87	18.54	4.81	20.67	4.80	21.18	4.82	13.22	4.82	22.64	7.17	16.81
4.90	18.21	4.84	22.01	4.83	21.95	4.85	13.57	4.84	21.08	7.21	14.75
4.92	19.48	4.87	23.27	4.86	20.68	4.88	12.71	4.87	21.47	7.25	14.74
4.95	20.33	4.90	22.43	4.88	20.58	4.90	12.32	4.90	22.38	7.29	13.80
4.98	19.99	4.92	22.30	4.91	20.88	4.93	12.71	4.92	21.17	7.33	13.84
5.01	21.58	4.95	21.67	4.94	22.87	4.96	13.54	4.95	21.31	7.37	14.41
5.03	21.74	4.98	21.07	4.96	23.90	4.99	12.93	4.98	21.58	7.41	15.13
5.06	21.14	5.00	20.88	4.99	26.24	5.01	13.43	5.00	20.22	7.45	15.43
5.09	19.73	5.03	20.62	5.02	24.23	5.04	13.63	5.03	21.45	7.49	15.83
5.11	19.04	5.06	21.00	5.05	24.57	5.07	13.67	5.06	21.86	7.53	15.47
5.14	18.75	5.08	22.86	5.07	25.19	5.09	14.02	5.09	22.95	7.57	16.37
5.17	18.26	5.11	22.67	5.10	23.44	5.12	14.57	5.11	22.31	7.61	17.54
5.20	19.12	5.14	22.72	5.13	23.42	5.15	14.07	5.14	22.20	7.65	25.28
5.22	20.59	5.17	23.22	5.15	25.56	5.17	13.44	5.17	22.97	7.69	24.98
5.25	20.26	5.19	23.14	5.18	24.41	5.20	12.23	5.19	23.25	7.73	15.19
5.28	20.58	5.22	24.08	5.21	20.35	5.23	11.53	5.22	22.54	7.77	14.14
5.31	20.71	5.25	25.91	5.23	19.94	5.25	11.64	5.25	21.88	7.81	13.45
5.33	21.67	5.27	24.24	5.26	19.99	5.28	11.47	5.27	21.71	7.85	12.07

5.36	21.70	5.30	23.83	5.29	20.61	5.31	11.00	5.30	21.01	7.89	12.34
5.39	23.01	5.33	27.76	5.31	18.72	5.34	10.44	5.33	22.44	7.93	13.39
5.41	22.06	5.35	28.34	5.34	18.92	5.36	11.24	5.35	22.96	7.97	14.12
5.44	20.59	5.38	29.69	5.37	19.46	5.39	11.43	5.38	22.78	8.01	13.55
5.47	20.26	5.41	28.03	5.39	18.54	5.42	11.92	5.41	22.41	8.05	12.77
5.50	22.46	5.43	27.32	5.42	16.81	5.44	12.79	5.44	20.99	8.09	12.19
5.52	23.81	5.46	27.42	5.45	16.64	5.47	12.71	5.46	20.00	8.13	11.25
5.55	24.35	5.49	28.30	5.48	16.47	5.50	12.75	5.49	19.34	8.17	11.78
5.58	22.50	5.52	29.84	5.50	15.92	5.52	12.91	5.52	20.99	8.21	11.16
5.60	22.33	5.54	30.89	5.53	15.68	5.55	13.57	5.54	20.85	8.25	11.38
5.63	23.01	5.57	29.90	5.56	15.65	5.58	14.32	5.57	20.60	8.29	12.50
5.66	23.07	5.60	30.80	5.58	17.26	5.61	14.32	5.60	22.35	8.33	12.83
5.69	20.98	5.62	29.10	5.61	17.46	5.63	14.86	5.62	22.65	8.37	12.98
5.71	19.85	5.65	27.72	5.64	18.59	5.66	14.78	5.65	22.62	8.41	13.06
5.74	19.48	5.68	27.70	5.66	19.59	5.69	14.49	5.68	20.45	8.45	13.73
5.77	19.98	5.70	26.54	5.69	17.90	5.71	14.00	5.71	19.52	8.49	14.84
5.80	20.22	5.73	29.25	5.72	18.05	5.74	13.43	5.73	20.69	8.53	14.70
5.82	20.23	5.76	30.19	5.74	18.68	5.77	14.04	5.76	22.53	8.57	14.70
5.85	20.34	5.78	27.59	5.77	18.43	5.79	16.63	5.79	23.43	8.61	14.80
5.88	21.20	5.81	28.28	5.80	18.42	5.82	17.77	5.81	23.58	8.65	14.23
5.90	21.15	5.84	30.43	5.83	17.48	5.85	18.30	5.84	22.14	8.69	13.49
5.93	21.37	5.87	28.11	5.85	17.40	5.87	18.92	5.87	20.04	8.73	13.07
5.96	20.52	5.89	28.17	5.88	17.15	5.90	17.91	5.89	19.19	8.77	13.16
5.99	21.00	5.92	28.07	5.91	16.90	5.93	18.69	5.92	19.06	8.81	12.37
6.01	21.67	5.95	27.60	5.93	16.53	5.96	19.48	5.95	20.23	8.85	12.01
6.04	23.03	5.97	25.72	5.96	16.48	5.98	20.11	5.97	19.89	8.89	11.66
6.07	22.73	6.00	24.92	5.99	15.61	6.01	19.73	6.00	20.32	8.93	12.21
6.09	22.31	6.03	24.29	6.01	15.14	6.04	18.42	6.03	20.24	8.97	12.19
6.12	20.54	6.05	25.19	6.04	16.16	6.06	18.75	6.06	21.83	9.01	12.15
6.15	19.44	6.08	25.64	6.07	17.42	6.09	19.56	6.08	23.05	9.05	12.43
6.18	18.96	6.11	26.23	6.09	16.65	6.12	19.41	6.11	23.13	9.09	12.95
6.20	20.19	6.14	26.76	6.12	16.76	6.14	20.44	6.14	24.24	9.13	13.11
6.23	21.35	6.16	26.63	6.15	15.74	6.17	22.09	6.16	22.70	9.17	12.82
6.26	21.40	6.19	27.77	6.17	14.92	6.20	22.91	6.19	25.68	9.21	11.69

6.29	21.38	6.22	28.56	6.20	14.46	6.23	22.67	6.22	29.88	9.25	10.97
6.31	20.74	6.24	30.16	6.23	13.53	6.25	21.24	6.24	31.59	9.29	11.40
6.34	20.23	6.27	29.83	6.26	12.33	6.28	20.51	6.27	32.40	9.33	12.12
6.37	20.89	6.30	27.53	6.28	12.20	6.31	21.53	6.30	31.63	9.37	11.44
6.39	21.78	6.32	25.67	6.31	12.81	6.33	21.27	6.32	27.88	9.41	11.77
6.42	22.11	6.35	26.85	6.34	12.68	6.36	20.94	6.35	26.55	9.45	12.74
6.45	20.53	6.38	24.18	6.36	11.92	6.39	20.24	6.38	24.18	9.49	11.66
6.48	18.87	6.40	23.39	6.39	12.74	6.41	19.67	6.41	22.04	9.53	11.36
6.50	18.60	6.43	23.90	6.42	13.39	6.44	19.19	6.43	21.56	9.57	13.64
6.53	19.26	6.46	24.96	6.44	13.01	6.47	19.00	6.46	21.85	9.61	15.05
6.56	19.50	6.49	25.37	6.47	13.32	6.49	18.85	6.49	21.14	9.65	14.02
6.58	19.94	6.51	24.71	6.50	12.88	6.52	20.49	6.51	22.77	9.69	13.45
6.61	18.88	6.54	24.20	6.52	12.55	6.55	20.11	6.54	22.88	9.73	12.53
6.64	17.63	6.57	25.39	6.55	12.70	6.58	18.59	6.57	21.85	9.77	11.82
6.67	17.67	6.59	27.46	6.58	13.58	6.60	16.22	6.59	20.94	9.81	12.15
6.69	19.50	6.62	27.84	6.61	13.10	6.63	16.16	6.62	20.79	9.85	12.30
6.72	16.53	6.65	28.62	6.63	14.43	6.66	16.28	6.65	22.40	9.89	12.15
6.75	13.73	6.67	26.82	6.66	16.39	6.68	16.83	6.67	22.48	9.93	12.07
6.78	13.62	6.70	25.37	6.69	15.28	6.71	15.38	6.70	22.98	9.97	12.12
6.80	15.08	6.73	25.05	6.71	14.02	6.74	15.02	6.73	22.82	10.01	12.27
6.83	16.63	6.75	24.18	6.74	13.90	6.76	14.85	6.76	21.30	10.05	12.12
6.86	16.51	6.78	24.30	6.77	14.45	6.79	16.04	6.78	20.58	10.09	12.49
6.88	17.62	6.81	23.81	6.79	14.91	6.82	16.61	6.81	20.31	10.13	12.75
6.91	16.64	6.84	23.44			6.84	14.98	6.84	23.69	10.17	12.63
6.94	15.56	6.86	22.04			6.87	14.50	6.86	20.71	10.21	12.31
6.97	15.27	6.89	21.64			6.90	14.48	6.89	16.83	10.25	12.62
6.99	16.61	6.92	22.06			6.93	15.15	6.92	16.71	10.29	12.29
7.02	17.08	6.94	23.62			6.95	15.65	6.94	17.97	10.33	12.27
7.05	16.51	6.97	24.75			6.98	15.99	6.97	19.75	10.37	12.52
7.07	16.10	7.00	24.82			7.01	16.69	7.00	20.13	10.41	13.71
7.10	16.56	7.02	21.47			7.03	15.97	7.03	21.35	10.45	13.96
7.13	15.80	7.05	21.22			7.06	15.34	7.05	20.46	10.49	13.01
7.16	16.11	7.08	24.29			7.09	14.93	7.08	20.59	10.53	14.01
7.18	15.79	7.11	26.25			7.11	15.72	7.11	21.02	10.57	15.02

7.21	15.63	7.13	25.53	7.14	16.04	7.13	19.34	10.61	14.38
7.24	15.05	7.16	26.85	7.17	16.05	7.16	18.85	10.65	13.59
7.27	14.31	7.19	24.75	7.20	16.12	7.19	18.58	10.69	13.47
7.29	14.67	7.21	23.76	7.22	16.04	7.21	19.17	10.73	13.61
7.32	16.14	7.24	23.87	7.25	15.70	7.24	20.90	10.77	13.73
7.35	16.46	7.27	23.24	7.28	14.87	7.27	20.07	10.81	12.39
7.37	14.69	7.29	20.76	7.30	15.34	7.29	18.60	10.85	11.59
7.40	14.01	7.32	19.93	7.33	16.94	7.32	19.15	10.89	12.54
7.43	14.75	7.35	19.53	7.36	16.25	7.35	19.24	10.93	14.02
7.46	15.50	7.37	20.73	7.38	15.45	7.38	19.45	10.97	14.48
7.48	15.44	7.40	19.47	7.41	15.01	7.40	19.48	11.01	14.82
7.51	15.15	7.43	19.94	7.44	14.62	7.43	17.54	11.05	15.36
7.54	15.03	7.46	20.41	7.46	15.55	7.46	17.00	11.09	14.99
7.56	15.95	7.48	18.94	7.49	16.71	7.48	17.80	11.13	15.31
7.59	15.43	7.51	19.28	7.52	18.09	7.51	18.23	11.17	14.88
7.62	14.87	7.54	18.38	7.55	18.89	7.54	18.43	11.21	15.23
7.65	14.89	7.56	17.77	7.57	17.77	7.56	18.22	11.25	14.75
7.67	14.28	7.59	17.60	7.60	17.70	7.59	18.68	11.29	14.42
7.70	13.16	7.62	17.75	7.63	18.38	7.62	20.05	11.33	13.62
7.73	12.78	7.64	18.74	7.65	18.16	7.64	19.85	11.37	13.43
7.76	13.34	7.67	19.60	7.68	18.19	7.67	18.23	11.41	14.72
7.78	13.09	7.70	20.71	7.71	19.00	7.70	18.48	11.45	15.06
7.81	12.87	7.72	21.49	7.73	19.77	7.73	18.53	11.49	14.91
7.84	12.56	7.75	20.22	7.76	19.11	7.75	17.95	11.53	15.02
7.86	12.24	7.78	20.05	7.79	17.90	7.78	18.70	11.57	13.94
7.89	12.90	7.81	20.02	7.81	17.57	7.81	17.47	11.61	15.31
7.92	13.23	7.83	20.26	7.84	16.98	7.83	17.17	11.65	16.44
7.95	12.43	7.86	19.36	7.87	16.19	7.86	16.85	11.69	15.37
7.97	11.88	7.89	18.44	7.90	16.95	7.89	16.14	11.73	13.62
8.00	12.16	7.91	19.18	7.92	18.04	7.91	17.47	11.77	14.05
8.03	11.99	7.94	19.57	7.95	19.32	7.94	18.06	11.81	14.03
8.05	11.24	7.97	18.95	7.98	18.98	7.97	19.67	11.85	13.53
8.08	11.01	7.99	20.80	8.00	19.67	7.99	21.76	11.89	14.71
8.11	11.31	8.02	21.20	8.03	20.05	8.02	19.72	11.93	15.95

8.14	11.56	8.05	17.80	8.06	20.79	8.05	21.44	11.97	14.72
8.16	12.89	8.08	15.75	8.08	21.18	8.08	22.52	12.01	15.26
8.19	13.95	8.10	16.03	8.11	22.66	8.10	24.35	12.05	15.62
8.22	12.72	8.13	16.90	8.14	22.65	8.13	26.44	12.09	20.87
8.25	12.23	8.16	17.16	8.17	22.90	8.16	26.36	12.13	20.55
8.27	12.78	8.18	16.70	8.19	21.51	8.18	27.53	12.17	12.15
8.30	13.22	8.21	17.26	8.22	19.88	8.21	27.15	12.21	11.66
8.33	11.82	8.24	17.39	8.25	19.07	8.24	23.77	12.25	12.02
8.35	10.90	8.26	17.87	8.27	17.82	8.26	20.77	12.29	14.44
8.38	11.55	8.29	17.20	8.30	18.69	8.29	20.51	12.33	16.77
8.41	11.48	8.32	16.56	8.33	19.06	8.32	20.03	12.37	17.21
8.44	11.03	8.34	16.59	8.35	18.99	8.35	20.89	12.41	18.94
8.46	11.74	8.37	16.98	8.38	19.47	8.37	20.39	12.46	20.15
8.49	12.17	8.40	16.99	8.41	19.83	8.40	17.85	12.49	20.58
8.52	11.83	8.43	16.32	8.43	19.84	8.43	17.58	12.53	18.62
8.54	11.85	8.45	16.31	8.46	19.09	8.45	18.02	12.57	18.83
8.57	11.81	8.48	15.89	8.49	17.29	8.48	19.74	12.62	20.79
8.60	11.38	8.51	15.49	8.52	17.09	8.51	18.56	12.66	21.89
8.63	11.18	8.53	15.90	8.54	16.81	8.53	16.43	12.70	20.08
8.65	10.94	8.56	14.23	8.57	16.73	8.56	14.75	12.74	19.57
		8.59	14.35	8.60	17.13	8.59	14.67	12.78	20.44
		8.61	14.28	8.62	16.69	8.61	14.39	12.82	21.88
		8.64	14.55	8.65	16.62	8.64	14.79	12.86	19.84
		8.67	13.93	8.68	17.41	8.67	14.48	12.90	19.60
		8.69	14.44	8.70	18.64	8.70	13.54	12.94	19.40
		8.72	14.12	8.73	20.44	8.72	12.93	12.98	17.64
		8.75	13.27	8.76	19.32	8.75	14.29	13.02	17.05
		8.78	13.13	8.78	18.45	8.78	14.08	13.06	16.60
		8.80	13.13	8.81	17.84	8.80	14.95	13.10	16.44
		8.83	13.17	8.84	18.29	8.83	15.89	13.14	18.36
		8.86	13.31	8.87	18.20	8.86	15.57	13.18	18.54
		8.88	13.03	8.89	17.11	8.88	15.13	13.22	16.06
		8.91	12.59	8.92	17.67	8.91	16.01	13.26	16.53
		8.94	12.83	8.95	18.64	8.94	15.85	13.30	18.43

8.96	13.76	8.97	18.83	8.96	16.06
8.99	13.41	9.00	19.71	8.99	16.58
9.02	13.42	9.03	18.97	9.02	17.60
9.04	13.97	9.05	16.77	9.05	18.97
9.07	13.59	9.08	16.77	9.07	18.73
9.10	13.40	9.11	17.20	9.10	17.77
9.13	12.95	9.14	17.77	9.13	17.75
		9.16	17.88	9.15	17.18
		9.19	17.58	9.18	16.38
		9.22	17.23	9.21	16.45
		9.24	18.08	9.23	15.70
		9.27	17.72	9.26	16.47
		9.30	16.02	9.29	15.88
		9.32	15.47	9.31	15.38
		9.35	15.39	9.34	14.39
		9.38	16.21	9.37	14.60
		9.40	16.32	9.40	15.02
		9.43	15.73	9.42	17.52
		9.46	14.15	9.45	18.95
		9.49	14.85	9.48	18.06
		9.51	16.07	9.50	16.31
		9.54	16.23	9.53	15.44
		9.57	15.69	9.56	14.58
		9.59	14.73	9.58	14.64
		9.62	14.83	9.61	15.22
		9.65	14.62	9.64	16.52
		9.67	14.20	9.67	17.71
		9.70	13.87	9.69	19.77
		9.73	13.99	9.72	20.54
		9.75	14.40	9.75	19.91
		9.78	14.87	9.77	18.47
		9.81	15.86	9.80	18.46
		9.84	15.24	9.83	18.76
		9.86	15.33	9.85	18.91

13.34	19.02
13.38	18.26
13.42	16.64
13.46	16.81
13.50	17.10
13.54	16.03
13.58	15.33
13.62	14.76
13.66	15.29
13.70	16.53
13.74	17.35
13.78	16.81
13.82	14.97
13.86	15.00
13.90	15.42
13.94	15.85
13.98	15.71
14.02	13.75
14.06	14.01
14.10	14.42
14.14	14.00
14.18	14.06
14.22	13.59
14.26	13.37
14.30	13.07
14.34	13.17
14.38	12.72
14.42	11.92
14.46	11.60
14.50	10.95
14.54	10.70
14.58	10.72
14.62	11.62
14.66	11.54

9.89	15.48	9.88	20.61	14.70	11.67
9.92	15.94	9.91	20.69	14.74	11.16
9.94	15.93	9.93	19.70	14.78	11.67
9.97	15.81	9.96	17.49	14.82	12.37
10.00	14.87	9.99	17.53		
10.02	14.62	10.02	16.78		
10.05	14.09	10.04	16.10		
10.08	13.84	10.07	17.74		
10.11	14.30	10.10	18.26		
10.13	14.53	10.12	17.17		
10.16	14.66	10.15	14.94		
10.19	15.81	10.18	15.19		
10.21	16.25	10.20	15.62		
10.24	15.36	10.23	15.55		
10.27	14.20	10.26	15.39		
10.29	13.99	10.28	15.58		
10.32	14.08	10.31	16.67		
10.35	14.90	10.34	17.19		
10.37	14.28	10.37	18.90		
10.40	13.31	10.39	16.79		
10.43	13.64	10.42	13.78		
10.46	13.35	10.45	13.06		
10.48	12.97	10.47	13.68		
10.51	13.10	10.50	15.32		
10.54	13.80	10.53	16.56		
10.56	15.11	10.55	16.87		
10.59	14.82	10.58	17.12		
10.62	13.89	10.61	16.99		
10.64	13.82	10.63	16.34		
10.67	13.97	10.66	16.40		
10.70	13.64	10.69	17.07		
10.72	13.62	10.72	15.97		
10.75	13.24	10.74	16.00		
10.78	12.38	10.77	17.32		

10.81	11.17	10.80	16.03
10.83	10.77	10.82	14.91
10.86	10.63	10.85	14.32
10.89	10.23	10.88	14.44
10.91	10.39	10.90	14.21
10.94	10.98	10.93	14.49
10.97	11.40	10.96	14.67
10.99	11.14	10.99	14.87
11.02	10.85	11.01	14.30
11.05	10.64	11.04	15.91
11.08	10.17	11.07	17.81
11.10	10.40	11.09	17.04
11.13	10.42	11.12	16.79
11.16	9.42	11.15	17.83
11.18	9.04	11.17	18.72
11.21	9.43	11.20	16.54
11.24	10.15	11.23	15.80
11.26	10.20	11.25	15.70
11.29	10.75	11.28	15.11
11.32	11.26	11.31	15.47
11.34	10.46	11.34	16.37
11.37	9.58	11.36	15.37
11.40	9.61	11.39	14.98
11.43	10.06	11.42	15.63
11.45	9.73	11.44	15.44
11.48	9.61	11.47	16.33
11.51	8.83	11.50	20.01
11.53	8.11	11.52	22.91
		11.55	19.27
		11.58	15.91
		11.60	17.10
		11.63	16.55
		11.66	17.07
		11.69	16.90

11.71	17.09
11.74	16.38
11.77	17.17
11.79	16.97
11.82	16.23
11.85	15.67
11.87	16.51
11.90	16.79
11.93	18.23
11.95	21.30
11.98	22.17
12.01	18.89
12.04	17.90
12.06	18.31
12.09	18.50
12.12	18.80
12.14	22.07
12.17	23.56
12.20	23.37
12.22	27.70
12.25	28.54
12.28	24.80
12.30	21.86
12.33	20.51
12.36	20.11
12.39	20.32
12.41	18.63
12.44	17.11
12.47	17.94
12.49	18.34
12.52	19.97
12.55	24.16
12.57	24.77
12.60	23.20

12.63	22.81
12.66	21.34
12.68	19.21
12.71	18.49
12.74	17.99
12.76	19.60
12.79	21.98
12.82	21.27
12.84	19.53
12.87	21.64
12.90	22.05
12.92	19.22
12.95	19.64
12.98	19.58
13.01	18.25
13.03	17.54
13.06	16.11
13.09	16.01
13.11	15.10
13.14	14.10
13.17	13.59
13.19	14.29
13.22	15.49
13.25	15.80
13.27	16.84
13.30	15.30
13.33	14.60
13.36	15.06
13.38	16.23
13.41	16.91
13.44	16.76
13.46	14.42
13.49	14.06
13.52	14.34

13.54	14.82
13.57	14.84
13.60	14.93
13.62	14.72
13.65	14.99
13.68	15.00
13.71	14.26
13.73	14.39
13.76	13.17
13.79	12.87
13.81	12.33
13.84	12.13
13.87	11.93
13.89	10.84
13.92	10.93
13.95	11.36
13.97	10.61
14.00	9.32
14.03	9.19
14.06	9.41
14.08	9.89
14.11	10.16
14.14	9.93

Table A4.9. Sandstone Point midden *Saccostrea glomerata* Mg/Ca ratios.

SSPSg005 Distance along growth axis (mm)	SSPSg005 Mg/Ca (mmol/mol)	SSPSg009 Distance along growth axis (mm)	SSPSg009 Mg/Ca (mmol/mol)
14.74	15.49	16.50	16.38
14.73	16.10	16.47	15.77
14.70	15.97	16.44	16.28
14.67	16.29	16.41	14.38
14.65	16.89	16.38	13.38
14.62	15.92	16.35	12.47
14.59	14.81	16.32	11.57
14.57	14.08	16.29	12.71
14.54	14.17	16.26	12.91
14.51	13.41	16.24	12.63
14.49	12.73	16.21	12.18
14.46	12.76	16.18	12.21
14.43	14.08	16.15	12.44
14.41	14.95	16.12	12.07
14.38	13.63	16.09	12.50
14.35	12.67	16.06	12.87
14.33	13.40	16.03	11.46
14.30	15.15	16.00	10.64
14.27	13.46	15.97	10.32
14.25	10.64	15.94	11.04
14.22	9.90	15.91	11.51
14.19	9.98	15.89	12.06
14.17	10.70	15.86	11.80
14.14	12.01	15.83	11.42
14.11	11.70	15.80	10.93
14.09	10.25	15.77	10.74
14.06	10.08	15.74	12.07
14.03	9.88	15.71	12.67
14.00	9.30	15.68	12.16
13.98	10.65	15.65	12.19
13.95	11.20	15.62	11.56
13.92	10.52	15.59	11.50
13.90	10.27	15.56	12.37
13.87	10.52	15.53	14.23
13.84	10.86	15.51	15.68
13.82	11.00	15.48	16.35
13.79	10.35	15.45	15.56
13.76	10.16	15.42	15.68
13.74	11.09	15.39	16.37
13.71	12.16	15.36	17.48
13.68	11.61	15.33	18.27
13.66	12.21	15.30	18.22
13.63	17.30	15.27	17.77
13.60	17.30	15.24	15.87
13.58	14.78	15.21	18.26
13.55	13.78	15.18	17.95
13.52	12.36	15.15	16.53
13.50	12.63	15.13	16.35
13.47	12.95	15.10	17.46
13.44	12.86	15.07	17.95
13.42	13.61	15.04	17.69
13.39	14.67	15.01	16.78
13.36	14.38	14.98	16.21
13.34	14.18	14.95	16.63

13.31	14.71	14.92	16.74
13.28	14.83	14.89	16.28
13.26	15.56	14.86	17.28
13.23	15.46	14.83	16.96
13.20	14.66	14.80	17.05
13.17	13.66	14.78	16.59
13.15	14.93	14.75	16.56
13.12	17.21	14.72	16.03
13.09	18.60	14.69	15.23
13.07	19.49	14.66	14.90
13.04	18.69	14.63	14.91
13.01	15.26	14.60	14.14
12.99	15.52	14.57	13.40
12.96	15.88	14.54	13.84
12.93	16.27	14.51	13.90
12.91	15.92	14.48	13.58
12.88	17.61	14.45	13.32
12.85	17.99	14.42	13.01
12.83	17.35	14.40	12.41
12.80	16.06	14.37	12.12
12.77	15.41	14.34	12.03
12.75	15.97	14.31	11.22
12.72	16.13	14.28	10.91
12.69	16.44	14.25	10.30
12.67	17.37	14.22	10.52
12.64	18.12	14.19	11.28
12.61	17.46	14.16	12.48
12.59	17.36	14.13	13.44
12.56	16.77	14.10	14.40
12.53	15.67	14.07	14.52
12.51	14.82	14.05	14.59
12.48	15.06	14.02	14.14
12.45	15.15	13.99	13.85
12.42	16.68	13.96	14.99
12.40	15.17	13.93	14.71
12.37	14.19	13.90	14.29
12.34	13.00	13.87	13.54
12.32	13.07	13.84	15.00
12.29	13.76	13.81	14.78
12.26	14.76	13.78	15.15
12.24	15.55	13.75	16.67
12.21	14.98	13.72	18.17
12.18	15.26	13.69	18.37
12.16	15.80	13.67	17.95
12.13	15.14	13.64	17.23
12.10	14.69	13.61	17.44
12.08	15.67	13.58	17.64
12.05	15.50	13.55	17.42
12.02	13.67	13.52	17.32
12.00	13.67	13.49	18.07
11.97	13.86	13.46	17.24
11.94	14.28	13.43	15.10
11.92	13.50	13.40	13.67
11.89	13.38	13.37	13.51
11.86	14.44	13.34	13.24
11.84	12.93	13.32	13.30
11.81	11.82	13.29	13.66
11.78	12.35	13.26	13.47
11.76	12.78	13.23	12.31
11.73	15.47	13.20	11.21

11.70	15.20	13.17	11.13
11.68	11.56	13.14	11.00
11.65	11.04	13.11	11.47
11.62	10.65	13.08	11.96
11.59	10.04	13.05	12.61
11.57	10.30	13.02	12.78
11.54	10.15	12.99	12.36
11.51	9.76	12.96	11.89
11.49	9.38	12.94	11.90
11.46	9.69	12.91	12.62
11.43	9.96	12.88	12.13
11.41	9.54	12.85	11.40
11.38	9.03	12.82	11.23
11.35	8.81	12.79	12.38
11.33	8.88	12.76	13.76
11.30	8.60	12.73	14.02
11.27	8.43	12.70	14.13
11.25	8.42	12.67	13.79
11.22	9.32	12.64	14.01
11.19	10.12	12.61	14.04
11.17	10.16	12.59	13.82
11.14	10.24	12.56	14.13
11.11	9.95	12.53	13.65
11.09	9.14	12.50	13.24
11.06	8.19	12.47	14.01
11.03	7.91	12.44	15.36
11.01	8.65	12.41	15.90
10.98	9.78	12.38	15.56
10.95	9.70	12.35	16.07
10.93	8.83	12.32	16.29
10.90	9.16	12.29	16.38
10.87	9.45	12.26	17.73
10.85	9.20	12.23	17.72
10.82	9.51	12.21	16.73
10.79	9.84	12.18	16.86
10.76	10.26	12.15	17.63
10.74	10.05	12.12	17.27
10.71	9.88	12.09	17.33
10.68	10.02	12.06	16.65
10.66	10.66	12.03	16.49
10.63	11.17	12.00	15.14
10.60	10.73	11.97	14.87
10.58	9.71	11.94	15.23
10.55	9.84	11.91	15.84
10.52	10.30	11.88	16.38
10.50	9.72	11.86	14.84
10.47	9.74	11.83	14.04
10.44	9.96	11.80	14.06
10.42	11.02	11.77	13.95
10.39	11.51	11.74	13.17
10.36	11.56	11.71	13.03
10.34	10.83	11.68	12.66
10.31	11.11	11.65	12.73
10.28	11.38	11.62	12.38
10.26	12.86	11.59	11.52
10.23	12.83	11.56	11.64
10.20	11.18	11.53	11.64
10.18	10.99	11.51	12.46
10.15	12.33	11.48	11.49
10.12	14.76	11.45	11.09

10.10	15.70	11.42	11.17
10.07	15.86	11.39	11.43
10.04	16.50	11.36	11.63
10.02	15.91	11.33	11.72
9.99	15.23	11.30	11.07
9.96	15.08	11.27	10.40
9.93	14.88	11.24	9.53
9.91	14.98	11.21	9.31
9.88	15.74	11.18	9.90
9.85	15.90	11.15	10.85
9.83	15.68	11.13	12.31
9.80	15.36	11.10	12.70
9.77	15.24	11.07	11.83
9.75	15.50	11.04	11.44
9.72	15.52	11.01	11.80
9.69	15.29	10.98	12.54
9.67	15.72	10.95	13.30
9.64	16.33	10.92	11.89
9.61	17.67	10.89	11.30
9.59	18.83	10.86	11.67
9.56	17.04	10.83	11.79
9.53	15.31	10.80	11.95
9.51	14.53	10.78	11.59
9.48	13.93	10.75	11.71
9.45	14.00	10.72	12.92
9.43	13.85	10.69	14.88
9.40	13.59	10.66	17.08
9.37	13.38	10.63	17.64
9.35	13.31	10.60	15.36
9.32	15.19	10.57	14.05
9.29	15.96	10.54	15.23
9.27	14.34	10.51	16.07
9.24	13.42	10.48	16.37
9.21	13.35	10.45	17.34
9.18	15.24	10.42	17.92
9.16	16.91	10.40	18.95
9.13	17.67	10.37	19.89
9.10	16.79	10.34	18.59
9.08	15.24	10.31	17.62
9.05	14.67	10.28	17.68
9.02	16.31	10.25	17.93
9.00	16.44	10.22	18.03
8.97	16.62	10.19	21.06
8.94	15.85	10.16	25.17
8.92	15.53	10.13	25.60
8.89	14.90	10.10	23.78
8.86	15.03	10.07	21.82
8.84	14.59	10.05	19.39
8.81	14.19	10.02	16.73
8.78	15.59	9.99	16.08
8.76	16.72	9.96	15.99
8.73	16.11	9.93	15.41
8.70	15.38	9.90	14.83
8.68	14.83	9.87	14.64
8.65	14.48	9.84	15.24
8.62	14.89	9.81	16.23
8.60	15.00	9.78	15.43
8.57	15.23	9.75	15.13
8.54	15.36	9.72	14.89
8.52	13.85	9.69	15.59

8.49	14.11	9.67	16.56
8.46	14.70	9.64	16.18
8.43	14.96	9.61	16.40
8.41	15.57	9.58	16.02
8.38	14.16	9.55	15.86
8.35	13.06	9.52	15.15
8.33	13.21	9.49	15.70
8.30	13.44	9.46	15.55
8.27	12.87	9.43	15.78
8.25	12.82	9.40	15.31
8.22	14.11	9.37	16.20
8.19	13.36	9.34	15.59
8.17	13.79	9.32	13.68
8.14	14.25	9.29	13.28
8.11	12.67	9.26	13.59
8.09	11.88	9.23	13.68
8.06	11.83	9.20	13.10
8.03	11.64	9.17	12.70
8.01	11.31	9.14	13.07
7.98	10.87	9.11	13.03
7.95	10.93	9.08	12.87
7.93	10.76	9.05	12.18
7.90	11.64	9.02	12.40
7.87	12.08	8.99	12.18
7.85	10.72	8.96	11.94
7.82	10.17	8.94	12.23
7.79	10.57	8.91	12.57
7.77	11.29	8.88	12.47
7.74	13.01	8.85	12.31
7.71	11.63	8.82	12.34
7.69	10.28	8.79	12.44
7.66	10.39	8.76	11.76
7.63	10.90	8.73	10.52
7.61	10.79	8.70	10.26
7.58	10.46	8.67	10.78
7.55	10.51	8.64	10.65
7.52	10.35	8.61	10.35
7.50	9.99	8.58	10.29
7.47	10.57	8.56	10.63
7.44	11.11	8.53	10.47
7.42	10.46	8.50	9.93
7.39	9.68	8.47	9.89
7.36	8.89	8.44	10.37
7.34	8.97	8.41	10.81
7.31	9.21	8.38	11.82
7.28	9.35	8.35	12.65
7.26	9.23	8.32	12.76
7.23	8.62	8.29	12.46
7.20	8.76	8.26	12.19
7.18	8.88	8.23	12.28
7.15	9.83	8.21	12.16
7.12	10.16	8.18	10.52
7.10	10.84	8.15	9.58
7.07	11.59	8.12	10.08
7.04	11.54	8.09	11.33
7.02	11.76	8.06	12.44
6.99	12.36	8.03	12.77
6.96	12.43	8.00	13.49
6.94	10.60	7.97	13.75
6.91	10.59	7.94	13.97

6.88	11.29	7.91	13.74
6.86	11.40	7.88	14.30
6.83	11.60	7.86	14.64
6.80	11.82	7.83	14.67
6.77	12.12	7.80	15.11
6.75	12.87	7.77	14.85
6.72	12.76	7.74	14.84
6.69	12.42	7.71	14.84
6.67	13.02	7.68	16.00
6.64	12.58	7.65	17.05
6.61	12.45	7.62	17.37
6.59	12.43	7.59	17.86
6.56	12.42	7.56	18.03
6.53	11.85	7.53	17.67
6.51	11.37	7.50	16.77
6.48	11.63	7.48	15.70
6.45	11.75	7.45	14.03
6.43	11.49	7.42	13.38
6.40	12.34	7.39	14.96
6.37	13.42	7.36	17.41
6.35	13.36	7.33	20.00
6.32	13.40	7.30	20.61
6.29	13.86	7.27	18.75
6.27	14.43	7.24	16.99
6.24	14.78	7.21	15.12
6.21	14.92	7.18	14.19
6.19	15.70	7.15	14.44
6.16	15.92	7.13	16.14
6.13	15.33	7.10	18.03
6.11	15.34	7.07	19.28
6.08	15.59	7.04	18.69
6.05	15.86	7.01	17.34
6.03	16.17	6.98	16.27
6.00	16.61	6.95	16.81
5.97	15.71	6.92	17.70
5.94	15.12	6.89	19.69
5.92	15.64	6.86	20.39
5.89	16.13	6.83	20.91
5.86	16.61	6.80	21.98
5.84	16.91	6.77	21.67
5.81	17.37	6.75	19.97
5.78	17.52	6.72	19.18
5.76	17.01	6.69	18.09
5.73	17.02	6.66	16.44
5.70	17.15	6.63	16.77
5.68	17.45	6.60	18.87
5.65	17.84	6.57	20.89
5.62	17.75	6.54	21.58
5.60	16.84	6.51	21.46
5.57	15.09	6.48	22.39
5.54	15.10	6.45	23.76
5.52	16.31	6.42	26.10
5.49	16.96	6.39	28.34
5.46	16.75	6.37	30.12
5.44	16.00	6.34	29.50
5.41	17.11	6.31	24.68
5.38	16.95	6.28	19.91
5.36	17.51	6.25	17.94
5.33	17.68	6.22	18.08
5.30	16.17	6.19	18.25

5.28	15.57	6.16	16.40
5.25	16.49	6.13	15.60
5.22	16.97	6.10	14.79
5.19	16.49	6.07	15.99
5.17	15.26	6.04	16.76
5.14	14.85	6.02	15.70
5.11	16.32	5.99	15.49
5.09	17.19	5.96	15.46
5.06	17.35	5.93	14.85
5.03	17.43	5.90	14.92
5.01	16.10	5.87	16.66
4.98	16.45	5.84	16.99
4.95	17.13	5.81	15.97
4.93	16.50	5.78	16.35
4.90	15.26	5.75	17.52
4.87	14.70	5.72	17.72
4.85	14.83	5.69	16.69
4.82	14.96	5.67	15.34
4.79	15.08	5.64	14.41
4.77	15.25	5.61	15.91
4.74	15.26	5.58	16.99
4.71	15.57	5.55	16.60
4.69	16.12	5.52	16.06
4.66	15.84	5.49	16.38
4.63	15.03	5.46	16.84
4.61	14.61	5.43	17.19
4.58	14.92	5.40	16.34
4.55	14.40	5.37	17.14
4.53	14.90	5.34	18.28
4.50	15.16	5.31	17.39
4.47	14.90	5.29	17.56
4.45	14.08	5.26	16.34
4.42	13.98	5.23	15.07
4.39	13.99	5.20	14.32
4.36	13.44	5.17	13.72
4.34	13.26	5.14	13.75
4.31	12.56	5.11	13.96
4.28	12.15	5.08	13.52
4.26	11.63	5.05	12.74
4.23	11.19	5.02	13.01
4.20	10.96	4.99	12.66
4.18	11.06	4.96	12.34
4.15	11.36	4.94	13.67
4.12	10.86	4.91	14.63
4.10	10.42	4.88	13.62
4.07	10.06	4.85	12.67
4.04	9.76	4.82	12.32
4.02	9.80	4.79	12.63
3.99	10.21	4.76	13.06
3.96	11.38	4.73	13.06
3.94	11.39	4.70	13.56
3.91	11.64	4.67	14.09
3.88	11.39	4.64	14.06
3.86	11.12	4.61	14.27
3.83	11.06	4.58	14.04
3.80	11.50	4.56	14.29
3.78	12.74	4.53	13.05
3.75	13.37	4.50	11.81
3.72	13.00	4.47	11.73
3.70	13.30	4.44	12.09

3.67	13.65	4.41	13.33
3.64	14.15	4.38	14.33
3.61	13.49	4.35	15.06
3.59	14.28	4.32	15.36
3.56	14.53	4.29	14.70
3.53	14.90	4.26	15.39
3.51	15.00	4.23	15.63
3.48	14.95	4.20	14.57
3.45	15.02	4.18	13.34
3.43	16.93	4.15	13.09
3.40	17.73	4.12	13.11
3.37	16.43	4.09	13.37
3.35	16.10	4.06	14.14
3.32	18.07	4.03	14.54
3.29	20.16	4.00	15.20
3.27	23.94	3.97	16.23
3.24		3.94	16.39
3.21		3.91	16.70
3.19	17.83	3.88	16.21
3.16	18.05	3.85	16.22
3.13	19.29	3.83	16.51
3.11	19.76	3.80	15.53
3.08	24.17	3.77	16.21
3.05	24.71	3.74	15.97
3.03	21.38	3.71	15.77
3.00	17.89	3.68	17.12
2.97	17.79	3.65	18.05
2.95	17.48	3.62	18.03
2.92	15.78	3.59	17.62
2.89	14.83	3.56	17.63
2.87	15.09	3.53	18.25
2.84	16.30	3.50	15.47
2.81	18.17	3.47	14.99
2.78	17.38	3.45	18.57
2.76	16.66	3.42	20.81
2.73	16.25	3.39	20.56
2.70	16.21	3.36	22.62
2.68	16.57	3.33	25.10
2.65	17.37	3.30	23.60
2.62	16.32	3.27	22.63
2.60	16.25	3.24	22.04
2.57	15.43	3.21	21.54
2.54	14.22	3.18	22.37
2.52	14.25	3.15	24.57
2.49	14.30	3.12	24.77
2.46	15.52	3.10	24.57
2.44	19.09	3.07	22.53
2.41	22.08	3.04	20.57
2.38	21.63	3.01	19.44
2.36	21.25	2.98	18.68
2.33	23.53	2.95	19.62
2.30	21.49	2.92	19.39
2.28	17.77	2.89	20.85
2.25	18.06	2.86	22.79
2.22	16.01	2.83	22.22
2.20	14.72	2.80	21.80
2.17	16.03	2.77	22.57
2.14	16.12	2.74	22.16
2.12	16.28	2.72	18.70
2.09	14.46	2.69	18.28

2.06	11.53	2.66	19.24
2.04	13.44	2.63	19.10
2.01	18.71	2.60	18.83
1.98		2.57	18.57
1.95		2.54	17.34
1.93	11.65	2.51	15.96
1.90	4.38	2.48	15.93
1.87		2.45	15.83
1.85		2.42	16.76
1.82	5.03	2.39	16.33
1.79	7.03	2.37	15.59
1.77	10.59	2.34	15.60
1.74	11.60	2.31	15.15
1.71	11.51	2.28	14.99
1.69	12.72	2.25	14.56
1.66	14.56	2.22	15.00
1.63	14.58	2.19	15.40
1.61	14.09	2.16	15.17
1.58	13.85	2.13	15.94
1.55	12.62	2.10	16.18
1.53	9.36	2.07	16.14
1.50	10.87	2.04	14.10
1.47	13.88	2.01	13.16
1.45	10.68	1.99	15.06
1.42	9.50	1.96	16.04
1.39	10.71	1.93	15.42
1.37	11.09	1.90	14.78
1.34	8.96	1.87	15.11
1.31	8.45	1.84	17.40
1.29	7.58	1.81	17.81
1.26	6.29	1.78	16.22
1.23	5.96	1.75	16.09
1.21	6.47	1.72	14.79
1.18	7.76	1.69	13.51
1.15	7.58	1.66	13.51
1.12	6.85	1.64	13.36
1.10	6.79	1.61	12.22
1.07	6.38	1.58	10.71
1.04	6.46	1.55	9.26
1.02	5.18	1.52	9.85
0.99	4.04	1.49	9.98
0.96	4.54	1.46	8.17
0.94	5.91	1.43	7.61
0.91	6.49	1.40	7.20
0.88	6.34	1.37	6.24
0.86	6.49	1.34	5.80
0.83	7.09	1.31	6.38
0.80	8.59	1.28	8.21
0.78	10.09	1.26	9.46
0.75	10.65	1.23	9.99
0.72	10.54	1.20	8.81
0.70	10.76	1.17	7.07
0.67	11.34	1.14	6.03
0.64	11.67	1.11	5.49
0.62	12.11	1.08	5.12
0.59	9.12	1.05	4.79
0.56	5.90	1.02	4.52
0.54	4.39	0.99	4.53
0.51	4.70	0.96	4.14
0.48	4.22	0.93	3.98

0.46	3.94	0.91	3.81
0.43	5.69	0.88	3.78
0.40	7.77	0.85	3.83
0.38	10.54	0.82	4.14
0.35		0.79	4.20
0.32	11.54	0.76	3.75
0.29	5.95	0.73	3.58
0.27	7.93	0.70	3.57
0.24	6.57	0.67	3.34
0.21	5.45	0.64	3.29
0.19	6.82	0.61	3.44
0.16	6.90	0.58	3.68
0.13	6.43	0.55	3.82
0.11	6.68	0.53	3.94
0.08	8.27	0.50	3.71
0.05	11.16	0.47	3.48
0.03	15.83	0.44	3.59
0.00	17.20	0.41	3.52
		0.38	3.14
		0.35	3.29
		0.32	3.57
		0.29	3.52
		0.26	3.38
		0.23	3.44
		0.20	3.52
		0.18	3.65
		0.15	3.57
		0.12	3.53
		0.09	3.74
		0.06	3.84
		0.03	3.62
		0.00	3.30

Table A4.10. Pambula Lake and Little Swanport *Mytilus galloprovincialis* Mg/Ca ratios.

PLMg016 Distance along growth axis (mm)	PLMg016 (mmol/mol)	PLMg024 Distance along growth axis (mm)	PLMg024 (mmol/mol)	PLMg047 Distance along growth axis (mm)	PLMg047 (mmol/mol)	LSMg362 Distance along growth axis (mm)	LSMg362 (mmol/mol)	LSMg399 Distance along growth axis (mm)	LSMg399 (mmol/mol)	LSMg531 Distance along growth axis (mm)	LSMg531 (mmol/mol)
0.00	9.87	0.00	6.22	0.00	8.65	0.00	0.46	0.00	5.47	0.00	5.93
0.02	11.05	0.08	6.84	0.08	10.20	0.05	0.49	0.08	5.48	0.08	8.14
0.05	10.16	0.15	7.19	0.16	8.86	0.10	0.54	0.16	5.38	0.16	7.43
0.07	10.84	0.23	6.98	0.25	9.30	0.15	0.59	0.24	5.01	0.24	9.03
0.10	11.89	0.30	7.50	0.33	8.45	0.21	0.58	0.32	5.17	0.32	6.82
0.13	12.52	0.38	7.79	0.41	7.77	0.26	0.59	0.40	4.68	0.39	7.15
0.15	10.93	0.45	7.47	0.49	7.71	0.31	0.54	0.47	3.97	0.47	6.67
0.18	9.79	0.53	6.55	0.57	8.21	0.37	0.60	0.55	4.51	0.55	6.21
0.21	10.63	0.60	7.32	0.66	9.88	0.42	0.57	0.63	3.74	0.63	5.67
0.23	12.00	0.68	6.69	0.74	10.03	0.47	0.61	0.71	3.79	0.71	5.89
0.26	12.79	0.75	6.94	0.82	7.24	0.53	0.64	0.79	4.68	0.79	6.30
0.29	11.80	0.83	7.83	0.90	7.10	0.58	0.64	0.87	5.40	0.87	6.03
0.31	11.15	0.90	7.44	0.98	7.40	0.63	0.63	0.95	5.13	0.95	6.20
0.34	11.63	0.98	7.72	1.07	8.31	0.69	0.69	1.03	3.74	1.03	6.80
0.37	10.72	1.05	7.88	1.15	10.26	0.74	0.66	1.11	4.80	1.10	6.58
0.39	10.93	1.13	8.13	1.23	10.51	0.79	0.67	1.19	2.76	1.18	6.96
0.42	9.31	1.21	7.90	1.31	11.94	0.85	0.72	1.27	1.64	1.26	6.13
0.45	9.12	1.28	7.96	1.39	11.80	0.90	0.68	1.34	1.01	1.34	5.96
0.47	9.32	1.36	8.14	1.48	11.13	0.95	0.67	1.42	1.38	1.42	6.06
0.50	9.02	1.43	7.64	1.56	10.94	1.01	0.69	1.50	1.84	1.50	5.75
0.53	8.74	1.51	6.47	1.64	10.65	1.06	0.65	1.58	1.38	1.58	6.29
0.55	9.49	1.58	5.71	1.72	9.35	1.11	0.67	1.66	1.40	1.66	6.43
0.58	10.15	1.66	5.19	1.80	6.80	1.17	0.66	1.74	1.56	1.74	6.43
0.61	10.04	1.73	3.87	1.89	4.60	1.22	0.70	1.82	1.07	1.81	6.22
0.63	8.31	1.81	2.74	1.97	3.56	1.27	0.63	1.90	0.95	1.89	6.51
0.66	8.07	1.88	1.87	2.05	3.19	1.33	0.69	1.98	1.42	1.97	6.40
0.69	8.22	1.96	1.98	2.13	4.34	1.38	0.71	2.06	1.95	2.05	7.02

0.71	7.38	2.03	2.10	2.21	6.23	1.43	0.74	2.14	3.30	2.13	6.87
0.74	7.61	2.11	2.36	2.30	8.35	1.49	0.67	2.22	4.09	2.21	7.02
0.77	7.37	2.18	2.31	2.38	8.65	1.54	0.72	2.29	4.58	2.29	6.53
0.79	7.94	2.26	3.37	2.46	9.29	1.59	0.61	2.37	5.03	2.37	6.83
0.82	10.33	2.34	4.44	2.54	9.52	1.65	0.70	2.45	4.70	2.44	6.84
0.85	12.46	2.41	5.79	2.62	9.69	1.70	0.73	2.53	4.60	2.52	6.81
0.90	15.72	2.49	7.07	2.71	10.51	1.75	0.69	2.61	5.02	2.60	6.94
0.93	12.98	2.56	7.35	2.79	9.23	1.81	0.67	2.69	5.23	2.68	6.70
0.95	12.02	2.64	8.62	2.87	8.31	1.86	0.72	2.77	5.45	2.76	7.04
0.98	7.38	2.71	9.42	2.95	7.56	1.91	0.67	2.85	6.55	2.84	6.57
1.01	7.11	2.79	9.97	3.03	7.00	1.96	0.68	2.93	6.38	2.92	6.56
1.03	7.65	2.86	10.06	3.12	7.24	2.02	0.71	3.01	6.40	3.00	6.47
1.06	8.38	2.94	10.11	3.20	7.29	2.07	0.68	3.09	7.45	3.08	6.46
1.09	10.32	3.01	10.27	3.28	7.43	2.12	0.68	3.16	6.89	3.15	6.28
1.11	8.28	3.09	9.88	3.36	7.88	2.18	0.65	3.24	6.77	3.23	6.26
1.14	7.36	3.16	9.87	3.44	8.18	2.23	0.67	3.32	5.91	3.31	6.69
1.17	7.32	3.24	9.95	3.52	8.28	2.28	0.69	3.40	6.15	3.39	6.66
1.19	8.14	3.32	8.16	3.61	7.64	2.34	0.69	3.48	5.78	3.47	6.72
1.22	13.10	3.39	7.22	3.69	8.34	2.39	0.67	3.56	5.44	3.55	6.56
1.24	15.61	3.47	6.40	3.77	8.25	2.44	0.69	3.64	5.69	3.63	6.96
1.43	8.92	3.54	5.36	3.85	8.53	2.50	0.77	3.72	6.00	3.71	6.32
1.46	7.30	3.62	5.40	3.93	8.79	2.55	0.75	3.80	6.01	3.79	6.62
1.48	6.58	3.69	5.07	4.02	8.87	2.60	0.67	3.88	5.79	3.86	6.67
1.51	6.07	3.77	5.35	4.10	9.52	2.66	0.72	3.96	5.55	3.94	6.43
1.54	6.38	3.84	6.67	4.18	10.51	2.71	0.71	4.04	5.56	4.02	6.39
1.56	6.65	3.92	7.24	4.26	10.60	2.76	0.70	4.11	5.17	4.10	6.81
1.59	6.59	3.99	8.03	4.34	11.83	2.82	0.71	4.19	5.21	4.18	6.84
1.62	6.63	4.07	8.23	4.43	12.10	2.87	0.67	4.27	5.34	4.26	7.55
1.64	6.61	4.14	8.30	4.51	12.32	2.92	0.68	4.35	5.91	4.34	8.32
1.67	6.84	4.22	8.67	4.59	11.63	2.98	0.76	4.43	6.85	4.42	6.53
1.70	6.94	4.29	9.21	4.67	11.21	3.03	0.68	4.51	6.15	4.50	5.80
1.72	6.23	4.37	9.44	4.76	10.23	3.08	0.74	4.59	6.61	4.57	6.05
1.75	6.23	4.45	10.38	4.84	9.95	3.14	0.70	4.67	6.83	4.65	5.90
1.78	6.39	4.52	10.50	4.92	9.91	3.19	0.72	4.75	7.33	4.73	6.03

1.80	6.61	4.60	11.33	5.00	9.81	3.24	0.65	4.83	7.93	4.81	5.93
1.83	6.62	4.67	11.17	5.08	9.87	3.30	0.76	4.91	7.46	4.89	5.87
1.86	6.08	4.75	11.27	5.17	9.42	3.35	0.64	4.98	7.24	4.97	6.01
1.88	5.51	4.82	11.60	5.25	9.34	3.40	0.67	5.06	6.38	5.05	6.09
1.91	4.16	4.90	12.94	5.33	9.84	3.46	0.63	5.14	6.63	5.13	5.87
1.94	2.87	4.97	10.21	5.41	8.98	3.51	0.63	5.22	6.07	5.21	6.08
1.96	2.04	5.05	10.65	5.49	8.40	3.56	0.65	5.30	6.06	5.28	6.19
1.99	1.32	5.12	10.08	5.57	8.27	3.61	0.81	5.38	5.62	5.36	5.83
2.02	1.13	5.20	9.44	5.66	7.66	3.67	0.66	5.46	6.07	5.44	5.80
2.04	1.53	5.27	9.51	5.74	7.51	3.72	0.67	5.54	5.76	5.52	6.08
2.07	2.52	5.35	9.16	5.82	7.88	3.77	0.77	5.62	6.17	5.60	5.81
2.10	3.83	5.42	9.03	5.90	9.69	3.83	0.89	5.70	5.90	5.68	5.70
2.12	5.04	5.50	8.71	5.98	10.92	3.88	0.98	5.78	5.89	5.76	5.74
2.15	6.41	5.58	8.78	6.07	11.89	3.93	1.60	5.86	5.68	5.84	5.73
2.18	7.02	5.65	9.16	6.15	11.62	3.99	2.58	5.93	5.52	5.92	5.85
2.20	7.28	5.73	9.07	6.23	12.23	4.04	3.89	6.01	6.12	5.99	5.94
2.23	7.03	5.80	9.82	6.31	11.68	4.09	4.73	6.09	5.79	6.07	6.05
2.26	6.49	5.88	10.08	6.39	11.57	4.15	5.61	6.17	6.03	6.15	5.86
2.28	5.84	5.95	9.85	6.48	10.81	4.20	6.35	6.25	5.75	6.23	6.03
2.31	4.89	6.03	10.58	6.56	11.26	4.25	7.63	6.33	5.71	6.31	6.32
2.34	5.11	6.10	10.90	6.64	12.28	4.31	8.15	6.41	5.69	6.39	6.24
2.36	4.25	6.18	11.08	6.72	11.70	4.36	8.99	6.49	5.63	6.47	6.57
2.39	4.57	6.25	10.37	6.80	11.97	4.41	9.59	6.57	5.25	6.55	6.49
2.41	4.15	6.33	11.06	6.89	11.96	4.47	10.15	6.65	5.32	6.62	6.86
2.44	4.62	6.40	11.02	6.97	11.72	4.52	9.49	6.73	5.10	6.70	7.02
2.47	4.50	6.48	11.42	7.05	12.58	4.57	10.20	6.80	5.22	6.78	7.00
2.49	3.73	6.55	11.28	7.13	12.88	4.63	10.10	6.88	5.05	6.86	7.06
2.52	2.68	6.63	11.64	7.21	12.91	4.68	10.50	6.96	5.04	6.94	7.07
2.55	2.70	6.71	11.17	7.30	12.97	4.73	10.43	7.04	5.07	7.02	7.42
2.57	2.57	6.78	11.31	7.38	13.76	4.79	10.75	7.12	5.18	7.10	7.59
2.60	2.68	6.86	11.68	7.46	14.33	4.84	11.63	7.20	4.99	7.18	7.48
2.63	2.89	6.93	11.04	7.54	12.88	4.89	10.88	7.28	5.12	7.26	7.24
2.65	2.93	7.01	11.34	7.62	13.23	4.95	10.94	7.36	5.25	7.33	7.07
2.68	3.27	7.08	11.72	7.71	13.64	5.00	10.48	7.44	4.93	7.41	7.63

2.71	3.55	7.16	11.68	7.79	12.71	5.05	10.51	7.52	4.92	7.49	7.53
2.73	4.47	7.23	11.56	7.87	12.81	5.11	9.98	7.60	4.60	7.57	8.17
2.76	4.04	7.31	12.15	7.95	11.98	5.16	10.45	7.67	4.52	7.65	8.10
2.79	5.95	7.38	12.41	8.03	10.93	5.21	10.83	7.75	4.98	7.73	7.65
2.81	6.26	7.46	12.57	8.12	10.70	5.27	10.82	7.83	4.91	7.81	7.52
2.84	5.82	7.53	12.12	8.20	9.57	5.32	11.04	7.91	5.17	7.89	7.51
2.87	7.32	7.61	12.78	8.28	8.84	5.37	11.05	7.99	5.03	7.97	7.37
2.89	7.61	7.69	12.14	8.36	8.85	5.43	11.50	8.07	5.27	8.04	7.48
2.92	9.70	7.76	12.64	8.44	8.47	5.48	11.31	8.15	5.54	8.12	7.68
2.95	8.28	7.84	12.39	8.53	8.96	5.53	10.90	8.23	5.79	8.20	7.73
2.97	10.05	7.91	12.20	8.61	9.33	5.59	10.12	8.31	5.52	8.28	7.73
3.00	10.28	7.99	12.18	8.69	9.47	5.64	10.45	8.39	5.40	8.36	7.93
3.03	11.27	8.06	12.15	8.77	9.03	5.69	11.22	8.47	5.73	8.44	7.85
3.05	11.09	8.14	12.24	8.85	9.36	5.75	10.75	8.55	5.86	8.52	7.82
3.08	11.71	8.21	12.37	8.94	8.71	5.80	11.46	8.62	5.86	8.60	7.15
3.11	10.60	8.29	12.41	9.02	9.24	5.85	10.56	8.70	5.87	8.68	7.38
3.13	8.92	8.36	12.36	9.10	9.65	5.90	10.13	8.78	5.90	8.75	7.39
3.16	6.90	8.44	11.78	9.18	11.00	5.96	9.27	8.86	6.08	8.83	6.87
3.19	5.28	8.51	11.88	9.26	11.63	6.01	8.97	8.94	5.76	8.91	7.26
3.21	4.78	8.59	11.51	9.35	12.45	6.06	9.47	9.02	5.62	8.99	7.16
3.24	4.76	8.66	11.66	9.43	12.82	6.12	9.66	9.10	6.13	9.07	7.35
3.27	4.91	8.74	11.14	9.51	12.79	6.17	9.65	9.18	6.36	9.15	7.53
3.29	4.82	8.82	10.68	9.59	12.83	6.22	9.71	9.26	6.84	9.23	7.05
3.32	4.75	8.89	10.53	9.67	13.40	6.28	10.22	9.34	7.05	9.31	7.27
3.35	5.09	8.97	10.48	9.75	12.98	6.33	10.24	9.42	7.62	9.39	7.07
3.37	5.21	9.04	10.59	9.84	13.15	6.38	10.17	9.49	7.52	9.46	7.53
3.40	4.98	9.12	10.33	9.92	12.85	6.44	10.15	9.57	7.25	9.54	7.26
3.43	5.19	9.19	10.03	10.00	11.68	6.49	10.46	9.65	7.68	9.62	7.22
3.45	5.27	9.27	9.89	10.08	10.94	6.54	11.06	9.73	7.88	9.70	7.03
3.48	4.91	9.34	9.91	10.16	10.21	6.60	10.07	9.81	8.52	9.78	7.08
3.51	4.68	9.42	9.90	10.25	10.28	6.65	10.49	9.89	8.57	9.86	7.16
3.53	4.67	9.49	10.01	10.33	10.41	6.70	10.38	9.97	8.03	9.94	7.33
3.56	4.72	9.57	9.52	10.41	10.33	6.76	10.49	10.05	7.65	10.02	6.83
3.59	4.79	9.64	9.49	10.49	11.22	6.81	10.05	10.13	7.18	10.10	7.24

3.61	5.42	9.72	9.60	10.57	10.92	6.86	9.16	10.21	6.56	10.17	7.25
3.64	5.48	9.79	9.37	10.66	11.21	6.92	9.27	10.29	6.75	10.25	7.15
3.67	6.39	9.87	9.45	10.74	11.31	6.97	9.18	10.37	7.35	10.33	7.31
3.69	6.94	9.95	9.58	10.82	11.40	7.02	9.36	10.44	7.41	10.41	7.21
3.72	7.58	10.02	9.55	10.90	10.73	7.08	9.10	10.52	7.12	10.49	7.07
3.74	7.46	10.10	9.96	10.98	11.03	7.13	8.68	10.60	7.09	10.57	6.80
3.77	7.97	10.17	10.57	11.07	10.88	7.18	7.55	10.68	7.45	10.65	6.75
3.80	7.72	10.25	11.05	11.15	10.43	7.24	7.18	10.76	7.29	10.73	7.54
3.82	7.98	10.32	11.69	11.23	10.38	7.29	6.01	10.84	7.58	10.80	6.76
3.85	8.08	10.40	12.40	11.31	10.34	7.34	6.26	10.92	7.63	10.88	7.25
3.88	8.03	10.47	12.41	11.39	10.28	7.40	6.20	11.00	9.00	10.96	7.17
3.90	8.54	10.55	11.90	11.48	9.48	7.45	6.55	11.08	9.27	11.04	7.18
3.93	8.64	10.62	12.39	11.56	9.79	7.50	6.35	11.16	9.69	11.12	7.25
3.96	8.91	10.70	12.35	11.64	9.56	7.56	6.92	11.24	8.89	11.20	7.38
3.98	9.31	10.77	13.11	11.72	9.57	7.61	6.96	11.31	8.75	11.28	7.18
4.01	10.54	10.85	12.97	11.80	9.24	7.66	6.88	11.39	7.99	11.36	7.21
4.04	10.27	10.93	12.48	11.89	9.49	7.71	6.72	11.47	7.48	11.44	6.91
4.06	9.95	11.00	13.26	11.97	9.28	7.77	6.69	11.55	7.04	11.51	7.16
4.09	10.10	11.08	12.68	12.05	9.48	7.82	7.39	11.63	6.66	11.59	7.12
4.12	10.44	11.15	13.91	12.13	9.72	7.87	7.53	11.71	6.80	11.67	7.44
4.14	10.48	11.23	12.97	12.21	9.21	7.93	7.62	11.79	6.38	11.75	7.26
4.17	10.45	11.30	13.35	12.30	9.37	7.98	7.67	11.87	6.99	11.83	7.08
4.20	10.48	11.38	13.83	12.38	8.88	8.03	6.90	11.95	7.88	11.91	6.90
4.22	10.34	11.45	13.81	12.46	9.20	8.09	6.70	12.03	8.47	11.99	7.40
4.25	10.33	11.53	13.70	12.54	9.03	8.14	7.43	12.11	8.67	12.07	7.05
4.28	11.10	11.60	14.36	12.62	9.16	8.19	8.51	12.19	8.88	12.15	7.01
4.30	11.21	11.68	14.22	12.71	9.72	8.25	8.15	12.26	8.77	12.22	7.24
4.33	12.11	11.75	14.14	12.79	10.25	8.30	8.19	12.34	9.10	12.30	7.22
4.36	10.38	11.83	13.99	12.87	10.65	8.35	7.98	12.42	8.50	12.38	7.28
4.38	10.44	11.90	14.97	12.95	12.41	8.41	7.08	12.50	8.80	12.46	7.90
4.41	10.88	11.98	14.42	13.03	13.52	8.46	6.74	12.58	8.37	12.54	7.27
4.44	10.63	12.06	15.28	13.12	13.87	8.51	6.98	12.66	7.90	12.62	7.48
4.46	10.24	12.13	14.56	13.20	14.95	8.57	7.31	12.74	7.74	12.70	7.32
4.49	10.54	12.21	14.61	13.28	15.77	8.62	7.50	12.82	7.93	12.78	6.98

4.52	11.22	12.28	14.92	13.36	16.90	8.67	7.23	12.90	8.43	12.86	6.48
4.54	10.61	12.36	14.60	13.44	16.16	8.73	6.66	12.98	8.44	12.93	6.41
4.57	11.06	12.43	14.15	13.53	17.08	8.78	7.32	13.06	8.90	13.01	6.26
4.60	11.74	12.51	13.90	13.61	15.78	8.83	7.60	13.13	8.51	13.09	6.33
4.62	10.81	12.58	13.63	13.69	15.38	8.89	8.42	13.21	8.19	13.17	6.29
4.65	11.14	12.66	12.92	13.77	15.17	8.94	8.59	13.29	7.58	13.25	6.45
4.68	11.02	12.73	12.32	13.85	14.71	8.99	8.63	13.37	8.08	13.33	5.90
4.70	11.06	12.81	12.22	13.94	14.15	9.05	9.94	13.45	7.81	13.41	5.83
4.73	10.34	12.88	12.12	14.02	13.61	9.10	8.91	13.53	7.57	13.49	5.72
4.76	11.13	12.96	12.14	14.10	12.84	9.15	9.84	13.61	7.51	13.57	5.66
4.78	11.39	13.04	12.30	14.18	12.53	9.21	10.46	13.69	7.43	13.64	5.77
4.81	11.38	13.11	11.85	14.26	12.13	9.26	10.50	13.77	7.39	13.72	5.91
4.84	11.59	13.19	11.56	14.35	11.89	9.31	11.03	13.85	7.13	13.80	6.43
4.86	11.19	13.26	11.06	14.43	11.93	9.37	11.11	13.93	7.29	13.88	6.29
4.89	11.26	13.34	10.52	14.51	12.43	9.42	10.77	14.00	6.96	13.96	6.73
4.92	11.00	13.41	10.92	14.59	12.03	9.47	10.32	14.08	6.26	14.04	6.79
4.94	10.52	13.49	11.27	14.67	12.25	9.53	11.45	14.16	5.99	14.12	6.61
4.97	9.99	13.56	12.54	14.76	12.05	9.58	9.96	14.24	5.56	14.20	7.24
4.99	10.18	13.64	11.78	14.84	12.09	9.63	9.86	14.32	5.32	14.28	7.19
5.02	9.66	13.71	12.03	14.92	11.36	9.68	9.97	14.40	5.04	14.35	7.34
5.05	9.87	13.79	10.32	15.00	11.65	9.74	10.23	14.48	5.33	14.43	7.25
5.07	10.60	13.86	10.88	15.08	11.61	9.79	10.52	14.56	5.46	14.51	7.18
5.10	10.85	13.94	11.41	15.17	11.51	9.84	8.40	14.64	5.22	14.59	7.43
5.13	10.42	14.01	13.48	15.25	11.60	9.90	10.44	14.72	5.08	14.67	7.46
5.15	11.22	14.09	13.98	15.33	11.44	9.95	9.60	14.80	4.92	14.75	7.46
5.18	10.29	14.17	15.37	15.41	11.60	10.00	11.82	14.88	5.21	14.83	7.31
5.21	10.38	14.24	15.19	15.49	11.32	10.06	13.02	14.95	5.75	14.91	6.90
5.23	10.31	14.32	15.38	15.58	11.45	10.11	13.17	15.03	5.65	14.98	7.61
5.26	9.71	14.39	15.46	15.66	11.15	10.16	12.05	15.11	5.92	15.06	7.62
5.29	10.58	14.47	16.07	15.74	11.37	10.22	9.94	15.19	6.07	15.14	7.50
5.31	9.68	14.54	16.26	15.82	11.58	10.27	7.44	15.27	6.44	15.22	7.64
5.34	9.88	14.62	18.13	15.90	11.71	10.32	7.28	15.35	6.27	15.30	7.65
5.37	10.58	14.69	18.25	15.98	11.59	10.38	7.21	15.43	6.55	15.38	8.08
5.39	10.20	14.77	16.05	16.07	11.51	10.43	7.22	15.51	6.70	15.46	8.21

5.42	9.81	14.84	14.78	16.15	11.38	10.48	7.31	15.59	7.12	15.54	8.37
5.45	9.86	14.92	13.83	16.23	11.80	10.54	7.57	15.67	7.29	15.62	8.27
5.47	9.65	14.99	13.17	16.31	11.47	10.59	7.51	15.75	7.81	15.69	8.52
5.50	9.36	15.07	12.17	16.40	11.56	10.64	8.02	15.82	7.56	15.77	8.77
5.53	8.89	15.14	14.31	16.48	11.47	10.70	8.78	15.90	7.52	15.85	8.95
5.55	9.15	15.22	12.61	16.56	11.03	10.75	7.60	15.98	7.70	15.93	8.66
5.58	9.16	15.30	13.40	16.64	11.18	10.80	6.78	16.06	7.82	16.01	8.80
5.61	9.00	15.37	11.84	16.72	11.21	10.86	6.60	16.14	8.03	16.09	8.43
5.63	8.92	15.45	12.56	16.81	11.32	10.91	6.83	16.22	7.72	16.17	8.96
5.66	9.25	15.52	12.35	16.89	12.43	10.96	6.91	16.30	7.79	16.25	8.38
5.69	9.09	15.60	12.47	16.97	12.22	11.02	7.07	16.38	7.79	16.33	8.78
5.71	9.43	15.67	12.43	17.05	13.48	11.07	7.35	16.46	7.33	16.40	8.34
5.74	9.92	15.75	11.85	17.13	14.14	11.12	7.20	16.54	7.78	16.48	8.88
5.77	9.34	15.82	12.09	17.21	14.76	11.18	7.45	16.62	7.45	16.56	8.76
5.79	9.33	15.90	12.20	17.30	14.81	11.23	7.33	16.69	7.24	16.64	8.71
5.82	8.89	15.97	12.56	17.38	15.20	11.28	7.53	16.77	7.36	16.72	8.17
5.85	9.00	16.05	11.90	17.46	15.51	11.34	7.52	16.85	7.44	16.80	8.01
5.87	8.91	16.12	12.06	17.54	15.95	11.39	7.67	16.93	7.40	16.88	7.95
5.90	8.68	16.20	11.63	17.62	17.05	11.44	8.04	17.01	7.35	16.96	7.97
5.93	8.55	16.27	10.84	17.71	17.89	11.50	8.03	17.09	7.70	17.04	7.64
5.95	8.65	16.35	10.83	17.79	17.73	11.55	7.89	17.17	7.90	17.11	7.79
5.98	8.91	16.43	11.04	17.87	17.74	11.60	7.27	17.25	8.03	17.19	7.81
6.01	8.95	16.50	10.39	17.95	16.35	11.66	7.44	17.33	7.87	17.27	7.42
6.03	8.87	16.58	10.39	18.03	16.77	11.71	7.78	17.41	7.95	17.35	7.14
6.06	9.14	16.65	10.86	18.12	17.38	11.76	8.66	17.49	7.95	17.43	6.67
6.09	9.37	16.73	10.54	18.20	17.38	11.81	9.92	17.57	8.01	17.51	6.61
6.11	9.40	16.80	11.06	18.28	17.17	11.87	10.17	17.64	8.40	17.59	6.33
6.14	9.48	16.88	11.07	18.36	17.98	11.92	9.84	17.72	8.41	17.67	6.21
6.17	10.13	16.95	10.39	18.44	16.96	11.97	8.45	17.80	8.98	17.74	6.50
6.19	10.21	17.03	10.14	18.53	16.39	12.03	6.40	17.88	8.79	17.82	6.22
6.22	10.00	17.10	10.27	18.61	16.14	12.08	5.82	17.96	8.89	17.90	6.63
6.25	10.21	17.18	10.61	18.69	16.57	12.13	5.68	18.04	8.31	17.98	6.25
6.27	10.24	17.25	9.92	18.77	17.62	12.19	5.33	18.12	7.99	18.06	6.48
6.30	10.11	17.33	10.22	18.85	15.42	12.24	5.55	18.20	8.31	18.14	6.53

6.32	10.43	17.41	10.37	18.94	15.84	12.29	5.44	18.28	8.00	18.22	6.58
6.35	10.34	17.48	10.01	19.02	15.59	12.35	4.99	18.36	7.13	18.30	6.68
6.38	10.25	17.56	10.53	19.10	16.98	12.40	5.36	18.44	6.83	18.38	6.69
6.40	10.35	17.63	10.08	19.18	16.95	12.45	5.44	18.51	7.10	18.45	7.07
6.43	10.83	17.71	9.64	19.26	17.25	12.51	5.30	18.59	6.97	18.53	6.97
6.46	10.98	17.78	10.05	19.35	16.93	12.56	5.49	18.67	6.82	18.61	7.23
6.48	10.86	17.86	9.83	19.43	17.00	12.61	5.75	18.75	6.74	18.69	7.40
6.51	10.72	17.93	10.26	19.51	16.67	12.67	5.02	18.83	6.67	18.77	7.67
6.54	10.00	18.01	9.86	19.59	15.76	12.72	5.00	18.91	6.85	18.85	7.52
6.56	10.05	18.08	9.67	19.67	16.70	12.77	4.64	18.99	6.66	18.93	7.43
6.59	9.69	18.16	9.70	19.76	16.71	12.83	4.67	19.07	7.09	19.01	7.05
6.62	9.76	18.23	9.93	19.84	16.53	12.88	4.54	19.15	7.78	19.09	6.88
6.64	9.69	18.31	9.61	19.92	17.12	12.93	4.63	19.23	8.21	19.16	7.18
6.67	9.81	18.38	9.40	20.00	16.78	12.99	4.84	19.31	9.56	19.24	6.98
6.70	9.20	18.46	9.92	20.08	16.93	13.04	5.06	19.38	10.15	19.32	7.24
6.72	8.98	18.54	10.73	20.17	16.73	13.09	5.90	19.46	10.82	19.40	7.19
6.75	9.45	18.61	10.56	20.25	17.01	13.15	5.71	19.54	11.14	19.48	7.32
6.78	9.00	18.69	10.82	20.33	15.95	13.20	5.67	19.62	11.21	19.56	7.51
6.80	9.40	18.76	11.32	20.41	16.07	13.25	5.35	19.70	10.65	19.64	7.11
6.83	9.41	18.84	10.81	20.49	16.01	13.31	5.86	19.78	10.89	19.72	7.64
6.86	9.42	18.91	10.97	20.58	16.14	13.36	5.22	19.86	11.66	19.80	7.13
6.88	8.97	18.99	11.46	20.66	15.77	13.41	5.52	19.94	12.14	19.87	7.87
6.91	8.90	19.06	11.60	20.74	14.69	13.47	5.71	20.02	12.33	19.95	8.24
6.94	8.96	19.14	11.64	20.82	15.56	13.52	5.68	20.10	11.90	20.03	8.56
6.96	9.46	19.21	12.07	20.90	15.68	13.57	5.41	20.18	12.93	20.11	7.82
6.99	9.18	19.29	11.76	20.99	15.93	13.62	5.66	20.25	12.16	20.19	7.79
7.02	9.42	19.36	11.39	21.07	16.54	13.68	5.61	20.33	11.42	20.27	8.02
7.04	8.88	19.44	10.80	21.15	17.12	13.73	5.99	20.41	12.85	20.35	8.41
7.07	9.29	19.51	10.27	21.23	17.07	13.78	6.28	20.49	12.70	20.43	8.57
7.10	9.35	19.59	9.84	21.31	15.97	13.84	5.79	20.57	11.34	20.51	8.82
7.12	9.50	19.67	9.31	21.40	16.41	13.89	5.58	20.65	11.00	20.58	9.00
7.15	9.59	19.74	9.75	21.48	15.73	13.94	5.68	20.73	9.20	20.66	8.68
7.18	10.09	19.82	9.87	21.56	16.22	14.00	6.20	20.81	9.55	20.74	9.15
7.20	10.35	19.89	9.46	21.64	14.48	14.05	5.95	20.89	8.26	20.82	9.36

7.23	9.99	19.97	9.79	21.72	14.95	14.10	5.57	20.97	10.48	20.90	8.97
7.26	9.79	20.04	9.43	21.81	13.17	14.16	5.82	21.05	9.98	20.98	8.76
7.28	9.67	20.12	9.34	21.89	13.80	14.21	6.03	21.13	9.51	21.06	8.42
7.31	9.12	20.19	9.86	21.97	12.75	14.26	5.89	21.20	9.69	21.14	8.73
7.34	9.42	20.27	9.67	22.05	12.48	14.32	5.88	21.28	9.57	21.22	8.93
7.36	9.81	20.34	9.06	22.13	13.23	14.37	5.93	21.36	8.87	21.29	8.85
7.39	9.83	20.42	9.65	22.22	13.07	14.42	5.53	21.44	9.15	21.37	8.75
7.42	9.72	20.49	9.95	22.30	14.17	14.48	5.41	21.52	9.76	21.45	8.93
7.44	9.99	20.57	10.04	22.38	13.80	14.53	5.16	21.60	8.55	21.53	8.73
7.47	9.82	20.64	9.90	22.46	14.55	14.58	4.90	21.68	8.31	21.61	8.93
7.50	9.85	20.72	9.98	22.54	14.11	14.64	4.95	21.76	7.82	21.69	8.85
7.52	9.31	20.80	9.86	22.62	14.34	14.69	5.16	21.84	7.17	21.77	8.55
7.55	9.61	20.87	10.05	22.71	14.10	14.74	4.92	21.92	7.52	21.85	8.93
7.57	9.33	20.95	9.47	22.79	14.33	14.80	5.00	22.00	6.75	21.92	8.99
7.60	9.25	21.02	9.66	22.87	13.70	14.85	4.80	22.07	6.77	22.00	9.57
7.63	9.04	21.10	9.45	22.95	13.46	14.90	5.08	22.15	6.64	22.08	8.98
7.65	9.66	21.17	9.72	23.03	13.24	14.96	4.92	22.23	6.91	22.16	9.26
7.68	9.13	21.25	9.84	23.12	13.06	15.01	4.63	22.31	6.67	22.24	9.46
7.71	9.05	21.32	10.39	23.20	12.92	15.06	5.14	22.39	6.65	22.32	9.02
7.73	8.81	21.40	9.65	23.28	13.33	15.12	5.12	22.47	6.48	22.40	9.84
7.76	8.40	21.47	9.77	23.36	13.54	15.17	5.05	22.55	7.35	22.48	9.23
7.79	8.38	21.55	10.00	23.44	13.12	15.22	5.21	22.63	8.26	22.56	9.78
7.81	7.90	21.62	9.93	23.53	14.34	15.28	4.83	22.71	7.40	22.63	9.81
7.84	7.77	21.70	9.93	23.59	11.49	15.33	4.56	22.79	7.21	22.71	9.73
7.87	7.38	21.77	9.93	23.59	15.00	15.38	4.31	22.87	7.36	22.79	9.73
7.89	6.89	21.85	10.76	23.67	11.43	15.44	4.19	22.95	8.03	22.87	9.31
7.92	7.14	21.93	9.80	23.75	11.52	15.49	4.20	23.02	8.65	22.95	9.57
7.95	7.40	22.00	9.89	23.82	12.18	15.54	4.36	23.10	8.11	23.03	9.54
7.97	7.58	22.08	10.30	23.90	12.03	15.60	4.18	23.18	7.48	23.11	9.15
8.00	7.69	22.15	11.13	23.97	12.09	15.65	4.23	23.26	8.95	23.19	9.18
8.03	8.54	22.23	10.70	24.05	12.46	15.70	4.26	23.34	8.20	23.27	8.87
8.05	9.13	22.30	10.75	24.12	12.00	15.75	4.31	23.42	8.35	23.34	9.00
8.08	9.17	22.38	11.60	24.20	12.80	15.81	3.96	23.50	7.94	23.42	9.25
8.11	9.76	22.45	11.12	24.27	13.13	15.86	3.52	23.58	9.88	23.50	8.01

8.13	9.82	22.53	11.53	24.35	13.02	15.91	3.72	23.66	10.44	23.58	8.16
8.16	10.40	22.60	11.60	24.43	12.47	15.97	3.80	23.74	11.35	23.66	8.66
8.19	10.94	22.68	11.95	24.50	12.89	16.02	3.70	23.82	10.12	23.74	8.03
8.21	11.27	22.75	12.19	24.58	12.37	16.07	3.84	23.89	9.22	23.82	7.70
8.24	12.03	22.83	11.80	24.65	13.09	16.13	3.89	23.97	10.51	23.90	7.31
8.27	12.83	22.90	11.29	24.73	12.83	16.18	3.63	24.05	9.74	23.98	7.19
8.29	13.18	22.98	12.15	24.80	12.84	16.23	3.70	24.13	10.25	24.05	7.22
8.32	13.02	23.06	10.05	24.88	13.24	16.29	4.00	24.21	10.30	24.13	7.41
8.35	13.95	23.13	11.68	24.95	11.30	16.34	4.03	24.29	9.23	24.21	7.67
8.37	14.17	23.21	11.55	25.03	13.71	16.39	4.14	24.37	9.97	24.29	7.89
8.40	13.98	23.28	11.29	25.10	13.52	16.45	4.22	24.45	9.54	24.37	7.97
8.43	13.44	23.33	14.31	25.18	13.23	16.50	3.93	24.53	8.61	24.45	7.35
8.45	13.76	23.33	12.04	25.26	13.34	16.55	3.97	24.61	9.19	24.53	7.53
8.48	12.77	23.41	14.25	25.33	12.30	16.61	4.02	24.69	9.13	24.61	8.25
8.51	11.95	23.49	14.96	25.41	12.91	16.66	3.79	24.77	8.74	24.68	7.40
8.53	12.09	23.56	14.53	25.48	12.70	16.71	3.69	24.84	7.98	24.76	7.92
8.56	11.87	23.64	15.13	25.56	12.91	16.77	3.85	24.92	7.37	24.84	8.17
8.59	11.74	23.72	14.77	25.63	13.51	16.82	3.69	25.00	7.08	24.92	7.54
8.61	11.25	23.79	14.72	25.71	13.07	16.87	3.60	25.08	7.59	25.00	7.89
8.64	10.77	23.87	13.91	25.78	12.84	16.93	3.35	25.16	6.93	25.08	7.96
8.67	11.44	23.95	14.18	25.86	12.88	16.98	3.46	25.24	7.50	25.16	8.30
8.69	11.10	24.02	14.06	25.94	13.71	17.03	3.35	25.32	7.68	25.24	8.28
8.72	11.73	24.10	14.26	26.01	13.25	17.09	3.43	25.40	8.89	25.32	8.49
8.75	10.92	24.18	13.52	26.09	13.08	17.14	3.52	25.48	9.72	25.39	8.86
8.77	11.65	24.26	13.56	26.16	12.35	17.19	3.77	25.56	9.39	25.47	9.14
8.80	11.48	24.33	13.05	26.24	11.71	17.25	3.82	25.64	10.60	25.55	9.19
8.82	11.65	24.41	13.97	26.31	11.38	17.30	3.66	25.71	8.56	25.63	9.06
8.85	11.90	24.49	12.81	26.39	12.05	17.35	3.56	25.79	8.75	25.71	8.65
8.88	12.63	24.56	13.33	26.46	12.50	17.41	3.73	25.87	7.47	25.79	9.03
8.90	12.26	24.64	12.98	26.54	12.33	17.46	4.08	25.95	7.51	25.87	8.26
8.93	12.28	24.72	12.78	26.61	12.49	17.51	4.24	26.03	7.32	25.95	8.32
8.96	12.21	24.79	13.04	26.69	12.66	17.56	4.32	26.11	6.33	26.03	7.69
8.98	12.47	24.87	12.09	26.77	13.11	17.62	4.29	26.19	6.25	26.10	7.84
9.01	12.72	24.95	12.84	26.84	12.59	17.67	4.36	26.27	6.65	26.18	7.15

9.04	11.98	25.03	12.27	26.92	13.23	17.72	4.39	26.35	7.50	26.26	7.56
9.06	12.06	25.10	13.09	26.99	12.40	17.78	4.35	26.43	8.73	26.34	7.02
9.09	11.82	25.18	12.45	27.07	13.16	17.83	4.56	26.51	8.86	26.42	7.19
9.12	11.72	25.26	12.53	27.14	13.04	17.88	4.37	26.58	7.24	26.50	7.36
9.14	12.86	25.33	11.82	27.22	13.05	17.94	3.47	26.66	6.40	26.58	7.46
9.17	12.97	25.41	10.84	27.29	13.11	17.99	3.58	26.74	6.30	26.66	8.02
9.20	11.87	25.49	10.35	27.37	13.32	18.04	3.58	26.82	6.41	26.74	7.64
9.22	13.21	25.56	11.32	27.44	13.20	18.10	3.53	26.90	6.37	26.81	8.17
9.25	13.09	25.64	12.55	27.52	12.80	18.15	3.64	26.98	6.54	26.89	7.17
9.28	13.20	25.72	11.63	27.60	11.66	18.20	3.45	27.06	6.65	26.97	7.08
9.30	12.33	25.80	11.81	27.67	12.37	18.26	3.35	27.14	6.67	27.05	7.36
9.33	13.76	25.87	11.65	27.75	11.44	18.31	3.48	27.22	6.56	27.13	7.07
9.36	12.00	25.95	11.38	27.82	10.99	18.36	3.45	27.30	6.48	27.21	7.64
9.38	12.36	26.03	11.54	27.90	10.78	18.42	3.75	27.38	8.78	27.29	6.94
9.41	12.16	26.10	11.05	27.97	11.21	18.47	3.93	27.46	8.42	27.37	7.88
9.44	11.68	26.18	11.14	28.05	11.26	18.52	4.30	27.53	9.48	27.45	7.61
9.46	12.00	26.26	10.87	28.12	11.63	18.58	3.50	27.61	8.85	27.52	7.74
9.49	12.74	26.33	10.92	28.20	12.15	18.63	3.36	27.69	8.13	27.60	7.80
9.52	12.38	26.41	10.57	28.28	11.12	18.68	3.17	27.77	8.44	27.68	7.53
9.54	12.65	26.49	10.57	28.35	11.59	18.74	3.68	27.85	8.44	27.76	7.24
9.57	12.92	26.57	10.49	28.43	11.76	18.79	3.50	27.93	7.72	27.84	7.04
9.60	12.40	26.64	10.32	28.50	11.79	18.84	3.76	28.01	8.13	27.92	7.29
9.62	12.86	26.72	10.18	28.58	11.91	18.90	3.76	28.09	8.73	28.00	7.51
9.65	12.65	26.80	10.16	28.65	12.09	18.95	4.03	28.17	9.18	28.08	7.88
9.68	12.71	26.87	9.70	28.73	12.27	19.00	4.07	28.25	7.29	28.16	8.51
9.70	12.59	26.95	9.43	28.80	12.23	19.06	4.31	28.33	7.85	28.23	8.32
9.73	12.56	27.03	8.82	28.88	11.93	19.11	4.43	28.40	7.55	28.31	7.80
9.76	12.87	27.10	8.88	28.95	12.75	19.16	4.52	28.48	8.90	28.39	8.55
9.78	12.83	27.18	8.79	29.03	12.51	19.22	4.52	28.56	9.87	28.47	8.55
9.81	12.99	27.26	9.23	29.11	12.52	19.27	4.07	28.64	9.43	28.55	8.67
9.84	12.70	27.33	8.60	29.18	12.96	19.32	4.22	28.72	7.95	28.63	8.72
9.86	12.81	27.41	8.86	29.26	12.77	19.38	4.52	28.80	9.48	28.71	9.47
9.89	13.19	27.49	8.42	29.33	12.66	19.43	4.34	28.88	7.74	28.79	8.96
9.92	13.03	27.57	8.28	29.41	11.63	19.48	4.34	28.96	8.35	28.87	8.51

9.94	12.79	27.64	7.75	29.48	12.23	19.53	3.90	29.04	8.12	28.94	7.92
9.97	12.66	27.72	8.14	29.56	12.10	19.59	4.18	29.12	7.76	29.02	8.76
10.00	12.54	27.80	8.25	29.63	12.56	19.64	4.01	29.20	6.36	29.10	8.67
10.02	13.11	27.87	8.93	29.71	11.82	19.69	4.17	29.28	6.28	29.18	8.38
10.05	12.71	27.95	7.99	29.79	12.69	19.75	4.13	29.35	5.75	29.26	8.42
10.08	13.13	28.03	7.74	29.86	11.42	19.80	4.04	29.43	5.95	29.34	8.27
10.10	13.05	28.10	8.11	29.94	12.02	19.85	4.03	29.51	5.64	29.42	8.05
10.13	12.92	28.18	8.08	30.01	11.11	19.91	4.08	29.59	6.87	29.50	9.23
10.15	13.08	28.26	8.83	30.09	11.14	19.96	4.53	29.67	7.24	29.57	9.18
10.18	12.35	28.34	8.99	30.16	11.15	20.01	4.50	29.75	6.90	29.65	9.05
10.21	12.40	28.41	8.90	30.24	10.67	20.07	5.34	29.83	6.40	29.73	8.96
10.23	12.35	28.49	8.38	30.31	10.42	20.12	4.19	29.91	7.06	29.81	8.48
10.26	12.48	28.57	8.01	30.39	11.61	20.17	4.60	29.99	6.31	29.89	9.42
10.29	12.03	28.64	8.43	30.46	11.50	20.23	4.47	30.07	6.03	29.97	8.67
10.31	11.93	28.72	8.71	30.54	11.41	20.28	4.55	30.15	6.08	30.05	8.12
10.34	12.38	28.80	8.63	30.62	11.09	20.33	4.86	30.22	5.43	30.13	8.72
10.37	12.39	28.87	8.64	30.69	10.92	20.39	4.58	30.30	5.20	30.21	7.72
10.39	12.32	28.95	9.47	30.77	11.28	20.44	4.67	30.38	5.34	30.28	8.50
10.42	12.53	29.03	9.30	30.84	11.55	20.49	4.60	30.46	4.85	30.36	8.73
10.45	12.52	29.11	8.57	30.92	10.92	20.55	4.64	30.54	5.07	30.44	9.27
10.47	12.46	29.18	8.49	30.99	11.25	20.60	4.10	30.62	4.67	30.52	7.98
10.50	12.79	29.26	7.96	31.07	10.87	20.65	3.33	30.70	4.89	30.60	7.76
10.53	12.44	29.34	8.09	31.14	11.12	20.71	3.28	30.78	4.14	30.68	6.92
10.55	12.50	29.41	8.04	31.22	10.62	20.76	3.00	30.86	4.70	30.76	7.04
10.58	12.12	29.49	7.55	31.30	10.81	20.81	2.63	30.94	4.79	30.84	6.94
10.61	12.49	29.57	7.40	31.37	10.49	20.87	2.69	31.02	4.96	30.92	6.62
10.63	12.29	29.64	7.53	31.45	10.42	20.92	2.48	31.09	5.48	30.99	6.84
10.66	12.61	29.72	7.55	31.52	10.38	20.97	2.67	31.17	4.83	31.07	6.26
10.69	12.51	29.80	7.96	31.60	10.33	21.03	2.77	31.25	5.01	31.15	6.98
10.71	12.48	29.88	7.25	31.67	10.94	21.08	2.81	31.33	6.00	31.23	6.68
10.74	12.45	29.95	7.75	31.75	10.29	21.13	3.00	31.41	4.64	31.31	6.51
10.77	12.10	30.03	7.73	31.82	10.36	21.19	3.09	31.49	5.21	31.39	6.52
10.79	12.27	30.11	7.55	31.90	9.79	21.24	3.29	31.57	5.80	31.47	6.27
10.82	11.74	30.18	7.51	31.97	9.40	21.29	3.14	31.65	5.14	31.55	6.24

10.85	12.18	30.26	7.49	32.05	8.83	21.35	3.01	31.73	6.01	31.62	6.04
10.87	11.74	30.34	7.78	32.13	8.69	21.40	3.28	31.81	5.86	31.70	6.44
10.90	12.21	30.41	7.48	32.20	8.24	21.45	3.39	31.89	5.06	31.78	6.79
10.93	11.91	30.49	7.80	32.28	8.66	21.50	3.29	31.96	5.21	31.86	7.30
10.95	12.30	30.57	7.71	32.35	8.40	21.56	3.87	32.04	5.33	31.94	7.67
10.98	12.43	30.65	6.76	32.43	8.74	21.61	4.12	32.12	5.43	32.02	7.33
11.01	11.95	30.72	7.70	32.50	9.05	21.66	3.34	32.20	5.49	32.10	7.93
11.03	12.29	30.80	7.60	32.58	8.87	21.72	3.51	32.28	5.76	32.18	8.08
11.06	12.05	30.88	7.38	32.65	8.73	21.77	3.59	32.36	5.95	32.26	8.41
11.09	12.24	30.95	7.23	32.73	9.03	21.82	4.10	32.44	5.50	32.33	7.96
11.11	12.27	31.03	7.33	32.80	9.01	21.88	4.35	32.52	6.28	32.41	8.05
11.14	12.15	31.11	8.77	32.88	8.14	21.93	4.33	32.60	6.33	32.49	7.41
11.17	12.33	31.18	8.18	32.96	8.17	21.98	4.02	32.68	5.66	32.57	6.84
11.19	12.08	31.26	8.85	33.03	8.98	22.04	3.86	32.76	5.73	32.65	6.71
11.22	12.33	31.34	7.07	33.11	8.85	22.09	4.54	32.84	5.80	32.73	6.31
11.25	11.49	31.42	6.63	33.18	8.91	22.14	5.03	32.91	5.65	32.81	5.20
11.27	11.85	31.49	6.96	33.26	8.64	22.20	4.74	32.99	6.49	32.89	5.32
11.30	11.97	31.57	6.82	33.33	8.93	22.25	4.97	33.07	5.40	32.97	5.27
11.33	11.38	31.65	6.89	33.41	9.43	22.30	5.15	33.15	5.71	33.04	4.87
11.35	11.21	31.72	6.90	33.48	9.02	22.36	5.09	33.23	5.20	33.12	5.33
11.38	11.06	31.80	7.20	33.56	9.08	22.41	5.24	33.31	5.19	33.20	4.96
11.40	11.01	31.88	7.07	33.63	9.43	22.46	4.97	33.39	5.11	33.28	5.52
11.43	10.77	31.95	7.26	33.71	9.13	22.52	5.01	33.47	5.57	33.36	5.80
11.46	10.40	32.03	7.50	33.79	8.84	22.57	5.08	33.55	5.38	33.44	5.42
11.48	11.33	32.11	7.47	33.86	8.73	22.62	4.94	33.63	5.90	33.52	5.44
11.51	11.21	32.19	7.95	33.94	8.51	22.68	4.98	33.71	6.13	33.60	5.29
11.54	11.51	32.26	7.50	34.01	8.48	22.73	5.01	33.78	6.26	33.68	5.61
11.56	11.79	32.34	7.57	34.09	8.09	22.78	4.95	33.86	4.90	33.75	5.22
11.59	11.90	32.42	7.82	34.16	7.84	22.84	5.34	33.94	5.04	33.83	4.59
11.62	11.91	32.49	8.11	34.24	7.96	22.89	5.12	34.02	5.65	33.91	4.38
11.64	11.74	32.57	7.22	34.31	7.58	22.94	5.09	34.10	6.07	33.99	4.62
11.67	11.67	32.65	7.36	34.39	7.63	23.00	5.03	34.18	5.69	34.07	5.09
11.70	12.04	32.72	7.50	34.47	7.51	23.05	5.15	34.26	5.74	34.15	5.08
11.72	12.39	32.80	6.93	34.54	7.85	23.10	4.71	34.34	5.97	34.23	5.06

11.75	12.47	32.88	6.58	34.62	7.38	23.16	5.10	34.42	4.55	34.31	4.88
11.78	13.13	32.96	6.69	34.69	8.22	23.21	4.83	34.50	5.14	34.39	5.18
11.80	13.00	33.03	6.60	34.77	8.29	23.26	5.10	34.58	5.43	34.46	6.07
11.83	13.26	33.11	6.87	34.84	8.92	23.31	4.75	34.66	4.43	34.54	5.32
11.86	13.14	33.19	6.53	34.92	8.71	23.37	4.60	34.73	5.26	34.62	4.97
11.88	13.03	33.26	6.97	34.99	8.84	23.42	4.99	34.81	5.11	34.70	4.87
11.91	13.27	33.34	6.51	35.07	9.13	23.47	5.33	34.89	5.84	34.78	5.34
11.94	13.58	33.42	6.58	35.15	8.78	23.53	5.12	34.97	5.34	34.86	4.95
11.96	13.81	33.49	6.97	35.22	8.44	23.58	5.54	35.05	6.48	34.94	4.89
11.99	15.25	33.57	7.42	35.30	8.10	23.63	5.70	35.13	6.20	35.02	4.98
12.02	14.64	33.65	7.37	35.37	8.43	23.69	5.37	35.21	5.30	35.10	4.64
12.04	14.87	33.73	7.46	35.45	8.53	23.74	5.12	35.29	6.11	35.17	4.52
12.07	12.49	33.80	7.06	35.52	8.26	23.79	5.69	35.37	5.58	35.25	4.33
12.10	11.61	33.88	6.92	35.60	8.22	23.85	5.99	35.45	5.67	35.33	4.49
12.12	11.30	33.96	7.05	35.67	7.67	23.90	5.58	35.53	5.63	35.41	4.70
12.15	11.22	34.03	7.05	35.75	7.63	23.95	6.08	35.60	5.53	35.49	4.55
12.18	10.30	34.11	7.23	35.82	7.83	24.01	5.69	35.68	5.27	35.57	4.27
12.20	10.36	34.19	7.48	35.90	7.76	24.06	6.20	35.76	6.23	35.65	4.71
12.23	9.82	34.26	7.37	35.98	7.78	24.11	5.54	35.84	5.79	35.73	4.46
12.26	9.39	34.34	7.67	36.05	7.68	24.17	5.84	35.92	5.27	35.81	4.66
12.28	9.31	34.42	7.34	36.13	7.75	24.22	5.93	36.00	5.67	35.88	4.91
12.31	9.29	34.50	7.29	36.20	8.11	24.27	5.88	36.08	5.18	35.96	5.16
12.34	9.45	34.57	7.37	36.28	8.37	24.33	5.39	36.16	5.64	36.04	5.12
12.36	9.20	34.65	7.39	36.35	8.18	24.38	5.37	36.24	5.47	36.12	5.00
12.39	9.09	34.73	7.00	36.43	8.65	24.43	5.66	36.32	5.92	36.20	4.81
12.42	8.93	34.80	7.09	36.50	8.94	24.49	5.74	36.40	5.76	36.28	5.86
12.44	9.09	34.88	6.99	36.58	9.25	24.54	5.63	36.48	5.45	36.36	5.32
12.47	8.75	34.96	6.81	36.65	8.79	24.59	6.20	36.55	5.49	36.44	5.40
12.50	8.95	35.03	6.67	36.73	9.01	24.65	5.56	36.63	6.08	36.51	5.76
12.52	8.80	35.11	6.56	36.81	8.32	24.70	5.95	36.71	6.65	36.59	6.10
12.55	8.31	35.19	6.40	36.88	8.62	24.75	6.82	36.79	5.91	36.67	5.18
12.58	8.39	35.27	6.18	36.96	8.57	24.81	6.11	36.87	6.19	36.75	5.39
12.60	8.38	35.34	6.41	37.03	8.78	24.86	6.07	36.95	6.08	36.83	5.13
12.63	8.32	35.42	6.31	37.11	8.66	24.91	6.88	37.03	6.14	36.91	5.34

12.66	8.60	35.50	6.25	37.18	8.30	24.97	5.87	37.11	5.76	36.99	4.78
12.68	8.76	35.57	6.29	37.26	8.28	25.02	5.92	37.19	6.07	37.07	4.91
12.71	8.70	35.65	6.10	37.33	8.03	25.07	6.09	37.27	5.41	37.15	5.79
12.73	8.46	35.73	6.39	37.41	7.78	25.13	6.62	37.35	5.38	37.23	6.13
12.76	8.69	35.80	6.23	37.49	7.45	25.18	6.71	37.42	4.71	37.30	5.84
12.79	9.04	35.88	5.99	37.56	7.61	25.23	6.73	37.50	5.15	37.38	5.39
12.81	8.66	35.96	6.36	37.64	7.84	25.29	7.18	37.58	5.31	37.46	5.07
12.84	9.20	36.04	6.36	37.71	7.84	25.34	7.97	37.66	5.22	37.54	5.26
12.87	9.28	36.11	6.02	37.79	7.26	25.39	6.61	37.74	5.88	37.62	5.70
12.89	9.49	36.19	4.86	37.86	7.31	25.44	6.38	37.82	5.62	37.70	5.08
12.92	9.59	36.27	4.34	37.94	7.68	25.50	7.02	37.90	5.51	37.78	5.30
12.95	9.63	36.34	3.62	38.01	7.34	25.55	6.82	37.98	5.33	37.86	5.14
12.97	9.63	36.42	3.57	38.09	7.30	25.60	5.96	38.06	5.47	37.93	4.97
13.00	9.92	36.50	3.76	38.16	7.37	25.66	5.56	38.14	5.32	38.01	4.91
13.03	10.24	36.57	4.07	38.24	7.17	25.71	5.40	38.22	5.50	38.09	4.97
13.05	10.51	36.65	4.60	38.32	7.45	25.76	5.86	38.29	5.03	38.17	5.16
13.08	10.62	36.73	4.76	38.39	7.43	25.82	5.92	38.37	4.73	38.25	5.30
13.11	10.68	36.80	4.46	38.47	7.49	25.87	6.65	38.45	5.23	38.33	4.70
13.13	10.68	36.88	4.46	38.54	7.17	25.92	6.78	38.53	4.99	38.41	4.75
13.16	11.20	36.96	4.53	38.62	7.25	25.98	6.52	38.61	5.28	38.49	4.78
13.19	11.17	37.04	4.93	38.69	7.79	26.03	6.33	38.69	5.41	38.57	4.34
13.21	11.10	37.11	4.93	38.77	7.90	26.08	5.85	38.77	4.82	38.64	4.67
13.24	11.53	37.19	5.06	38.84	7.79	26.14	6.29	38.85	4.74	38.72	4.69
13.27	11.29	37.27	5.39	38.92	8.10	26.19	6.50	38.93	5.00	38.80	4.72
13.29	11.46	37.34	5.62	38.99	8.08	26.24	6.64	39.01	5.40	38.88	5.08
13.32	11.78	37.42	5.67	39.07	8.18	26.30	6.48	39.09	4.46	38.96	4.76
13.35	12.02	37.50	5.96	39.15	7.94	26.35	6.58	39.17	4.26	39.04	4.79
13.37	12.22	37.57	5.96	39.22	8.22	26.40	6.65	39.24	4.96	39.12	5.15
13.40	12.29	37.65	6.48	39.30	8.53	26.46	5.89	39.32	4.98	39.20	4.71
13.43	12.18	37.73	6.66	39.37	8.66	26.51	6.21	39.40	5.74	39.28	4.58
13.45	12.72	37.81	7.00	39.45	8.93	26.56	5.83	39.48	5.63	39.35	4.46
13.48	12.56	37.88	7.81	39.52	9.30	26.62	5.32	39.56	6.04	39.43	4.61
13.51	12.79	37.96	5.64	39.60	9.22	26.67	5.95	39.64	6.55	39.51	4.85
13.53	13.02	38.04	5.51	39.67	9.37	26.72	5.37	39.72	4.84	39.59	4.98

13.56	13.12	38.11	5.04	39.75	9.13	26.78	5.85	39.80	5.24	39.67	4.83
13.59	13.08	38.19	5.28	39.82	9.27	26.83	6.09	39.88	5.87	39.75	4.44
13.61	13.34	38.27	5.36	39.90	8.96	26.88	6.33	39.96	4.81	39.83	4.35
13.64	13.49	38.35	5.68	39.98	8.37	26.94	7.02	40.04	4.91	39.91	4.15
13.67	13.25	38.42	6.53	40.05	8.03	26.99	5.91	40.11	4.61	39.99	4.27
13.69	12.97	38.50	5.75	40.13	8.07	27.04	5.78	40.19	4.79	40.06	4.22
13.72	13.38	38.58	6.29	40.20	7.92	27.10	5.92	40.27	5.01	40.14	4.61
13.75	13.39	38.65	6.00	40.28	7.92	27.15	5.64	40.35	5.37	40.22	5.22
13.77	13.49	38.73	6.58	40.35	8.11	27.20	6.63	40.43	5.81	40.30	5.24
13.80	14.10	38.81	7.00	40.43	7.58	27.26	6.48	40.51	5.87	40.38	4.96
13.83	13.85	38.88	7.53	40.50	7.59	27.31	6.35	40.59	5.61	40.46	5.40
13.85	13.98	38.96	8.25	40.58	7.59	27.36	6.77	40.67	5.65	40.54	4.79
13.88	13.76	39.04	7.10	40.66	7.29	27.41	6.92	40.75	6.24	40.62	5.03
13.91	13.12	39.11	7.53	40.73	7.70	27.47	7.33	40.83	4.88	40.69	5.33
13.93	13.46	39.19	7.15	40.81	7.58	27.52	7.13	40.91	5.37	40.77	5.11
13.96	13.61	39.27	7.27	40.88	7.83	27.57	7.72	40.98	5.04	40.85	5.87
13.98	13.66	39.35	7.07	40.96	8.05	27.63	6.80	41.06	4.42	40.93	5.76
14.01	13.64	39.42	6.91	41.03	7.98	27.68	6.49	41.14	4.79	41.01	6.03
14.04	13.60	39.50	6.61	41.11	7.79	27.73	7.55	41.22	5.51	41.09	5.72
14.06	13.54	39.58	6.78	41.18	7.70	27.79	8.32	41.30	5.42	41.17	5.53
14.09	13.41	39.65	6.61	41.26	7.43	27.84	7.44	41.38	4.72	41.25	5.03
14.12	12.86	39.73	6.40	41.33	7.48	27.89	7.23	41.46	5.55	41.33	4.50
14.14	13.26	39.81	6.21	41.41	7.32	27.95	7.33	41.54	5.07	41.40	4.55
14.17	13.10	39.88	6.43	41.49	7.82	28.00	6.48	41.62	5.56	41.48	4.61
14.20	13.47	39.96	6.43	41.56	7.05	28.05	6.69	41.70	5.64	41.56	4.45
14.22	13.08	40.04	5.97	41.64	7.19	28.11	6.00	41.78	5.15	41.64	4.56
14.25	13.30	40.12	5.94	41.71	6.93	28.16	6.40	41.86	5.31	41.72	4.78
14.28	12.37	40.19	5.73	41.79	6.97	28.21	6.03	41.93	6.03	41.80	4.93
14.30	12.91	40.27	5.65	41.86	7.41	28.27	6.23	42.01	5.15	41.88	4.78
14.33	12.91	40.35	5.49	41.94	9.52	28.32	6.74	42.09	4.90	41.96	4.78
14.36	13.05	40.42	5.42	42.01	11.51	28.37	6.90	42.17	5.08	42.04	4.42
14.38	12.98	40.50	5.51	42.09	14.76	28.43	6.47	42.25	5.47	42.11	4.60
14.41	13.00	40.58	5.50	42.16	15.85	28.48	6.57	42.33	4.76	42.19	5.07
14.44	12.65	40.65	5.74	42.24	12.19	28.53	6.84	42.41	5.52	42.27	4.55

14.46	12.58	40.73	5.43	42.32	6.95	28.59	6.54	42.49	4.00	42.35	4.85
14.49	12.68	40.81	5.65	42.39	5.60	28.64	6.37	42.57	4.77	42.43	5.18
14.52	12.67	40.89	5.85	42.47	6.34	28.69	6.15	42.65	4.85	42.51	4.89
14.54	12.77	40.96	6.23	42.54	6.80	28.75	6.76	42.73	5.37	42.59	5.72
14.57	12.56	41.04	5.85	42.62	7.95	28.80	6.40	42.80	5.13	42.67	5.03
14.60	12.23	41.12	5.98	42.69	7.62	28.85	6.19	42.88	5.19	42.75	5.52
14.62	12.59	41.19	6.13	42.77	7.93	28.91	7.00	42.96	4.62	42.82	4.49
14.65	12.69	41.27	5.97	42.84	7.29	28.96	7.45	43.04	5.08	42.90	4.83
14.68	12.01	41.35	5.87	42.92	6.37	29.01	6.23	43.12	4.24	42.98	5.32
14.70	11.86	41.43	6.36	42.99	5.56	29.07	7.06	43.20	4.38	43.06	5.39
14.73	12.54	41.50	6.10	43.07	5.57	29.12	7.79	43.28	4.93	43.14	5.49
14.76	12.61	41.58	6.07	43.15	5.49	29.17	6.80	43.36	4.80	43.22	4.70
14.78	12.78	41.66	6.16	43.22	5.07	29.23	7.02	43.44	4.42	43.30	5.90
14.81	12.70	41.73	6.19	43.30	5.13	29.28	6.49	43.52	4.61	43.38	4.03
14.84	12.98	41.81	6.13	43.37	4.89	29.33	6.01	43.60	4.66	43.46	5.00
14.86	12.46	41.89	6.61	43.45	4.82	29.39	5.94	43.67	4.24	43.53	3.80
14.89	12.38	41.96	6.07	43.52	4.54	29.44	5.30	43.75	4.72	43.61	4.57
14.92	13.06	42.04	6.45	43.60	4.46	29.49	5.64	43.83	4.43	43.69	4.26
14.94	12.94	42.12	6.32	43.67	4.63	29.54	5.45	43.91	3.67	43.77	4.59
14.97	13.01	42.19	6.43	43.75	4.35	29.60	5.99	43.99	4.98	43.85	4.18
15.00	13.05	42.27	5.93	43.83	5.02	29.65	5.38	44.07	4.50	43.93	4.40
15.02	13.62	42.35	6.40	43.90	4.95	29.70	5.70	44.15	4.88	44.01	4.20
15.05	13.27	42.43	6.24	43.98	4.92	29.76	5.82	44.23	4.95	44.09	4.47
15.08	13.48	42.50	6.20	44.05	5.40	29.81	5.65	44.31	4.48	44.17	4.68
15.10	12.99	42.58	5.85	44.13	5.67	29.86	5.97	44.39	4.79	44.24	4.16
15.13	13.13	42.66	5.85	44.20	6.84	29.92	5.63	44.47	4.00	44.32	4.33
15.16	13.05	42.73	6.03	44.28	6.77	29.97	5.82	44.55	4.54	44.40	4.19
15.18	13.10	42.81	5.93	44.35	6.47	30.02	5.76	44.62	4.73	44.48	4.55
15.21	13.43	42.89	5.84	44.43	6.13	30.08	5.73	44.70	3.78	44.56	4.98
15.23	14.15	42.96	5.89	44.50	6.51	30.13	5.76	44.78	4.58	44.64	4.48
15.26	14.10	43.04	6.40	44.58	6.78	30.18	6.06	44.86	3.84	44.72	4.31
15.29	14.63	43.12	5.87	44.66	6.92	30.24	5.97	44.94	4.03	44.80	4.12
15.31	14.46	43.20	5.68	44.73	6.75	30.29	6.23	45.02	3.76	44.87	4.10
15.34	13.65	43.27	5.85	44.81	6.58	30.34	5.91	45.10	4.05	44.95	4.06

15.37	13.99	43.35	5.72	44.88	6.07	30.40	6.57	45.18	4.10	45.03	3.95
15.39	14.04	43.43	5.56	44.96	6.20	30.45	6.15	45.26	4.15	45.11	4.17
15.42	13.36	43.50	5.53	45.03	6.01	30.50	6.87	45.34	4.81	45.19	4.73
15.45	14.38	43.58	5.86	45.11	6.08	30.56	7.00	45.42	3.78	45.27	4.86
15.47	13.84	43.66	5.58	45.18	6.25	30.61	7.45	45.49	3.81	45.35	4.47
15.50	13.94	43.73	5.34	45.26	6.07	30.66	6.58	45.57	4.91	45.43	4.85
15.53	13.75	43.81	5.00	45.34	6.08	30.72	7.15	45.65	3.63	45.51	5.07
15.55	14.37	43.89	4.95	45.41	6.12	30.77	6.85	45.73	4.97	45.58	5.25
15.58	14.16	43.97	4.79	45.49	6.23	30.82	6.90	45.81	4.36	45.66	4.50
15.61	14.26	44.04	5.07	45.56	5.99	30.88	7.84	45.89	4.87	45.74	4.68
15.63	14.72	44.12	4.80	45.64	6.13	30.93	6.89	45.97	5.14	45.82	3.97
15.66	14.46	44.20	4.95	45.71	5.89	30.98	5.87	46.05	4.20	45.90	4.62
15.69	13.82	44.27	4.73	45.79	6.19	31.04	6.04	46.13	4.14	45.98	4.51
15.71	14.35	44.35	4.77	45.86	6.34	31.09	6.88	46.21	5.20	46.06	4.17
15.74	14.27	44.43	4.53	45.94	5.93	31.14	7.08	46.29	4.13	46.14	4.20
15.77	14.30	44.50	4.65	46.01	5.97	31.20	6.07	46.37	4.20	46.22	4.23
15.79	14.53	44.58	4.49	46.09	5.96	31.25	6.22	46.44	4.42	46.29	4.12
15.82	14.70	44.66	4.93	46.17	5.81	31.30	5.87	46.52	4.54	46.37	3.95
15.85	14.18	44.74	5.44	46.24	6.04	31.35	5.60	46.60	3.11	46.45	4.18
15.87	14.70	44.81	5.36	46.32	5.51	31.41	5.54	46.68	2.99	46.53	3.53
15.90	13.95	44.89	5.75	46.39	5.61	31.46	5.62	46.76	2.94	46.61	3.62
15.93	14.72	44.97	5.96	46.47	5.64	31.51	5.46	46.84	2.62	46.69	3.96
15.95	14.59	45.04	5.39	46.54	5.51	31.57	4.71	46.92	3.02	46.77	3.73
15.98	13.75	45.12	4.70	46.62	5.61	31.62	4.81	47.00	3.05	46.85	4.02
16.01	15.70	45.20	4.52	46.69	5.60	31.67	5.04	47.08	2.80	46.93	3.57
16.03	14.11	45.27	4.73	46.77	5.97	31.73	5.61	47.16	2.78	47.00	4.62
16.06	14.15	45.35	5.14	46.85	5.64	31.78	5.49	47.24	3.08	47.08	3.83
16.09	13.71	45.43	5.92	46.92	5.87	31.83	5.79	47.31	3.07	47.16	4.29
16.11	13.56	45.50	5.96	47.00	6.24	31.89	5.43	47.39	2.96	47.24	3.18
16.14	14.19	45.58	6.33	47.07	6.11	31.94	5.13	47.47	2.69	47.32	3.19
16.17	14.25	45.66	7.35	47.15	6.45	31.99	6.12	47.55	3.38	47.40	3.65
16.19	13.52	45.74	7.22	47.22	6.22	32.05	6.05	47.63	3.37	47.48	3.47
16.22	13.96	45.81	6.55	47.30	6.56	32.10	5.93	47.71	3.25	47.56	3.79
16.25	13.51	45.89	6.65	47.37	5.95	32.15	6.41	47.79	3.35	47.64	4.20

16.27	14.16	45.97	6.78	47.45	5.93	32.21	6.66	47.87	2.96	47.71	4.23
16.30	13.91	46.04	6.69	47.52	5.77	32.26	5.90	47.95	3.38	47.79	4.07
16.33	14.09	46.12	6.95	47.60	5.76	32.31	7.01	48.03	3.38	47.87	4.01
16.35	14.19	46.20	7.16	47.68	5.40	32.37	7.07	48.11	3.68	47.95	3.45
16.38	13.58	46.27	7.10	47.75	5.89	32.42	7.16	48.18	3.54	48.03	4.50
16.40	13.20	46.35	7.23	47.83	5.87	32.47	6.82	48.26	3.64	48.11	4.37
16.43	13.01	46.43	6.53	47.90	6.23	32.53	7.15	48.34	3.55	48.19	4.48
16.46	13.98	46.51	6.80	47.98	6.22	32.58	7.29	48.42	3.32	48.27	4.83
16.48	13.77	46.58	6.94	48.05	5.78	32.63	7.05	48.50	3.33	48.35	4.74
16.51	14.34	46.66	6.95	48.13	5.89	32.69	6.93	48.58	3.32	48.42	4.36
16.54	13.61	46.74	6.39	48.20	5.69	32.74	6.75	48.66	3.35	48.50	4.62
16.56	14.34	46.81	7.08	48.28	5.83	32.79	6.90	48.74	2.62	48.58	4.33
16.59	14.61	46.89	6.69	48.35	6.40	32.85	6.20	48.82	3.22	48.66	4.24
16.62	14.38	46.97	6.54	48.43	5.70	32.90	6.44	48.90	3.85	48.74	4.39
16.64	14.24	47.04	6.59	48.51	5.50	32.95	5.83	48.98	3.22	48.82	4.44
16.67	14.48	47.12	6.60	48.58	5.38	33.01	5.98	49.06	2.89	48.90	3.96
16.70	14.71	47.20	6.60	48.66	5.59	33.06	6.56	49.13	4.04	48.98	3.82
16.72	14.09	47.28	6.18	48.73	5.38	33.11	6.02	49.21	3.99	49.06	4.09
16.75	14.29	47.35	6.64	48.81	5.79	33.16	5.88	49.29	4.47	49.13	3.61
16.78	14.49	47.43	6.35	48.88	5.19	33.22	6.66	49.37	4.54	49.21	3.33
16.80	14.42	47.51	6.22	48.96	5.47	33.27	6.98	49.45	4.98	49.29	4.14
16.83	14.38	47.58	6.32	49.03	5.32	33.32	6.29	49.53	4.82	49.37	4.12
16.86	14.63	47.66	6.33	49.11	5.55	33.38	6.42	49.61	4.89	49.45	4.79
16.88	14.26	47.74	6.00	49.19	5.41	33.43	5.98	49.69	4.39	49.53	4.00
16.91	13.57	47.81	6.17	49.26	5.19	33.48	6.97	49.77	4.53	49.61	3.74
16.94	14.27	47.89	6.10	49.34	5.92	33.54	6.74	49.85	4.12	49.69	3.97
16.96	14.37	47.97	5.96	49.41	6.02	33.59	6.43	49.93	4.10	49.76	3.67
16.99	14.40	48.05	5.69	49.49	6.18	33.64	6.41	50.00	5.25	49.84	4.63
17.02	14.46	48.12	5.97	49.56	5.79	33.70	6.79	50.08	4.35	49.92	3.47
17.04	14.34	48.20	5.94	49.64	6.04	33.75	6.16	50.16	3.83	50.00	3.64
17.07	13.82	48.28	5.91	49.71	6.26	33.80	6.13	50.24	4.44	50.08	4.05
17.10	13.61	48.35	5.99	49.79	6.39	33.86	6.09	50.32	4.24	50.16	3.94
17.12	13.83	48.43	6.00	49.86	7.08	33.91	6.41	50.40	4.32	50.24	4.11
17.15	13.78	48.51	5.81	49.94	6.87	33.96	6.62	50.48	4.71	50.32	4.31

17.18	13.23	48.58	6.11	50.02	6.58	34.02	6.92	50.56	4.40	50.40	4.85
17.20	13.35	48.66	6.18	50.09	6.41	34.07	6.10	50.64	5.08	50.47	4.10
17.23	13.27	48.74	6.66	50.17	6.22	34.12	6.34	50.72	5.50	50.55	4.90
17.26	13.77	48.82	6.53	50.24	6.32	34.18	6.43	50.80	4.87	50.63	4.95
17.28	13.34	48.89	6.50	50.32	6.87	34.23	6.47	50.87	4.61	50.71	4.92
17.31	13.54	48.97	6.27	50.39	6.78	34.28	6.59	50.95	5.62	50.79	4.33
17.34	13.25	49.05	6.09	50.47	6.75	34.34	6.64	51.03	4.56	50.87	4.92
17.36	13.82	49.12	6.03	50.54	7.45	34.39	6.93	51.11	5.66	50.95	4.80
17.39	13.28	49.20	6.39	50.62	7.88	34.44	6.58	51.19	5.85	51.03	4.73
17.42	13.79	49.28	6.01	50.70	8.34	34.50	6.46	51.27	5.54	51.11	4.17
17.44	13.22	49.35	6.37	50.77	7.82	34.55	7.33	51.35	4.89	51.18	4.52
17.47	13.19	49.43	5.85	50.85	7.98	34.60	6.98	51.43	5.82	51.26	4.68
17.50	12.63	49.51	5.91	50.92	8.39	34.66	6.62	51.51	5.06	51.34	4.56
17.52	12.88	49.58	5.90	51.00	8.26	34.71	6.24	51.59	4.99	51.42	5.19
17.55	12.80	49.66	5.26	51.07	8.38	34.76	6.51	51.67	5.48	51.50	4.58
17.58	12.74	49.74	5.05	51.15	7.82	34.82	6.27	51.75	4.99	51.58	5.61
17.60	13.08	49.82	4.81	51.22	8.72	34.87	5.74	51.82	4.74	51.66	6.08
17.63	12.99	49.89	4.98	51.30	8.76	34.92	6.03	51.90	5.71	51.74	5.64
17.66	12.43	49.97	4.94	51.37	8.60	34.98	5.83	51.98	4.38	51.82	6.33
17.68	12.45	50.05	5.18	51.45	7.81	35.03	5.94	52.06	4.47	51.89	6.19
17.71	12.94	50.12	5.55	51.53	7.56	35.08	5.43	52.14	4.00	51.97	6.06
17.73	12.72	50.20	5.69	51.60	7.64	35.13	5.66	52.22	5.23	52.05	5.03
17.76	12.08	50.28	5.83	51.68	7.33	35.19	6.30	52.30	5.74	52.13	5.99
17.79	12.34	50.35	5.24	51.75	7.81	35.24	5.79	52.38	5.47	52.21	7.39
17.81	12.56	50.43	5.71	51.83	7.12	35.29	6.15	52.46	5.03	52.29	5.46
17.84	12.43	50.51	6.02	51.90	7.31	35.35	5.85	52.54	5.04	52.37	5.63
17.87	12.66	50.59	5.92	51.98	6.84	35.40	5.37	52.62	4.98	52.45	5.66
17.89	12.77	50.66	6.17	52.05	7.45	35.45	5.96	52.69	4.80	52.52	4.92
17.92	12.67	50.74	6.01	52.13	7.07	35.51	6.53	52.77	5.46	52.60	4.98
17.95	13.13	50.82	5.89	52.20	7.37	35.56	6.27	52.85	5.57	52.68	5.31
17.97	12.24	50.89	5.46	52.28	7.16	35.61	5.86	52.93	5.69	52.76	5.35
18.00	12.83	50.97	5.46	52.36	6.80	35.67	6.39	53.01	5.01	52.84	5.50
18.03	11.70	51.05	5.38	52.43	6.93	35.72	6.62	53.09	5.59	52.92	5.14
18.05	12.53	51.12	5.32	52.51	7.12	35.77	6.74	53.17	5.19	53.00	5.05

18.08	11.83	51.20	5.71	52.58	7.42	35.83	7.22	53.25	4.72	53.08	5.15
18.11	12.23	51.28	7.12	52.66	7.52	35.88	7.27	53.33	5.49	53.16	5.05
18.13	12.51	51.36	7.32	52.73	7.32	35.93	7.26	53.41	4.86	53.24	5.60
18.16	11.81	51.43	7.15	52.81	7.48	35.99	6.70	53.49	5.58	53.31	5.21
18.19	12.76	51.51	5.63	52.88	7.37	36.04	6.82	53.56	4.65	53.39	5.35
18.21	12.81	51.59	6.01	52.96	7.55	36.09	6.99	53.64	5.96	53.47	4.71
18.24	11.37	51.66	5.44	53.04	7.30	36.15	6.74	53.72	5.56	53.55	4.46
18.27	11.16	51.74	5.52	53.11	7.63	36.20	6.63	53.80	5.86	53.63	5.33
18.29	12.55	51.82	6.16	53.19	7.79	36.25	6.74	53.88	5.13	53.71	5.37
18.32	12.09	51.89	5.52	53.26	7.92	36.31	6.87	53.96	5.86	53.79	5.44
18.35	11.08	51.97	6.32	53.34	7.66	36.36	5.85	54.04	6.28	53.87	4.90
18.37	12.38	52.05	6.56	53.41	7.54	36.41	6.04	54.12	5.52	53.94	5.07
18.40	11.31	52.13	7.22	53.49	7.61	36.47	6.03	54.20	6.09	54.02	4.86
18.43	12.02	52.20	7.17	53.56	6.53	36.52	6.24	54.28	4.96	54.10	4.33
18.45	12.36	52.28	7.48	53.64	6.45	36.57	6.07	54.36	4.88	54.18	4.88
18.48	11.34	52.36	7.50	53.71	6.21	36.63	5.58	54.44	4.90	54.26	4.94
18.51	11.57	52.43	7.42	53.79	5.39	36.68	5.99	54.51	5.97	54.34	4.48
18.53	11.82	52.51	7.24	53.87	5.17	36.73	5.71	54.59	4.83	54.42	4.86
18.56	12.48	52.59	6.92	53.94	5.02	36.79	5.79	54.67	5.08	54.50	4.09
18.59	12.06	52.66	6.88	54.02	5.27	36.84	5.30	54.75	5.10	54.58	5.39
18.61	11.61	52.74	6.49	54.09	5.59	36.89	5.91	54.83	5.23	54.65	5.52
18.64	11.20	52.82	6.43	54.17	5.76	36.95	7.05	54.91	4.25	54.73	5.38
18.67	11.89	52.90	6.81	54.24	5.93	37.00	6.62	54.99	6.43	54.81	5.99
18.69	12.56	52.97	6.78	54.32	6.05	37.05	6.32	55.07	4.79	54.89	4.33
18.72	13.29	53.05	6.42	54.39	5.95	37.10	7.27	55.15	5.30	54.97	5.26
18.75	12.56	53.13	6.18	54.47	6.02	37.16	7.17	55.23	5.03	55.05	4.79
18.77	13.15	53.20	5.74	54.54	5.90	37.21	7.66	55.31	5.85	55.13	4.04
18.80	13.04	53.28	5.31	54.62	6.02	37.26	7.27	55.38	5.87	55.21	6.26
18.83	13.73	53.36	5.20	54.70	6.44	37.32	6.65	55.46	4.41	55.29	5.15
18.85	14.33	53.43	5.52	54.77	7.11	37.37	6.68	55.54	4.23	55.36	5.67
18.88	13.98	53.51	5.39	54.85	7.12	37.42	6.49	55.62	3.93	55.44	5.52
18.91	13.36	53.59	5.74	54.92	7.02	37.48	6.46	55.70	5.20	55.52	4.55
18.93	16.63	53.67	5.65	55.00	7.41	37.53	6.51	55.78	4.73	55.60	5.25
18.96	16.72	53.74	5.53	55.07	7.43	37.58	6.55	55.86	5.76	55.68	5.71

18.99	17.30	53.82	5.35	55.15	7.39	37.64	6.31	55.94	6.30	55.76	4.94
19.01	17.66	53.90	5.55	55.22	7.43	37.69	6.11	56.02	6.01	55.84	5.72
19.04	20.15	53.97	5.30	55.30	7.28	37.74	6.77	56.10	5.53	55.92	5.44
19.06	19.89	54.05	5.28	55.37	7.73	37.80	6.47	56.18	4.45	56.00	5.79
19.09	19.64	54.13	5.65	55.45	8.05	37.85	6.76	56.26	6.83	56.07	5.08
19.12	20.09	54.20	5.44	55.53	8.00	37.90	6.24	56.33	5.29	56.15	4.77
19.14	19.92	54.28	5.26	55.60	7.71	37.96	6.21	56.41	5.01	56.23	4.85
19.17	19.73	54.36	5.12	55.68	7.19	38.01	7.09	56.49	5.84	56.31	5.55
19.20	20.41	54.44	5.45	55.75	7.32	38.06	6.82	56.57	4.81	56.39	6.11
19.22	19.94	54.51	5.63	55.83	9.78	38.12	6.71	56.65	6.28	56.47	5.91
19.25	19.48	54.59	5.12	55.90	9.18	38.17	7.08	56.73	5.99	56.55	6.16
19.28	20.70	54.67	5.59	55.98	7.81	38.22	7.12	56.81	6.20	56.63	5.11
19.30	19.72	54.74	5.94	56.05	7.75	38.28	6.62	56.89	6.83	56.71	3.76
19.33	16.90	54.82	5.97	56.13	7.27	38.33	6.57	56.97	6.52	56.78	3.19
19.36	18.32	54.90	5.77	56.21	6.74	38.38	6.32	57.05	5.50	56.86	3.34
19.38	16.62	54.97	6.27	56.28	7.83	38.44	6.22	57.13	5.70	56.94	3.05
19.41	16.78	55.05	6.62	56.36	6.98	38.49	6.54	57.20	4.92	57.02	2.68
19.44	16.49	55.13	6.58	56.43	7.04	38.54	6.36	57.28	6.01	57.10	3.28
19.46	15.72	55.21	6.46	56.51	6.91	38.60	6.06	57.36	6.02	57.18	3.45
19.49	16.67	55.28	6.41	56.58	7.16	38.65	6.13	57.44	5.32	57.26	3.52
19.52	16.19	55.36	6.66	56.66	6.62	38.70	6.60	57.52	4.92	57.34	3.07
19.54	16.84	55.44	7.08	56.73	6.86	38.76	5.90	57.60	5.55	57.41	3.77
19.57	16.32	55.51	7.25	56.81	6.65	38.81	6.10	57.68	5.07	57.49	3.33
19.60	16.14	55.59	7.80	56.88	6.54	38.86	5.93	57.76	6.00	57.57	4.19
19.62	14.72	55.67	8.30	56.96	6.56	38.92	5.57	57.84	5.43	57.65	4.43
19.65	14.64	55.74	8.44	57.04	7.15	38.97	6.00	57.92	5.79	57.73	4.81
19.68	14.90	55.82	9.46	57.11	6.74	39.02	6.19	58.00	5.11	57.81	4.98
19.70	14.06	55.90	9.72	57.19	7.10	39.07	5.93	58.07	5.75	57.89	3.67
19.73	14.98	55.98	9.08	57.26	7.25	39.13	6.07	58.15	5.93	57.97	4.97
19.76	14.13	56.05	8.56	57.34	7.22	39.18	5.93	58.23	6.69	58.05	4.59
19.78	13.71	56.13	8.44	57.41	7.59	39.23	6.22	58.31	6.29	58.12	3.98
19.81	12.99	56.21	8.55	57.49	7.51	39.29	6.87	58.39	6.03	58.20	3.68
19.84	13.49	56.28	9.62	57.56	7.42	39.34	6.61	58.47	5.12	58.28	4.00
19.86	12.44	56.36	9.53	57.64	7.95	39.39	6.46	58.55	5.86	58.36	4.30

19.89	12.16	56.44	10.27	57.71	8.49	39.45	7.51	58.63	4.81	58.44	3.65
19.92	12.48	56.51	10.06	57.79	8.44	39.50	8.30	58.71	5.25	58.52	4.90
19.94	12.24	56.59	9.79	57.87	8.44	39.55	8.02	58.79	6.44	58.60	4.07
19.97	12.18	56.67	9.69	57.94	8.80	39.61	7.09	58.87	6.50	58.68	4.53
20.00	12.51	56.74	9.32	58.02	8.52	39.66	6.70	58.94	5.87	58.76	5.42
20.02	12.25	56.82	9.13	58.09	9.18	39.71	6.63	59.02	6.66	58.83	5.09
20.05	13.13	56.90	8.69	58.17	8.88	39.77	6.73	59.10	5.95	58.91	4.39
20.08	13.38	56.98	9.13	58.24	9.01	39.82	6.14	59.18	7.55	58.99	5.01
20.10	14.10	57.05	9.09	58.32	8.36	39.87	6.87	59.26	6.40	59.07	4.48
20.13	13.19	57.13	8.61	58.39	8.74	39.93	6.50	59.34	5.20	59.15	4.00
20.15	13.11	57.21	9.53	58.47	9.31	39.98	7.42	59.42	6.86	59.23	4.51
20.18	12.37	57.28	9.61	58.55	9.06	40.03	6.74	59.50	6.04	59.31	5.72
20.21	12.43	57.36	9.38	58.62	8.33	40.09	7.20	59.58	5.53	59.39	5.53
20.23	12.03	57.44	9.52	58.70	8.77	40.14	6.49	59.66	4.99	59.47	6.15
20.26	12.38	57.51	9.10	58.77	8.43	40.19	7.64	59.74	6.41	59.54	5.18
20.29	11.63	57.59	8.90	58.85	8.45	40.25	7.44	59.81	6.22	59.62	6.22
20.31	12.32	57.67	9.37	58.92	8.64	40.30	8.14	59.89	5.34	59.70	4.90
20.34	11.75	57.75	9.07	59.00	8.52	40.35	7.18	59.97	6.51	59.78	4.13
20.37	12.36	57.82	9.06	59.07	8.32	40.41	6.78	60.05	6.04	59.86	4.94
20.39	12.47	57.90	8.81	59.15	8.73	40.46	6.59	60.13	6.73	59.94	4.61
20.42	12.14	57.98	8.44	59.22	8.74	40.51	6.36	60.21	7.30	60.02	5.44
20.45	12.62	58.05	8.92	59.30	8.58	40.57	6.31	60.29	7.77	60.10	3.88
20.47	12.35	58.13	8.22	59.38	9.13	40.62	6.18	60.37	5.74	60.18	4.43
20.50	13.78	58.21	8.37	59.45	8.70	40.67	6.38	60.45	6.79	60.25	4.22
20.53	13.50	58.28	8.43	59.53	8.43	40.73	6.82	60.53	6.61	60.33	4.63
20.55	12.73	58.36	8.11	59.60	8.25	40.78	6.93	60.61	8.82	60.41	3.87
20.58	13.62	58.44	8.47	59.68	8.62	40.83	6.45	60.69	8.04	60.49	5.37
20.61	14.46	58.52	8.55	59.75	8.43	40.88	7.19	60.76	6.11	60.57	5.59
20.63	13.97	58.59	8.20	59.83	8.39	40.94	7.18	60.84	6.59	60.65	5.72
20.66	13.63	58.67	7.68	59.90	8.31	40.99	7.16	60.92	7.18	60.73	5.57
20.69	13.89	58.75	7.97	59.98	8.39	41.04	6.46	61.00	7.90	60.81	6.09
20.71	13.87	58.82	7.89	60.06	9.00	41.10	6.42	61.08	6.49	60.89	6.26
20.74	13.75	58.90	8.07	60.13	8.87	41.15	6.60	61.16	7.35	60.96	4.52
20.77	12.68	58.98	7.96	60.21	8.65	41.20	6.84	61.24	7.94	61.04	4.92

20.79	13.13	59.05	8.33	60.28	8.49	41.26	6.56	61.32	6.37	61.12	5.36
20.82	12.98	59.13	8.75	60.36	8.40	41.31	6.22	61.40	6.03	61.20	5.74
20.85	13.46	59.21	8.58	60.43	8.63	41.36	6.88	61.48	7.15	61.28	5.32
20.87	12.10	59.29	8.98	60.51	7.98	41.42	6.22	61.56	6.90	61.36	5.93
20.90	11.77	59.36	9.10	60.58	7.98	41.47	6.20	61.63	6.46	61.44	4.55
20.93	12.80	59.44	8.90	60.66	7.86	41.52	6.72	61.71	7.05	61.52	5.62
20.95	12.02	59.52	9.20	60.73	7.95	41.58	6.79	61.79	7.21	61.60	5.58
20.98	12.52	59.59	9.28	60.81	7.74	41.63	6.61	61.87	5.77	61.67	6.37
21.01	12.98	59.67	9.27	60.89	7.84	41.68	6.52	61.95	6.50	61.75	4.71
21.03	13.91	59.75	9.20	60.96	8.18	41.74	5.97	62.03	5.87	61.83	5.34
21.06	15.28	59.82	9.24	61.04	8.16	41.79	6.72	62.11	6.38	61.91	6.44
21.09	15.89	59.90	8.90	61.11	8.42	41.84	6.50	62.19	6.98	61.99	5.71
21.11	17.38	59.98	8.90	61.19	8.01	41.90	7.43	62.27	7.40	62.07	5.74
21.14	19.89	60.06	8.46	61.26	8.43	41.95	7.42	62.35	7.10	62.15	5.57
21.17	19.06	60.13	8.08	61.34	8.68	42.00	6.75	62.43	8.27	62.23	4.73
21.19	19.85	60.21	8.02	61.41	8.14	42.06	6.86	62.51	6.11	62.30	4.89
21.22	20.19	60.29	8.11	61.49	8.32	42.11	7.96	62.58	5.80	62.38	5.30
21.25	21.11	60.36	7.72	61.56	8.70	42.16	6.68	62.66	5.82	62.46	5.08
21.27	19.36	60.44	8.18	61.64	9.15	42.22	6.94	62.74	7.44	62.54	5.33
21.30	20.25	60.52	8.27	61.72	8.92	42.27	7.28	62.82	7.16	62.62	6.68
21.32	18.53	60.59	8.28	61.79	9.30	42.32	6.72	62.90	8.48	62.70	5.23
21.35	19.29	60.67	8.19	61.87	10.06	42.38	7.05	62.98	7.94	62.78	4.52
21.38	19.91	60.75	7.99	61.94	9.34	42.43	7.50	63.06	7.29	62.86	6.20
21.40	18.68	60.83	7.84	62.02	10.25	42.48	6.95	63.14	7.51	62.94	5.27
21.43	18.75	60.90	7.70	62.09	9.78	42.54	7.25	63.22	7.12	63.01	5.63
21.46	18.81	60.98	7.92	62.17	9.90	42.59	7.48	63.30	8.98	63.09	6.38
21.48	18.84	61.06	7.15	62.24	9.78	42.64	6.85	63.38	7.49	63.17	6.27
21.51	18.36	61.13	6.71	62.32	9.40	42.70	6.91	63.45	7.86	63.25	4.92
21.54	17.95	61.21	7.01	62.40	9.87	42.75	6.13	63.53	7.66	63.33	6.35
21.56	19.95	61.29	6.61	62.47	9.60	42.80	6.63	63.61	6.39	63.41	5.32
21.59	18.26	61.36	6.50	62.55	9.59	42.86	7.24	63.69	7.03	63.49	6.15
21.62	18.80	61.44	6.50	62.62	9.50	42.91	6.89	63.77	6.98	63.57	6.17
21.64	20.95	61.52	6.44	62.70	9.15	42.96	8.10	63.85	6.65	63.65	6.01
21.67	18.90	61.60	6.60	62.77	9.22	43.01	7.40	63.93	5.62	63.72	5.75

21.70	19.82	61.67	6.56	62.85	9.67	43.07	8.43	64.01	6.63	63.80	4.86
21.72	19.43	61.75	6.79	62.92	9.46	43.12	7.81	64.09	5.45	63.88	4.78
21.75	19.99	61.83	6.94	63.00	9.17	43.17	8.56	64.17	7.52	63.96	5.46
21.78	19.21	61.90	7.70	63.07	9.39	43.23	7.90	64.25	6.76	64.04	5.93
21.80	19.32	61.98	7.22	63.15	9.22	43.28	7.71	64.33	6.01	64.12	5.42
21.83	18.35	62.06	7.11	63.23	9.12	43.33	7.82	64.40	4.97	64.20	5.19
21.86	19.63	62.13	7.74	63.30	9.04	43.39	8.34	64.48	5.56	64.28	5.59
21.88	15.86	62.21	7.47	63.38	9.58	43.44	7.34	64.56	5.65	64.36	4.80
21.91	15.27	62.29	7.33	63.45	8.85	43.49	6.77	64.64	5.64	64.43	5.29
21.94	16.37	62.37	7.29	63.53	9.13	43.55	7.71	64.72	5.11	64.51	5.19
21.96	14.40	62.44	7.08	63.60	9.20	43.60	7.12	64.80	6.46	64.59	6.11
21.99	13.10	62.52	6.27	63.68	7.92	43.65	7.12	64.88	6.59	64.67	5.33
22.02	14.40	62.60	5.97	63.75	8.08	43.71	6.96	64.96	6.15	64.75	5.61
22.04	13.24	62.67	6.33	63.83	8.33	43.76	7.09	65.04	5.77	64.83	4.58
22.07	13.14	62.75	6.38	63.91	7.46	43.81	7.51	65.12	5.47	64.91	6.51
22.10	12.92	62.83	7.05	63.98	6.62	43.87	7.19	65.20	7.14	64.99	4.84
22.12	12.94	62.90	7.44	64.06	6.94	43.92	7.66	65.27	6.09	65.07	4.60
22.15	13.03	62.98	7.10	64.13	7.26	43.97	7.08	65.35	6.22	65.14	5.24
22.18	12.91	63.06	6.78	64.21	7.01	44.03	7.58	65.43	5.79	65.22	4.20
22.20	12.26	63.14	7.25	64.28	7.65	44.08	7.32	65.51	6.81	65.30	5.33
22.23	12.43	63.21	8.29	64.36	7.96	44.13	6.80	65.59	6.42	65.38	5.18
22.26	12.34	63.29	8.84	64.43	8.58	44.19	8.01	65.67	6.38	65.46	5.15
22.28	12.88	63.37	8.95	64.51	8.56	44.24	7.22	65.75	6.58	65.54	4.62
22.31	13.39	63.44	9.30	64.58	8.53	44.29	7.40	65.83	6.64	65.62	4.50
22.34	12.85	63.52	8.79	64.66	7.87	44.35	7.60	65.91	7.08	65.70	4.78
22.36	13.61	63.60	7.80	64.74	8.62	44.40	7.74	65.99	6.09	65.78	4.52
22.39	13.74	63.67	8.27	64.81	7.90	44.45	7.20	66.07	5.74	65.85	4.66
22.42	13.67	63.75	7.55	64.89	7.46	44.51	7.00	66.15	7.02	65.93	4.99
22.44	14.55	63.83	7.42	64.96	7.32	44.56	6.88	66.22	6.97	66.01	5.51
22.47	14.59	63.90	6.98	65.04	7.48	44.61	7.27	66.30	7.57	66.09	5.04
22.50	14.81	63.98	6.94	65.11	7.97	44.66	6.67	66.38	6.50	66.17	5.41
22.52	15.33	64.06	6.30	65.19	7.84	44.72	6.64	66.46	6.63	66.25	6.75
22.55	14.67	64.14	6.53	65.26	7.98	44.77	5.82	66.54	6.20	66.33	8.95
22.57	15.70	64.21	6.24	65.34	8.44	44.82	6.55	66.62	5.98	66.41	8.80

22.60	15.77	64.29	5.72	65.41	8.94	44.88	6.44	66.70	4.65	66.48	9.15
22.63	15.19	64.37	6.16	65.49	9.50	44.93	6.93	66.78	7.25	66.56	8.17
22.65	16.54	64.44	5.79	65.57	9.44	44.98	6.13	66.86	6.14	66.64	6.58
22.68	16.56	64.52	5.24	65.64	9.22	45.04	7.05	66.94	5.11	66.72	8.07
22.71	16.24	64.60	5.54	65.72	8.35	45.09	6.65	67.02	4.23	66.80	7.56
22.73	15.98	64.67	5.41	65.79	8.46	45.14	6.84	67.09	5.61	66.88	7.18
22.76	17.69	64.75	5.58	65.87	8.36	45.20	6.94	67.17	6.88	66.96	5.49
22.79	15.27	64.83	5.59	65.94	7.40	45.25	5.97	67.25	5.42	67.04	5.95
22.81	15.78	64.91	6.05	66.02	8.84	45.30	6.75	67.33	5.20	67.12	7.35
22.84	15.07	64.98	5.67	66.09	8.40	45.36	7.10	67.41	5.16	67.19	6.85
22.87	15.79	65.06	5.97	66.17	8.63	45.41	7.54	67.49	5.95	67.27	4.65
22.89	15.81	65.14	6.20	66.25	8.77	45.46	7.10	67.57	6.92	67.35	5.71
22.92	16.65	65.21	5.92	66.32	8.95	45.52	7.79	67.65	6.52	67.43	5.81
22.95	15.99	65.29	6.39	66.40	8.29	45.57	7.14	67.73	5.69	67.51	8.04
22.97	16.20	65.37	5.86	66.47	8.87	45.62	7.25	67.81	6.58	67.59	7.49
23.00	14.61	65.44	5.10	66.55	9.10	45.68	6.80	67.89	6.50	67.67	8.27
23.03	15.54	65.52	5.17	66.62	10.32	45.73	7.09	67.96	7.23	67.75	9.48
23.05	14.31	65.60	5.71	66.70	9.09	45.78	8.08	68.04	6.09	67.83	7.76
23.08	14.39	65.68	5.81	66.77	10.60	45.84	7.46	68.12	6.70	67.90	8.66
23.11	13.18	65.75	6.09	66.85	9.67	45.89	6.64	68.20	6.70	67.98	9.23
23.13	12.41	65.83	6.78	66.92	9.48	45.94	8.03	68.28	6.68	68.06	7.20
23.16	13.89	65.91	6.26	67.00	9.46	46.00	7.36	68.36	7.55	68.14	6.89
23.19	13.79	65.98	6.07	67.08	9.18	46.05	7.43	68.44	6.98	68.22	6.46
23.21	13.60	66.06	6.00	67.15	9.72	46.10	7.55	68.52	7.59	68.30	7.40
23.24	14.15	66.14	6.41	67.23	9.25	46.16	7.79	68.60	7.48	68.38	6.67
23.27	13.05	66.21	7.30	67.30	9.29	46.21	8.24	68.68	7.42	68.46	4.84
23.29	13.39	66.29	7.76	67.38	9.55	46.26	7.37	68.76	8.83	68.54	6.62
23.32	14.13	66.37	8.22	67.45	9.32	46.32	7.34	68.83	7.98	68.61	6.78
23.35	12.33	66.45	8.49	67.53	8.98	46.37	7.71	68.91	5.64	68.69	6.42
23.37	13.25	66.52	7.99	67.60	9.32	46.42	6.71	68.99	8.01	68.77	5.67
23.40	12.21	66.60	8.59	67.68	8.61	46.48	6.85	69.07	7.66	68.85	7.06
23.43	12.89	66.68	7.59	67.76	9.25	46.53	6.99	69.15	7.62	68.93	6.01
23.45	13.31	66.75	8.50	67.83	10.09	46.58	6.24	69.23	6.96	69.01	4.83
23.48	14.32	66.83	8.59	67.91	9.52	46.64	6.29	69.31	6.56	69.09	5.06

23.51	13.89	66.91	8.66	67.98	9.37	46.69	6.69	69.39	6.38	69.17	6.46
23.53	13.66	66.98	8.78	68.06	9.19	46.74	6.43	69.47	7.27	69.24	4.51
23.56	13.99	67.06	8.35	68.13	9.19	46.79	6.11	69.55	5.76	69.32	6.21
23.59	12.50	67.14	8.39	68.21	9.10	46.85	6.39	69.61	7.38	69.40	5.64
23.61	12.47	67.22	9.28	68.28	8.96	46.90	5.76			69.48	6.04
23.64	11.55	67.29	10.13	68.36	9.32	46.95	6.09			69.56	5.45
23.67	12.10	67.37	10.32	68.43	8.98	47.01	5.56			69.64	6.19
23.69	12.47	67.45	9.69	68.51	8.78	47.06	6.01			69.72	4.75
23.72	11.95	67.52	10.47	68.59	8.59	47.11	6.03			69.80	5.07
23.75	12.04	67.60	8.27	68.66	7.78	47.17	5.81			69.88	5.00
23.77	12.60	67.68	8.11	68.74	8.04	47.22	6.17			69.95	5.69
23.80	11.92	67.75	8.49	68.81	8.24	47.27	5.88			70.03	6.16
23.82	12.72	67.83	7.93	68.89	8.73	47.33	6.32			70.11	5.37
23.85	12.59	67.91	8.82	68.96	9.11	47.38	6.37			70.19	5.99
23.88	12.96	67.99	9.07	69.04	9.66	47.43	6.78			70.27	6.12
23.90	12.54	68.06	9.71	69.11	9.61	47.49	7.48			70.35	5.41
23.93	12.78	68.14	9.24	69.19	10.34	47.54	6.91			70.43	5.68
23.96	13.73	68.22	8.97	69.26	9.04	47.59	7.56			70.51	4.75
23.98	13.52	68.29	11.53	69.34	8.75	47.65	7.19			70.59	4.64
24.01	13.54	68.37	9.26	69.42	8.71	47.70	7.85			70.66	6.27
24.04	13.49	68.45	8.65	69.49	7.97	47.75	7.68			70.74	6.67
24.06	12.89	68.52	8.38	69.57	8.40	47.81	7.93			70.82	7.22
24.09	13.84	68.60	8.44	69.64	8.76	47.86	7.44			70.90	8.39
24.12	12.84	68.68	11.04	69.72	9.36	47.91	7.65			70.98	6.34
24.14	13.90	68.76	11.63	69.79	10.14	47.97	8.49			71.06	6.06
24.17	15.84	68.83	11.12	69.87	9.93	48.02	8.18			71.14	6.22
24.20	16.61	68.91	8.88	69.94	10.56	48.07	8.41			71.22	6.20
24.22	16.70	68.99	9.16	70.02	10.83	48.13	8.05			71.30	5.92
24.25	16.04	69.06	9.82	70.10	11.67	48.18	7.95			71.37	6.27
24.28	15.93	69.14	10.69	70.17	11.18	48.23	7.39			71.45	4.30
24.30	15.98	69.22	10.00	70.25	11.88	48.29	7.49			71.53	5.71
24.33	15.89	69.29	10.21	70.32	12.07	48.34	6.61			71.61	4.75
24.36	16.83	69.37	10.23	70.40	11.11	48.39	7.03			71.69	5.29
24.38	17.77	69.45	10.44	70.47	10.96	48.45	6.86			71.77	5.52

24.41	16.06	69.53	10.24	70.55	11.00	48.50	6.37	71.85	5.16
24.44	16.95	69.60	10.41	70.62	11.75	48.55	6.53	71.93	4.82
24.46	16.53	69.68	10.22	70.70	11.70	48.61	5.51		
24.49	14.51	69.76	9.94	70.77	11.31	48.66	6.30		
24.52	16.52	69.83	10.75	70.85	11.40	48.71	6.26		
24.54	14.47	69.91	10.05	70.93	10.17	48.77	5.95		
24.57	14.01	69.99	11.57	71.00	10.49	48.82	6.13		
24.60	13.65	70.06	10.66	71.08	10.31	48.87	5.87		
24.62	13.83	70.14	11.79	71.15	11.31	48.92	6.12		
24.65	14.39	70.22	11.17	71.23	12.13	48.98	6.06		
24.68	13.93	70.29	11.66	71.30	11.04	49.03	6.74		
24.70	14.52	70.37	10.59	71.38	11.51	49.08	6.30		
24.73	14.33	70.45	10.79	71.45	11.55	49.14	6.16		
24.76	13.73	70.53	12.12	71.53	11.04	49.19	6.08		
24.78	12.64	70.60	12.93	71.60	11.55	49.24	5.98		
24.81	14.74	70.68	13.00	71.68	10.88	49.30	6.19		
24.84	14.71	70.76	11.87	71.76	10.58	49.35	5.78		
24.86	12.93	70.83	13.43	71.83	10.29	49.40	6.07		
24.89	12.82	70.91	14.24	71.91	9.66	49.46	5.77		
24.92	11.67	70.99	15.50	71.98	7.74	49.51	5.98		
24.94	11.83	71.06	15.30	72.06	6.74	49.56	5.39		
24.97	11.74	71.14	20.11	72.13	7.07	49.62	5.66		
25.00	11.95	71.22	17.88	72.21	7.02	49.67	5.68		
25.02	11.62	71.30	17.39	72.28	7.36	49.72	5.43		
25.05	11.31	71.37	14.72	72.36	7.20	49.78	5.74		
25.07	11.37	71.45	14.39	72.44	7.40	49.83	5.96		
25.10	11.58	71.53	14.32	72.51	7.67	49.88	6.03		
25.13	10.89	71.60	16.35	72.59	7.89	49.94	6.34		
25.15	11.90	71.68	13.35	72.66	8.06	49.99	6.15		
25.18	11.39	71.76	12.56	72.74	9.10	50.04	7.01		
25.21	13.39	71.84	12.87	72.81	9.03	50.10	6.62		
25.23	13.05	71.91	12.22	72.89	9.43	50.15	6.81		
25.26	12.75	71.99	11.58	72.96	9.10	50.20	7.16		
25.29	11.76	72.07	12.38	73.04	9.85	50.26	7.78		

25.31	12.91	72.14	11.76	73.11	9.47	50.31	6.76
25.34	13.59	72.22	9.81	73.19	8.91	50.36	7.11
25.37	12.66	72.30	11.36	73.27	8.62	50.42	7.44
25.39	11.99	72.37	10.56	73.34	9.05	50.47	7.29
25.42	11.53	72.45	11.30	73.42	9.68	50.52	7.25
25.45	11.15	72.53	10.30	73.49	8.90	50.58	7.70
25.47	11.95	72.61	11.90	73.57	8.99	50.63	7.50
25.50	10.70	72.68	12.12	73.64	9.01	50.68	8.25
25.53	12.49	72.76	13.94	73.72	8.49	50.74	8.15
25.55	11.89	72.84	11.64	73.79	8.79	50.79	7.62
25.58	11.60	72.91	9.55	73.87	8.82	50.84	7.39
25.61	12.61	72.99	9.43	73.94	8.79	50.89	7.48
25.63	12.06	73.07	10.31	74.02	8.71	50.95	7.59
25.66	11.71	73.14	10.97	74.10	8.41	51.00	7.34
25.69	11.09	73.22	9.17	74.17	8.08	51.05	8.56
25.71	12.16	73.30	9.45	74.25	8.52	51.11	8.43
25.74	12.66	73.38	8.16	74.32	7.98	51.16	8.90
25.77	13.41	73.45	8.96	74.40	8.11	51.21	9.18
25.79	13.41	73.53	9.64	74.47	8.41	51.27	9.24
25.82	14.37	73.61	10.50	74.55	8.14	51.32	9.42
25.85	12.23	73.68	9.61	74.62	8.55	51.37	8.61
25.87	15.31	73.76	10.25	74.70	8.23	51.43	8.12
25.90	13.19	73.84	8.62	74.78	8.32	51.48	8.04
25.93	13.65	73.91	8.94	74.85	7.96	51.53	7.95
25.95	15.47	73.99	9.06	74.93	7.81	51.59	7.67
25.98	14.43	74.07	8.63	75.00	8.59	51.64	7.17
26.01	13.23	74.15	9.36	75.08	8.42	51.69	7.59
26.03	15.10	74.22	9.65	75.15	8.14	51.75	7.22
26.06	14.64	74.30	9.10	75.23	8.69	51.80	6.92
26.09	13.11	74.38	10.47	75.30	8.83	51.85	7.36
26.11	13.64	74.45	10.67	75.38	9.43	51.91	7.77
26.14	14.19	74.53	9.81	75.45	9.06	51.96	7.04
26.17	14.52	74.61	10.22	75.53	8.09	52.01	7.09
26.19	14.59	74.68	11.43	75.61	9.57	52.07	8.16

26.22	14.14	74.76	10.39	75.68	8.51	52.12	7.75
26.25	14.03	74.84	10.31	75.76	9.59	52.17	6.86
26.27	13.46	74.92	10.21	75.83	9.32	52.23	7.13
26.30	13.87	74.99	10.24	75.91	9.79	52.28	7.92
26.32	15.46	75.07	10.89	75.98	11.24	52.33	7.73
26.35	13.65	75.15	11.57	76.06	10.20	52.39	7.25
26.38	14.00	75.22	11.64	76.13	10.45	52.44	7.25
26.40	14.84	75.30	11.67	76.21	10.44	52.49	7.10
26.43	15.75	75.38	12.39	76.28	10.28	52.55	6.61
26.46	15.80	75.45	12.90	76.36	11.65	52.60	6.56
26.48	16.87	75.53	10.66	76.44	9.76	52.65	6.55
26.51	17.15	75.61	9.35	76.51	11.88	52.70	5.99
26.54	18.61	75.69	8.24	76.59	13.26	52.76	5.72
26.56	18.54	75.76	7.99	76.66	10.67	52.81	5.17
26.59	20.49	75.84	7.82	76.74	12.16	52.86	5.78
26.62	21.67	75.92	7.23	76.81	12.11	52.92	5.45
26.64	19.37	75.99	8.11	76.89	12.81	52.97	6.04
26.67	17.16	76.07	6.86	76.96	12.36	53.02	6.20
26.70	17.05	76.15	8.15	77.04	10.73	53.08	6.00
26.72	17.31	76.22	8.22	77.12	12.39	53.13	5.81
26.75	16.40	76.30	8.84	77.19	9.99	53.18	6.08
26.78	17.20	76.38	8.25	77.27	10.93	53.24	6.27
26.80	16.72	76.45	7.56	77.34	10.62	53.29	5.87
26.83	18.48	76.53	7.68	77.42	9.82	53.34	5.89
26.86	15.52	76.61	7.20	77.49	9.89	53.40	5.35
26.88	16.38	76.69	6.83	77.57	9.71	53.45	5.72
26.91	16.14	76.76	6.33	77.64	10.51	53.50	5.98
26.94	16.17	76.84	6.69	77.72	10.88	53.56	6.55
26.96	15.34	76.92	6.07	77.79	9.81	53.61	6.13
26.99	15.60	76.99	5.47	77.87	11.18	53.66	6.14
27.02	14.88	77.07	5.87	77.95	11.14	53.72	6.27
27.04	14.70	77.15	5.58	78.02	10.38	53.77	6.51
27.07	15.28	77.22	5.65	78.10	9.04	53.82	6.02
27.10	15.19	77.30	6.72	78.17	9.20	53.88	6.29

27.12	15.34	77.38	7.29	78.25	9.58	53.93	6.64
27.15	16.08	77.46	7.96	78.32	9.09	53.98	6.38
27.18	12.80	77.53	8.29	78.40	9.72	54.04	6.44
27.20	14.82	77.61	8.72	78.47	9.74	54.09	5.96
27.23	14.09	77.69	8.91	78.55	9.44	54.14	5.77
27.26	15.99	77.76	8.42	78.62	10.65	54.20	6.24
27.28	15.32	77.84	9.07	78.70	10.19	54.25	6.02
27.31	14.08	77.92	8.78	78.78	10.74	54.30	6.11
27.33	12.60	77.99	9.49	78.85	12.57	54.36	6.61
27.36	14.10	78.07	9.26	78.93	12.62	54.41	6.27
27.39	15.54	78.15	8.00	79.00	13.48	54.46	6.03
27.41	14.85	78.23	8.14	79.08	11.65	54.52	6.05
27.44	15.67	78.30	9.04	79.15	12.13	54.57	5.92
27.47	15.02	78.38	8.34	79.23	11.51	54.62	5.15
27.49	16.26	78.46	8.45	79.30	11.14	54.67	5.19
27.52	15.34	78.53	8.21	79.38	11.97	54.73	4.74
27.55	15.56	78.61	8.11	79.46	10.70	54.78	4.94
27.57	14.35	78.69	9.17	79.53	11.27	54.83	4.78
27.60	15.85	78.76	9.43	79.61	11.73	54.89	5.13
27.63	14.93	78.84	7.77	79.68	11.73	54.94	4.86
27.65	13.78	78.92	8.80	79.76	13.92	54.99	5.31
27.68	15.54	78.99	7.78	79.83	15.08	55.05	5.40
27.71	14.93	79.07	7.68	79.91	13.99	55.10	5.56
27.73	14.60	79.15	7.08	79.98	12.27	55.15	4.99
27.76	15.11	79.23	6.83	80.06	12.00	55.21	5.09
27.79	15.81	79.30	5.75	80.13	11.36	55.26	5.11
27.81	14.78	79.38	6.08	80.21	10.71	55.31	4.81
27.84	16.88	79.46	5.61	80.29	10.96	55.37	4.57
27.87	16.50	79.53	6.02	80.36	9.96	55.42	4.36
27.89	17.51	79.61	5.85	80.44	9.43	55.47	4.35
27.92	16.05	79.69	6.34	80.51	9.04	55.53	4.52
27.95	17.59	79.76	6.63	80.59	9.40	55.58	4.76
27.97	17.18	79.84	6.63	80.66	9.60	55.63	4.62
28.00	16.60	79.92	6.04	80.74	10.09	55.69	4.19

28.03	15.24	80.00	6.45	80.81	9.94	55.74	3.79
28.05	17.84	80.07	5.90	80.89	11.15	55.79	3.96
28.08	16.32	80.15	5.71	80.97	11.29	55.85	3.95
28.11	15.41	80.23	5.58	81.04	11.50	55.90	4.05
28.13	16.99	80.30	5.95	81.12	11.24	55.95	4.37
28.16	17.67	80.38	5.89	81.19	11.62	56.01	4.59
28.19	14.56	80.46	5.78	81.27	10.22	56.06	4.35
28.21	17.69	80.53	6.28	81.34	12.32	56.11	4.32
28.24	15.38	80.61	5.76	81.42	11.71	56.17	4.47
28.27	17.97	80.69	6.36	81.49	11.68	56.22	3.93
28.29	15.15	80.77	7.17	81.57	11.03	56.27	4.03
28.32	11.86	80.84	6.96	81.64	12.49	56.33	4.17
28.32	15.82	80.92	6.98	81.72	11.41	56.38	4.71
28.36	11.47	81.00	6.38	81.80	12.56	56.43	5.76
28.41	13.55	81.07	5.98	81.87	12.26		
28.46	12.98	81.15	6.09	81.95	12.33		
28.52	12.96	81.23	6.11	82.02	13.08		
28.57	13.49	81.30	6.67	82.10	11.28		
28.62	14.60	81.38	6.71	82.17	11.22		
28.68	13.99	81.46	7.14	82.25	11.49		
28.73	14.04	81.54	7.23	82.32	9.72		
28.78	13.92	81.61	7.70	82.40	10.09		
28.83	14.58	81.69	6.93	82.47	9.45		
28.89	14.25	81.77	6.61	82.55	10.07		
28.94	15.51	81.84	6.09	82.63	11.12		
28.99	13.15	81.92	6.33	82.70	8.99		
29.05	13.52	82.00	6.26	82.78	9.92		
29.10	16.93	82.07	6.50	82.85	11.74		
29.15	15.52	82.15	5.23	82.93	10.21		
29.21	14.53	82.23	6.05	83.00	10.04		
29.26	13.58	82.31	6.13	83.08	10.20		
29.31	13.54	82.38	6.30	83.15	10.42		
29.37	13.83	82.46	6.47	83.23	10.97		
29.42	14.13	82.54	7.60	83.31	9.61		

29.47	15.14	82.61	7.11	83.38	9.58
29.53	14.45	82.69	5.49	83.46	9.91
29.58	12.48	82.77	5.97	83.53	8.59
29.63	13.59	82.84	6.30	83.61	9.40
29.69	11.20	82.92	5.47	83.68	8.93
29.74	12.86	83.00	4.74	83.76	8.52
29.79	12.34	83.08	4.88	83.83	9.50
29.85	13.91	83.15	4.39	83.91	7.55
29.90	12.97	83.23	4.86	83.98	8.68
29.95	15.12	83.31	5.37	84.06	8.62
30.01	14.82	83.38	4.43	84.14	8.17
30.06	12.90	83.46	4.08	84.21	8.27
30.11	13.21	83.54	4.84	84.29	9.20
30.17	14.05	83.61	4.47	84.36	8.53
30.22	14.21	83.69	4.25	84.44	8.42
30.27	14.19	83.77	4.89	84.51	7.71
30.32	15.81	83.85	4.86	84.59	6.80
30.38	16.56	83.92	4.44	84.66	8.39
30.43	14.68	84.00	4.30	84.74	7.21
30.48	14.63	84.08	4.15	84.82	6.78
30.54	14.37	84.15	5.34	84.89	7.35
30.59	14.99	84.23	5.18	84.97	8.68
30.64	14.07	84.31	4.86	85.04	7.26
30.70	14.83	84.38	5.10	85.12	7.32
30.75	14.17	84.46	4.91	85.19	7.33
30.80	12.86	84.53	4.64	85.27	6.77
30.86	14.51			85.34	7.24
30.91	12.95			85.42	7.43
30.96	15.03			85.49	7.20
31.02	13.52			85.57	7.75
31.07	13.95			85.65	7.44
31.12	13.03			85.72	7.56
31.18	13.17			85.80	7.51
31.23	12.22			85.87	7.37

31.28	16.48	85.95	6.70
31.34	14.20	86.02	7.10
31.39	13.30	86.10	6.86
31.44	10.82	86.17	8.57
31.50	12.26	86.25	8.04
31.55	12.54	86.33	6.10
31.60	13.57	86.40	6.08
31.65	14.12	86.48	5.59
31.71	15.17	86.55	6.58
31.76	13.44	86.63	5.92
31.81	15.09	86.70	5.86
31.87	13.11	86.78	6.74
31.92	13.75	86.85	6.63
31.97	13.22	86.93	5.85
32.03	12.17	87.00	5.49
32.08	13.99	87.08	7.57
32.13	14.53	87.16	5.67
32.19	13.63	87.23	5.65
32.24	13.37	87.31	5.67
32.29	12.98	87.38	4.61
32.35	12.33	87.46	4.58
32.40	10.87	87.53	5.07
32.45	13.17	87.61	4.77
32.51	13.45	87.68	5.67
32.56	14.78	87.76	5.39
32.61	14.86	87.83	4.74
32.67	14.84	87.91	5.09
32.72	13.50	87.99	5.41
32.77	13.30	88.06	4.62
32.83	14.13	88.14	4.92
32.88	14.41	88.21	5.36
32.93	14.83	88.29	3.97
32.99	14.73	88.36	5.95
33.04	15.27	88.44	4.28

33.09	14.34
33.14	16.79
33.20	14.10
33.25	13.09
33.30	13.05
33.36	14.83
33.41	16.32
33.46	16.40
33.52	15.92
33.57	13.83
33.62	12.68
33.68	12.73
33.73	14.38
33.78	14.10
33.84	13.14
33.89	13.63
33.94	13.08
34.00	11.45
34.05	12.80
34.10	10.93
34.16	10.37
34.21	10.99
34.26	11.45
34.32	10.33
34.37	11.86
34.42	10.29
34.47	9.15
34.53	10.45
34.58	10.16
34.63	10.39
34.69	10.43
34.74	9.30
34.79	12.66
34.85	10.57
88.51	6.63
88.59	5.20
88.67	4.64
88.74	5.33
88.82	5.55
88.89	5.61
88.94	4.35

34.90	11.91
34.95	11.47
35.01	10.34
35.06	11.42
35.11	12.13
35.17	11.81
35.22	11.42
35.27	11.24
35.33	11.72
35.38	10.54
35.43	10.84
35.49	11.55
35.54	10.55
35.59	11.29
35.65	10.91
35.70	10.69
35.75	10.58
35.81	9.29
35.86	9.90
35.91	9.77
35.97	10.99
36.02	10.18
36.07	11.29
36.12	11.91
36.18	11.15
36.23	11.91
36.28	12.57
36.34	10.99
36.39	12.62
36.44	12.32
36.50	12.38
36.55	11.30
36.60	10.50
36.66	10.52

36.71	10.36
36.76	9.79
36.82	9.56
36.87	10.30
36.92	9.96
36.98	8.98
37.03	9.78
37.08	9.83
37.14	8.99
37.19	9.73
37.24	9.04
37.30	10.11
37.35	9.16
37.40	9.88
37.45	9.67
37.51	9.65
37.56	9.98
37.61	8.50
37.67	8.39
37.72	7.68
37.77	6.39
37.83	7.27
37.88	6.48
37.93	7.03
37.99	6.18
38.04	7.33
38.09	6.39
38.15	7.80
38.20	7.88
38.25	7.06
38.31	6.89
38.36	7.74
38.41	8.12
38.47	6.83

38.52	7.19
38.57	6.93
38.63	9.95
38.68	8.34
38.73	9.24
38.78	6.69
38.84	6.67
38.89	6.94
38.94	6.16
39.00	6.54
39.05	5.80
39.10	6.14
39.16	6.51
39.21	6.50
39.26	6.44
39.32	6.45
39.37	7.13
39.42	7.78
39.48	6.07
39.53	5.39
39.58	6.28
39.64	6.53
39.69	7.88
39.74	7.51
39.80	8.28
39.85	9.02
39.90	9.17
39.96	9.21
40.01	8.16
40.06	8.36
40.11	8.19
40.17	8.01
40.22	8.48
40.27	9.00

40.33	8.76
40.38	9.74
40.43	9.47
40.49	7.63
40.54	8.33
40.59	8.31
40.65	9.42
40.70	8.25
40.75	9.17
40.81	9.04
40.86	9.73
40.91	8.49
40.97	9.27
41.02	9.99
41.07	8.71
41.13	9.37
41.18	8.15
41.23	8.40
41.29	9.92
41.34	8.35
41.39	7.45
41.45	8.45
41.50	8.32
41.55	8.67
41.60	9.27
41.66	7.90
41.71	8.02
41.76	7.27
41.82	9.13
41.87	8.01
41.92	8.18
41.98	7.39
42.03	7.58
42.08	7.30

42.14	8.21
42.19	7.73
42.24	7.93
42.30	7.95
42.35	7.40
42.40	7.81
42.46	8.27
42.51	6.95
42.56	8.45
42.62	7.78
42.67	8.21
42.72	7.89
42.78	7.95
42.83	6.76
42.88	8.25
42.93	7.50
42.99	7.40
43.04	7.35
43.09	7.56
43.15	7.63
43.20	7.07
43.25	6.98
43.31	5.70
43.36	5.44
43.41	5.53
43.47	5.17
43.52	5.46
43.57	4.67
43.63	4.85
43.68	5.31
43.73	4.76
43.79	5.03
43.84	5.75
43.89	6.09

43.95	5.43
44.00	5.95
44.05	5.78
44.11	6.09
44.16	5.44
44.21	5.73
44.27	4.86
44.32	5.60
44.37	5.98
44.43	6.75
44.48	6.23
44.53	6.37
44.58	5.92
44.64	5.95
44.69	5.89
44.74	5.53
44.80	5.25
44.85	6.54
44.90	6.01
44.96	6.85
45.01	6.92
45.06	8.21
45.12	7.31
45.17	6.75
45.22	7.49
45.28	7.52
45.33	7.73
45.38	7.15
45.44	7.18
45.49	6.45
45.54	6.31
45.60	6.44
45.65	5.59
45.70	5.92

45.76	6.41
45.81	5.76
45.86	6.54
45.91	5.75
45.97	5.98
46.02	6.18
46.07	5.49
46.13	5.25
46.18	5.31
46.23	4.77
46.29	5.01
46.34	6.10
46.39	5.97
46.45	7.01
46.50	6.35
46.55	5.92
46.61	5.90
46.66	4.88
46.71	5.16
46.77	5.07
46.82	4.89
46.87	5.62
46.93	4.91
46.98	4.14
47.03	4.58
47.09	4.26
47.14	4.21
47.19	3.95
47.24	4.65
47.30	4.72
47.35	4.57
47.40	5.09
47.46	5.87
47.51	6.67

47.56	6.13
47.62	6.38
47.67	5.69
47.72	5.65
47.78	5.89
47.83	5.58
47.88	5.94
47.94	6.23
47.99	6.16
48.04	6.16
48.10	6.18
48.15	6.78
48.20	6.11
48.26	6.50
48.31	6.80
48.36	7.12
48.42	7.29
48.47	7.35
48.52	7.57
48.58	7.65
48.63	7.98
48.68	8.28
48.73	9.63
48.79	8.65
48.84	8.24
48.89	8.97
48.95	8.60
49.00	9.37
49.05	9.59
49.11	8.73
49.16	9.08
49.21	9.35
49.27	9.35
49.32	9.96

49.37	9.52
49.43	10.03
49.48	8.72
49.53	10.17
49.59	9.40
49.64	9.33
49.69	10.27
49.75	9.93
49.80	10.17
49.85	10.15
49.91	9.39
49.96	9.51
50.01	9.92
50.07	9.43
50.12	10.51
50.17	10.28
50.22	10.55
50.28	10.49
50.33	9.53
50.38	9.51
50.44	9.94
50.49	9.43
50.54	9.18
50.60	9.32
50.65	8.87
50.70	7.95
50.76	9.95
50.81	9.47
50.86	9.12
50.92	8.92
50.97	9.07
51.02	9.19
51.08	9.18
51.13	9.84

51.18	9.04
51.24	9.91
51.29	9.35
51.34	9.36
51.40	8.80
51.45	9.74
51.50	9.27
51.56	8.98
51.61	9.04
51.66	9.52
51.71	10.44
51.77	10.22
51.82	10.66
51.87	9.91
51.93	9.30
51.98	9.95
52.03	10.43
52.09	8.50
52.14	9.48
52.19	9.28
52.25	10.54
52.30	10.23
52.35	11.77
52.41	10.27
52.46	10.05
52.51	8.94
52.57	10.85
52.62	10.14
52.67	10.64
52.73	10.22
52.78	9.14
52.83	9.29
52.89	10.20
52.94	10.83

52.99	11.81
53.05	10.25
53.10	10.13
53.15	12.01
53.20	10.99
53.26	10.63
53.31	11.37
53.36	10.71
53.42	10.39
53.47	11.42
53.52	10.53
53.58	10.93
53.63	10.73
53.68	10.61
53.74	9.60
53.79	10.37
53.84	10.21
53.90	10.24
53.95	9.80
54.00	9.21
54.06	8.66
54.11	7.14
54.16	6.64
54.22	7.21
54.27	7.74
54.32	7.65
54.38	8.63
54.43	8.28
54.48	8.47
54.53	8.87
54.59	8.34
54.64	7.95
54.69	9.61
54.75	9.24

54.80	8.72
54.85	9.20
54.91	8.57
54.96	8.70
55.01	7.96
55.07	7.56
55.12	9.42
55.17	11.22
55.23	10.25
55.28	11.47
55.33	11.09
55.39	10.93
55.44	11.90
55.49	9.93
55.55	10.94
55.60	11.25
55.65	10.80
55.71	10.13
55.76	11.39
55.81	11.39
55.87	10.58
55.92	13.03
55.97	10.88
56.02	11.01
56.08	9.39
56.13	10.34
56.18	10.39
56.24	9.26
56.29	8.73
56.34	9.33
56.40	9.66
56.45	9.82
56.50	9.64
56.56	10.00

56.61	9.59
56.66	9.56
56.72	9.87
56.77	10.07
56.82	10.00
56.88	9.49
56.93	10.69
56.98	9.56
57.04	10.00
57.09	9.98
57.14	9.48
57.20	9.54
57.25	9.27
57.30	9.49
57.35	8.39
57.41	9.30
57.46	8.58
57.51	10.10
57.57	10.21
57.62	10.20
57.67	9.39
57.73	9.10
57.78	9.04
57.83	9.86
57.89	8.89
57.94	10.02
57.99	8.52
58.05	8.66
58.10	9.51
58.15	9.18
58.21	9.33
58.26	9.09
58.31	10.16
58.37	10.56

58.42	10.03
58.47	10.65
58.53	11.33
58.58	9.59
58.63	10.27
58.69	10.28
58.74	9.81
58.79	10.83
58.84	10.14
58.90	10.64
58.95	10.62
59.00	10.15
59.06	10.41
59.11	10.91
59.16	10.33
59.22	9.29
59.27	9.85
59.32	9.78
59.38	9.03
59.43	9.46
59.48	9.69
59.54	9.28
59.59	8.74
59.64	9.30
59.70	9.87
59.75	9.68
59.80	9.60
59.86	9.23
59.91	9.52
59.96	8.96
60.02	8.80
60.07	9.07
60.12	8.40
60.18	8.30

60.23	8.31
60.28	9.53
60.33	8.73
60.39	9.14
60.44	9.04
60.49	8.51
60.55	8.53
60.60	9.33
60.65	9.11
60.71	8.71
60.76	9.34
60.81	9.24
60.87	9.33
60.92	9.18
60.97	9.19
61.03	8.62
61.08	9.19
61.13	9.63
61.19	8.86
61.24	8.65
61.29	8.07
61.35	8.86
61.40	8.24
61.45	9.86
61.51	8.75
61.56	9.39
61.61	8.98
61.66	10.08
61.72	9.88
61.77	8.88
61.82	9.94
61.88	9.67
61.93	10.36
61.98	10.05

62.04	9.97
62.09	9.79
62.14	10.67
62.20	10.24
62.25	10.59
62.30	12.09
62.36	10.99
62.41	9.59
62.46	11.47
62.52	11.33
62.57	11.60
62.62	10.96
62.68	10.28
62.73	11.41
62.78	11.53
62.84	9.53
62.89	11.02
62.94	10.46
62.99	9.94
63.05	10.05
63.10	9.14
63.15	9.18
63.21	9.53
63.26	8.35
63.31	8.71
63.37	9.27
63.42	9.29
63.47	8.20
63.53	9.42
63.58	8.50
63.63	8.22
63.69	8.24
63.74	8.54
63.79	9.08

63.85	9.94
63.90	9.10
63.95	9.76
64.01	8.97
64.06	9.30
64.11	9.52
64.17	10.20
64.22	9.47
64.27	9.85
64.33	10.25
64.38	9.77
64.43	11.08
64.48	11.66
64.54	10.93
64.59	10.75
64.64	10.99
64.70	11.32
64.75	11.65
64.80	12.73
64.86	11.87
64.91	11.56
64.96	10.67
65.02	12.27
65.07	12.03
65.12	11.92
65.18	11.56
65.23	11.35
65.28	11.71
65.34	11.40
65.39	11.27
65.44	11.39
65.50	11.87
65.55	12.50
65.60	11.60

65.66	10.99
65.71	11.49
65.76	13.32
65.81	11.54
65.87	12.21
65.92	11.71
65.97	12.91
66.03	11.67
66.08	11.06
66.13	11.39
66.19	12.28
66.24	12.18
66.29	12.64
66.35	12.60
66.40	12.30
66.45	12.14
66.51	11.76
66.56	11.76
66.61	11.92
66.67	13.20
66.72	11.42
66.77	12.05
66.83	11.96
66.88	11.36
66.93	11.72
66.99	12.14
67.04	13.62
67.09	13.74
67.15	12.28
67.20	10.94
67.25	9.45
67.31	8.33
67.36	7.22
67.41	7.20

67.46	7.37
67.52	6.73
67.57	6.85
67.62	6.71
67.68	6.93
67.73	6.45
67.78	7.33
67.84	7.47
67.89	7.45
67.94	8.00
68.00	7.14
68.05	8.01
68.10	8.19
68.16	7.95
68.21	8.37
68.26	8.68
68.32	8.57
68.37	8.77
68.42	8.49
68.48	8.10
68.53	8.26
68.58	8.26
68.64	8.84
68.69	8.68
68.74	8.17
68.80	8.63
68.85	8.45
68.90	8.49
68.95	7.41
69.01	8.25
69.06	7.94
69.11	7.41
69.17	7.43
69.22	8.03

69.27	7.15
69.33	7.89
69.38	7.54
69.43	7.68
69.49	7.49
69.54	7.64
69.59	7.45
69.65	7.74
69.70	7.99
69.75	8.54
69.81	7.82
69.86	8.50
69.91	7.11
69.97	8.33
70.02	7.53
70.07	7.71
70.13	7.25
70.18	7.70
70.23	8.08
70.29	7.67
70.34	7.88
70.39	7.45
70.44	7.10
70.50	7.22
70.55	7.28
70.60	7.75
70.66	7.88
70.71	8.11
70.76	8.83
70.82	8.62
70.87	8.36
70.92	8.82
70.98	8.54
71.03	8.76

71.08	9.28
71.14	9.83
71.19	9.70
71.24	9.10
71.30	9.07
71.35	9.58
71.40	10.24
71.46	10.29
71.51	9.89
71.56	9.68
71.62	9.66
71.67	8.90
71.72	8.82
71.78	8.62
71.83	8.18
71.88	8.25
71.93	7.90
71.99	7.67
72.04	8.09
72.09	8.57
72.15	8.42
72.20	8.94
72.25	8.61
72.31	8.61
72.36	7.96
72.41	8.29
72.47	7.86
72.52	7.63
72.57	7.50
72.63	7.64
72.68	8.02
72.73	8.29
72.79	8.12
72.84	8.02

72.89	7.92
72.95	7.90
73.00	8.43
73.05	9.47
73.11	8.83
73.16	8.39
73.21	8.64
73.27	8.60
73.32	8.20
73.37	8.39
73.42	9.98
73.48	11.61
73.53	12.29
73.58	12.64
73.64	11.80
73.69	10.47
73.74	9.24
73.80	9.42
73.85	8.92
73.90	8.50
73.96	8.80
74.01	9.54
74.06	9.19
74.12	9.00
74.17	9.53
74.22	9.25
74.28	9.55
74.33	8.91
74.38	8.85
74.44	9.03
74.49	8.69
74.54	8.15
74.60	8.27
74.65	7.83

74.70	7.71
74.75	8.11
74.81	8.61
74.86	9.08
74.91	9.56
74.97	10.07
75.02	9.57
75.07	10.78
75.13	10.57
75.18	10.52
75.23	10.65
75.29	11.64
75.34	10.76
75.39	11.39
75.45	10.75
75.50	10.69
75.55	9.96
75.61	10.37
75.66	11.19
75.71	11.63
75.77	10.74
75.82	11.70
75.87	12.79
75.93	11.86
75.98	11.46
76.03	10.87
76.09	10.93
76.14	11.02
76.19	11.00
76.24	10.82
76.30	10.55
76.35	10.16
76.40	9.81
76.46	9.46

76.51	8.94
76.56	8.40
76.62	8.44
76.67	8.00
76.72	8.25
76.78	8.13
76.83	8.03
76.88	8.18
76.94	8.35
76.99	8.74
77.04	9.47
77.10	9.34
77.15	10.07
77.20	9.53
77.26	9.01
77.31	8.38
77.36	8.43
77.42	7.57
77.47	8.35
77.52	8.63
77.57	8.69
77.63	8.32
77.68	7.82
77.73	7.45
77.79	7.68
77.84	7.21
77.89	6.73
77.95	5.84
78.00	5.62
78.05	5.37
78.11	5.42
78.16	5.50
78.21	5.62
78.27	5.54

78.32	5.29
78.37	5.58
78.43	5.88
78.48	6.22
78.53	6.89
78.59	7.57
78.64	7.96
78.69	7.89
78.75	7.97
78.80	8.48
78.85	8.54
78.91	8.73
78.96	8.47
79.01	8.23
79.06	8.73
79.12	8.28
79.17	8.32
79.22	8.28
79.28	8.44
79.33	8.69
79.38	8.63
79.44	9.06
79.49	8.73
79.54	9.25
79.60	10.53
79.65	9.01
79.70	8.70
79.76	8.35
79.81	8.23
79.86	8.08
79.92	8.07
79.97	8.01
80.02	7.91
80.08	7.89

80.13	7.67
80.18	7.88
80.24	7.44
80.29	7.62
80.34	7.02
80.40	7.04
80.45	6.97
80.50	7.01
80.55	7.11
80.61	7.27
80.66	7.04
80.71	7.06
80.77	7.27
80.82	7.15
80.87	6.70
80.93	6.67
80.98	6.86
81.03	6.73
81.09	6.79
81.14	6.72
81.19	6.77
81.25	6.61
81.30	6.82
81.35	6.72
81.41	6.76
81.46	6.71
81.51	6.75
81.57	6.38
81.62	6.65
81.67	6.28
81.73	6.49
81.78	6.25
81.83	6.15
81.89	6.23

81.94	6.27
81.99	6.13
82.05	6.18
82.10	5.74
82.15	5.82
82.20	5.69
82.26	5.47
82.31	4.78
82.36	4.57
82.42	4.06
82.47	3.67
82.52	3.30
82.58	3.62
82.63	3.62
82.68	3.95
82.74	4.10
82.79	3.91
82.84	3.93
82.90	3.50
82.95	3.39
83.00	3.42
83.06	3.29
83.11	3.42
83.16	3.57
83.22	3.48
83.27	3.25
83.32	2.80
83.38	2.59
83.43	2.60
83.48	2.58
83.53	2.74
83.59	2.91
83.64	3.06
83.69	3.43

83.75	3.86
83.80	4.09
83.85	3.95
83.91	4.13
83.96	4.14
84.01	3.95
84.07	4.29
84.12	4.33
84.17	4.60
84.23	3.89
84.28	4.08
84.33	3.95
84.39	3.71
84.44	3.67
84.49	3.89
84.55	3.94
84.60	3.90
84.65	3.98
84.71	4.10
84.76	3.65
84.81	3.62
84.87	3.50
84.92	3.63
84.97	3.91
85.02	3.92
85.08	4.02
85.13	4.16

Table 4A.11. Pambula Lake water parameter data.

Date	Salinity	$\delta^{18}O$ (VSMOW)	Ca (ppm)	Mg (ppm)	Mg me/l	Ca me/l	Mg/Ca
05-Jun-06			279.41	885.03	73.72	13.97	5.28
7-Jul-06		1.40	404.86	1324.50	110.33	20.24	5.45
8-Sep-06	31.7	0.90	463.43	1533.65	127.75	23.17	5.51
22-Sep-06	32.8	0.82					
6-Oct-06	33.3	0.98					
20-Oct-06	33.2	0.89	483.19	1598.83	133.18	24.16	5.51
3-Nov-06	33.4	1.11	472.90	1562.28	130.14	23.64	5.50
21-Nov-06	33.7	1.13	491.69	1628.43	135.65	24.58	5.52
1-Dec-06	31.8	1.93	462.96	1537.99	128.11	23.15	5.53
15-Dec-06	34	1.35	470.76	1551.96	129.28	23.54	5.49
30-Dec-06	32.9	1.39	471.22	1547.47	128.90	23.56	5.47
12-Jan-07	33	0.97	460.80	1526.91	127.19	23.04	5.52
19-Jan-07			469.78	1554.32	129.48	23.49	5.51
29-Jan-07	33.7	0.93					
12-Feb-07	27.2	0.73	203.48	572.00	47.65	10.17	4.68
16-Feb-07	2.67						
6-Mar-07		-0.66	351.24	1065.00	88.71	17.56	5.05
21-Mar-07		0.79	452.41	1454.63	121.17	22.62	5.36
30-Mar-07	32.60	0.86	447.08	1429.98	119.12	22.35	5.33
8-Apr-07	32.60						
20-Apr-07	33.40	0.89	451.10	1484.76	123.68	22.56	5.48
30-Apr-07	32.60						
8-May-07	33.40						
11-May-07	33.20						
25-May-07	34.00	0.83	463.16	1534.53	127.83	23.16	5.52
12-Jun-07	33.10	1.04					
22-Jun-07	27.80						
6-Jul-07	24.30						
9-Jul-07	20.00	-2.88					
16-Jul-07	24.50						

Table 4A.12. Little Swanport water parameter data.

Date	Salinity	d18o (VSMOW)	Mg (ppm)
7-Sep-06	36.38	0.58	1560.92
26-Sep-06	35.44	0.71	1514.56
10-Oct-06	35.71	0.74	1513.33
24-Oct-06	36.05	0.84	1434.69
9-Nov-06	35.78	0.80	1583.37
23-Nov-06	35.98	0.68	1542.35
5-Dec-06	35.91	1.00	1607.53
19-Dec-06	35.78	1.00	1631.13
9-Jan-07	36.38	1.21	1592.14
2-Feb-07	37.05	1.20	1568.00
13-Feb-07	37.12	1.06	1638.30
27-Feb-07	36.45	0.81	1517.50
27-Mar-07	36.58	0.90	1577.22
12-Apr-07	36.38	0.89	1491.18
24-Apr-07	36.31	0.75	1500.51
8-May-07	36.52	0.75	1462.88
22-May-07	36.45	0.71	1576.73
5-Jun-07	35.91	0.59	1572.12
19-Jun-07	36.05	0.45	1596.33
3-Jul-07	35.38	0.30	1585.61
17-Jul-07	34.64	0.37	1543.32